

Disease mechanisms and markers of progression in cerebral small vessel disease



Dr Robin Barney Brown

Jesus College

Dept of Clinical Neurosciences

University of Cambridge

This dissertation is submitted for the degree of Doctor of Philosophy
April 2023

Declaration

This thesis is the result of my own work and includes nothing which is the outcome of work done in collaboration except as declared in the preface and specified in the text.

It is not substantially the same as any work that has already been submitted before for any degree or other qualification except as declared in the preface and specified in the text.

It does not exceed the prescribed word limit for the Clinical Medicine and Clinical Veterinary Medicine Degree Committee.

Abstract

Introduction

Cerebral small vessel disease (SVD) is a common disease process accounting for a quarter of all ischaemic strokes, around 80% of haemorrhagic strokes, and is the major contributor to vascular cognitive impairment and dementia. Despite it being a major public health burden, understanding of the natural history is incomplete and the specific pathophysiological processes involved have not been fully elucidated. Consequently, there are few effective disease modifying treatments. In part I of this thesis I aimed to clarify elements of the natural history of white matter hyperintensity lesions (WMHs) in SVD. These are a key radiological feature of SVD that are strongly correlated with clinical sequelae, and I further tested whether brain lesion volume can regress over time. In part II I investigated the role of two novel pathophysiological mechanisms (inflammation and the permeability of the blood-brain barrier), and their relationship with SVD severity and progression.

Methods

I performed a systematic review of WMH growth and used inverse variance-weighted meta-analysis to determine the expected WMH change over time in high-risk populations. I next used a novel timepoint-blind WMH marking technique to assess whether WMH volume regresses over time in three separate SVD cohorts. Finally I studied a cohort of patients with SVD undergoing PET-MRI imaging, phlebotomy and neuropsychometric testing.

Results

WMHs typically expand at 2.50 ± 3.02 cc/year in patients with SVD and this is significantly more likely in patients with hypertension and who currently smoke. I found only 12/417 participants (2.9%) who showed modest WMH regression on longitudinal imaging, and this was more likely in patients with less severe disease at baseline. I demonstrated significant differences between patient and control groups in

both microglial signal and blood-brain barrier permeability, and associations between microglial signal and both clinical and radiological markers of SVD severity. These disease processes did not predict disease progression at one year.

Conclusions

I calculated the expected rate of WMH growth in relevant populations and how these data affect the sample sizes required to show a treatment effect, which should inform future trials. My results investigating WMH regression suggest that this is unlikely to be a significant factor in severe SVD.

I showed that both microglial signal and blood-brain barrier permeability are likely to be relevant in SVD, but whether they are disease causing remains unclear. I further discussed the ongoing interventional study in which the data collection for this thesis was nested (MINERVA). The MINERVA trial aims to answer this question by testing whether minocycline can inhibit activated microglia and stabilise the blood-brain barrier, and I presented baseline data from the trial.

Acknowledgements

This work was conducted with the help of the following individuals:

Dr Audrey Low (Research Associate, University of Cambridge) assisted with the data collection and analysis in chapter two.

Dr Marco Egle (Postdoctoral Research Fellow, National Institutes of Health, USA) assisted with the data collection and analysis in chapter three.

Dr Anil Tuladhar (Neurologist and Junior Principal Investigator, Radboud UMC, Nijmegen, Netherlands) supervised the image acquisition in the RUN DMC study and assisted with the data analysis and interpretation in chapter three.

Prof Frank-Erik de Leeuw (Professor of Neurology, Radboud UMC, Nijmegen, Netherlands) is the principal investigator of the RUN DMC study and assisted with the data analysis and interpretation in chapter three.

Dr Jessica Walsh (Clinical Neuroimaging Research Facilitator, University of Oxford) recruited participants to the observational PET-MRI cohort and acquired portions of the data used in chapters five, six, seven and eight.

Dr Daniel Tozer (Senior Research Associate, University of Cambridge) developed the methods, and performed aspects of data analysis and interpretation (chapters five, six, seven and eight).

Dr Young Hong (Senior Research Associate, University of Cambridge) and Dr Tim Fryer (Assistant Director of Research, University of Cambridge) developed the methods and performed aspects of data analysis and interpretation (chapters five, six, seven and eight).

Prof Martin Graves (Professor of Radiology), Prof Franklin Aigbirhio (Professor of Molecular Imaging Chemistry) and Prof John O'Brien (Professor of Old Age Psychiatry) were involved in obtaining funding for the observation and interventional PET-MRI studies (chapters four, five, six, seven and eight).

Malin Overmars (PhD student, University of Utrecht, Netherlands) assisted with the statistical analysis in chapter six.

Dr Amanda Heslegrave (Senior Research Associate, UK Dementia Research Institute, University College London) provided advice on the cerebrospinal fluid analysis (chapter six and seven) and supervised the neurofilament and GFAP assays.

Prof Hugh Markus (Professor of Stroke Medicine, University of Cambridge) supervised this work throughout.

Dedication

I am grateful to my parents for instilling in me a love of learning and a drive to challenge myself, without which I would never have pursued this PhD project with such enthusiasm. My family have made enormous sacrifices for my research work, particularly my wife Jennifer, whose unwavering support has been incredible and who has helped me to focus at critical moments and to relax at times of great challenge. It is clichéd but still appropriate to say that this thesis is as much hers as it is mine! My daughter Hattie and my sons Alex and Isaac have been a constant source of delight and distraction and I would also like to dedicate this work to them in the hope that one day they may even read it (although this seems unlikely to be necessary as their respective ambitions lie in becoming an artist, a fireman and a unicorn)!

I am very grateful to the Association of British Neurologists for awarding me a Clinical Research Training Fellowship to support my PhD work, and to the Guarantors of Brain for funding the award. My thanks also go to the other funders of this work including the Medical Research Council, the British Heart Foundation, and particularly the British Medical Association Foundation for awarding me my first independent grant funding without which this research wouldn't have been possible.

I would also like to thank the many friends and colleagues working in stroke in Cambridge who have helped to nurture my enthusiasm for the subject and made coming to work every day a genuine pleasure. This includes the “downstairs” team of junior doctors, consultants, therapists, and both clinical and research nurses (particularly Jo, Elaine, Sarah and Jenny who I regard as big sisters) and the “upstairs” team who have helped to teach, train, stimulate and on many occasions and without complaint stepped in to help with patient visits and data collection.

It has been fantastic to work with generations of co-conspirators in the Fellows' room, especially Jess, from whose excellent work many of my thoughts developed, and Chris and Bernard who barrelled down the home straight at the same time. Particular thanks go to Dan for training me with patience, and to Laurence for being my confidante and moral compass.

I am also very grateful to Hugh for entrusting me with this project, for stretching me academically and for giving me the opportunity to develop as a clinician and as a scientist throughout our work together. You have been a brilliant supervisor and extremely supportive when times were difficult, and I appreciate it greatly!

Finally my thanks go to the participants and their families and carers who gave up their time so willingly to make this work possible. We have gathered a huge amount of data and I cannot express enough gratitude for every single brain scan, blood sample, lumbar puncture and cognitive testing session. I sincerely hope that this information will continue to be useful in the advancement of small vessel disease research for many years to come and I am grateful to you all for being a part of it.

Publications

1. **Brown RB**, Tozer DJ, Egle M, Tuladhar AM, de Leeuw F-E & Markus HS – How often does white matter hyperintensity volume regress in cerebral small vessel disease? *Int J Stroke* 2023 [published online ahead of print; doi: 10.1177/17474930231169132]
2. Tozer DJ, **Brown RB**, Walsh J, Hong YT, Williams GB, O'Brien JT, Aigbirhio FI, Fryer TD & Markus HS - Do Regions of Increased Inflammation Progress to New White Matter Hyperintensities?: A Longitudinal Positron Emission Tomography- Magnetic Resonance Imaging Study. *Stroke* 2023;54(2):549-558
3. **Brown RB**, Tozer DJ, Loubière LH, Hong YT, Fryer TD, Williams GB, Graves MJ, Aigbirhio FI, O'Brien JT & Markus HS - MINocyclinE to Reduce inflammation and blood brain barrier leakage in small Vessel disease (MINERVA) trial study protocol. *Eur J Stroke* 2022;7(3):323-330
4. Ohlmeier L, Nannoni S, Pallucca C, **Brown RB**, Loubiere L, Markus HS - Prevalence of, and Risk Factors for, Cognitive Impairment in Lacunar Stroke. *Int J Stroke* 2022;18(1):62-69
5. **Brown RB**, Low A & Markus HS - Rate of, and risk factors for, white matter hyperintensity growth: a systematic review and meta-analysis with implications for clinical trial design. *JNNP* 2021;92:1271-1277
6. Nannoni SN, Ohlmeier L, **Brown RB**, Morris RG, MacKinnon A & Markus HS - Cognitive impact of cerebral microbleeds in patients with symptomatic small vessel disease. *Int J Stroke* 2021;17(4):415-424
7. Fernando J, **Brown RB**, Edwards H, Egle M, Markus HS & Tay J - Individual markers of cerebral small vessel disease and domain-specific quality of life deficits. *Brain & Behaviour* 2021;00:ee02106
8. **Brown RB**, Traylor M, Burgess S, Sawcer S & Markus HS - Do cerebral small vessel disease and multiple sclerosis share common mechanisms of white matter injury? A genetic study. *Stroke* 2019;50:1968- 1972

Presentations

1. **Brown RB** – Inflammation in cerebral small vessel disease: friend or foe? Invited talk at NIHR Stroke Workshop, London, 27/09/2023
2. **Brown RB**, Tozer DJ, Loubière LH, Harshfield E, Hong YT, Fryer TD, Williams GB, Graves MJ, Aigbirhio FI, O'Brien JT & Markus HS - MINocyclinE to Reduce neuroinflammation and blood brain barrier leakage in small Vessel disease: results of the MINERVA trial. Platform presentation at European Stroke Organisation Conference, Munich, 11/05/2023
3. **Brown RB** – Central and peripheral inflammation in cerebral small vessel disease. Oral presentation at British Heart Foundation Centre of Research Excellence annual symposium, Cambridge, 20/04/2023
4. **Brown RB**, Tozer DJ, Loubière LH, Hong YT, Fryer TD, Williams GB, Graves MJ, Aigbirhio FI, O'Brien JT & Markus HS – Central and peripheral inflammation in cerebral small vessel disease. Oral presentation at European Molecular Biology Organisation stroke inflammation workshop, Munich, 9-11/03/2022

Table of contents

DECLARATION	1
ABSTRACT	2
ACKNOWLEDGEMENTS	4
DEDICATION.....	6
PUBLICATIONS.....	7
PRESENTATIONS	8
TABLE OF CONTENTS	9
GLOSSARY OF TERMS.....	13
CHAPTER ONE	15
INTRODUCTION TO CEREBRAL SMALL VESSEL DISEASE AND DEFINITIONS	16
SUBTYPES OF SVD	18
CLINICAL FEATURES OF SPORADIC SVD.....	21
<i>Stroke</i>	21
<i>Vascular cognitive impairment and dementia</i>	21
<i>Mood and motivation</i>	23
<i>Mobility, gait apraxia and vascular Parkinsonism</i>	23
NEUROIMAGING HALLMARKS OF SVD.....	24
<i>Lacunar infarcts</i>	25
<i>White matter hyperintensity lesions</i>	26
<i>Cerebral microbleeds</i>	29
<i>Enlarged perivascular spaces</i>	30
<i>Multifocal and novel imaging markers</i>	34
PATHOPHYSIOLOGY OF SVD.....	36
<i>Classical hypothesis and cerebrovascular risk factors</i>	36
<i>Genetic factors</i>	40
<i>Neurodegeneration and the relationship between SVD and Alzheimer’s disease</i>	42
<i>Blood-brain barrier permeability</i>	43
<i>Neuroinflammation and the peripheral immune response</i>	48
<i>Synthesis of pathophysiological mechanisms</i>	51
DISEASE-MODIFYING TREATMENT AND EVIDENCE FROM PREVIOUS CLINICAL TRIALS	52
AIMS OF THESIS	54
PART I.....	57
CHAPTER TWO	58
INTRODUCTION.....	59
METHODS	60
<i>Systematic review and data extraction</i>	60
<i>Statistical analysis</i>	61
RESULTS.....	62
<i>Rates of WMH progression and comparison between studies</i>	63

<i>Sample size calculations for a clinical trial based on WMH progression ..</i>	67
<i>Individual patient risk factors for WMH progression</i>	69
DISCUSSION	72
CHAPTER THREE.....	76
INTRODUCTION.....	77
METHODS.....	78
<i>Study populations</i>	78
<i>Image acquisition</i>	79
<i>Image analysis</i>	80
<i>Statistical analysis</i>	81
RESULTS.....	82
<i>Proportion of regressors.....</i>	82
<i>Effects of brain atrophy on proportion of regressors.....</i>	85
<i>Effect of using different thresholds to define regression.....</i>	85
<i>Individual patient factors associated with regression</i>	86
<i>Intra-rater reliability in WMH marking technique</i>	88
DISCUSSION	88
PART II	92
CHAPTER FOUR.....	93
INTRODUCTION.....	94
PHASE I: OBSERVATIONAL PET-MRI STUDY	94
<i>Patient selection</i>	95
<i>Imaging acquisition.....</i>	97
<i>Image analysis</i>	97
<i>Blood sampling, processing, and analysis</i>	99
<i>Neuropsychometric testing</i>	100
<i>Ethical and regulatory approval</i>	101
PHASE II: THE MINOCYCLINE TO REDUCE BLOOD-BRAIN BARRIER PERMEABILITY AND INFLAMMATION IN SMALL VESSEL DISEASE (MINERVA) TRIAL	101
<i>Patient selection</i>	104
<i>Imaging acquisition.....</i>	104
<i>Image analysis</i>	104
<i>Blood sampling, processing, and analysis</i>	106
<i>Neuropsychometric testing</i>	107
<i>Cerebrospinal fluid sampling</i>	107
<i>Statistical analysis and power calculations.....</i>	110
<i>Safety and adverse event reporting</i>	110
<i>Data capture / data access</i>	111
<i>Ethical and regulatory approval</i>	111
<i>Potential limitations</i>	112
POOLED PET-MRI COHORT	112
CHAPTER FIVE.....	114
INTRODUCTION.....	115
METHODS.....	116
<i>Statistical analysis</i>	116

RESULTS.....	116
<i>Observational phase recruitment</i>	116
<i>MINERVA trial recruitment</i>	117
<i>Comparison of patient groups and control</i>	118
<i>Comparison of observational cohort with MINERVA trial interventional cohort</i>	121
<i>Baseline neuropsychiatric test performance</i>	124
DISCUSSION	128
CHAPTER SIX	131
INTRODUCTION.....	132
<i>Evidence for central inflammation</i>	132
<i>Evidence for peripheral inflammation</i>	133
<i>Interaction between peripheral and central compartments</i>	134
<i>Hypotheses and study design</i>	135
METHODS.....	136
<i>Image analysis</i>	136
<i>Blood processing</i>	136
<i>Neuropsychometric testing</i>	137
<i>Statistical analysis</i>	137
RESULTS.....	139
<i>Determination of optimal PET marker</i>	139
<i>Relationship of PET binding to MRI markers of SVD</i>	141
<i>Relationship of PET binding to cognition</i>	148
<i>Relationship of peripheral blood proteomic panel with markers of SVD severity</i>	154
<i>Relationship of circulating monocytes to radiological SVD markers</i>	157
<i>Interactions between peripheral and central compartments</i>	158
DISCUSSION	160
CHAPTER SEVEN	165
INTRODUCTION.....	166
<i>Evidence for the role of BBB permeability in SVD</i>	166
<i>Role of markers of neurogliovascular unit breakdown in SVD</i>	168
<i>Hypotheses and study design</i>	169
METHODS.....	170
<i>Image analysis</i>	170
<i>Blood processing</i>	170
<i>Cerebrospinal fluid processing</i>	171
<i>Neuropsychiatric testing</i>	171
<i>Statistical analysis</i>	171
RESULTS.....	173
<i>Determination of optimal DCE-MRI marker for BBB permeability</i>	173
<i>Relationship of BBB permeability to MRI markers of SVD</i>	174
<i>Relationship of BBB permeability to cognition</i>	180
<i>Relationship of peripheral blood proteomic panel with BBB permeability</i>	185
RELATIONSHIP OF Q_{ALB} TO RADIOLOGICAL SVD MARKERS AND COGNITION.....	187

<i>Relationship of Qalb to DCE-MRI markers</i>	189
<i>Association of GFAP with SVD severity</i>	190
<i>Association of NfL with SVD severity</i>	195
<i>Relationship between CSF/serum GFAP and NfL</i>	200
CHAPTER EIGHT	205
INTRODUCTION	206
METHODS	209
<i>Image analysis</i>	210
<i>Neuropsychiatric test scoring</i>	210
<i>Statistical analysis</i>	211
RESULTS	211
<i>Predictors of radiological disease progression</i>	212
<i>Predictors of change in cognition</i>	218
DISCUSSION	224
<i>Radiological progression</i>	224
<i>Progression of cognition</i>	227
<i>Conclusions and further directions</i>	228
CHAPTER NINE	230
APPENDIX A. STUDIES INCLUDED IN WMH PROGRESSION REVIEW (CHAPTER TWO)	278
APPENDIX B. MRI SEQUENCE DETAILS (CHAPTERS FOUR TO EIGHT).	285
APPENDIX C. INTRA- AND INTER-ASSAY RELIABILITY DATA FORPROTEOMICS PANEL DATA.	286
APPENDIX D. UNIVARIATE REGRESSION MODEL RESULTS FOR INDIVIDUAL OLINK BIOMARKERS AS PREDICTORS OF RADIOLOGICAL FEATURES OF SVD (CHAPTER SIX).	287
APPENDIX E. UNIVARIATE REGRESSION MODEL RESULTS FOR INDIVIDUAL OLINK BIOMARKERS AS PREDICTORS OF BBB PERMEABILITY (CHAPTER SEVEN).	290

Glossary of terms

AD: Alzheimer's disease

ApoE: Apolipoprotein E

ASL: arterial spin labelling

BAM: border-associated macrophage

BBB: blood-brain barrier

BMI: body mass index

CAA: cerebral amyloid angiopathy

CADASIL: cerebral autosomal dominant arteriopathy with subcortical infarcts and leukoencephalopathy

CBF: cerebral blood flow

CD14 *[etc.]*: cluster of differentiation 14

CI: confidence interval

CMB: cerebral microbleed

CNS: central nervous system

CRP: C-reactive protein

CSF: cerebrospinal fluid

CSF1R: colony stimulating factor 1 receptor

DBP: diastolic blood pressure

DCE-MRI: dynamic contrast-enhanced magnetic resonance imaging

DTI: diffusion tensor imaging

DWI: diffusion-weighted imaging

dWMH: deep white matter hyperintensity

ECM: extracellular matrix

EF: executive function

eGFR: estimated glomerular filtration rate

ELISA: enzyme-linked immunosorbent assay

EPVS: enlarged perivascular space

FA: fractional anisotropy

FDR: false discovery rate

FLAIR: fluid-attenuated inversion recovery

GC: global cognition

GFAP: glial fibrillary acidic protein

GWAS: genome-wide association study

ICAM-1: intercellular adhesion molecule 1

ICH: intracerebral haemorrhage

IL-6 *[etc.]*: interleukin-6

IQR: interquartile range

K_{in} : permeability constant

LTM: long-term memory

MCI: mild cognitive impairment

MCP-1: monocyte chemo-attractant protein 1

MD: mean diffusivity

MDPH: mean diffusivity peak height

MMP-2 *[etc.]*: matrix metalloprotease 2

MRI: magnetic resonance imaging

NART: National Adult Reading Test

NAWM: normal-appearing white matter

NfL: neurofilament light

OR: odds ratio

PDGFR β : platelet-derived growth factor receptor- β

PET: positron emission tomography

PS: processing speed

PVS: perivascular space

pWMH: periventricular white matter hyperintensity

Q_{alb}: serum / cerebrospinal fluid albumin quotient

RNA: ribonucleic acid

SBP: systolic blood pressure

SE: standard error

SNP: single nucleotide polymorphism

SVD: small vessel disease

SWAN: susceptibility-weighted angiogram

SWI: susceptibility-weighted imaging

TIA: transient ischaemic attack

TIMP-1 [*etc.*]: tissue inhibitor of metalloproteases 4

TGF- β : tumour growth factor β

TNF- α : tumour necrosis factor α

TSPO: translocator protein

t-PA: tissue plasminogen activator

VaD: vascular dementia

VCAM-1: vascular adhesion molecule 1

VCI: vascular cognitive impairment

VEGF: vascular endothelial growth factor

vWF: von Willebrand factor

WMHs: white matter hyperintensities

WoM: working memory

CHAPTER ONE

Introduction, aims and thesis outline

Introduction to cerebral small vessel disease and definitions

Cerebral small vessel disease (SVD) is a common disease process underlying stroke and cognitive impairment/dementia. SVD refers to a pathological dysfunction of the small vessels that make up a network of brain vasculature (principally but not confined to the small perforating arteries and arterioles in the deep/subcortical anatomical areas, though superficial regions and the venous system are also involved).^{1,2} This small vessel dysfunction leads to a constellation of potential symptoms consistent with the vascular territory or neuronal networks affected and the time course of dysfunction, ranging from cognitive impairment and dementia caused by low grade progressive ischaemia over many years, to acute stroke when an affected vessel becomes suddenly occluded intracerebral haemorrhage (ICH) when it ruptures.

SVD is extremely common, affecting millions of people worldwide. It is responsible for $\frac{1}{5}$ to $\frac{1}{4}$ of ischaemic strokes³, the majority of haemorrhagic strokes¹ and around 45% of vascular cognitive impairment (VCI) or vascular dementia (VaD)⁴ - though VaD commonly arises due to multiple overlapping disease processes⁵ and conversely SVD is also an important risk factor for the development of Alzheimer's disease⁶, so the precise contribution of SVD to all-cause dementia risk is difficult to summarise. In the UK this corresponds to around 20,000 strokes per year, 10,000 cases of ICH and 35,000 cases of VCI/VaD.⁷ The economic burden of VaD alone is an estimated £15.7 billion per year, projected to rise to over £45 billion per year in 2040.⁸ However, despite its importance, understanding of the underlying pathophysiology is incomplete and there are few effective disease-modifying treatments.⁹ It is therefore critical to understand this disease process and how it can be therapeutically modified.

The aetiology of SVD is linked to the structure and behaviour of the affected vessels. The cerebral arterial circulation can be thought of as large vessels (>2mm diameter) that give multiple branches to supply blood to a large area of cortical and subcortical tissue, and small vessels (typically <2mm diameter but tapering down to 100-200µm

in diameter) that provides the blood supply to a much smaller area of tissue.¹⁰ Figure 1.1 illustrates the typical configuration of large and small vessels.

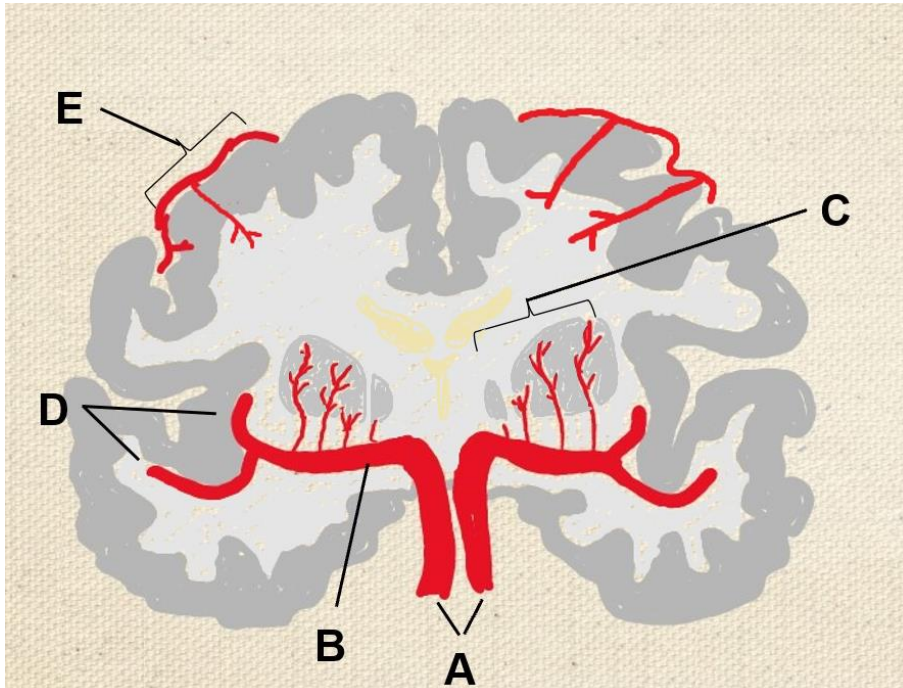


Figure 1.1. Sketch of cerebral circulation in coronal plane. Labelled are (A) internal carotid arteries; (B) middle cerebral artery; (C) lenticulostriate perforator arteries; (D) distal middle cerebral artery branches; (E) leptomeningeal arteries with cortical arterioles

Large vessels and small vessels have different haemodynamic properties and are subject to differing disease processes. A key difference is that small perforator vessels are end-arterioles with no collateral circulation; accordingly, the areas they supply (typically subcortical regions containing myelinated neuronal tracts that have high metabolic demand) are more vulnerable to ischaemia.¹¹ As can readily be inferred from the diagram of cerebral circulation in figure 1.1, occlusion of one of the perforating arterioles (in this case the lenticulostriate arteries) causes ischaemia in a small volume of subcortical tissue downstream from the occlusion. Conversely, occlusion of a large artery (for example the middle cerebral artery) compromises the blood flow to a much larger volume of tissue including both cortical and subcortical areas. The cause of such an occlusion is likely to be different and these are more often caused by plaque rupture

from large artery disease in the carotid artery or cardioembolic (typically secondary to atrial fibrillation) rather than intrinsic disease within the vessel.¹²

Symptoms from SVD can arise in one of three main ways:

(1) Acute occlusion of a vessel, presumed to be intrinsically diseased before the event – this can cause symptoms consistent with ischaemia in the area affected.

(2) Chronic occlusion or stenosis of a vessel or network of vessels – this can lead to chronic ischaemia.

(3) Rupture of a diseased vessel – this can lead either to microscopic bleeding that does not usually cause symptoms acutely, or macroscopic bleeding, which usually does. The risk factors, neuroimaging findings and treatments for ICH in SVD are beyond the scope of this thesis and not further discussed (although the disease mechanisms are likely to be similar in deep/subcortical ICH).

Subtypes of SVD

There are several subtypes of SVD, characterised principally by the distribution of vessels affected and further by aetiology. The chief distinction is between SVD affecting the deep white matter and subcortical structures (including the basal ganglia, thalamus, midbrain, brainstem and cerebellum – vessels marked “C” in figure 1) and SVD affecting the cortical/leptomeningeal arterial beds (vessels marked “E” in figure 1). SVD affecting the leptomeningeal vessels is usually reflective of cerebral amyloid angiopathy (CAA), a condition in which β -amyloid (a key protein implicated in Alzheimer’s disease when deposited in the parenchyma) accumulates in the vessel walls, rendering these vessels prone to chronic ischaemia and to rupture, causing ICH.¹³ This is common, affecting roughly 5-7% of elderly people, and considerably more in populations such as patients with cognitive impairment or lobar ICH.¹⁴ CAA is generally sporadic but has a significant genetic component driven by the *ApoE* genotype; *ApoE* codes for the Apolipoprotein E protein which chaperones lipids in the

blood and interstitium, and the presence of the *ApoE* $\epsilon 4$ allele is known to be a risk factor for CAA, conferring a fivefold risk of diagnosis in one descriptive study.¹⁵ Less commonly it can be inherited in an autosomal dominant Mendelian pattern due to mutations in the β -amyloid precursor protein (APP)¹⁶ and extremely rarely it can be acquired iatrogenically due to exposure via certain neurosurgical procedures to cadaveric dura, presumably containing a reservoir of β -amyloid.¹⁷ This thesis does not consider CAA, which affects a different distribution of vessels, has a distinct risk factor profile, and might consequently have different pathogenic mechanisms to SVD affecting the subcortical structures.

SVD affecting the deep and subcortical areas is usually sporadic and associated with individual cardiovascular risk factors, typically hypertension¹⁸⁻²³, hypercholesterolaemia¹⁸⁻²⁰, diabetes mellitus^{18,24,25} and smoking.^{18,20,22,23} Age is also a risk factor for SVD and there are robust associations between older age and the measurement of various radiological hallmarks of SVD described below; however, in later life not all patients show clinical or radiological signs of subcortical SVD and there is a rightly a philosophical question as to whether this should be considered part of *normal* ageing.²⁶ Despite its prevalence, the terminology describing this subtype of SVD has been somewhat inconsistently divided between descriptors of the aetiology (such as “hypertensive arteriopathy”) and histopathological findings (including “arteriosclerosis” and “lipohyalinosis”).¹⁰ None of these terms truly captures the breadth of vascular risk factor-mediated subcortical SVD; henceforth, for simplicity I refer to this form of SVD as sporadic SVD.

There are also monogenic forms of subcortical SVD such as congenital autosomal dominant arteriopathy with subcortical infarcts and leukoencephalopathy (CADASIL), which arises due to a cysteine-altering mutation in the *Notch3* gene. *Notch3* codes for a transmembrane receptor protein predominantly expressed in vascular smooth muscle cells.²⁷ In CADASIL, the loss or gain of a cysteine residue leads to an unpaired cysteine that is unable to make a disulphide bond and this disrupts the 3D architecture of the protein. CADASIL is the commonest inherited stroke syndrome with an estimated

prevalence of 1-2 per 100,000²⁸ (though mutations in the *Notch3* gene may be significantly more common and were discovered in around 1 in 450 out of over 200,000 participants in the UK Biobank cohort, a large prospective observational cohort study investigating a wide range of health outcomes in the UK²⁹) and is characterised by migraine with aura early in life, young stroke and early onset dementia.³⁰ Less common mutations that cause familial SVD syndromes include other genes involved in extracellular matrix maintenance such as *HTRA1* (either in an autosomal dominant fashion or in congenital autosomal recessive arteriopathy with subcortical infarcts and leukoencephalopathy; CARASIL) and *COL4A1*. Genetic forms of SVD affect younger patients and may also have differing pathologies, and so this thesis focuses on sporadic SVD alone except where otherwise specified when consideration of other subtypes is informative (figure 1.2).

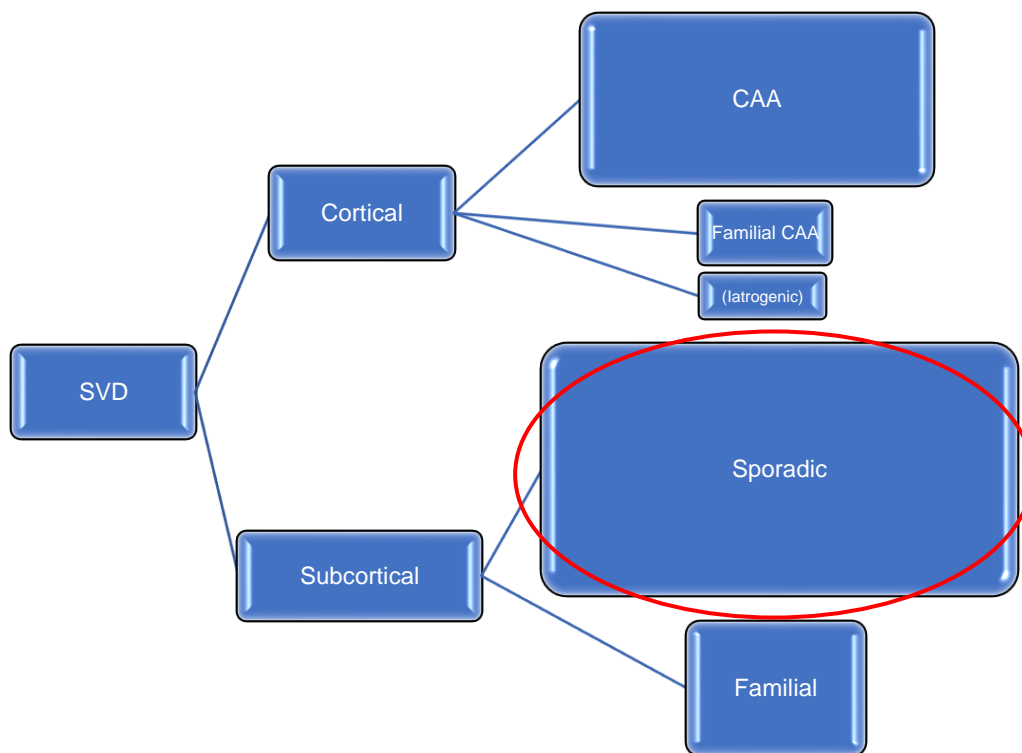


Figure 1.2. Classification of small vessel diseases. In reality, the picture is likely to be more complex as multiple pathologies can occur in parallel, particularly in the presence of cardiovascular risk factors.

Clinical features of sporadic SVD

The symptoms caused by SVD relate to the chronicity of small vessel occlusion and anatomical location; these range from sudden-onset stroke (hyperacutely) to long-term cognitive and psychiatric symptoms over many years.

Ischaemic stroke

SVD can manifest acutely when arterial or arteriolar occlusion leads to ischaemia; this is typically in vascular territories supplied by subcortical perforator vessels including the subcortical white matter (centrum semiovale, corona radiata, periventricular white matter and internal/external capsules), basal ganglia, thalamus, midbrain and brainstem. Clinically this causes a lacunar syndrome that typically presents as pure motor stroke, pure sensory stroke, sensorimotor stroke, ataxic hemiparesis or a “clumsy hand – dysarthria” syndrome depending on the anatomical location affected.³¹

A further manifestation of small vessel stroke is the capsular warning syndrome, a sequence of transient ischaemic attacks (TIAs) causing recurrent symptoms in keeping with the syndromes above that usually precede a subcortical stroke.³² Symptoms typically occur three to five times in a period of up to 72 hours and in around 50% of cases the area affected includes the internal capsule, for which it is named; however, other small vessel territories can be affected. This study also found that there was an eventual infarct visible on neuroimaging in 71.2% of patients; but the outcomes were favourable with a modified Rankin scale score of 0-1 after three years (corresponding to complete recovery or mild symptoms not affecting daily function) in around 80%. It may be that a diseased perforator vessel reaches a critical occlusive threshold with vascular supply alternately meeting or not meeting metabolic requirements; and this may provide some opportunity for neuronal compensation.³³

Vascular cognitive impairment and dementia

Cerebrovascular disease can cause a wide range of symptoms relating to several domains of thinking and memory, and forms a spectrum from VCI (where there is objective mild cognitive dysfunction and symptoms relating to it, but no significant

interruption to independent activities of daily life) to VaD, in which independent activities become progressively more difficult and patients require increasing levels of support.⁵ Diagnostic criteria broadly require two components:

- (1) objective evidence of cognitive dysfunction based on neuropsychological tests
- (2) supportive evidence from neuroimaging of cerebrovascular disease consistent with the symptoms

Robust clinical categorisations have been suggested by The American Heart Association / American Stroke Association³⁴ and the Vascular Impairment of Cognition Classification Consensus Study (VICCCS),³⁵ although other classifications exist and have largely been used as research tools.^{36,37} The American Heart Stroke Association criteria propose that VaD should be diagnosed based on deficits in cognition that significantly affect daily life, independent of physical symptoms arising from stroke and from any other medical issues including delirium, intoxication or medication side effects and affecting at least two of the following domains: executive function and attention, memory, language and visuospatial function. VCI is subdivided into four subtypes which include amnesic syndromes, amnesic syndromes with deficits in additional domains, non-amnesic symptoms in a single domain or non-amnesic symptoms in multiple domains.

Aetiologically, VCI and VaD can be caused by multiple infarcts, a single “strategic” infarct (for example in the medial temporal lobe or thalamus), mixed dementia (where there are overlapping vascular pathologies or additional conditions such as Alzheimer’s disease) or subcortical SVD. The latter is the most common cause of VCI/VaD^{1,38} and there is a specific pattern of cognitive impairment seen in sporadic SVD which is typified by early impairments in executive function and processing speed with preserved long-term memory.³⁹ The typical clinical picture of SVD-related VCI is a patient with long-term cardiovascular risk factors developing executive dysfunction with difficulties in concentration, attention and the ability to remember lists or perform multi-step tasks such as following a recipe.⁴⁰ Patients take longer to complete physical

and intellectual tasks that require concentration, and episodic and semantic memory remain intact. Language is not known to be affected in SVD though anecdotally many patients in our SVD research clinic describe hesitancy initiating speech. Longitudinal studies have characterised the progression of cognitive impairment in sporadic SVD with drop-off more evident in the domains that were most affected at baseline⁴¹; this cohort of patients with moderate to severe SVD is discussed further in chapter three.

Mood and motivation

Symptoms of mood are common in SVD and disease severity on MRI is known to be associated with the risk of depression.⁴² This has led to a proposed “vascular depression” model, in which vascular disease influences brain networks that mediate the development and progression of depression as distinct from conventional unipolar depression.⁴³

More recently, neuropsychiatric symptoms in SVD have been further divided into either low mood/depression or predominantly apathy, the loss of motivation and reduction in goal directed behaviour. One study measuring sub-scores of the Geriatric Depression Scale in patients with SVD found 15.8% showed evidence of apathy, compared to 11.8% with evidence of apathy and low mood, and only 1.0% showing evidence of isolated depression.⁴⁴ Apathy is thought to reflect global disruption of white matter networks rather than any specific brain region⁴⁵ and, interestingly, predicts incident dementia in longitudinal studies where depression alone does not.⁴⁶

Mobility, gait apraxia and vascular Parkinsonism

Sporadic SVD is known to be associated with declining mobility, which occur in the presence or absence of disability caused by lacunar stroke.⁴⁷ Several studies have assessed the relationship SVD burden and gait, and found there to be a significant negative correlation both with gait speed^{48,49} and certain gait parameters reflecting the coordination of walking such as cadence and step length.⁵⁰ Key anatomical locations that mediate this response include the pyramidal tract projections to the thalamus,

corpus callosum which is key for bilateral coordinated movements and the cerebellum.^{51,52}

Gait apraxia is a specific pathological motor pattern relating to the failure of movement initiation and motor planning.⁵³ Patients are unable to start walking, but can make accurate stepping movements when lying on their back; while upright, they can describe a feeling of falling backwards or of losing trunk control. The authors postulate that this particular gait disorder can be due to disruption of the subcortical white matter network around the supplementary motor area, which is a typical site for SVD pathology.

More general motor symptoms can arise in SVD and these can mimic the symptoms of Parkinson's disease (PD), a neurodegenerative condition characterised by bradykinesia, rigidity, and tremor in addition to systemic and neuropsychiatric symptoms. At three years after lacunar stroke, up to 33% of patients displayed one or more signs of Parkinsonism in one longitudinal study,⁵⁴ with 10% displaying a Parkinsonian syndrome. Key to differentiating the two conditions are the symmetry of symptom onset (PD is usually asymmetric at onset), absence of a tremor and the presence of cerebrovascular disease over a consistent time period with the onset of symptoms.⁵⁵ Patients with vascular Parkinsonism display a typical gait characterised by slow, short and shuffling steps and a marked inability to turn quickly (the *marche à petits pas*).⁵³

Neuroimaging hallmarks of SVD

Neuroimaging in patients with sporadic SVD is complex and reveals a number of characteristic lesions that can occur in isolation or in combination. These imaging features are important clinically for diagnosis and prognosis; they are equally important in research studies as they provide objective metrics of disease severity which can be used to determine aetiology, associations with risk factors, and in some cases, the outcome of interventional studies. Not all SVD lesions can be seen on computed

tomography (CT) scans, and so this thesis considers only evidence of SVD as visualised on MRI.

Key radiological hallmarks of SVD include lacunar infarcts (acutely as recent small subcortical infarcts and chronically as lacunes), white matter hyperintensity lesions (WMHs), cerebral microbleeds (CMBs), enlarged perivascular spaces (EPVSs), and cortical atrophy, consensus guidelines for the identification and reporting of which were provided by the STAndards for ReportIng Vascular changes on nEuroimaging (STRIVE) consortium⁵⁶, recently updated as STRIVE-2.⁵⁷ Figure 1.3 shows a sketched representation of the typical size, shape and location of these lesions which are described in turn below.

Of note, the resolution of neuroimaging has thus far precluded accurate assessment of the perforator vessels themselves *in vivo*, though the advent of higher field (7T) MRI means this is becoming technically possible.⁵⁸

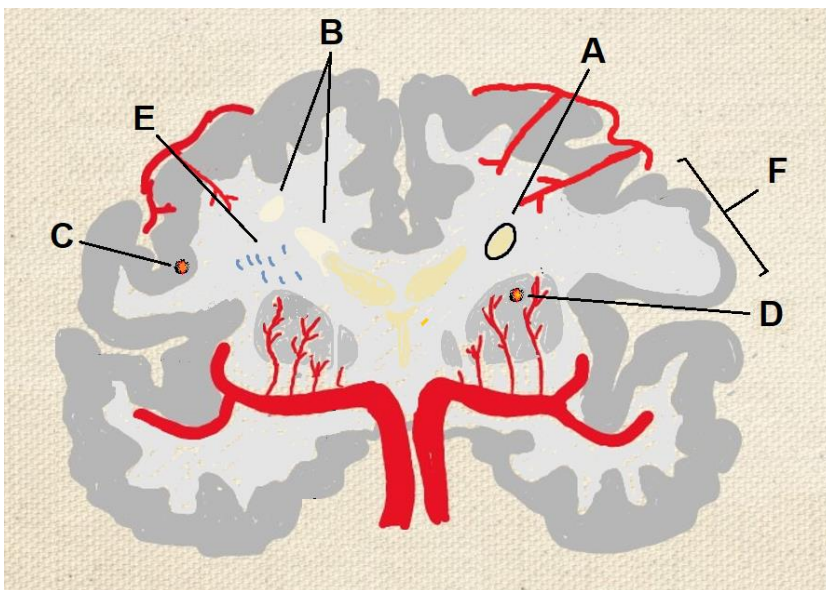


Figure 1.3. Sketch of cerebral circulation in coronal plane with diagrams of representative SVD lesions: (A) lacune; (B) deep and periventricular WMHs; (C) cortical CMB; (D) subcortical CMB; (E) EPVSs; (F) cortical atrophy

Lacunar infarcts

Small vessel disease strokes range from a diameter of 3-20mm (with some authors giving an upper limit of 15mm particularly in the chronic phase as the lesions generally

contract) and occur in subcortical areas typically in the territory of perforating arterioles; acutely they have high signal on diffusion weighted imaging (DWI) sequences and are termed recent small subcortical strokes. So-named because they often cavitate to form a “lake-like” area isointense with CSF, lacunar infarcts in the chronic phase show low signal on T1 images, high signal on T2 and low signal marked by a rim of high signal on FLAIR sequences. Not all acute subcortical infarcts progress to cavitation; estimates range for 61%⁵⁹ to 97%⁶⁰ after three months or longer. Lacunes arise in a continuum of shapes from round to elongated ovoid with little to complex extension into the third dimension, and usually in line with the afferent arteriole presumed to be supplying this anatomical region.⁶¹ They occur preferentially at the edge of areas of WMHs (see below)⁶² and this provides further evidence of their relationship with SVD.

Small subcortical infarcts can occur symptomatically causing syndromes as above, or asymptotically, most likely due to increasing distance from key white matter tracts involved in sensorimotor function.⁶³ In one population-based cohort study assessing participants aged 60-64, 7.8% were found to have at least one lacune on MRI scan.⁶⁴ Furthermore, 1.6% developed incident lacunes between baseline and a four year follow up appointment; asymptomatic lacunar infarcts form a significant part of the burden of covert / subclinical SVD⁶⁵ and are independently associated with deterioration in cognition in domains that are typically affected by SVD such as executive function and processing speed.⁶⁶ They are also associated with quality of life metrics, though part of this relationship is mediated by physical disability in the case of symptomatic lacunar stroke.⁶⁷

White matter hyperintensity lesions

White matter hyperintensity lesions (WMHs) are areas of high signal on T2 and FLAIR, thought to represent gliosis due to chronic low-grade ischaemia. They are a second key radiological hallmark of SVD⁶⁸ and independently predict stroke, dementia and all-cause mortality in longitudinal studies, as well as intracerebral haemorrhage risk and incidence of Alzheimer’s disease.⁶⁹

WMHs arise initially as isolated punctate lesions, typically in the periventricular and deep white matter, but with progressive disease severity can become clustered together (early confluent) and eventually coalesce.⁷⁰ Although in the early literature these were graded according to subjective visual scoring systems (e.g. the Fazekas scale⁷¹), they can also be measured volumetrically and this produces a continuous distribution of objective values which may be more informative both at assessing the relationship with risk factors and also measuring progression.⁷² Large multicentre studies still use visual rating systems although the improvement of automated WMH lesion marking may lead to volumetric analysis being used preferentially even in this context.

Several theories have been proposed as to what exactly the MRI signal change in WMH represents. The nature of the increased signal on T2 weighted MRI has led some authors to suggest that it represents oedema, perhaps as a response to tissue damage.⁷³ Pathological studies show axonal destruction and gliosis, suggesting that these are neurons that are irreversibly damaged, consistent with chronic hypoxic injury.⁷⁴ Demyelination and infiltration of microglial cells have also been observed, suggesting that these areas represent immune activation.⁷⁵ In any case, it is very challenging to draw direct radiological/pathological comparisons, principally because there can be a considerable time (up to even several decades) between WMHs arising and death. This means that MRI and post-mortem both provide a single timepoint assessment and there can be minimal inference about the progression (or improvement) of disease in the interim.⁷⁶ SVD severity and other comorbidities at time of death may overwrite any assessment of the disease process earlier in life. In addition, it can be difficult to co-register *in vivo* imaging to *ex vivo* histopathology samples.⁷⁷

Regardless of their macro- and micro-structural composition, WMHs are the commonest radiological sign of SVD and are nearly ubiquitous in the most severe clinical manifestation of SVD, vascular dementia;⁷⁶ despite this, the WMH volume and distribution is heterogeneous and lesions have variable clinical implications.⁷⁵ There is no consensus threshold that demarcates normal brain ageing from pathological SVD, though some authors have found that WMHs exert an effect on brain atrophy

(as a surrogate for biological ageing) that is distinct from chronological age.⁷⁸ Large scale population based cohort studies such as the UK Biobank will help to create normative population values.⁷⁹ WMH volumes from the first 45,000 participants in the UK Biobank are publicly available and give WMH volume as $5229.8\text{mm}^3 \pm 6883.4\text{mm}^3$ in an asymptomatic population with a mean age of 62 years (<https://biobank.ctsu.ox.ac.uk/crystal/refer.cgi?id=9028>).

There have been some suggestions that periventricular WMHs (pWMHs) may be distinct from deep WMHs (dWMHs) in the deep subcortical white matter, basal ganglia, thalamus and brainstem. Although the concordance between assessments of severity of dWMHs and pWMHs is high⁸⁰, the microvascular configuration is slightly different; dWMHs are supplied by longer penetrating arterioles and consequently subject to a slightly lower perfusion pressure, while pWMHs are supplied by shorted arterioles and are often more directly related to a large systemic artery.⁸¹ It has therefore been suggested that pWMHs are related more to hypertension and dWMHs are related more to hypoperfusion⁸², and this might be consistent with the anatomy of the blood supply, although several studies have shown correlation between dWMH burden and hypertension nevertheless.⁸³⁻⁸⁵ Additional evidence at least for a mechanistic difference is provided by genetic studies, which have elucidated differing genetic variants as a risk for dWMHs and pWMHs.⁸⁶ WMHs in these two areas may be associated with different clinical phenotypes; visual rating scales scores of pWMH correlated with cognitive impairment in the typical domains affected in patients with SVD⁸⁷ while dWMH volumes were associated with risk of depression.⁸⁸ Discrimination between the two categories can be difficult, particularly in severe disease when pWMH and dWMH lesions become confluent.

A recent development on the idea that WMHs are discrete lesions with a clearly demarcated border (as is typically visible on imaging) proposes that lesions exist on a continuum of microstructural damage, thus giving rise to the concept of a WMH penumbra that is potentially salvageable. This evidence is supported by findings that the FLAIR signal of surrounding normal appearing white matter (NAWM) is also

abnormal⁸⁹, as are DTI markers of white matter microstructural integrity such as fractional anisotropy (FA).⁹⁰ This study demonstrated that blood flow is reduced in proximity to WMHs and normalises in a stepwise manner with distance from the lesion⁹¹; however, it is not clear whether this phenomenon represents the cause of lesion formation or a response to decreased neuronal activity and even correlations established in a longitudinal follow may simple represent disease severity.⁹²

Some authors have developed this idea further and provide evidence that WMHs may regress over time, both in healthy community dwelling participants⁸⁹ and in patients with minor stroke⁹³; a recent pre-print review article found explicit mention of WMH reduction in around a third of all studies that measured WMH longitudinally (accounting for 4%-45% of participants).⁹⁴ These findings challenge the idea that WMHs represent irreversible tissue damage and might change the target for interventional studies (for example, whether trials should aim to reverse WMHs rather than slow progression). They might also have implications for the statistical analysis of such projects.

Cerebral microbleeds

Cerebral microbleeds (CMBs) are small signal voids that produce a blooming artefact 2-5mm in diameter on paramagnetic MRI sequences such as T2*-weighted gradient echo-based sequences or susceptibility weighted images/angiography (SWI/SWAN).⁶⁸ They are thought to represent deposition of haemosiderin following microvascular rupture.⁹⁵

CMBs occur in two principal distributions:

- (1) cortical – usually at the cortico-subcortical junction or deep grey matter
- (2) subcortical – typically in the white matter, basal ganglia, brainstem and cerebellum

Generally cortical CMBs are thought to arise in CAA due to pathology of the leptomenigeal and cortical vasculature, while subcortical CMBs are thought to be hypertensive and indicative of underlying vascular risk factors, particularly

hypertension.⁹⁶ In practice the picture is often unclear and individual patients may have both cortical and subcortical CMBs; however, the presence of exclusively cortical CMBs is indicative of CAA and is an important radiological component of the diagnostic criteria.⁹⁷ There is a robust association between CMBs and other small vessel disease markers in patients with presumed arteriolosclerosis, including WMHs and lacunes.⁹⁸

The extent of symptoms caused by CMBs remains unclear. In CAA, patients can experience temporary neurological symptoms which are usually positive (paraesthesia, limb jerking or positive visual phenomena), though they can be negative with loss of function. These transient focal neurological episodes can often be attributable to areas of haemosiderin deposition in a concordant anatomical location (most often convexity subarachnoid haemorrhage and superficial siderosis).⁹⁹ CMBs are also associated with impairment in long-term memory and executive function in community-based populations¹⁰⁰ and with impairment in the typical domains affected by SVD in patients with stroke¹⁰¹ and specifically lacunar stroke.¹⁰² These associations with impairment in varying cognitive domains depending on the population tested and the likely predominance of Alzheimer's disease pathology compared to SVD suggest that CMBs may be an overall marker of disease severity rather than causative of any specific dysfunction individually. The anatomical distribution may suggest aetiology, and hence other associated symptoms.¹⁰³

Enlarged perivascular spaces

Perivascular spaces (PVSs; formerly known as Virchow-Robin spaces) are small fluid-filled areas in the extracellular interstitium that run parallel to arterioles, capillaries and venules within the brain. While generally microscopic, they can become dilated and visible on MRI scans with high signal on T2-weighted sequences and low signal on T1-weighted and FLAIR sequences, and this finding is thought to be a further radiological hallmark of SVD.⁶⁸ It can be difficult to distinguish enlarged PVSs (EPVSs) from small lacunes, even on multimodal imaging; accordingly the STRIVE

consortium recommended a threshold of <3mm to define lesions as PVSs rather than lacunes.

EPVSs are seen in typical locations within the brain including centrum semiovale running towards the ventricles, basal ganglia and internal capsule, the base of the brain and parts of the posterior circulation territory including the hippocampus, midbrain, brainstem, and cerebellum.¹⁰⁴ Some authors have reported an association with ageing independent of SVD and vascular risk factors¹⁰⁵ while others have not found this association to be significant¹⁰⁶; however, there is clear relationship with severity of SVD that has been demonstrated in several studies¹⁰⁶⁻¹⁰⁸ and EPVSs may predict anticoagulant-related intracranial haemorrhage in some populations.¹⁰⁹

The role of PVSs and the process that leads to PVS enlargement have not been fully elucidated. They are thought to facilitate drainage of fluid and soluble molecules via a paravascular route, and this hypothesis has been supported by experimental labelling of large molecules subsequently detected in the PVS.^{110,111} However this idea is controversial and others have calculated that perivascular flow of water and solutes is implausible due to the high force and low resistance that would be needed.¹¹² Other theories include that PVSs facilitate the mixing of peri-arteriolar and peri-venular circulation and the transport of substances by convection.¹¹³ In parallel with these competing suggestions for PVS function, the mechanism of PVS enlargement in disease is also unclear: this may be due to arteriolar stiffening typically seen in hypertension or alternatively the aggregation of protein, particularly β -amyloid.¹¹⁴

EPVSs do not cause focal symptoms and different authors have found slightly different associations with cognitive performance. Some studies have found a significant relationship between number of EPVSs and cognitive impairment, measured using total brain EPVSs in neurologically normal participants with cardiovascular risk factors¹¹⁵ or basal ganglia EPVSs in patients with minor stroke or TIA¹¹⁶; however, others have found there to be no association using visual rating scales in stroke patients¹¹⁷ or volumetric measurements in patients with moderate to severe

symptomatic SVD.¹⁰⁶ It may be that they are an early hallmark in mild disease in which they represent the underlying burden of SVD, but that in advanced disease they cease to become the most important radiological predictor of severity. Additionally, the measurement of EPVSs is challenging as they are small and there can be hundreds or thousands of lesions; heterogeneity in the techniques used to assess their effect on cognitive profiles may be responsible for these varying findings and this question remains unresolved.

Lacunar infarcts, WMHs, CMBs and EPVSs make up the four key focal radiological hallmarks of SVD. A comparison of these lesions is shown in figure 1.4.

Cerebral atrophy

Cerebral atrophy is a common feature of neurological and neurodegenerative diseases and brain volume can reduce either generally (which is a non-specific finding) or focally in a specific location linked with a particular condition (for example and most commonly, medial temporal lobe atrophy in Alzheimer's disease¹¹⁸). Atrophy may represent neuronal loss, thinning of the cortex, contraction of the white matter or secondary neurodegeneration⁶⁸ and is known to be associated both with other markers of SVD¹¹⁹⁻¹²¹ and with impairment in cognitive domains that it typically affects.^{39,122} Anatomically-specific relationships have been found both between WMHs and areas of cortical atrophy⁷⁸ and subcortical infarcts and regional volume loss¹²³, suggesting that although atrophy is non-specific, it has a relevant association with SVD burden.

One consideration in the radiological assessment of SVD is the association between brain atrophy and other hallmarks of SVD. It is possible that atrophy of the surrounding cortex can distort other lesions or make them appear relatively more prominent; this relationship has not been formally tested.

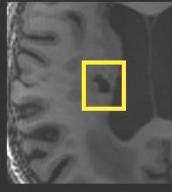
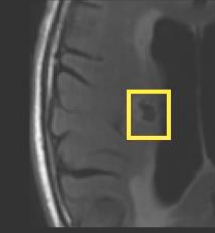
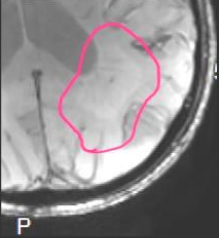
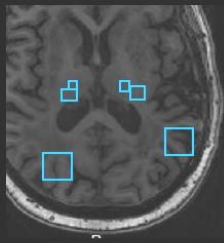
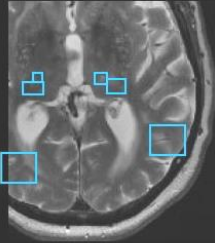
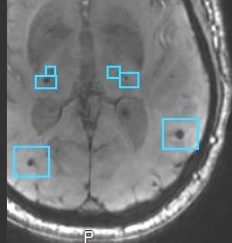
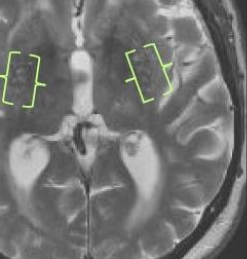
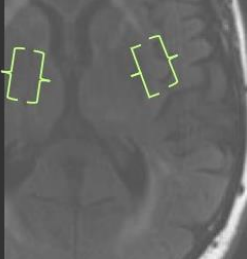
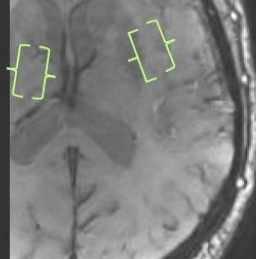
	T1	T2	FLAIR	SWAN
Lacunar infarct (chronic phase)				
White matter hyperintensities				
Cerebral microbleeds				
Enlarged perivascular spaces				

Figure 1.4. Appearance of typical SVD-related lesions on T1-weighted, T2-weighted, FLAIR and SWAN images. In the acute phase, recent subcortical infarcts appear bright on DWI (*not shown*). In the chronic phase these can cavitate and become lacunar infarcts, typically showing a hyperintense rim on FLAIR sequences with internal signal isointense to CSF. WMHs are typically bright on T2 and FLAIR sequences and can be isointense with surrounding brain on T1 or, as shown here, slightly hypointense. The signal within the lesion is not usually as low as that within a cavitated lacunar infarct. CMBs are hypointense on SWAN sequences and display a ‘blooming’ artefact; these can be difficult to appreciate on other sequences and are not clearly seen in this patient. EPVSs are best seen as streaks of high signal on T2 images, and can be hypointense on T1 images or FLAIR (particularly if present within a WMH).

Multifocal and novel imaging markers

In addition to the specific focal lesions above that are associated with SVD, generalised measurements of white matter microstructure can be used to assess disease severity. This provides as meaningful outcome measure as SVD is known to be a whole-brain disease with abnormalities of vessel structure and function quite remote from MRI-visible focal lesions.¹²⁴ White matter integrity can be quantified using diffusion tensor imaging (DTI). DTI is based on diffusion weighted imaging (DWI), a technique in which a pair of magnetic diffusion gradient pulses are applied during a spin-echo sequence to enhance signal from diffusing protons and suppress signal from stationary protons. DTI models the DWI signal as a 3D ellipsoid (the ‘tensor’) and from this can be calculated several scalar parameters:

- (1) the magnitude of diffusion, averaged in three dimensions (mean diffusivity; MD)
- (2) the proportion of diffusion along the lead axis compared to the two other planes (fractional anisotropy; FA, ranging from 0 in unconstrained isotropic diffusion to 1 in diffusion constrained exclusively to the lead axis)
- (3) the diffusion parallel to white matter tracts (axial diffusivity; AD)
- (4) the diffusion perpendicular to white matter tracts (radial diffusivity; RD)

These parameters are obtained for each voxel or can be averaged across an anatomical region, tissue class or the whole brain. Further metrics can be derived from the features of histograms of these values either across tissue class or the whole brain, and there is some uncertainty as to which of these metrics provides the most accurate assessment of SVD-related structural damage.¹²⁵ MD increases and FA decreases in microstructural disease.¹²⁶ Of the DTI parameters, these two measurements have provided the most consistent associations with cognitive performance^{127,128} and with WMH severity.¹²⁹ One study in patients with SVD¹³⁰ provides evidence that median FA and normalised peak height MD (MDPH; calculated from the histogram and negatively correlated with disease severity) have the most reliable relationship with cognition in multicentre studies. This has been taken further in a recent analysis that

compared six completed cohort studies with varying degrees of SVD burden; median FA and MDPH were significant predictors of dementia in all six cohorts, though median MD had the strongest association in this study.¹³¹

A further marker of SVD are cortical microinfarcts. Post-mortem histology often reveals very small areas of infarction (in the range of 0.2-1.0mm), sometimes in their hundreds or thousands; these are typically not seen on MRI at field strengths up to 1.5T¹³², but if large enough can be seen in the acute phase on DWI sequences at 3T and are considerably clearer at 7T.¹³³ Microinfarcts are known to occur in large artery disease where they are presumed to be embolic¹³⁴, and Alzheimer's disease^{135,136}; however, mounting evidence suggests that they are associated with SVD burden independent of other neurological conditions¹³⁷⁻¹³⁹ and that risk of histopathological features of Alzheimer's disease and radiological evidence of SVD combine in a non-linear fashion.¹⁴⁰ Caution should be taken however in interpreting DWI lesions of under 2mm diameter as microinfarcts or as a marker of SVD; in one large cohort study of over 2000 patients, DWI-positive lesions of this size appeared in 1.5% of participants and over 4.7 years of follow-up only 5.9% evolved into clearly defined microinfarcts.¹³⁷ Further evidence on the evolution of such lesions is provided by the RUN DMC-INTENSE study, a cohort of 54 participants known to have moderately severe and progressive SVD based on assessment of WMHs. In this cohort who had monthly MRI scans for ten months, the incidence of DWI lesions <2mm was 35%, and all lesions disappeared throughout the study follow-up.¹⁴¹

Novel imaging markers continue to emerge and may provide additional information both towards the assessment of disease severity and towards understanding the pathophysiological mechanism of SVD. These include the use of susceptibility-weighted sequences to identify clusters of multiple co-located perforator vessels, seen in around a third of patients with SVD in one study¹⁴² (and over two thirds of patients with CADASIL). The vessel-cluster sign was associated with other markers of disease severity including lacunes and WMH volume, and where present tended to occur in areas of WMH that were non- or partially cavitated, suggesting that these vessels may

be maximally dilated to maintain perfusion to tissue that is on the point of becoming irreversibly damaged.

Pathophysiology of SVD

The macropathological consequences of SVD are reasonably well defined, and the link between small vessel dysfunction and the clinico-radiological features above is secure. SVD has generally been thought of as the endpoint of various cardiovascular risk factors, leading to haemodynamic disturbance in the network of small vessels, direct impairment of function, and ischaemia. In this section I review the evidence for these associations, summarise the knowledge gained in pathological studies and discuss more novel pathogenic mechanisms that might have a role in the development and progression of SVD.

Classical hypothesis and cerebrovascular risk factors

The conventional understanding of SVD pathophysiology is that arterioles and venules become damaged in the context of typical cardiovascular risk factors, leading to intrinsic damage of the vessel walls which progresses over time.

Histopathological studies have also provided evidence that these processes may be relevant. The first post-mortem examinations of lacunar stroke patients were performed by Ferrand in the early 20th Century¹⁴³ and included some 88 patients, but it was not until 60 years later that a much larger pathological study became available.¹⁴⁴ This study was performed by Miller Fisher and included over 1000 elderly patients, around 10% of whom were found to have multiple lacunes and all but one of whom had evidence of intracranial atheroma, mainly in larger vessels proximal to the area of infarction but occasionally in smaller perforating arterioles leading directly to the infarct.

Miller Fisher went on to describe histopathological changes in the arterioles which he initially termed ‘segmental arterial disorganisation’ due to breakdown of the vessel wall, infiltration of connective tissue causing luminal narrowing.¹⁴⁵ This was

subsequently divided into predominantly fibrinous ('arteriosclerosis') and predominantly collagenous with lipid-containing macrophages ('lipohyalinosis') and was felt most likely to be a consequence of hypertension.¹⁴⁶ These findings suggest that the risk factors that contribute to atheromatous disease elsewhere in the body (such as coronary artery disease) may be relevant in SVD. Rarely, other histological patterns have been described: some authors describe evidence of partial and circumferential necrosis in the walls of damaged vessels ('fibrinoid necrosis') in a Japanese population with unselected cerebrovascular disease.¹⁴⁷ This is less obviously related to conventional cardiovascular risk factors albeit in a cohort that may have exhibited somewhat different pathophysiological mechanisms than Miller Fisher's original cohort.

A sketched diagram of how these histological patterns typically appear is given in figure 1.5. Although samples such as these provide evidence of the disease processes that occur in SVD, they are limited by the fact that post-mortem samples are usually taken some time after the stroke itself (lacunar stroke is rarely fatal and there can be considerable delays of up to decades between lesion formation and post-mortem¹⁴⁸).

Whether these pathological features represent distinct subtypes of sporadic SVD is unclear; an attractive hypothesis is that hypertension mediates a predominantly arteriosclerotic/lipohyalinotic picture while hypercholesterolaemia drives microatheromatous disease, but histological findings do not segregate neatly into these subtypes¹⁴⁹ and radiological correlates are not easily separable.⁶⁸

In addition to the chronic features of SVD detailed above, pathological changes underpinning acute lacunar infarcts has not yet been fully characterised, and proposed mechanisms include embolism from unstable atherosclerotic plaques in a proximal intracranial vessel and the sudden loss of flow in a vessel lumen that has already become pathologically narrowed.^{1,144} Intraluminal thrombus was not seen in any of Miller Fisher's cases¹⁴⁵, though it is unclear how long the interval between stroke and post-mortem was, and how long we should expect a thrombus to remain visible.

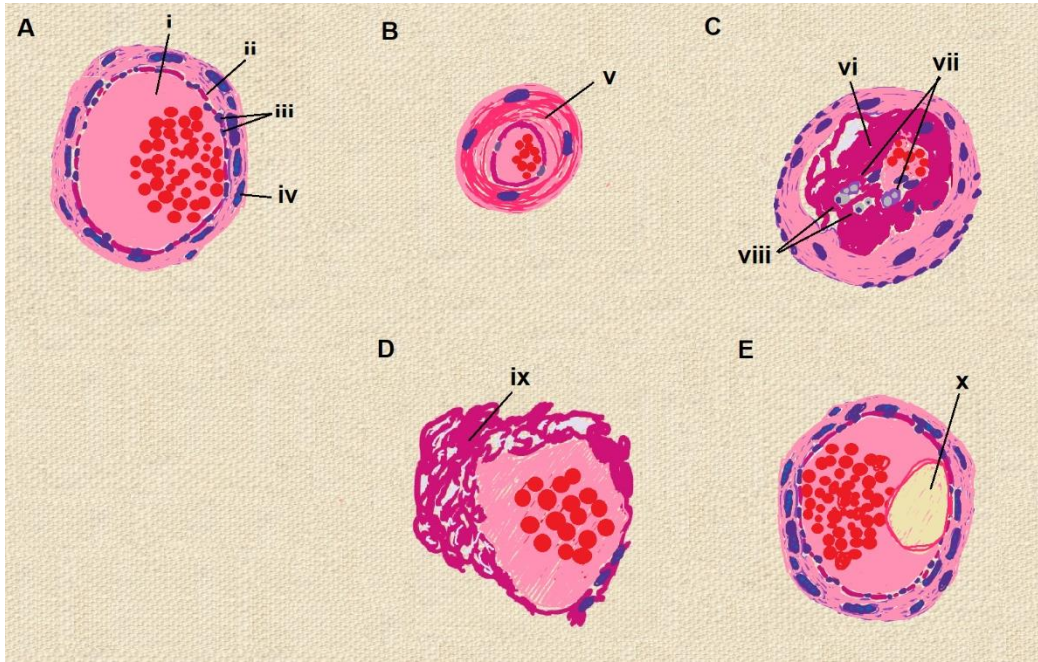


Figure 1.5. Sketch of histopathological features of SVD as they appear on post-mortem examination, typically stained with haematoxylin and eosin and represented as cross-section. (A) healthy arteriole including (i) lumen; (ii) basement membrane; (iii) endothelial cells; (iv) vascular smooth muscle cells. (B) arteriolosclerosis with (v) infiltration of fibrinous material markedly compressing lumen; (C) lipohyalinosis with (vi) infiltration of collagenous material; (vii) lipid-containing “foamy” macrophages and (viii) co-localising lymphocytes. (D) fibrinoid necrosis with degradation of the basement membrane and (ix) partially circumferential infiltration of fibrinous material (E) microatheroma in a vessel with (x) lipid plaque partially occluding lumen.

Intuitively, impairment of the afferent vascular supply might cause progressive ischaemia in an arteriolar territory, leading to oxidative or metabolic stress in that area. Neuroimaging resolution is not generally good enough to visualise cerebral perforator vessels directly, so the hypothesis that cerebral blood flow (CBF) is associated with SVD severity and progression has been investigated indirectly in several ways, typically using WMHs as a representative marker.^{82,150}

Non-invasive proxy measurements of CBF can be made using MRI techniques such as arterial spin labelling (ASL), in which a radiofrequency pulse is used to label blood in one slice and an image is acquired in a distal slice once the blood has circulated. ASL-derived CBF measurement is significantly lower in patients with SVD than control participants and correlates with cognitive function.¹⁵¹

Alternative methods to estimate CBF include assessment of the stiffness of the carotid arteries, including in one large prospective cohort study of patients with arterial disease.¹⁵² The authors found that this metric did not explain progression of WMHs, though the population was heterogeneous and there was no subgroup analysis assessing subjects with higher lesion burden at baseline. Transcranial doppler ultrasound can also be used to measure the resistance index along the middle cerebral artery and this was associated with linear change in semi-automatically measured WMH volume over 38 months ($r = 0.328$, $p < 0.001$) in one study.¹⁵³ This is likely to be a more accurate non-invasive proxy for flow in cerebral small vessels.¹⁵⁴

Specialist MRI techniques can also be used to assess CBF. One study¹⁵⁵ used dynamic contrast susceptibility-weighted MRI to calculate CBF in NAWM and found an odds ratio of 0.64 (per additional 1ml/100g brain tissue/min) for the development of new WMHs (95% CI 0.62-0.67, $p < 0.001$). Another study⁸² used phase contrast MR angiography to calculate CBF from carotid and basilar flow and did not show an association with WMH progression measured using an in-house probabilistic segmentation algorithm. Other authors have employed arterial spin labelling,¹⁵⁶ a non-invasive technique in which a frame of blood is magnetically tagged prior to transit into the tissue of interest, and showed that in the first five layers of voxels adjacent to lesions, there was a significantly lower flow in those that became WMHs at 18 month follow up than those voxels that remained NAWM. However, WMH voxels may have been under-estimated due to a histogram threshold-based method of defining WMHs at baseline and follow-up scans. These studies are summarised in a comprehensive review¹⁵⁷, which notes the potential for reverse causation that would follow if lesioned areas require less blood flow.

A final notion is that impairment of efferent fluid transport rather than afferent supply is responsible for the damage seen in SVD. Pathological studies have also shown involvement of venules¹⁵⁸ with endothelial abnormalities, collagen infiltration and venular tortuosity that has since been recapitulated using 7T MRI.¹⁵⁹ Tissue damage might also occur secondary to impaired drainage of toxins or reactive oxygen species

in the CSF either via the basement membrane of arterial walls, EPVSS, or recently described glia-lymphatic (“glymphatic”) channels¹⁰⁵. While there is indirect evidence for the role of CSF drainage in the progression of SVD (for example, increased levels of β -amyloid presumed due to impairment of clearance¹⁶⁰), and supportive animal models¹⁶¹, this phenomenon has not yet been demonstrated *in vivo* and is therefore some way from becoming a realistic outcome measure or therapeutic target.

This body of evidence detailing the role of cardiovascular risk factors and haemodynamic compromise in SVD is supported by large scale clinical studies, which provide information on the role of hypertension^{21,162,163}, hypercholesterolaemia^{164,165}, diabetes mellitus^{25,107} and smoking status.^{20,22} However, modification of these risk factors (for example treatment with perindopril¹⁶⁶, an antihypertensive, or pravastatin¹⁶⁷, a cholesterol-lowering drug) have had limited success in clinical trials to slow the progression of SVD as measured by WMH burden. This raises the possibility that while cardiovascular parameters are important for the incidence of WMHs in SVD, they are less crucial for progression which might be mediated by a second ‘hit.’

Other possible mechanisms might underlie this second ‘hit’ or provide parallel pathways through which SVD can occur include genetic factors, the neuroinflammatory response, alterations of the blood-brain barrier and also neurodegenerative processes, including the interaction between SVD and Alzheimer’s disease. These are summarised below in turn.

Genetic factors

A number of genes that might potentially contribute to the progression of SVD have been evaluated. Principal amongst these is *ApoE*, discussed above with reference to CAA where its role is most clearly significant; however, recent evidence has suggested that the $\epsilon 4$ allele specifically might directly affect the ability of cerebral white matter

to respond to ischaemia¹⁶⁸ and this has been proposed as a relevant disease mechanism in sporadic/vascular risk factor mediated SVD.

An association was found between the *ApoE* genotype and both baseline WMH volume and lesion progression rates in a large multicentre population study¹²⁰; smaller studies have shown that progression is more likely in *ApoE* $\epsilon 4$ carriers¹⁶⁹ and interestingly, that a measurable effect of diabetes on lesion growth was mediated by participants' *ApoE* genotype.¹⁷⁰ However, other authors have found no effect on the progression of WMHs outside populations with CAA.⁶ The $\epsilon 4$ allele has been shown to correlate with altered DTI parameters¹⁷¹; this was in a community-based population with relatively mild disease burden and therefore imaging might have been performed an earlier point in the disease process.

Genome wide association studies (GWAS) based on whole genome sequencing of large population-based cohorts have emerged as a useful tool assess genetic influence.¹⁷² This type of study can identify polymorphisms that contribute to small increased lifetime risks of conditions (as opposed to conventional Mendelian inheritance patterns)¹⁷³, typically explaining a few percent of the variability of the condition under investigation. GWAS studies have been applied to lacunar stroke^{174,175}, revealing 12 single nucleotide polymorphisms (SNPs) across five loci are that significantly associated with MRI-confirmed lacunar stroke and estimating the genetic contribution to lacunar stroke risk to be 6.5-8.1%. These genetic loci are associated with vascular extracellular matrix (ECM), differentiation of the blood-brain barrier (BBB), TGF- β signalling and myelination, suggesting an additional set of pathophysiological mechanisms that may be relevant.

GWAS studies have also been applied to WMH prevalence^{176,177}, and to DTI markers of white matter damage¹⁷⁸ revealing a number of SNPS with modest but statistically significant effect. The SNPS identified occur in genes that have broadly similar functions to those carrying genetic risk for lacunar infarcts, particularly in the ECM; however there are additional components that suggest the immune system has a role

in ischaemic white matter damage including several significant loci on the human leucocyte antigen (HLA) region on chromosome 6. Analogous GWAS studies for CMBs demonstrate associations only within the *ApoE* gene, as expected¹⁷⁹; studies investigating the genetic basis of EPVSs are at an earlier stage¹⁸⁰ and pre-print results indicate further significant results in SNPs implicated in ECM maintenance, but also endothelial cell development.

Neurodegeneration and the relationship between SVD and Alzheimer's disease

Multiple lines of observational evidence have linked SVD with measures of neurodegeneration. It seems plausible that a neurodegenerative process could have differential effects in the white matter and elsewhere in the brain (for example atrophy in grey matter, which has a collateral blood supply and might respond differently to ischaemia). There may also be a degree of Wallerian degeneration, though this has proven difficult to demonstrate experimentally.¹²⁷

Alzheimer's disease (AD) is a neurodegenerative condition characterised by accumulation of β -amyloid plaques and intracellular tau tangles. It causes a progressive amnesic and behavioural syndrome and is the commonest cause of dementia.¹⁸¹ The overlap between SVD and AD is potentially significant. There are risk factors in common, for example age and ApoE genotype, and the symptoms can be difficult to distinguish, potentially resulting in clinical dilemma (whether treatment should focus on cardiovascular risk optimisation or include acetyl cholinesterase inhibitors, which can have cardiac side effects) or having implications for the reliability of research results.

There is a bilateral interaction between the two conditions. Markers of endothelial activation in CSF such as ICAM-1 and VCAM-1 have been shown to predict the development of AD¹⁸², SVD burden accelerates the symptoms of AD⁶ and post-mortem studies have shown a significantly greater burden of cerebrovascular lesions in AD compared to other neurodegenerative conditions.¹⁸³ Of note, the latter study found

that AD patients with cerebrovascular lesions were likely to be younger and have less severe β -amyloid deposition, suggesting that in some way vascular disease may potentiate the effect of β -amyloid in AD. Conversely, AD pathology has also been linked to worsening markers of SVD; studies have shown that AD patients show faster progression of WMHs than in Lewy Body Dementia or Parkinson's Disease¹⁸⁴, and to healthy controls¹⁸⁵, and genetically determined risk of AD was associated with more severe WMH load in a cohort of cognitively normal midlife participants.¹⁸⁶ In many of these studies linking determining cause and effect is challenging, and there may be additional confounding factors that mediate the association between AD and SVD – particularly CAA, which is both a form of SVD and indicative of a β -amyloid burden that might be accompanied by the risk of AD.¹³

Blood-brain barrier permeability

Dysfunction of the blood-brain barrier (BBB) is another disease mechanism that has emerged as a novel pathological process relevant to SVD.¹⁸⁷ The BBB is a network of cells and ECM that surrounds capillary endothelium in the brain, regulates influx and efflux of molecules and cells into parenchyma and by doing so maintains the homeostasis of the delicate neuronal environment.¹⁸⁸ It comprises capillary endothelial cells, linked by “tight junctions” formed of protein complexes that occlude the usual paracellular transport of fluid and small molecules, pericytes that contribute to and maintain the ECM and astrocytes, differentiated glial cells that provide structure and nutrition to neurons, regulate extracellular ion concentration, modulate the neural response to injury and repair, and contribute to neuronal signalling.^{189,190} Microglia, resident immune cells in the brain parenchyma, are also found in close proximity to the BBB and can support tissue repair and metabolism in addition to their role in inflammation.¹⁹¹ Figure 1.6 shows a schematic representation of the structure of the BBB.

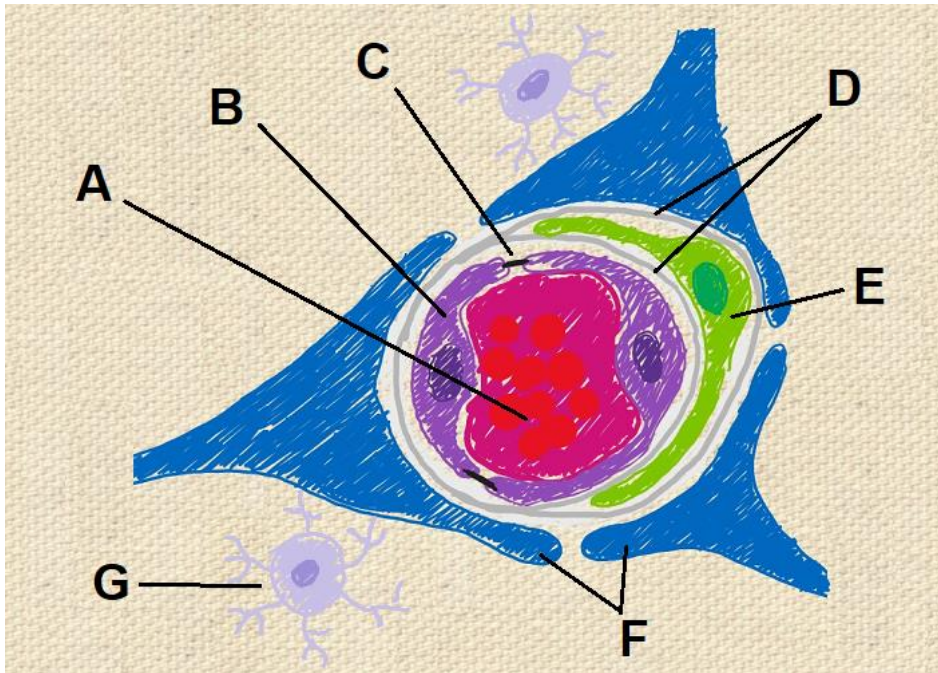


Figure 1.6. Sketch of the structure of the BBB, including (A) capillary lumen; (B) endothelial cell; (C) tight junctions between capillary cells; (D) basement membrane; (E) pericyte; (F) astrocytic foot processes (connections with other parenchymal cells not shown); (G) microglia

The BBB becomes more permeable in ageing, exhibiting altered pericyte morphology, loosening of tight junctions and structural changes in both the basement membrane and the ECM.¹⁹² It has also been suggested as an early marker of cognitive dysfunction independent of cardiovascular risk factors or biochemical markers of Alzheimer's disease.¹⁹³ Alongside these key relationships, BBB alterations have been investigated as a possible additional disease process in SVD.

Early studies assessing BBB function in SVD focused on post-mortem samples, and several molecules have been tested as a proxy for BBB leakage, with unclear overall results. Some authors have stained for immunoglobulins and fibrinogen, molecules that are thought to remain intravascular if the BBB is intact; increased parenchymal deposition was shown in patients with symptomatic cerebrovascular disease¹⁹⁴ and asymptomatic older adults with MRI evidence of WMHs.¹⁹⁵ However, a subsequent larger study did not demonstrate a significant relationship.¹⁹⁶ The authors of the latter study propose that these discrepancies may be methodological, as they targeted their histological analysis only to white matter areas that were macroscopically abnormal,

or simply because BBB dysfunction is common over a range of conditions in older adults. Other authors have tested alternative markers of BBB leakage, and found that albumin extravasation was increased around WMHs, though staining for tight junction proteins themselves was inconclusive as these were present in the healthy and diseased parenchyma of both patients and healthy control participants.¹⁹⁷ More recently transcriptomic studies have identified alterations in leukocyte gene expression related to WMH severity, principally in pathways related to extracellular matrix degradation and endothelial activation.¹⁹⁸

Further to these conflicting results from structural studies, functional studies have provided clearer data on the relationship between BBB function and SVD. The CSF/serum albumin ratio (or albumin quotient, Q_{alb}) has been suggested as the gold standard assessment of BBB function, and increases with BBB permeability as albumin can leak through tight junction deficiencies. This ratio has been found to be increased in a cohort of patients with symptomatic SVD (lacunar stroke or VCI/VaD)¹⁹⁹, patients with vascular risk factors in a mixed dementia cohort²⁰⁰ and a cohort explicitly with subcortical VaD.²⁰¹ Proving that this association is causative is challenging and this finding may simply reflect a response to tissue damage; these concerns might be addressed in subsequent longitudinal studies to test whether this metric predicts disease progression. To our knowledge, only two studies have assessed this. Bowman et al.²⁰² found no correlation between Q_{alb} and WMH volume change in 36 patients, albeit from a memory clinic population selected to minimise vascular pathology, and Jonsson et al.²⁰³ found that Q_{alb} was positively but not significantly correlated with WMH progression on a subjective visual rating scale in 53 patients with WMHs.

Other markers of BBB function have also been tested in longitudinal studies. One study²⁰⁴ measured extracellular vesicle proteins in the CSF (including Cystatin C and CD14) as a representative measure of BBB integrity and found a significant association with lesion progression, though with a small effect size. A similar association has been shown with Cystatin C in the blood.²⁰⁵

A limitation of these functional measurements of BBB integrity is that a single value predictor offers no geographically specific information about what is happening in a given anatomical location or tissue class. Hence, imaging techniques have been developed to allow quantify BBB permeability, using the administration of gadolinium-based contrast agents which ordinarily would not cross the BBB, but which enhance the T1 image signal and shorten the T1 relaxation time in parenchyma that they reach. This is termed dynamic contrast enhanced MRI (DCE-MRI).

Initial DCE-MRI studies measured the T1 signal enhancement after gadolinium administration and calculated the area under curve (AUC) for this signal across grey matter, white matter and WMHs.²⁰⁶ This study found that the AUC was positively correlated with WMH volume, in a cohort with severe sporadic SVD. A similar study in stroke patients used linear modelling of the associations between risk factors, SVD severity and the time course of T1 signal enhancement in these tissue classes²⁰⁷; patients with lacunar compared to cortical strokes were found to have higher BBB permeability in the NAWM as measured using this method.

DCE-MRI has been further developed by the application of more sophisticated pharmacokinetic modelling techniques. These include the two-compartment model, in which interstitium and plasma are explicitly modelled as separate compartments accounting for bidirectional movement of tracer between compartments and luminal flow, the Tofts model where plasma flow is assumed to be infinite, the modified Tofts model which incorporates a vascular binding component, and the Patlak model in which flow is assumed to be unidirectional out of the vascular space. Figure 1.7 shows these models graphically and gives the formula(e) used for calculation. These models have been compared using simulation and real world DCE-MRI data and these studies concluded that the Patlak model is most appropriate for low permeability data such as SVD in the chronic stage.^{208,209}

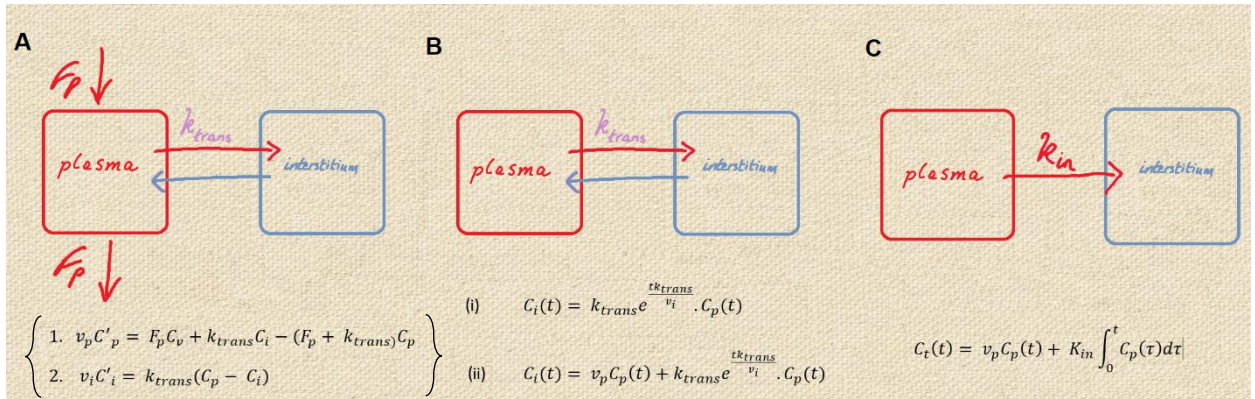


Figure 1.7. Schematic representations of kinetic models of BBB permeability. (A) standard two compartment model. Blood flows through the plasma space at rate F_p , and the tracer moves into the interstitium and back via competing processes that reach an equilibrium with rate k_{trans} . The model is described by the pair of equations (1) and (2) where v_p = plasma volume, C_p = plasma concentration, v_i = interstitial volume and C_i = interstitial concentration. (B) Tofts model. Plasma and interstitium form two compartments with no plasma flow. The standard model is described in (i) where $C_i(t)$ = interstitial concentration time series and $C_p(t)$ = plasma concentration time series. The extended Tofts model is described in (ii) and includes an additional term to account for plasma binding ($v_p * C_p(t)$). (C) Patlak model. Flow is unidirectional from plasma to interstitial compartment at rate k_{in} , with the inclusion of a vascular binding compartment.

Application of the Patlak model to DCE-MRI images has been used in several studies to investigate the relationship between the BBB and markers of SVD; these have found increased permeability in the NAWM of patients with lacunar compared to cortical strokes²¹⁰, in the white matter, WMHs and cortical grey matter of stroke-free individuals with higher scores on a compound SVD feature severity scale²¹¹ and that EPVSs in the basal ganglia are associated with increased BBB permeability.²¹² More informative results might be found by assessing ‘hotspots’ of BBB permeability (clusters of voxels where the permeability is above the 95th percentile of age-matched controls); this approach yielded results showing the permeability to be higher in NAWM than WMHs and that discriminated patients from controls very accurately.²¹³

The Patlak model has also been applied longitudinally to assess the role of the BBB in SVD progression. One such study²¹⁴ examined patients with Binswanger’s disease (defined as a severe form of SVD characterised by inflammation/demyelination and relatively quick progression to dementia). The authors found that while BBB

permeability was increased in this cohort, the signal was noisy and there was little overlap between areas of increased permeability on successive scans. Notably, they did find that areas of high permeability were located at the edge of WMHs or adjacent NAWM, and this supports the idea that WMH progression is a continuum with surrounding microscopically abnormal but potentially salvageable tissue. However, high permeability in voxels was not a statistically significant predictor of WMH development during the interscan interval.

Similar results have been described in a cohort of patients with mild/non-disabling stroke,²¹⁰ and showed a statistically significant correlation between voxels of increased BBB permeability and distance from WMH. Permeability was nevertheless not a significant predictor of incident WMH voxels at one year follow-up (though it did significantly predict cognitive decline). It is possible that BBB permeability is an effect of tissue damage rather than a predisposing factor but these studies do at least suggest that the increased permeability predates visible lesions.

Neuroinflammation and the peripheral immune response

Inflammation is a highly topical process in cardiovascular/cerebrovascular disease and emerging research suggests that it has a role in SVD. This evidence is largely circumstantial and derived from both pathology studies and inflammatory biomarkers. Post-mortem samples are associated with all the limitations discussed above, but nevertheless show inflammatory cells in the white matter around blood vessels and in the vicinity of demyelination.⁷⁵ Immune cells identified around vascular lesions are typically microglia, resident tissue phagocytic cells from the myeloid cell line. These have been further subtyped using immunohistochemistry²¹⁵; this study found differential microglial phenotypes in pWMHs compared to dWMHs and suggested there may be different triggers for this inflammatory activity. More recently the authors have also shown that microglial signatures vary widely even within anatomical regions and are associated with differential patterns of astrocyte recruitment.²¹⁶ This suggests that the stimuli for an inflammatory response may be diverse even in neighbouring areas.

Blood biomarkers of inflammation and their relationship with SVD have been extensively investigated, particularly canonical inflammatory pathways such as the IL-6 / C-reactive protein axis, which was associated with WMH volume and lacunar infarct count²¹⁷, and Intercellular Adhesion Molecule 1 (ICAM-1), a cell-cell adhesion molecule that is induced by inflammatory states; serum levels are elevated in the context of a distinct profile of pro-thrombotic inflammatory mediators²¹⁸ and predict WMH progression in follow-up studies²¹⁹. CRP and IL-6 have also been assessed longitudinally²²⁰ although this study did not find an association with the progression of WMH volume. A recent systematic review examining the associations between blood markers of inflammation and SVD, concluded that this association is moderately robust.²²¹ Moreover, biomarkers that were investigated tended to cluster into markers of vascular inflammation that were associated with sporadic SVD and markers of systemic inflammation that were associated with CAA. The advent of high throughput proteomic measurements allows more detailed biochemical pathways to be evaluated; a cluster of biomarkers of inflammation and endothelial activation that correlates with WMH burden has been identified using this technique.²²²

In addition to conventional biochemical markers of inflammation, the function of the immune cells involved in this cascade can also be assessed. In cardiovascular disease, inflammation is thought to be mediated by the innate immune response, including monocytes in the plasma compartment and macrophages in the tissue compartment. These cells are stimulated predominantly by IL-1 released from endothelial and vascular smooth muscle cells.²²³ Additional cellular components of this pathway include regulatory T cells producing TGF- β and T_H2 cells producing IL-4 and IL-10. Further to these systemic pathways, there are also local triggers, including oxidised phospholipids released from atheroma itself, which induce a pro-inflammatory phenotype in circulating monocytes.²²⁴ RNA sequencing data from isolated monocytes has shown that monocytes in patients with symptomatic atherosclerosis have an altered transcriptomic profile compared to those with asymptomatic atherosclerosis, and this favours innate immune cell activation.²²⁵ Application of these immunophenotyping

techniques to cerebrovascular disease is in progress, but it seems likely that similar mechanisms may be involved (particularly as the risk factor profile is very similar) and one early study has shown that the cytokine production capacity of monocytes was related to WMH volume and progression.²²⁶

No studies have yet addressed the mechanism of how peripheral inflammation might contribute to the central nervous system (CNS) tissue damage seen in SVD. It is possible that peripheral immune cells migrate directly through a permeable BBB, or that cytokines and other signalling molecules released from peripheral cells activate microglia within the brain tissue. Direct evidence via CSF measurement is limited and has focused exclusively on protein biomarkers rather than cell immunophenotyping; however, two studies have shown evidence of altered concentration of matrix metalloproteases (MMPs) in SVD, including MMP-2,²²⁷ MMP-9^{201,227}, and TIMP-1.²⁰¹ MMPs are inflammatory mediators that induce degradation of the ECM and these studies provide additional indirect evidence of the role of inflammation.

Evidence of inflammation within the CNS itself in SVD has however been provided by advanced neuroimaging, using positron emission tomography (PET) images. Administration of a radioligand that binds to translocator protein (TSPO), a mitochondrial surface protein that is thought to be upregulated in microglial activation,²²⁸ can be used to produce maps of microglial signal. This signal was found to be related to a compound score based on conventional radiological hallmarks of SVD in one study²²⁹, and can be used to identify focal areas of increased signal that are more prevalent in NAWM than in WMHs and in patients with SVD compared to controls.²¹³ However, interpretation of TSPO PET has been limited by confounds such as off-target and non-specific tissue binding²³⁰; moreover a recent large scale transcriptomic study has suggested that TSPO relates to microglial concentration rather than phenotype.²³¹ It is unclear whether inflammation in SVD is a primary driver of disease or merely a response to tissue damage; other authors have further suggested that microglial activation may be protective and that suppressing the immune response might be counterproductive.²³²

Synthesis of pathophysiological mechanisms

To fully define the pathophysiology of SVD, it would be necessary to demonstrate that all these processes (and perhaps others) contribute to the development and progression of clinical and radiological disease, and that reversal or modification of these factors can slow the progression of SVD. This requires further longitudinal cohort studies, supportive pre-clinical animal models and ultimately clinical trial data to prove the concept and the efficacy of treatment. Figure 1.8 illustrates how this model could be constructed.

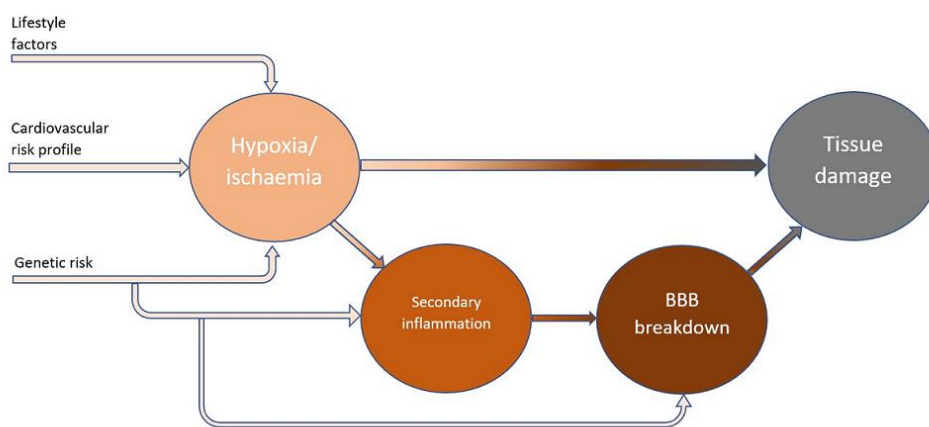


Figure 1.8. Conceptual model of parenchymal damage in SVD. Predisposing factors including cardiovascular risk factors and genetic risk profile predispose to hypoxia/ischaemia, which causes initial tissue damage and secondary inflammation which then leads to BBB breakdown and further tissue damage. Genetic factors might be relevant at both these stages.

Unifying evidence for the interaction between all these processes is incomplete. However, one synthesis has been proposed where an initial ‘hit’ due to haemodynamic factors (hypertension leading to hypoxia/ischaemia) is compounded by a secondary inflammatory response, and intracellular production of hypoxia-inducible factor (HIF)-1 α leads to degradation of the ECM and opening of the BBB.²³³ This has been supported by experiments using a spontaneously hypertensive / stroke-prone rat with unilateral carotid artery occlusion as a model of SVD.²³⁴ These animals develop similar white matter lesions to those seen in SVD, and an impaired behavioural phenotype; in this model, there was increased immunoreactivity to HIF-1 α and MMP-9 compared to control animals and a larger volume of WMHs on MRI.

Disease-modifying treatment and evidence from previous clinical trials

Literature around the treatment of SVD is heterogeneous due to the variety of ways in which it can be identified (symptomatically, radiologically etc.) and the range of outcome measurements considered (clinical or radiological). However, it is clear that disease-modifying treatments are currently limited. Antiplatelet agents including aspirin and clopidogrel are given to reduce recurrent stroke and are effective after lacunar stroke.²³⁵ Dual antiplatelet therapy with these medications in combination has also been tested explicitly in lacunar stroke patients as part of the Secondary Prevention of Small Subcortical Strokes (SPS3) trial, a two-by-two matrix study that also tested intensive blood pressure reduction. In this study dual antiplatelet treatment did not reduce recurrent stroke.²³⁶ There is no good evidence on which to recommend antiplatelet treatment for incidental / asymptomatic lacunar infarcts found on MRI.²³⁷

Modification of cardiovascular risk factors has been tested in a number of studies, for example treatment antihypertensives such as perindopril¹⁶⁶, or cholesterol-lowering medications such as simvastatin²³⁸ or pravastatin.¹⁶⁷ Multi-domain cardiovascular health interventions including counselling, long-term anthropometric measurements and medications have also been trialled unsuccessfully,²³⁹ though the studies may have been inadequately powered according to our calculations discussed in chapter two.

More recently, studies have used intensive blood pressure control based on a target value rather than a uniform medication strategy, and the Systolic blood Pressure INtervention – Memory and cognition IN Decreased hypertension (SPRINT-MIND) trial demonstrated that targeting a systolic pressure of less than 120mmHg can slow the progression of lesion growth compared to standard treatment.²⁴⁰ This was in a population with relatively mild SVD burden at baseline but encouragingly the radiological outcomes also translated to improved cognitive outcomes.²⁴¹

Other trials of intensive blood pressure treatment include the SPS3 study mentioned above, which showed a non-significant reduction in recurrent stroke and adverse cardiovascular events using a blood pressure target of 130/80mmHg²⁴², and the REcurrent Stroke PrEvention Clinical ouTcome (RESPECT) study, which also showed a non-significant reduction in recurrent stroke.²⁴³ However, the RESPECT authors performed a meta-analysis of their results and previous trials of intensive blood pressure treatment and calculated a pooled estimated odds ratio of 0.78 (95% CI 0.64-0.96) of stroke recurrence. More recently the PRESERVE study also tested a more restrictive blood pressure target of 120/80mmHg in patients with established SVD, and the authors found that this may delay white matter network disruption.²⁴⁴ However, there was no significant treatment effect on WMH volume, cognitive performance or on recurrent stroke / cardiovascular events, likely due to power.²⁴⁵ The mean participant age in all these trials was in the range 60-70 years; it is not clear if there is an optimal age for intervention or if there is an upper limit beyond which intensive blood pressure treatment is unhelpful (or indeed harmful). This is particularly important as the absence of experimental data in patients over 80 years of age limits the extrapolation of guidelines for blood pressure management.²⁴⁶

Novel pharmacological agents have been identified on the basis of the pathophysiological mechanisms discussed above. These include cilostazol, a weak antiplatelet agent and phosphodiesterase III inhibitor and isosorbide mononitrate, a NO donor that causes smooth muscle relaxation, which was associated with lower dependence and in combination with isosorbide mononitrate reduced a composite vascular endpoint in the LACunar Intervention trial 2 (LACI-2) study.²⁴⁷ This is in addition to the potential for secondary/subgroup analysis of ongoing secondary prevention trials in participants with unselected stroke; of particular interest are allopurinol, a xanthine oxidase inhibitor with anti-inflammatory properties²⁴⁸ and colchicine, an inflammasome / microtubule inhibitor that suppresses inflammatory cell proliferation.²⁴⁹

Other interventions that have previously been tested include B-vitamin supplementation, which did not have a significant effect on WMH progression in a cohort of patients with recent TIA or minor stroke²⁵⁰, regular moderate aerobic exercise, which had no significant effect on qualitative assessment of cognition and quality of life metrics in a population with clinically diagnosed vascular cognitive impairment²⁵¹, and resistance training, which had no significant effect on WMH progression in a population of community-dwelling older women.²⁵²

In summary, current evidence suggests that modification of cardiovascular risk factors has limited efficacy in slowing the progression of SVD once identified, and treatment should include aggressive blood pressure management (if tolerated) together with control of other risk factors such as hypercholesterolaemia, diabetes mellitus and smoking and general healthy lifestyle advice in line with guidelines outside SVD. Antiplatelet treatment should be used in patients with clinical stroke, but not necessarily in covert (asymptomatic) SVD.⁶⁵ Symptomatic treatments are beyond the scope of this thesis, but there are no medications that have been shown to improve cognition in VCI/VaD²⁵³ and pharmacological treatments for fatigue, depression and apathy have not been tested specifically in SVD populations.

Aims of thesis

This thesis is divided into two parts. In Part I, I consider WMHs specifically as a marker of SVD severity and a proxy for SVD pathophysiology. As discussed above, WMHs are straightforward to measure using a variety of analytical techniques, and increasingly used as outcome measurements in clinical trials. In Part I, I assess the following questions:

- (1) What is the expected rate of WMH volume progression?
- (2) Which study factors (population, imaging acquisition / analysis factors etc.) affect the measured rate of WMH progression?

(3) Which patient factors (i.e. demographic factors and potentially modifiable risk factors) affect WMH progression?

(4) How do these factors affect sample sizes required for clinical trials?

In addition to these questions, I hypothesise that in the natural history of SVD, WMH volume tends to increase over longitudinal follow-up measurements and that it is rare for individual participants to show decreases in WMH volume over time. I then further examine the following questions:

(5) What is the expected incidence of WMH regression in SVD?

(6) What factors are associated with WMH regression?

In Part II, I consider the pathophysiological mechanisms involved in SVD, focusing specifically on the innate immune response measured centrally (via PET imaging) and peripherally (via inflammatory biomarkers and cell phenotyping), and on BBB breakdown (using DCE-MRI and comparison of blood and CSF constituents).

I hypothesise that these processes are involved in SVD and associated with clinico-radiological severity, and further that they predict disease progression longitudinally. Using data from a cohort of patients with moderate to severe symptomatic SVD, Part II addresses the following questions:

(7) Are PET measurements of microglial signal associated with conventional MRI markers of SVD severity?

(8) Are BBB permeability measurements using DCE-MRI associated with conventional MRI markers of SVD severity?

(9) Are blood biomarkers and immunophenotyping associated with conventional MRI markers of SVD severity, and is there a relationship with PET and DCE-MRI measurements?

(10) Is Q_{alb} associated with DCE-MRI measurements of BBB permeability?

(11) Do baseline measurements of inflammation predict disease progression based on MRI or neuropsychometric testing?

(12) Do baseline measurements of BBB permeability predict disease progression in the same way?

These research questions aim to enhance understanding of the use of WMHs as an outcome measure with relevance for the design of future clinical trials, and to provide evidence of the role of novel disease mechanisms in SVD that might inform future disease-modifying treatments.

PART I

White matter hyperintensity lesions and their fate.

CHAPTER TWO

A systematic review and meta-analysis of white matter hyperintensity lesion progression in cerebral small vessel disease.

Content from this chapter was published as:

Brown, RB, Low, A & Markus, HS. Rate of, and risk factors for, white matter hyperintensity growth: A systematic review and meta-analysis with implications for clinical trial design. *J. Neurol. Neurosurg. Psychiatry* 92, 1271–1277 (2021)²⁵⁴

Figures 2.1, 2.2 and 2.4 are reproduced from this article courtesy of BMJ Publishing Group.

I designed the study, performed the literature search, extracted the data, critically reviewed references, analysed the data and wrote the first draft of the manuscript. Audrey Low assisted with data extraction, critically reviewed references, and critically reviewed the manuscript. Hugh Markus assisted with study design, critically reviewed references, and critically reviewed the manuscript.

Introduction

White matter hyperintensities (WMHs) visible on magnetic resonance imaging (MRI) become highly prevalent with increasing age.^{255,256} Increased WMH burden is seen in patients with stroke, particularly SVD or those patients with lacunesar disease.²¹ In community studies, WMHs predict the risk of both stroke and dementia.⁶⁹ Neuropathological studies demonstrate in the vast majority of cases they appear to result from cerebral small vessel disease, with histological changes of ischaemic demyelination, axonal loss, and gliosis.^{75,194} While potential risk factors for the prevalence of WMHs has been assessed in many of these cohorts, their contribution to the rate of WMH progression has not been studied in such detail.

The clinical relevance of WMHs, and the fact that they can be measured using MRI in a clinical trial setting, has led to their increasing use to assess potential therapeutic strategies for both SVD and dementia in phase 2 studies. This was recently illustrated in the SPRINT study²⁴⁰ in which intensive blood pressure lowering was associated with reduced cognitive impairment, in combination with a reduction in WMH lesion growth. This suggests a possible mechanistic pathway that might be targeted to develop disease-modifying treatments.

Designing and appropriately powering interventional studies depends on accurate estimate of WMH lesion growth over the timescale of a few years which is relevant for most trials. Individual studies have suggested this may vary depending on characteristics such as age, as well as characteristics of the cohort being studied. These differences could have a major impact on sample size calculations in any interventional study. To better understand WMH progression, I performed a systematic review and meta-analysis of longitudinal studies measuring change in WMH volume over time. I calculated absolute rates of WMH lesion growth and determined how these varied with cohort and individual patient characteristics. I further estimated sample sizes required for any interventional trial and the effects of population factors on these values.

Methods

Systematic review and data extraction

Systematic review was performed in accordance with PRISMA guidelines²⁵⁷ and registered prospectively in the International Prospective Register of Systematic Reviews (PROSPERO - identifier CRD42020191781). I first searched for studies where WMHs were evaluated longitudinally. I searched PubMed and Google Scholar for the following terms (("white matter hyperintens*" OR WMH OR "white matter lesion*" OR WML OR leukoaraiosis) AND (progress* OR develop* OR penumbra OR evol*) AND (longitudinal OR serial OR "follow-up") AND (MRI OR "magnetic resonance")) and selected publications up to and including 31 December 2020.

The review was limited to sporadic SVD and did not include either CAA, cohorts of patients with both ICH and WMHs, or monogenic forms of small vessel disease (e.g. CADASIL), which might have different pathological mechanisms. Review articles, case reports, trial protocols, and articles without numerical data were excluded. I also excluded studies investigating non-ischaemic causes of white matter disease, but included those addressing cognition and symptoms of mood/apathy/depression in older adults. Abstracts were screened by two authors (RBB and AL) and after consensus decision on inclusion data was extracted by a single author. The articles identified were hand-searched for further relevant references.

Where presented, WMH growth was extracted or calculated from the percentage of total brain volume and normalised to a rate of expansion in cubic centimetres per year. In the cases of multiple articles describing the same cohort, I used the reference with the largest sample size (or the most recent if analysis of the entire dataset had been published more than once). The standard deviation of this value was extracted where presented or calculated from parameters given in the article. Correlation coefficients for the effect of age and baseline WMH volume, and odds ratios for the effect of sex were also extracted. Data were captured using a standardised and predesigned template.

Participant groups in each study were categorised as community dwelling healthy control participants or patients in specific disease groups: SVD, all-cause stroke, dementia or mild cognitive impairment (MCI), depression/mood disorder or non-specific cardiovascular disease (CVD) including ischaemic heart disease, hypertension and hyperlipidaemia. Image analysis methods were categorised as manual (lesions traced on hard or digital copies of images), semi-automated (in which lesions were outlined using software and manually corrected) or automated if no supervision from the investigators was performed.

To examine risk factors for lesion progression in individual patients, odds ratios for the effects of hypertension, hypercholesterolaemia, diabetes and current smoking status on WMH progression were further extracted.

Statistical analysis

I used a multivariate mixed effects linear model to assess the effect of study population selection and image analysis methods on the annualised WMH growth rate, using restricted maximum likelihood estimation of heterogeneity and the Knapp-Hartung adjustment for estimates of significance.²⁵⁸ Population was modelled as a fixed effect and image analysis method as a random effect to account for the assumed relationship between these predictors and WMH growth. This form of meta-regression accounts for both within-study and between-study heterogeneity.²⁵⁹ All analysis was performed in the R project for statistical computing²⁶⁰ version 3.6.2 using the *meta* package.²⁶¹

I used the coefficients from the models above to estimate the sample sizes required to detect statistically significant reductions in WMH progression in a hypothetical clinical trial setting, stratified by population under investigation or baseline lesion volume and measured across a range of target treatment effect sizes.

Inverse variance-weighted univariate linear regression models were used to meta-analyse the effect of the above non-modifiable and potentially modifiable risk factors. For continuous predictor variables, correlation coefficients were scaled to represent the annual WMH growth (cc) per unit change in predictor (age in years or baseline WMH

volume in cc). For categorical predictor variables, the log odds ratio for the progression of WMH between categories was used.

Results

The initial literature search yielded 924 articles and manual searching provided a further 38 relevant publications. After reviewing the abstracts, 258 articles were selected for full text review. 52 studies met exclusion criteria based on the full text review, leaving a total of 206 articles that were included (figure 2.1). Each study was reviewed critically for its population selection, imaging acquisition and analysis methodology, and the risk factors investigated.

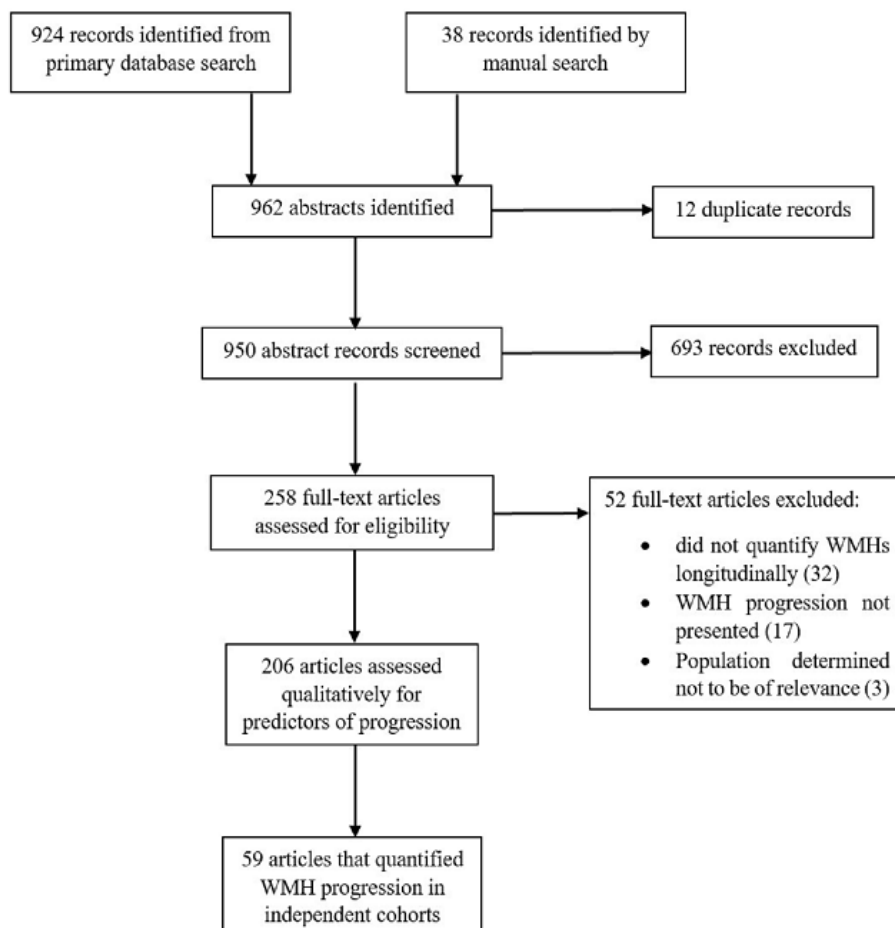


Figure 2.1. PRISMA flowchart of the literature search and selection of studies.

Rates of WMH progression and comparison between studies

I identified 59 studies that quantified WMH growth longitudinally in independent cohorts across 13,210 individuals. A further eight articles presented lesion expansion as a fraction of total brain or intracranial volume.

Studies specifically assessing patients with SVD reported highest rate of WMH progression (2.50cc/y, 95% CI -3.42-8.43cc/y), followed by intermediate rates in studies assessing patients with unselected ischaemic stroke (1.00cc/y, 95% CI -3.69-5.69cc/y). Lower estimates of WMH growth were calculated from studies including patients with depression (0.62 cc/y, 95% CI -2.55-3.79cc/y), cognitive impairment or dementia (0.46 cc/y, 95% CI -0.72-1.65cc/y) or cardiovascular disease (0.39cc/y, 95% CI 0.11-0.67cc/y). Studies assessing community dwelling control participants showed WMH growth of 0.46cc/y (95% CI -0.11-1.04cc/y).

WMH growth was broadly in the range of 0 – 1 cubic centimetres per year (inverse variance-weighted mean 0.41cc/y, 95% CI 0.17-0.66cc/y). 63.5% of the weighting of this estimate was assigned to the SPRINT-MIND study.²⁴⁰ Figure 2.2 shows these results as a forest plot of calculated values for the annual rate of WMH growth, stratified by diagnostic group. References, details of the cohorts, image analysis methods and extracted values are available in Appendix A, table 1.

There was no evidence of publication bias in the annualised WMH growth values we calculated. A funnel plot of these values is shown in figure 2.3; there was no significant asymmetry to indicate publication bias driven by the reporting of significant but less precise results and Egger's test for funnel plot asymmetry was non-significant ($t = 0.38$, $p = 0.70$).

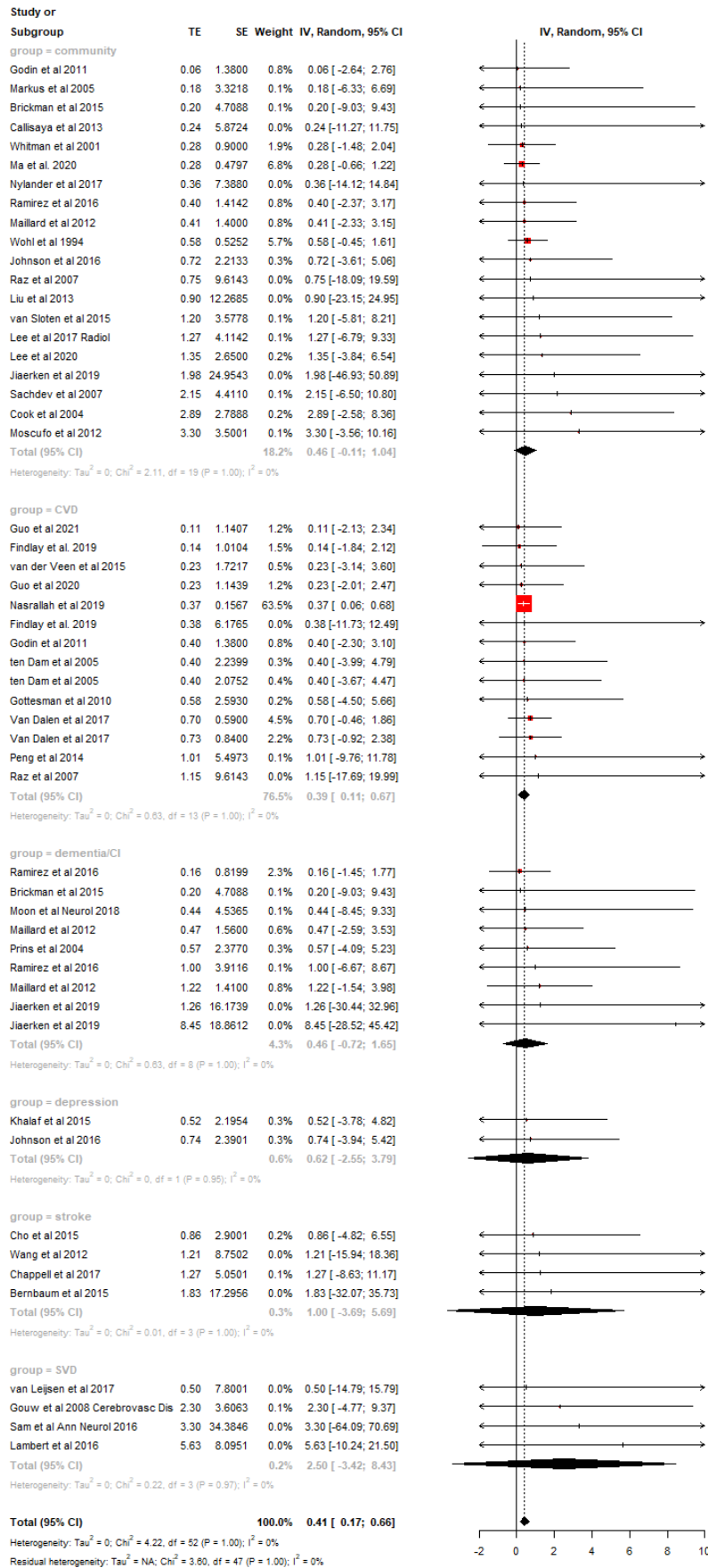


Figure 2.2. Forest plots showing inverse-variance weighted meta-analysis of annualised WMH growth (cc/y), stratified by diagnostic group.

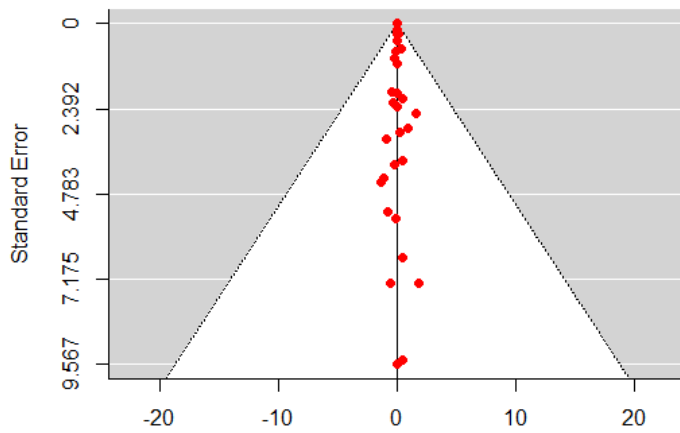


Figure 2.3. Funnel plot showing relative effect sizes across studies

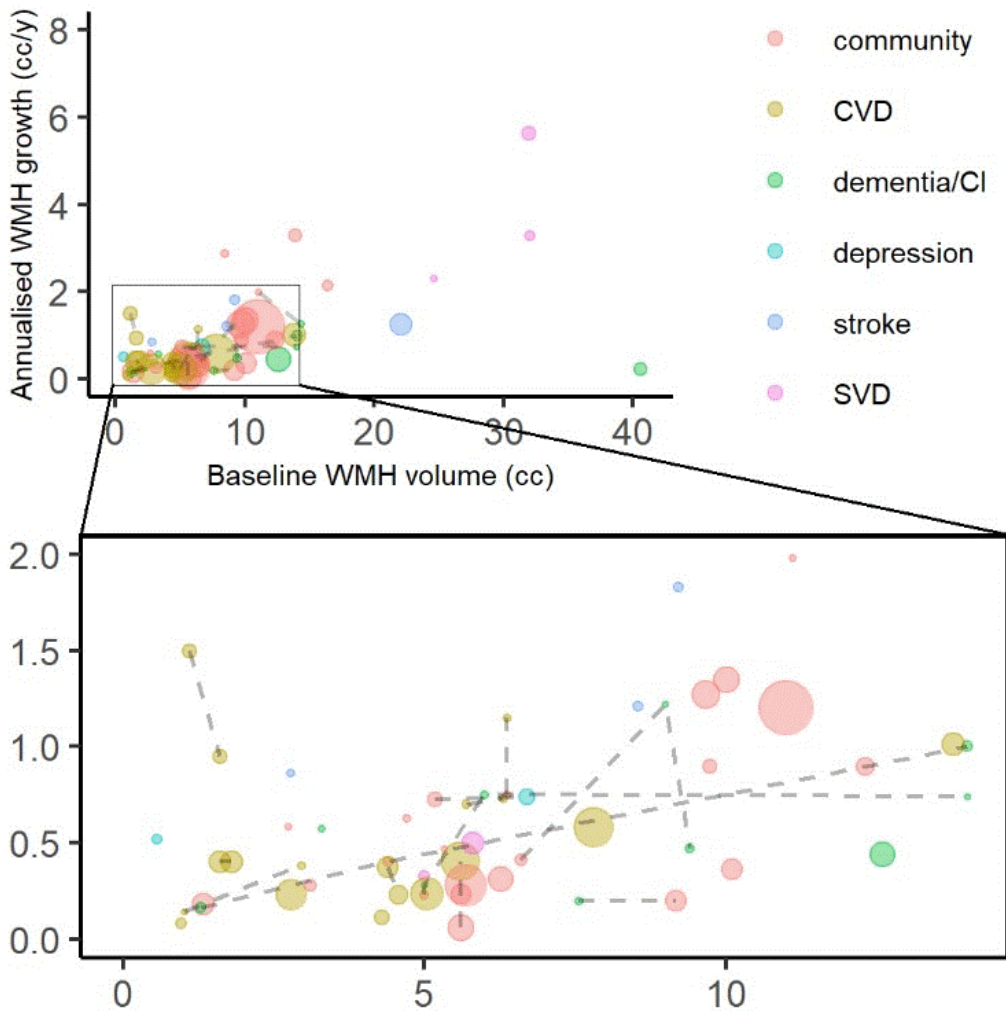


Figure 2.4. Bubble plots of WMH growth versus baseline volume. Plot points are scaled by study size and coloured by diagnosis of participant. Dashed lines link subgroups within an individual study. Disease-free control participants were assigned to the community-dwelling group.

Figure 2.4 shows a bubble plot of individual study WMH growth rates versus baseline WMH volumes, weighted by study size and stratified by diagnosis, with dashed lines connecting subgroups that were identified from a single study.

Diagnosis	Number of studies (patients)	Baseline WMH volume	WMH growth rate (cc/y)	vs depression	vs dementia /MCI	vs CVD	vs stroke
SVD	5 (494)	17.44	2.50	2.80 ($p = 0.049$)*	2.83 ($p = 0.043$)*	3.11 ($p = 0.036$)*	1.91 ($p = 0.13$)
Stroke	4 (377)	9.52	1.00	0.77 ($p = 0.03$)*	0.83 ($p = 0.013$)*	0.99 ($p = 0.15$)	
CVD	18 (4910)	4.28	0.39	-0.22 ($p = 0.02$)*	-1.17 ($p = 0.27$)		
Dementia/ MCI	13 (722)	1.89	0.46	-0.057 ($p = 0.68$)			
Depression	3 (178)	0.59	0.62				

Table 2.1. Annualised WMH growth rates for studies assessing different population categories and t-statistics for between group comparisons. SVD = small vessel disease; CVD = cardiovascular disease; MCI = mild cognitive impairment; * = significant at $p < 0.05$

In the multivariate model, studies examining patients with SVD predicted significantly higher lesion growth than those that recruited patients with cardiovascular risk factors, dementia/cognitive impairment or depression. This model explained 49.6% of the heterogeneity between studies (F-statistic on 7 and 43 d.f. 6.67, $p < 0.0001$). Weighted mean baseline lesion volumes, growth rates and post-hoc between group comparisons are shown in table 2.1.

The baseline lesion volume in each study was significantly associated with annualised growth rate in a univariate weighted linear regression model ($p = 2.0 \times 10^{-8}$, adjusted $r^2 = 0.39$, unstandardised β coefficient = 0.082, 95% CI 0.057 – 0.107). WMH growth rates were not significantly different between patient and control groups (β for patient cohorts = 0.124, 95% CI -1.03-1.27, $p = 0.83$).

Comparison of the methods of image analysis was limited by the range of different imaging analysis tools used and the fact that the pipelines described commonly used in-house code in addition to commercial software; there was no significant effect size of the choice of imaging analysis method on the rate of WMH progression. Compared to studies that were marked manually, semiautomated and automated were associated growth rates of -0.89cc/y (95% CI $-6.85\text{-}5.06\text{cc/y}$, $p = 0.75$) and -0.92cc/y (95% CI $-6.85\text{-}5.02$, $p = 0.76$) respectively.

Sample size calculations for a clinical trial based on WMH progression

I assumed a hypothetical clinical trial with two balanced arms representing intervention and control groups, using annual WMH progression as the primary outcome measure. I used the coefficients from the mixed effects model above to calculate the required samples sizes to detect a range of effect sizes with 80% power and significance level 0.05. For a study including patients with SVD, these ranged from 34 per arm to detect an effect size of 30% to 294 per arm to detect an effect size of 10%. For a study recruiting unselected stroke patients, the requisite sample sizes would be 54 per arm and 477 per arm respectively. Sample sizes for a trial recruiting participants with unselected cardiovascular disease, dementia/MCI or depression were considerably higher (table 2.2).

Population	Treatment effect sizes				
	30%	25%	20%	15%	10%
SVD	34	48	75	132	294
Stroke	54	78	120	213	477
CVD	113	162	253	448	1006
Dementia / MCI	556	880	1249	2218	4990

Table 2.2. Estimated prospective sample sizes (per arm) necessary to detect significant reduction in WMH progression, stratified by patient population, at power = 0.8 and $\alpha = 0.05$. CVD = cardiovascular disease; MCI = mild cognitive impairment; SVD = small vessel disease.

Baseline WMH volume	WMH	Treatment effect sizes				
		30%	25%	20%	15%	10%
0.25cc		44,522	69,565	123,670	278,257	>1,000,000
2.5cc		447	697	1,238	2,784	11,132
5.0cc		113	175	311	697	2,784
7.5cc		51	79	139	311	1,238
10.0cc		29	45	79	175	697
12.5cc		19	29	51	113	447
15.0cc		14	21	36	79	311
17.5cc		11	16	27	58	229
20.0cc		9	12	21	45	175
25.0cc		6	9	14	29	113
30.0cc		5	6	10	21	79
40.0cc		4	4	6	12	45

Table 2.3. Estimated prospective sample sizes (per arm) necessary to detect significant reduction in WMH progression, stratified by baseline WMH volume, at power = 0.8 and $\alpha = 0.05$. Highlighted values are those in which the required sample size is comparable to or less than the largest interventional trials that we reviewed.

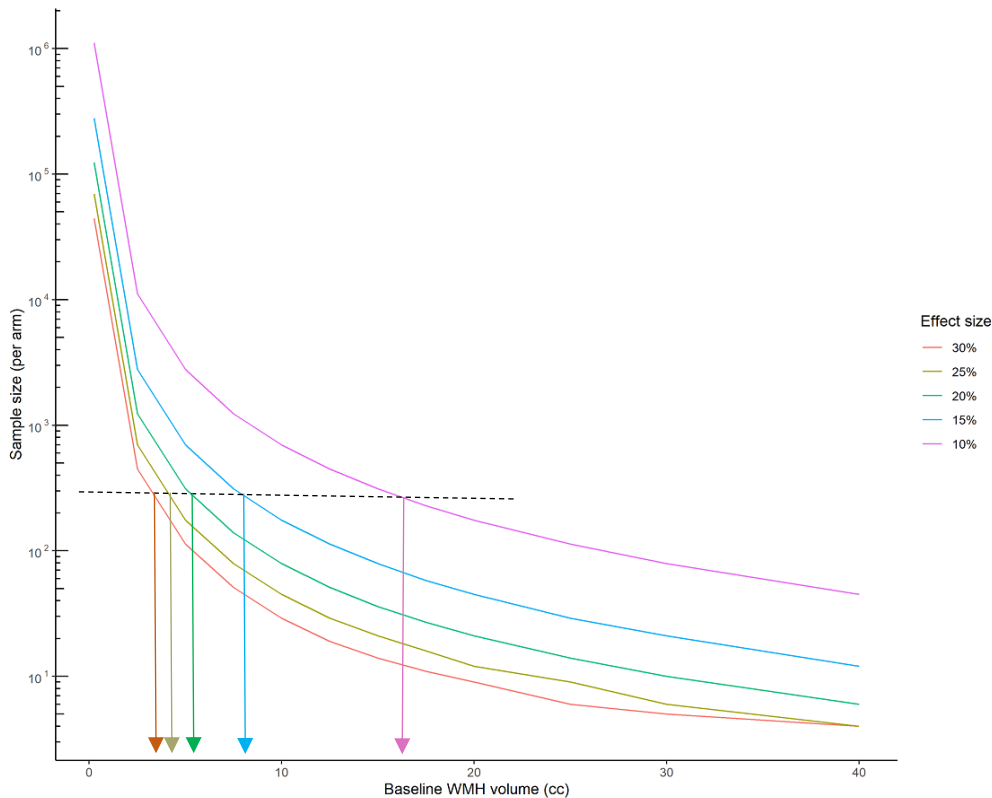


Figure 2.5. Estimated sample sizes for an interventional trial versus baseline WMH volume. The dashed line represents the largest interventional study included in our review, and the vertical lines the interceptions from this samples size to the required baseline lesion volume.

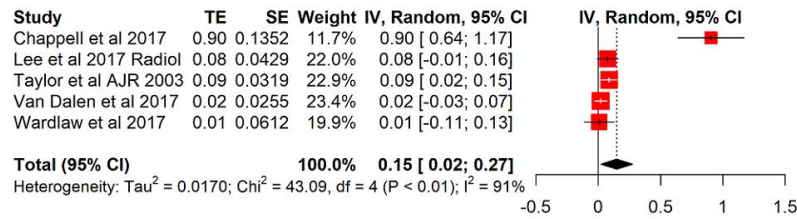
I also calculated how sample sizes required to show these treatment effects depends on the baseline lesion volume (table 2.3). As the largest interventional trials in the systematic review included close to 300 patients in each arm, applying this threshold for feasibility would require patients to have a mean baseline lesion volume of 5cc, 7.5cc, 10.0cc and 17.5cc to detect treatment effects of 30%, 20%, 15% and 10% respectively. Figure 2.5 shows the calculated sample sizes graphically, stratified by effect size.

Individual patient risk factors for WMH progression

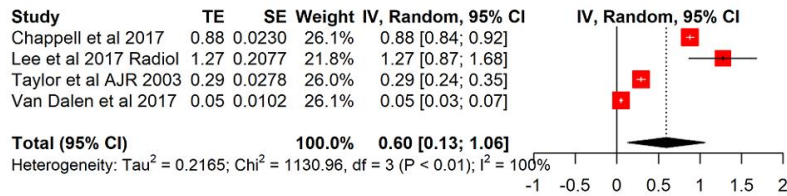
The most common predictor of WMH progression was baseline WMH volume/grade. This was significant in 14/44 articles that mentioned predictors^{83,84,265–268,93,153,164,166,238,262–264}, while one study explicitly stated that baseline lesion volume did not correlate with expansion.²⁶⁹ Meta-analysis of those studies that provided comparable metrics calculated that each unit increase in baseline lesion volume was associated with increased progression rate of 0.6cc/year (95% CI 0.13-1.06cc/y). Age at baseline significantly predicted progression independently of baseline lesion volume in a further 11/40 studies.^{82,93,272,273,153,238,264,265,268–271} In six studies, age was explicitly stated as not associated with lesion growth.^{84,155,205,262,263,274} I calculated that each year in age at baseline was associated with an additional 0.19cc/y in WMH expansion (95% CI 0.04 – 0.35cc/y).

Male sex was associated with decreased progression rate of 0.03cc/year (95% CI -0.21–0.16cc/year). However, while several additional studies found that sex was significantly associated with lesion growth, variations in the threshold for defining progression precluded incorporation of these results. Meta-analysis results are presented as a forest plot in figure 2.6. ApoE genotype was mentioned in several studies but only one presented numerical results for the association with WMH growth.

A. Effect of age on WMH growth



B. Effect of baseline volume on WMH growth



C. Effect of male sex on WMH growth

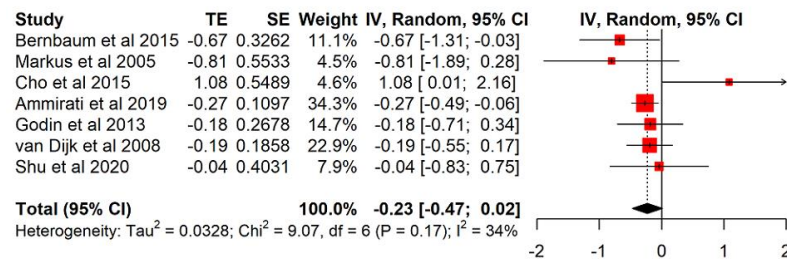
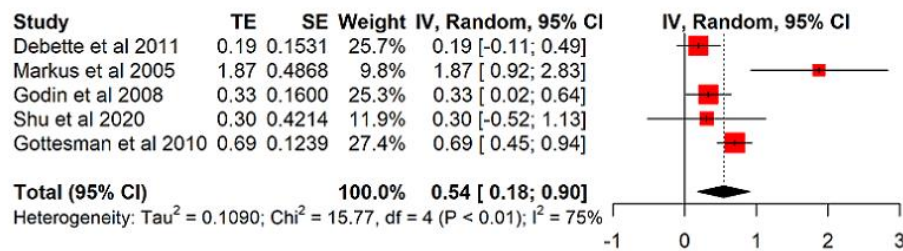


Figure 2.6. Forest plot showing meta-analysis results for demographic / non-modifiable risk factors for WMH progression. Effect sizes are correlation coefficients (age, baseline WMH) or odds ratio (sex).

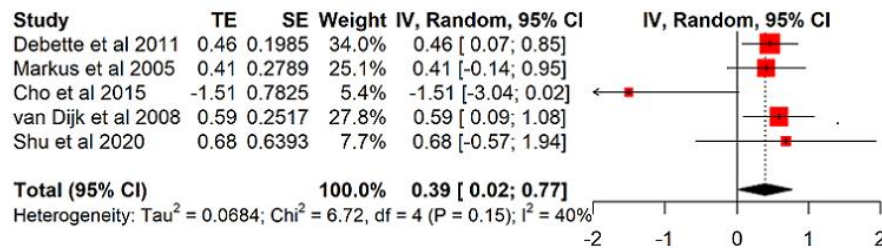
Potentially reversible factors influencing WMH progression were variably assessed in several studies. Hypertension was evaluated most frequently, and significantly associated with progression in 18 studies^{83,87,278–285,164,184,205,219,239,275–277}. However, no significant association was found in a further eight studies.^{84,93,155,166,262,270,274,286} Meta-analysis of these results was limited by heterogeneity of the definition of hypertension used and the statistical measures presented; however studies that presented the additional WMH progression conferred by a diagnosis of hypertension or blood pressure greater than 140/80 mmHg were meta-analysed. The combined effect size of having hypertension using this definition was 0.18cc/year (95% CI 0.12 – 0.30cc/year). These results are presented in figure 2.7(A). Current smoking status was also significantly associated with progression (OR 1.48, 95% CI 1.02-2.16, figure 2.7(B)).

Diabetes, hypercholesterolaemia, unspecified cardiovascular disease and BMI were mentioned in several studies without consensus as to the association with lesion growth. Sufficient data for meta-analysis were available for the effect of diabetes (figure 2.7(C)) and hypercholesterolaemia (figure 2.7(D)), both of which showed a trend towards association with the severity of WMH progression that was not statistically significant. All studies describing the effects of non-modifiable and potentially modifiable risk factors on WMH growth are given in Appendix A, table 2.

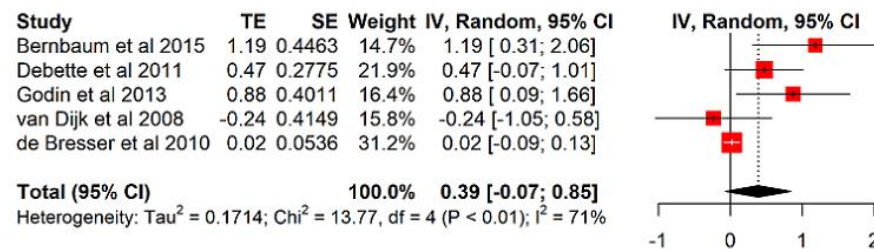
A. Effect of hypertension on WMH growth



B. Effect of smoking on WMH growth



C. Effect of diabetes on WMH growth



D. Effect of hypercholesterolaemia on WMH growth

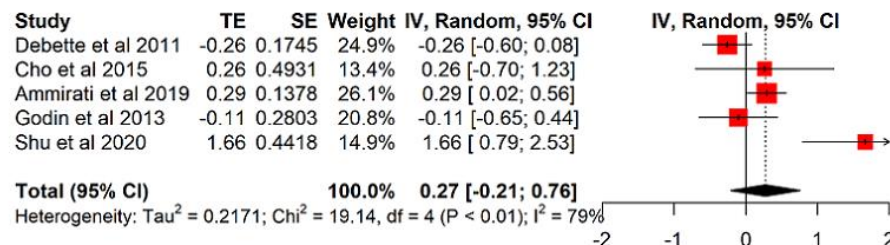


Figure 2.7. Forest plot showing meta-analysis results for potentially modifiable risk factors for WMH progression: hypertension (A), current smoking status (B), diabetes (C) and hypercholesterolaemia (D). Effect sizes are log odds ratios.

Discussion

WMHs are a common manifestation of SVD and importantly predict risk of stroke and dementia. WMH burden typically increases at a rate of up to 0-1 cubic centimetres per year in groups of susceptible participants, depending on the population examined, but can be considerably higher in specific populations, for example in patients who have already had symptoms due to SVD. This systematic review provides data on the expected rate of WMH progression and on study-level and individual patient factors that predict it. Studies in patients with unselected cardiovascular disease, cognitive impairment or depression show similar rates of WMH expansion to those assessing community-dwelling control participants, likely reflecting the high prevalence of these risk factors on a subclinical level in the general population.

A large proportion of the variance in the estimate of WMH growth in patients with cardiovascular disease and our overall estimate came from the SPRINT-MIND study (standard treatment group).²⁴⁰ This study used an automated WMH marking pipeline based on a UNet neural network algorithm accounting for co-registered T1 and FLAIR images²⁸⁷, quality assured by a neuroradiologist who was blinded to treatment allocation. Although the eligibility criteria for entry into the SPRINT study were relatively broad (participants needed to have hypertension plus additional cardiovascular risk factor(s) such as kidney disease, evidence of clinical or subclinical cardiovascular disease or be older than 75 years of age), the baseline WMH volumes were low and the distribution was narrow (median 4.40cc, IQR 3.80-5.00cc in the standard treatment group and median WMH 4.57cc, IQR 4.00-5.14cc). Given that the disease burden on baseline images was mild homogeneous, the low variance of the estimated annual WMH growth seems plausible.

The non-modifiable factors of baseline lesion volume and patient age are significant predictors of lesion growth, consistent with those predictors reported in individual studies. Lesion growth differs significantly across the diagnostic classifications used to recruit participants, and this directly affects the likely effect size that can be measured in interventional trials.

The meta-analysis of individual patient risk factors showed a significant association between both hypertension and smoking and WMH progression. However, how much of the disease process is reversible following treatment of these risk factors is yet unclear and it may be the case that these risk factors set in motion pathophysiological cascade that continues even in the absence of the risk factor itself. It has been suggested that areas of normal appearing white matter (NAWM) adjacent to WMHs are already altered on a microstructural level.^{156,288}

Modification of cardiovascular risk factors has been tested in a number of studies, for example treatment antihypertensives such as perindopril¹⁶⁶, or cholesterol-lowering medications such as simvastatin²³⁸ or pravastatin.¹⁶⁷ Multi-domain cardiovascular health interventions including counselling, long-term anthropometric measurements and medications have also been trialled unsuccessfully,²³⁹ though the studies may have been inadequately powered according to our calculations.

More recently, studies have used intensive blood pressure control based on a target value rather than a uniform medication strategy, and the SPRINT-MIND trial demonstrated that targeting a systolic pressure of less than 120mmHg can slow the progression of lesion growth compared to standard treatment.²⁴⁰ This was in a population with relatively mild SVD burden at baseline but encouragingly the radiological outcomes also translated to improved cognitive outcomes.²⁴¹

Choosing a population of interest and timepoint at which to intervene requires careful consideration. A cohort earlier in the disease course or with less severe disease will have a lower expected lesion growth; the imaging timepoints need to be separated by enough time to allow measurable progression and a larger sample size may be required. In contrast, a cohort with more advanced disease will demonstrate larger lesion growth, and though some authors have argued against a ceiling effect in WMH lesion progression²⁶⁸ it is still unclear to what extent the microstructural damage associated with WMH progression is reversible. Additionally, at a later stage in the disease course

there may be a level of cognitive impairment that stops any improvement in WMH progression from translating into functional benefit.

Strengths of this study include a robust search strategy and the inclusion of a large set of primary data covering a range of relevant populations. However, the study was limited to an extent by the heterogeneous image processing pipelines and statistical analysis used in the literature. I calculated annual lesion growth rates to allow the comparison of a wide range of studies including images over varying timescales, but the studies included used a range of inter-scan intervals from short months to five years, and an annualised rate simplifies values at either extreme which may be non-linear.^{62,268} Further limitations include that the duration of symptoms prior to baseline appointment was not considered in the analysis (and could feasibly have been heterogeneous due the possible routes of recruitment of participants with SVD either via an acute stroke centre or longer term secondary care).

I used summary statistics rather than patient level data, and while this is a reasonable proxy for estimating effect sizes between studies²⁵⁹, an individual study with significantly higher variance might require a considerably larger sample size than we calculated. Baseline lesion volume may not be known before study design or the completion of participant recruitment, but if patients are recruited to a trial on the basis of an MRI performed for clinical reasons then it might be possible to calculate the baseline lesion volume before enrolment. In this way investigators could ensure participants have baseline lesion volumes above a particular threshold compatible with the target sample size, though I consider that is likely to be impractical to select participants with similar baseline lesion volumes in order to minimise this variance. Adjusting analysis for baseline factors that influence progression might improve study power and lower further the required sample sizes that we calculated²⁶², but our data did not allow us pursue this approach.

A final limitation was the amount of data available for some potential risk factors and this may mean that this analysis could have missed associations with potentially

modifiable risk factors, for example diabetes. There were not enough data in the studies reviewed to meta-analyse certain other potentially significant non-modifiable risk factors, such as the ApoE genotype which has been suggested as a possible predictor of WMH progression.¹²⁰

Although the pathophysiological mechanisms underpinning WMH growth in SVD are not fully defined, WMHs represent a readily quantifiable target for novel interventions. They have been shown to be an effective endpoint for clinical trials based on multimodal population studies, conferring similar power to advanced MRI markers such as DTI and considerably more than using neuropsychometric measurements.²⁸⁹ These results show that age, baseline WMH volume, stroke and particularly SVD, hypertension and current smoking status are all predictors of disease progression. Prospective trials using WMH as an outcome measure should take these factors into account.

CHAPTER THREE

White matter hyperintensity regression and its predictors in cerebral small vessel disease

Content from this chapter has been accepted for publication as:

Brown, RB, Tozer, DJ, Egle M, Tuladhar, AM, de Leeuw, F-E & Markus, HS. White matter hyperintensity volume regression and its predictors in cerebral small vessel disease *[in press, International Journal of Stroke, 2023]*

Figures 3.1, 3.2, 3.3 and 3.4 are reproduced from this article under a Creative Commons Attribution 4.0 Licence.

I designed the study, marked the lesions in the PRESERVE and RUN DMC cohorts, performed the statistical analysis, and drafted the manuscript. Daniel Tozer supervised the image acquisition in the PRESERVE study and the image analysis. Marco Egle coordinated the PRESERVE study data collection and original analysis. Anil Tuladhar supervised the image acquisition in RUN DMC. Frank-Erik de Leeuw is the senior author of the RUN DMC study and was involved in gaining funding and ethical approval. Hugh Markus designed the study, edited the manuscript and as the senior author of the SCANS and PRESERVE studies was involved in gaining funding and ethical approval. All authors contributed to study design, provided interpretation of the results and statistical analysis, and were involved in critical editing of the manuscript.

Introduction

As discussed above, WMHs are a radiological hallmark of SVD and independently predict both stroke and dementia.⁶⁹ The previous chapter meta-analysed available data from the literature pertaining to the rate of WMH growth, with reference to sample sizes in clinical trials and individual risk factors for WMH progression. However, although WMH volume tends to increase over time (both in community dwelling participants^{83,290,291} and in specific patient groups with ischaemic stroke²⁹², hypertension²⁸⁵ and unselected cardiovascular disease^{293,294}), there have been recent reports of WMH regression in a proportion of patients with stroke and SVD^{270,295}. WMH volume reduction was noted in 37% in a population with minor stroke.⁹³ This finding has potentially important implications. If WMHs do regress, then better understanding of this process may inform potential treatment approaches. Secondly, this may make power calculations required for trial design more complex and increase requisite sample sizes for interventional studies.

There are various possible explanations for the regression of WMHs found in these studies. It may represent a true biological process such as the resolution of oedema or contraction of lesioned tissue as part of an inflammatory or scarring process (as has been proposed based on the finding of expanded free water compartment surrounding WMHs²⁹⁶). Alternatively, it could also be explained by radiological/technical factors causing apparent regression in some subjects. Such factors could include the necessary registration of images between scans, equipment changes between scans, and discrepancies between image quality and slice angle (the effect of which has not been assessed on longitudinal image analysis methods as far as we are aware). It might also reflect statistical factors such as the uncertainty caused by partial volume effects (particularly in periventricular areas), regression to the mean in lesion marking techniques or differential rates of atrophy affecting the mapping of lesioned tissue at follow-up to baseline space.²⁹⁷

This chapter aims to determine the frequency of WMH lesion volume regression using longitudinal volumetric measurements that account for these possible technical and methodological factors in three cohorts of patients with symptomatically defined SVD. I developed a novel analysis technique blinded to time point of scans to determine the frequency of participants showing WMH regression in each of the cohorts. Next I used pooled individual participant data to test the associations of patient and imaging factors (including more subtle measurements of white matter microstructural damage such as DTI measurements) with this regression.

Methods

Study populations

Three cohorts of patients with symptomatic SVD and differing degrees of WMH severity were studied. All participants provided written, informed consent prior to enrolment.

The St George's Cognition and Neuroimaging Study (SCANS)³⁹ was a prospective observational study that recruited patients with symptomatically-defined SVD presenting with a lacunar stroke syndrome and had both a compatible lacunar infarct and at least early confluent WMHs on MRI (Fazekas scale⁷¹ score ≥ 2). MRI scans were performed at least three months post-stroke. Patients were recruited from three South London hospitals between March 2007 and October 2010 and the study was approved by the Wandsworth Research Ethics Committee (ukctg.nihr.ac.uk; study ID: 4577).

The PRESERVE study²⁴⁵ was a multicentre randomised control trial of intensive versus standard blood pressure treatment in SVD. Patients with a lacunar stroke syndrome (and a compatible lacunar infarct on MRI) and WMHs of Fazekas score ≥ 2 were recruited at least three months post-stroke from six UK-wide hospitals between February 2012 and October 2015. MRI was performed at baseline and after two years; the trial was approved by the Harrow Research Ethics Committee (reference: 11/LO/0458) and registered with the International Standard Randomised Control

Trial Number registry (reference: ISRCTN37694103). I included only participants from the standard treatment arm in this analysis, because my aim was to describe the natural history of WMHs and lesion progression in the intensive arm may be confounded by effects of the intensive antihypertensive treatment.

The Radboud University Nijmegen Diffusion Tensor and Magnetic Resonance Cohort (RUN DMC) was a prospective long-term cohort study that recruited patients with any symptoms compatible with SVD and evidence of either lacune(s) or any WMHs on MRI.²⁹⁸ Patients were recruited at Radboud University Medical Centre, Netherlands and had MRI scans in 2006, 2011 and 2015. Due to equipment upgrade after the first timepoint in the RUN DMC study, we used images from the second and third timepoint only. The study was approved by the Arnhem-Nijmegen Medical Research Ethics Committee (No. 2005/256).

Image acquisition

MRI scanner and sequence details for studies above have previously been published^{39,298,299} and are summarised here in brief and fully in the supplementary material. MRI imaging in SCANS was performed on a 1.5T GE Signa HD MRI scanner at St George's, University of London and included T₁-weighted, fluid-attenuated inversion recovery (FLAIR) and diffusion tensor (DTI) images.

Images in PRESERVE were acquired using eight 3.0T MRI scanners across the six sites and acquisition parameters between sites were harmonised as much as possible and subject to rigorous quality control. T₁-weighted, FLAIR and DTI images were used for this analysis.

In the RUN DMC study MRI was acquired using a 1.5T Siemens Magnetom Avanto and included T₁-weighted, FLAIR and DTI sequences.

Image analysis

Two methods of measuring WMH lesion load were used. The analysis pipeline used in SCANS has previously been described.³⁰⁰ In brief images were pre-processed using Statistical Parametric Mapping 8 (<http://fil.ion.ucl.ac.uk/spm/software/spm8/>) to check orientation and co-register to MNI registration in 1mm isotropic voxels. Group average tissue probability maps were created using a modified multivariate mixture of Gaussians³⁰¹ and individual images were then segmented using these custom maps and repaired manually if required using ITK-SNAP (<http://www.itksnap.org>) including the removal of any lacunes and/or haemorrhages. Each subject image was then warped to an individual participant midpoint average image to create divergence maps for voxels containing WMHs.

WMH lesion load was determined in PRESERVE and RUN DMC using Jim version 8.0 (<http://xinapse.com/j-im-software/>), a semi-automated program in which a region of interest is selected by the rater and voxels within this contour delineated. The program was run on a Microsoft® Surface PC and manual adjustment performed using a stylus tool to correct lesion boundaries on the screen. To minimise errors relating to the selection of lesions, images were marked slice by slice on a parallel split screen and the image intensity was matched between scans. To reduce the risk of bias images were randomly displayed in terms of order of acquisition and the rater was blinded to image timepoint. Any haemorrhages or isolated lacunes were excluded from the lesion mask; in the case of lacunes within areas of confluent WMHs, the entire area of FLAIR high signal was marked and the area of low signal isointense with cerebrospinal fluid was then removed.

Previously published threshold values were used to determine whether there was progression or regression of WMH lesion load. Participants were categorised as “regressors” if they showed a decrease in the total WMH volume of at least 0.25cc between any sequential scans. This is the minimum difference between WMH volume that can be appreciated visually and has been used to define lesion regression.²⁶⁸ “Progressors” were defined as participants that showed an increase of greater than one

standard deviation of the interscan change within each study as has also been used previously.²⁶⁸

DTI images in SCANS and PRESERVE were pre-processed using the Eddy correct tool from Functional MRI of the Brain's Diffusion Toolbox (<http://fsl.fmrib.ox.ac.uk/fsl/fslwiki/FDTref>). In RUN DMC the DTI images were pre-processed using an in-house iteratively reweighted least squares algorithm.³⁰² In all three cohorts fractional anisotropy (FA) and mean diffusivity (MD) histograms were created using the FMRIB's DTIFit tool. White matter FA median and MD normalised peak height were used for analysis as these DTI parameters have been shown to be reproducible between sites in patients with SVD.³⁰³

Brain volumes in SCANS and RUN DMC were calculated by subtracting the WMH lesion maps from the grey and white matter masks derived from SPM8 and normalised for intracranial volume using SIENAX (<https://fsl.fmrib.ox.ac.uk/fsl/fslwiki/SIENA>). Brain volumes in PRESERVE were calculated by using applying SIENAX to images that had been intensity non-uniformity corrected by N4ITK and segmented using SPM12.

Statistical analysis

Differences in demographic factors, comorbidities and baseline imaging parameters between regressor/stable/progressor groups were tested using the student's t-test / one-way ANOVA for continuous variables and Pearson's chi-squared test for categorical variables (or Fisher's exact tests for cases where a category had fewer than five observations) as appropriate. All analyses were performed in the R project for statistical computing v3.6.3 (<https://www.R-project.org/>).²⁶⁰

As the PRESERVE and RUN DMC images were analysed using the same method, individual participant data were pooled and tested again using study site as a covariate. Ordered logistic regression models were performed using the "polr" function in the R package "MASS" (<https://www.rdocumentation.org/packages/mass/>) to test the association of demographic factors (age, sex, premorbid IQ and years in education),

participant comorbidities (hypertension, hypercholesterolaemia, diabetes and smoking history) and baseline imaging parameters (including MRI features of SVD such as lacunar infarcts, cerebral microbleeds and DTI metrics) with participant category. I used a mixed effects model with study site as a random factor and other predictors as fixed factors. Selection of predictor variable was conducted using stepwise forward selection of any predictors with $p < 0.05$ on univariate analysis and backwards selection of predictors that lost this significance in the multivariate model. I also used this method to test the effect of any change in brain volume on WMH regression.

Results

Proportion of regressors

98 participants were included from SCANS (mean age 69.0 years, 66.3% male, mean baseline WMH volume 37.3cc) who had four scans over a three year period. Of these, no participants showed lesion regression using the definition of a reduction of 0.25cc. I included 42 participants from PRESERVE (mean age 68.7 years, 65.4% male, mean WMH volume 31.0cc) who had repeat scans at two years. Of these, 6/42 (14.3%) showed lesion regression. 276 participants from RUN DMC were included (mean age 68.1 years, 57.5% male, mean WMH volume 7.75cc) who had repeat scans at five year; of these 6/276 (2.2%) showed lesion regression. Images from participants who were identified as showing WMH regression were visually inspected and no pairs of images showed discrepancies in image quality/positioning or artefacts that would explain a reduction in WMH volume. Figure 3.1 shows the WMH volume over time for the three cohorts, stratified by quintile of WMH change during the study.

Details of the cohorts are provided in table 3.1, together with the number of regressors, stable participants and progressors and differences in demographic and imaging parameters between the groups. Participants that demonstrated WMH progression tended to have larger baseline WMH volumes, though there were isolated participants with moderate disease who were categorised as stable or regressor.

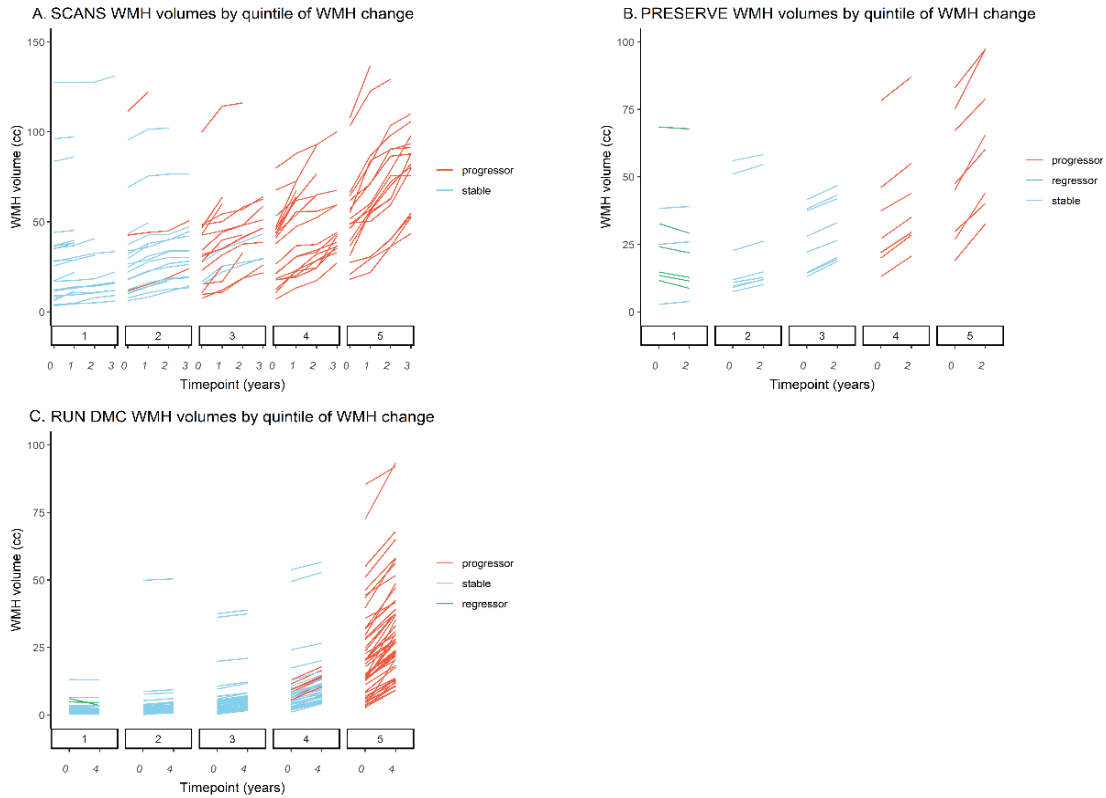


Figure 3.1. Spaghetti plots showing change of WMH volume across study duration, stratified by quintile of total WMH change in the SCANS study (A), the PRESERVE trial (B) and the RUN DMC study (C).

There was excellent correlation between the WMH lesion volumes calculated for this analysis and the previously marked and published values in RUN DMC²⁶⁸ (intraclass correlation coefficient for both timepoints 0.992, 95% CI 0.990-0.993, figure 3.2).

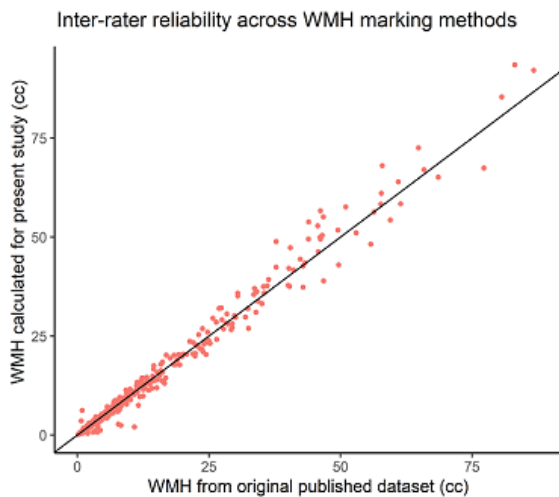


Figure 3.2. Inter-rater reliability data for the WMH volumes calculated for this study and those previously published in the literature. The black line illustrates perfect correlation.

	SCANS cohort (n = 98)				PRESERVE trial (n = 42)				RUN DMC cohort (n = 276)			
	Regressors	Stable	Progressors	P value	Regressors	Stable	Progressors	P value	Regressors	Stable	Progressors	P value
Number	0 (0)	41 (41.8)	57 (58.2)	-	6 (14.3)	18 (42.9)	18 (42.9)	-	6 (2.2)	199 (72.1)	71 (25.7)	-
Age	n/a	69.4 ± 9.8	68.7 ± 10.2	0.73	72.5 ± 5.5	66.9 ± 8.8	66.8 ± 8.8	0.32	61.5 ± 6.2	67.0 ± 7.3	71.8 ± 7.6	< 1 × 10 ⁻⁴
Sex (male)	n/a	26 (65.9)	38 (66.7)	0.99	3 (50)	9 (50)	6 (33.3)	0.63	5 (83.3)	113 (56.9)	40 (56.7)	0.52
NART	n/a	99.4 ± 14.9	100.1 ± 15.5	0.83	112.7 ± 11.4	114.7 ± 9.1	116.0 ± 8.8	0.77	-	-	-	-
Education (years)	n/a	11.7 ± 3.0	11.9 ± 3.5	0.81	-	-	-	-	10.7 ± 3.3	11.7 ± 3.3	10.4 ± 3.3	0.024
Hypertension (%)	n/a	92.7	93.0	1	100	100	100	1	66.7	77.1	84.5	0.33
Diabetes (%)	n/a	22.5	17.2	0.66	16.7	16.7	22.2	0.91	16.7	14.1	18.3	0.72
Hypercholesterolaemia (%)	n/a	87.8	84.2	0.99	50	83.3	83.3	0.19	50	44.1	60.6	0.099
Smoking (%)	n/a	24.3	19.2	0.99	0	16.7	16.7	0.58	16.7	16.5	16.9	0.99
Baseline WMH (cc)	n/a	30.1 ± 27.7	42.5 ± 25.0	0.026	27.6 ± 21.6	24.5 ± 15.7	38.7 ± 22.9	0.11	3.0 ± 2.0	4.217 ± 7.8	19.676 ± 17.0	< 1 × 10 ⁻⁴
Brain volume (cc)	n/a	1,313.6 ± 83.8	1,289.1 ± 87.6	0.016	1,372.3 ± 121.2	1,414.4 ± 122.9	1,313.4 ± 134.7	0.06	1,094.9 ± 94.4	1,074.9 ± 73.1	1,032.2 ± 83.9	<0.002
Lacunae	n/a	3.43	4.89	0.20	3	2.94	6	0.048	0.33	0.39	1.26	<0.001
Microbleeds	n/a	4.78	6.12	0.74	2	3.82	5	0.73	0	0.79	0.55	0.73
FA median	n/a	0.301 ± 0.03	0.287 ± 0.03	0.018	0.345 ± 0.02	0.344 ± 0.03	0.322 ± 0.03	0.046	0.347 ± 0.02	0.345 ± 0.03	0.321 ± 0.03	< 1 × 10 ⁻⁴
MD normalised peak height (mm ² /s)	n/a	0.0165 ± 0.003	0.0144 ± 0.002	0.00049	0.0143 ± 0.002	0.0140 ± 0.002	0.0125 ± 0.002	0.148	0.0143 ± 0.002	0.0140 ± 0.002	0.0120 ± 0.002	< 1 × 10 ⁻⁴

Table 3.1. Number of regressors, stable participants and regressors in each cohort and comparison of demographic details, comorbidities and baseline imaging markers of SVD.

Effects of brain atrophy on proportion of regressors

To test the effect of brain atrophy on lesion measurement, I also calculated WMH volumes normalised by total brain volume. Using this method, one participant from PRESERVE was reclassified from “regressor” to “stable” leaving 5/42 patients from PRESERVE and 6/276 from RUN DMC as regressors. Atrophy was not associated with WMH regression on univariate analysis (β -coefficient 0.178, $p = 0.12$). Figure 3.3 shows the relationship between change in brain volume and in WMH in each study.

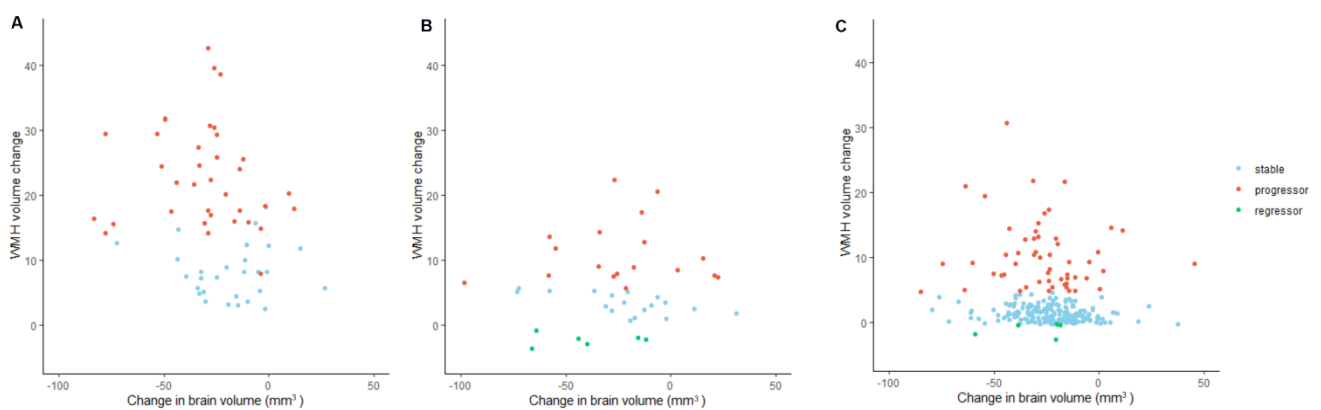


Figure 3.3. Scatter plot showing changes in measured brain volume and WMH volume over study duration in SCANS (A), PRESERVE (B) and RUN DMC (C).

Effect of using different thresholds to define regression

A secondary analysis was performed by defining “regressors” using a threshold of one standard deviation of the inter-scan WMH change (i.e. the inverse of the definition for characterising progressors). Using this definition, there were no regressors in any of the three populations. Conversely, matching the threshold of WMH growth to define “progressors” to 0.25cc led to all the participants originally marked as “stable” to be reclassified as “progressors” in all three cohorts, except for one participant in SCANS who showed an WMH increase of less than 0.25cc between each of the four timepoints.

Individual patient factors associated with regression

In RUN DMC the regressor subgroup had a lower age than the stable and progressor groups (61.5 years versus 67.0 and 71.8 years respectively, $p < 1 \times 10^{-4}$); no other between group differences in demographic variables or comorbidities for which data was available were identified in any of the studies. More severe imaging markers of SVD tended to be negatively associated with WMH regression; in RUN DMC the regressor group had lower baseline lesion volume (3.0cc vs 4.22 and 19.7cc in the stable and progressor groups respectively, $p < 1 \times 10^{-4}$), higher brain volume (1094.9cc versus 1074.9 and 1032.2cc, $p < 0.005$) and MD normalised peak height (0.0143mm²/s versus 0.0140 and 0.0120mm²/s). In both studies with regressor subjects, the regressor group was associated with lower lacune count (3.0 vs 2.94 and 6.0 in PRESERVE, $p = 0.048$; 0.33 versus 0.39 and 1.26 in RUN DMC, $p < 0.001$) and higher FA median (0.345 vs 0.344 and 0.322 in PRESERVE, $p = 0.046$; 0.347 versus 0.345 and 0.321 in RUN DMC, $p < 1 \times 10^{-4}$). Levene's test of homogeneity was used to ensure that ANOVA assumptions were valid in each cohort.

Using pooled individual participant data, significant predictors for WMH regression on univariate analysis were lower age, absence of hypercholesterolaemia, lower baseline WMH volume and lacune count, and higher brain volume, FA median and MD normalised peak height (see table 3.2).

On multivariate analysis including variables significant on univariate analysis only baseline WMH volume (OR 0.36, 95% CI 0.23–0.56) and baseline FA median (OR 1.55, 95% CI 1.07-2.24) were associated with lesion regression. Figure 3.4 shows how the probability of lesion regression depended on baseline WMH volume across the three cohorts, with regression being associated with lower baseline WMH volume; there was no clear WMH threshold beyond which lesion regression did not occur.

Predictor variables	Univariate models			Final multivariate model				
	β	SE	p value	β	SE	OR	t-statistic	p value
Study (RUN DMC vs PRESERVE)	-0.479	0.364	0.18					
Age (years)	-0.055	0.016	< 0.001					
Sex (male vs female)	0.259	0.252	0.304					
Hypertension (yes/ no)	-0.534	0.341	0.12					
Hypercholesterolaemia (yes/no)	-0.637	0.259	0.0014					
Diabetes (yes/no)	-0.295	0.34	0.39					
Smoking (yes/no)	-0.117	0.334	0.73					
Baseline WMH (cc)	-1.062	0.171	< 1 × 10⁻⁴	-1.021	0.227	0.361 (0.230 – 0.565)	< 1 × 10⁻⁶	< 1 × 10⁻⁴
Brain volume (cc)	0.520	0.131	< 1 × 10⁻⁴	0.191	0.218	1.210 (0.790 – 1.856)	0.88	0.38
Lacunae (count)	-0.239	0.058	< 1 × 10⁻⁴					
Microbleeds (count)	-0.017	0.023	0.45					
FA median	0.736	0.140	< 1 × 10⁻⁴	0.441	0.189	1.553 (1.07 – 2.251)	2.335	0.019
MD peak height (mm²/s)	0.820	0.145	< 1 × 10⁻⁴	0.054	0.260	1.05 (0.634 – 1.757)	0.209	0.83

Table 3.2. Predictors of WMH regression using ordered logistic regression assessed on both univariate and multivariate analysis. β = unstandardised β coefficient; SE = standard error; OR = odds ratio [(95%CI)]; WMH = white matter hyperintensities; FA = fractional anisotropy; MD = mean diffusivity

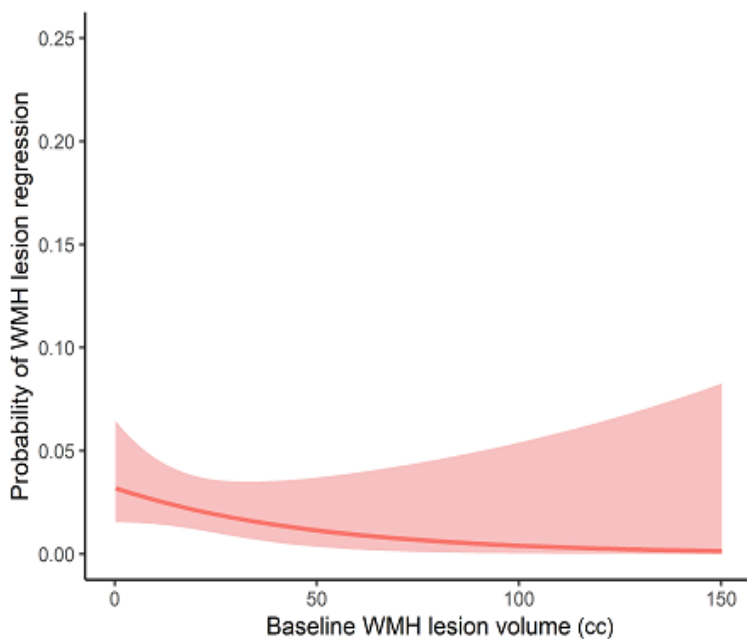


Figure 3.4. Probability of showing WMH regression versus baseline disease severity measured as WMH volume (cc).

Intra-rater reliability in WMH marking technique

Ten participants from the RUN DMC and PRESERVE studies were randomly selected and re-marked separately to the main study, in a re-randomised order and using the same blind-to-timepoint parallel method. The intraclass correlation coefficient was excellent at 0.93 (95% CI 0.87 – 0.95), and, importantly, when categorised as regressor / stable / progressor, all participants were in the same class as they had been during the original marking (figure 3.5).

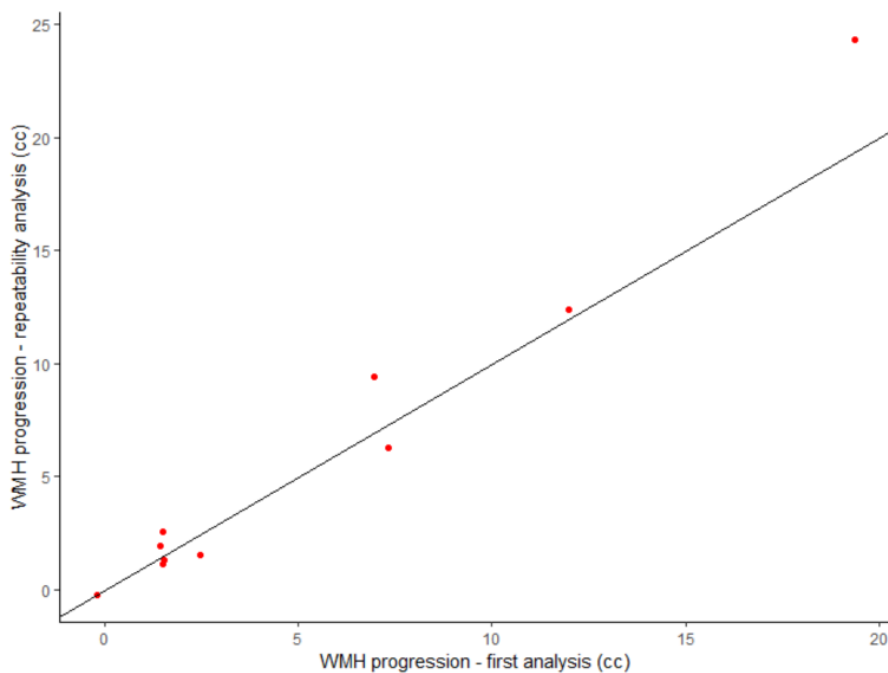


Figure 3.5. Calculated change in WMH difference between pairs of scans during original analysis and repeated analysis.

Discussion

I found only modest regression of WMH lesion volume in a small proportion of individuals over follow-up periods of between two and five years in this pooled study across three prospective cohorts with symptomatic SVD. Using a definition of 0.25cc to define regression, the proportion of participants demonstrating regression was 0%, 2.2% and 14.3% in SCANS, RUN DMC and PRESERVE respectively. When defining “regressors,” using a threshold of one standard deviation of the inter-scan WMH change, there were no regressors in any population. These values are lower than reported in recent literature.^{93,295}

The only factor that consistently predicted regression was a lower severity of SVD (and particularly less white matter damage) defined by other imaging variables. Participants who demonstrated lesion regression had a lower WMH burden at baseline. On multivariate analysis both WMH volume, and white matter microstructural integrity as assessed by FA, were associated with regression. Taken together, these results suggest that WMH regression may be more likely early in the disease process and in less severely affected patients.

Previous analysis of the RUN DMC cohort found lesion regression in 26 participants (9.4%) between 2006-2011 and in five participants (1.8%) between 2011-2015.²⁶⁸ The WMH lesion volumes I calculated, even though obtained by a different method, correlated very highly with previously published values. In this analysis I only used data from the 2011 and 2015 timepoints due to a scanner change between 2006 and 2011, and during this period our estimate of 2.2% is very similar to the 1.8% previously reported. The much higher proportion of regressors between 2006-2011 compared to 2011-2015 might be related to the measurement of WMH on different scanners.

In PRESERVE, there were a higher number of regressors. The reason for this is uncertain. Of note it was a multicentre study with image acquired on multiple scanners, and even in the standard blood pressure treatment arm in PRESERVE there was a reduction in mean blood pressure reduced by 15.3 mmHg²⁴⁵. It is possible that this led to regression in some patients, as blood pressure lowering has been shown to reduce WMH progression in the SPRINT-MIND trial.²⁴⁰ Additionally, patients may have better outcomes by virtue of their inclusion in clinical trials, potentially due to improved healthcare access and more detailed observation.³⁰⁴

Strengths of this study included the use of multiple cohorts that included participants with a range of mild to moderate to severe SVD, the larger sample size allowing associations between demographic risk factors / imaging markers and regression to be examined, and the rater being blinded to timepoint to minimise any bias in the

application of the semi-automated lesion marking technique that we used. The technique had excellent intra-rater reliability.

Limitations of the study include the differing intervals between follow-up imaging in each cohort. I was also limited by the understanding of scan-rescan reliability and the lack of consensus for acceptable noise in WMH measurement. This has been tested in small cohorts with various image analysis techniques^{305,306}, but it is still unclear to what extent small fluctuations in WMHs should be expected from imaging across multiple timepoints. If the measurement error in WMH calculation is similar to a definitive estimate of natural WMH variation then the WMH regression I observed in a small number of participants may be pathophysiologically insignificant.

A specific uncertainty is whether subtle differences in slice angle position chosen for the repeated MRI acquisitions may affect estimates of lesion progression. Conventionally it is thought that any discrepancies in slice position should offset each other in three dimensional space; however, if the slice thickness approaches lesion size (as is very plausibly the case in FLAIR images with an inter-slice gap of 3mm or 5mm), it may be possible for lesions to be captured on one set of images but fall between slices in another, producing an apparent reduction in WMH volume. (This is quite possible in the other direction producing an apparent WMH growth, but given that the magnitude of WMH change in progressors was considerably higher in regressors it is likely to have less influence on the overall measurements. An illustration of how this might be realised is given in figure 3.5.

This analysis does not exclude the fact that individual white matter lesions can regress, and this has been clearly demonstrated.⁸⁹ However it does suggest that in symptomatic SVD it is unusual for total WMH lesion volume to regress. This reassuring in the use of WMH as a surrogate endpoint in clinical trials and suggest that previous power calculations performed without considering regressors are likely to be accurate. Future studies testing interventions in SVD or performing longitudinal analysis of white matter damage in other populations (such as participants with cardiovascular risk

factors or cognitive impairment) should consider a similar blind-to-timepoint analysis method.

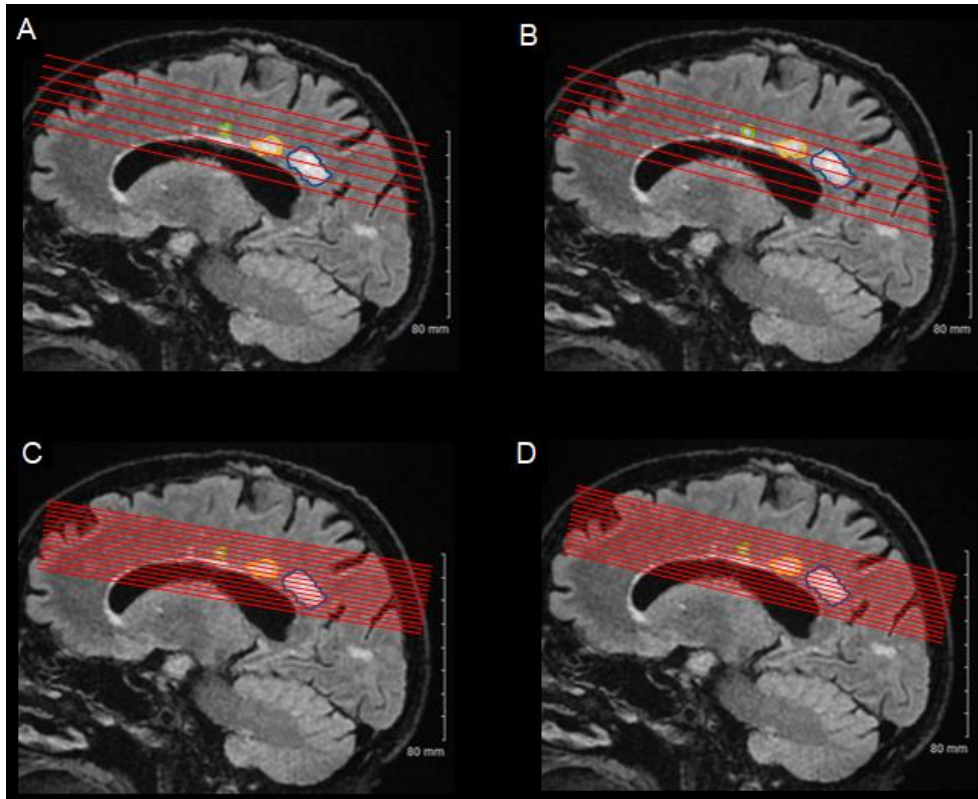


Figure 3.5. Sagittal FLAIR image of an SVD patient.. Red lines indicate hypothetical MRI slices used to acquire axial images with 5mm slices (A,B) or 2mm slices (C,D). In (A), the green lesion appears in two slices, the yellow lesion in three and the blue lesion in four slices, and the volume would be calculated accordingly. (B) shows an identical image with a pitch rotation of 10° applied to the image slices. In this case, the green lesion appears in one slice, the yellow lesion in two slices and the blue lesion in three slices. Although different surface areas are measured in the slices in (B), as the slice thickness approaches the lesion size the removal of a slice might cause an apparent reduction in lesion volume. This is not an issue when the slice thickness is much smaller than the lesion; in (C), the slices have the same angle as (A) and the green lesion appears in four slices, the yellow lesion in five slices and the blue lesion in nine slices. In (D), the slices are angled as in (B) and the lesions appear in the same number of slices as in (C).

PART II

Insights into small vessel disease pathophysiology from advanced neuroimaging, and the role of inflammation in cerebral small vessel disease.

CHAPTER FOUR

Methods, and the MINocycline to Reduce inflammation and blood brain barrier leakage in small Vessel disease (MINERVA) study protocol

Content from this chapter has been published as:

Brown, RB, Tozer, DJ, Loubière L, Hong YT, Fryer TD, Williams GB, Graves MJ, Aigbirhio FI, O'Brien JT & Markus HS. *Eur Stroke J* 2022; 7: 323-330³⁰⁷

Figures 4.4, 4.5 and 4.7 are reproduced from this article under a Creative Commons Attribution 4.0 Licence.

I am the clinician responsible for the MINERVA trial, contributed to specific trial design, gained ethical approval, recruited the participants, performed blood sampling and neuropsychometric testing and analysed the baseline trial data. I performed follow up imaging and neuropsychometric testing for the observational PET-MRI study. Jessica Walsh gained ethical approval for the observational PET-MRI study, recruited the participants, and performed blood sampling and neuropsychometric testing. Young Hong performed image pre-processing. Daniel Tozer and Tim Fryer developed aspects of the neuroimaging protocol, performed image pre-processing and image analysis, and gained funding for the studies. Guy Williams and Martin Graves developed aspects of the neuroimaging protocol and gained funding. Franklin Aigbirhio and John O'Brien gained funding for the studies. Hugh Markus designed the studies and gained funding.

Introduction

The experimental data presented in Part II were acquired from two phases of a research study funded by a Medical Research Council Experimental Medicine Programme Grant (MR/N026896/1). The first component is an observational study investigating the associations between microglial signal as a proxy measure of neuroinflammation (measured by PET imaging), blood brain barrier (BBB) permeability (measured by DCE-MRI) and conventional neuroimaging markers of SVD severity, peripheral inflammatory markers and neuropsychometric performance, with follow-up at the one year point including repeat structural MRI and cognitive testing as longer-term outcomes. The second phase of the study is an ongoing randomised, double-blind placebo-controlled clinical trial in patients with SVD, with primary outcomes based on these advanced neuroimaging markers. This chapter presents the experimental methods used to identify and recruit participants, and to analyse the neuroimaging and the blood samples, that are common across both studies. It goes on to present methods for dealing with additional laboratory analysis of blood and CSF that are implemented only in a subgroup of the trial participants, and the details of the intervention itself.

Phase I: Observational PET-MRI study

60 participants were recruited to the observational arm of this study and underwent baseline assessment including PET-MRI (using the radioligand ^{11}C -PK11195, which binds to microglia), phlebotomy and neuropsychometric testing and follow-up after one year including conventional MRI and repeat neuropsychometric testing. Of these, 20 had symptoms of lacunar stroke, cognitive impairment or gait apraxia attributable to SVD with at least moderately severe white matter damage on MRI (Fazekas scale⁷¹ ≥ 2); these constituted the sporadic SVD group. 20 had a monogenic form of SVD (CADASIL) with a proven cysteine changing mutation in the *Notch3* gene predicted to be pathogenic according to the Association of Clinical Genetic Science (UK). The

two patient subgroups were enrolled at least three months after clinical stroke to minimise the risk of enhanced ^{11}C -PK11195 binding or BBB permeability due to the acute lesion.^{308,309} The remaining 20 participants were healthy stroke-free control individuals.

Figure 4.1 illustrates the design of the observation PET-MRI study. The methods and main findings of this phase of the study have already been published²¹³ but are summarised here (methods) and in the introduction and relevant subsequent chapters where context is required (results).

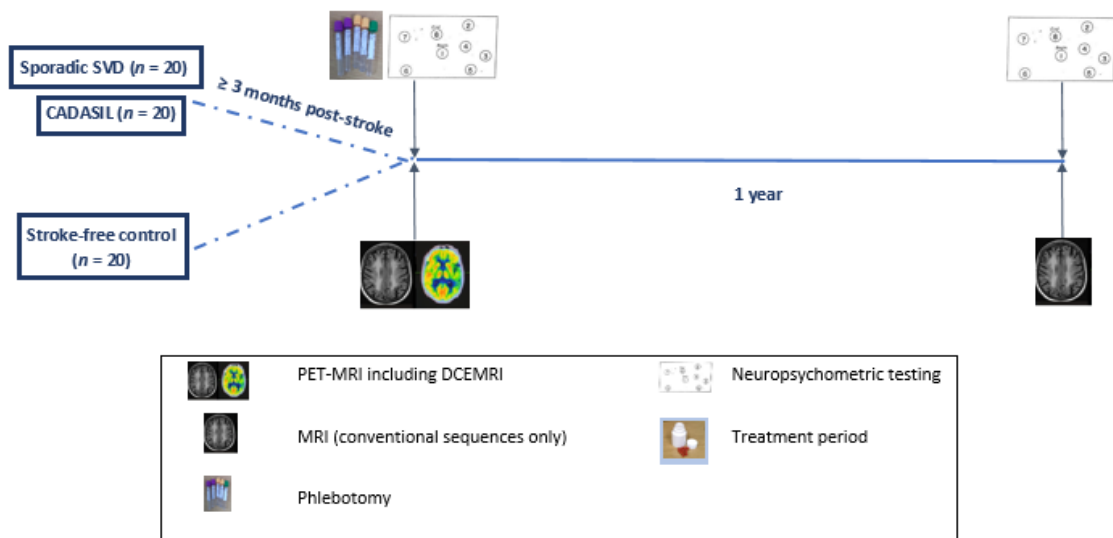


Figure 4.1. Observational phase study design.

Patient selection

Participants were recruited from inpatient and outpatient stroke services at Cambridge University Hospitals NHS Foundation Trust and the National CADASIL service run by Prof Hugh Markus. Figure 4.2 shows the inclusion and exclusion criteria for the study. Control participants were recruited from a database of healthy individuals who had indicated that they would be willing to take part in stroke research. Although presence of auto-immune and inflammatory diseases or prescription of immunomodulatory treatments were not explicit exclusion criteria for this study, in practice this did not apply to any of the recruited participants.

Inclusion criteria

Sporadic SVD group

- Clinical evidence of a lacunar stroke syndrome (eg pure motor stroke, pure sensory stroke, sensorimotor stroke or ataxic hemiparesis, or clumsy hand dysarthria syndrome) with a corresponding acute lacunar infarct on diffusion weighted imaging (DWI) for cases imaged (clinically) within 3 weeks of stroke or an anatomically compatible lacunar infarct on
- FLAIR/T1 MRI for cases imaged later after stroke (≤ 1.5 cm diameter).
- Confluent white matter hyper-intensities on T2 weighted MRI
- At least 3 months after last stroke to exclude BBB changes secondary to acute infarction.

CADASIL group

- Subjects with a confirmed genetic diagnosis due to a recognised NOTCH 3 mutation
- At least 3 months after last stroke to exclude BBB changes secondary to acute infarction.

Control group

- Stroke free subjects of similar age to patient groups
- No evidence of other major neurological conditions

Exclusion criteria

SVD and CADASIL group exclusion criteria:

- Unable/unwilling to consent
- MMSE < 21 (for consent issues)
- Age < 18
- Lacunar infarcts > 1.5 cm – as many of these are striatocapsular infarcts caused by embolism
- Evidence of cortical stroke
- Any stroke cause other than SVD including:
- Cardioembolic source
- Carotid or vertebral stenosis $> 50\%$ measured on NASCET criteria
- Estimated glomerular filtration rate (eGFR) $= < 59$ ml/min/1.73m² within past 3 months. Estimated GFR will be calculated using the Modification of Diet in Renal Disease (MDRD) equation:
- $186 \times (\text{Creatinine} / 88.4)^{1.154} \times (\text{Age} - 0.203 \times (0.742 \text{ if female}) \times (1.210 \text{ if black})$
- No contraindications to taking part in MRI study, e.g., pacemaker
- Women of child bearing age

Control groups exclusion criteria:

- Unable/unwilling to consent
- MMSE < 21 (for consent issues)
- Age < 18
- Any MRI evidence of lacunar infarcts or leukoaraiosis ($> \text{grade } 1$ in either periventricular or deep white matter regions on the Fazekas scale
- eGFR $= < 59$ within past 3 months
- No contraindications to taking part in MRI study, e.g., pacemaker
- Women of child bearing age

Figure 4.2. Inclusion and exclusion criteria of observational phase PET-MRI cohort.

Imaging acquisition

The neuroimaging protocol included PET and MRI which were co-acquired on a 3T GE SIGNA PET-MRI scanner (GE Healthcare, Waukesha, WI, USA) at the Wolfson Brain Imaging Centre in Cambridge, UK. Baseline imaging included:

1. PET data acquisition for 75 minutes following the injection of ^{11}C -PK11195 (target injection activity 500MBq) produced at the Wolfson Brain Imaging Centre Radiopharmaceutical Unit.
2. Simultaneous whole brain non-contrast MRI using a 32-channel head coil (Nova Medical, Wilmington, MA, USA) including T₁- and T₂-weighted images, FLAIR, DTI and susceptibility weighted images. Complete sequence details are given in Appendix B.
3. DCE-MRI to acquire dynamic T1 maps in a sub-volume of the brain chosen by the researcher to be representative of the burden of SVD in each patient. A Gadoterate meglumine, a Gadolinium-based contrast agent (Dotarem®) was injected at a sub-clinical dose of 0.025mmol/kg. The dynamic T1 relaxation time was mapped prior to injection and this was followed by eight cycles of post injection T1 mapping using an in-house developed pulse sequence that repeatedly acquires six 3D radiofrequency spoiled gradient echo images with different flip angles.

Follow-up MRI only imaging was performed after one year and included T1- and T2-weighted images, FLAIR, DTI and susceptibility-weighted images acquired on the same scanner.

Image analysis

WMH lesions were marked using Jim version 8.0 (<http://xinapse.com/j-im-software/>). The method described in chapter three was employed to blind the rater to timepoint;

baseline and follow-up images were marked slice by slice on a parallel split screen and displayed randomly in terms of order of acquisition to reduce the risk of bias. T1 images were processed using the ‘Segment’ routine in SPM12 to produce tissue probability maps for each tissue class after removal of the WMH mask. WMH and normal appearing white matter masks were then eroded by 3mm to eliminate contamination from CSF or grey matter.

The T1 maps from the DCE-MRI were calculated using the standard radiofrequency spoiled-gradient echo signal equation and used to estimate the gadolinium concentration in tissue using a Patlak graphical analysis to determine influx rate (K_{in}) as the measure of BBB permeability.³¹⁰ As there is no artery in the field of view, the superior sagittal sinus was used as an arterial input function, corrected by the factor $(1 - \text{haematocrit})$, which is assumed to be representative of the arterial concentration of contrast agent.³¹¹ Voxels of increased BBB permeability (‘hotspots’) were defined as those with a K_{in} greater than the 95th percentile of permeability derived from an existing cohort of stroke-free control participants.

List-mode PET data were histogrammed into 55 time bins and reconstructed using time-of-flight ordered subsets expectation-maximization (matrix size $128 \times 128 \times 89$, final resolution $2.0 \times 2.0 \times 2.8\text{mm}$).³¹² Attenuation correction was performed using a multi-subject atlas method.³¹³ Images were reconstructed to correct for random coincidences, dead time, normalization, scattered coincidences, radioactive decay, and sensitivity. SPM12 was used to realign each dynamic image series which was then co-registered with the T1 MRI sequence using a mean realigned PET image.

The specific binding of ^{11}C -PK11195 was estimated by determining the binding potential relative to a non-displaceable reference tissue (BP_{ND}) using a basis function implementation of the simplified reference tissue model, incorporating correction for vascular binding.³¹⁴ The white matter reference tissue input was estimated by supervised cluster analysis³¹⁵ using data from a library of previously-collected ^{11}C -PK11195 scans of healthy control participants using the same PET-MRI scanner.

Binding hotspots were defined similarly to the BBB permeability measures above as voxels about the 95th percentile of control participants. Figure 4.3 shows an example of the maps of ¹¹C-PK11195 binding and BBB permeability hotspots that were produced using this technique.

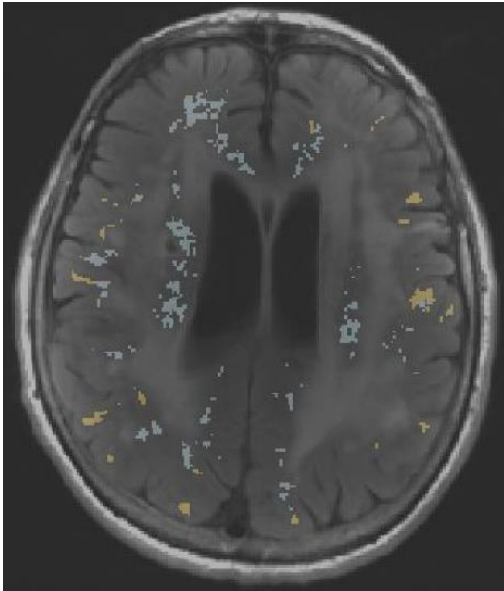


Figure 4.3. Representative FLAIR image from a study patient with hotspot maps of BBB permeability (yellow) and ¹¹C-PK11195 binding (blue) overlaid.

DTI images were analysed using FSL software ("FDT"; FMRIB's Diffusion Toolbox, <http://fsl.fmrib.ox.ac.uk/fsl/fslwiki/FDT>) to correct for eddy current effects and to create a binary brain mask in DTI space. Maps of FA and MD were created from this data using the DTIFIT tool. Spurious cerebrospinal fluid voxels based on thresholds of MD values above $2.6 \times 10^{-4} \text{ mm}^2\text{s}^{-1}$ and $\text{FA} > 1$ were removed. For each participant, the FMRIB Linear Image Registration Tool was used to register the FLAIR and B0 images. Tissue segments and WMH masks were then transformed into DTI space and used to create tissue specific FA and MD histograms.

Blood sampling, processing, and analysis

10ml of blood was collected at the baseline imaging appointment into serum separator tubes. After being left for at least 30 minutes to clot, the samples were centrifuged at 1000g for 15 minutes and the supernatant was aliquoted into 2ml Eppendorf tubes. Samples were stored at -80°C for *en bloc* analysis.

Samples were sent to the University of Cambridge Core Biochemical Assay Laboratory for measurement of high sensitivity C-reactive protein (hsCRP) using an enzyme-linked immunosorbent assay (Siemens Healthineers, Erlangen, Germany).

A further sample was sent for analysis using a commercially available proteomics platform (Olink; <https://olink.com/>). This platform uses a novel proximity extension assay technique incorporating a specific antibody against each target protein that has been modified with a single strand DNA primer; complementary pairs hybridise and are amplified by quantitative PCR where the numbers of cycles required is taken as a negative proxy for the concentration of the target protein. I selected the Cardiovascular Disease III panel which includes 92 protein biomarkers related to cardiovascular disease and inflammation, including cell adhesion molecules such as ICAM-2, matrix metalloproteases such as MMP-3, MMP-9 and TIMP-4, and conventional markers of cardiovascular endothelium activation or angiogenesis such as vWF and t-PA (<https://www.olink.com/products-services/target/cardiometabolic-panel/>).

Neuropsychometric testing

Participants underwent neuropsychometric testing at the baseline appointment using a panel of cognitive tests that have previously been optimised for use in patients with SVD.³⁹ These were specifically chosen to assess the cognitive domains that are typically impacted in SVD (executive function – EF, processing speed – PS and working memory – WoM). Long term memory (LTM) was also assessed. Details of the panel of tests included is given in table 4.1. In addition, an estimate of pre-morbid IQ was obtained using the National Adult Reading Test (NART – restandardised, 2nd Edition³¹⁶).

Performance on each task was transformed to a *z*-score by comparison with the best available age scaled reference data. The *z*-scores from each task were averaged within each domain tested to produce an overall domain score; an overall global cognition (GC) score was constructed by averaging across domains.

Neuropsychometric domain	Assessments used
Working memory	Digit span
Episodic (long term) memory	Logical memory I & II and visual reproduction I & II from the Wechsler Memory Scale-IV (www.pearsonclinical.co.uk)
Processing speed	Digit symbol substitution, Brain Injury Rehabilitation Trust Memory and Information Processing Battery (www.thedtgroup.org/research/bmipb), and the grooved pegboard task (https://www.advys.be/docs/)
Executive function	Trail-making test (part B, Reitan, R. M., & Wolfson, D. (1985). <i>The Halstead-Reitan Neuropsychological Test Battery: Therapy and clinical interpretation</i> . Tucson, AZ: Neuropsychological Press), single letter verbal fluency, and the Wisconsin card sort test (Grant, D. A., Berg, E. (1948). A behavioral analysis of degree of reinforcement and ease of shifting to new responses in a Weigl-type card-sorting problem. <i>Journal of Experimental Psychology</i> , 38, 404-411)

Table 4.1. Cognitive domains assessed and specific neuropsychometric test used in each domain in the observational phase.

Ethical and regulatory approval

This study was approved by the East of England -Cambridge South Research Ethics Committee (reference: 16/EE/0468) and the Administration of Radioactive Substances Advisory Committee (ARSAC ref: 83/3886/35752). All participants provided informed written consent.

Phase II: the MINocyclinE to Reduce blood-brain barrier permeability and inflammation in small Vessel disease (MINERVA) trial

44 participants were recruited to the interventional phase of the study. The MINocyclinE to Reduce blood-brain barrier permeability and inflammation in small

Vessel disease (MINERVA) study is a double-blind, placebo-controlled randomised clinical trial of Minocycline in patients with SVD.

Minocycline is a semi-synthetic tetracycline-derivative antibiotic that has been modified to increase its penetrance into the CNS. Minocycline is purported to have anti-inflammatory properties within the brain, reducing the activation of microglia,³¹⁷ and may be effective in stabilising the BBB.³¹⁸ In a rodent model of SVD (using the spontaneously hypertensive stroke-prone rat), it was significantly associated with reduced white matter damage and with improved behavioural and survival outcomes.²³⁴ Similar experiments in a different preclinical model (Wistar rats which underwent permanent bilateral carotid artery occlusion) showed that minocycline treatment was significantly associated with a reduction in ischaemic damage in white matter tracts and attenuated immunohistochemical staining of MMP-2.³¹⁹ Additionally, in mice with bilateral carotid artery stenosis, minocycline treatment was associated with preservation of electrophysiological response in the corpus callosum and with a reduction in microglial proliferation seen in post-mortem immunohistochemical studies.³²⁰

Primary outcomes from the MINERVA study should provide robust evidence of whether this intervention can influence the inflammatory response in SVD based on ¹¹C-PK11195 binding, and whether it can affect BBB permeability measured by DCE-MRI. If positive, it would imply that both processes can be altered in parallel, whereas if only the PET or DCE-MRI outcomes are positive it would provide further evidence that these changes occur at different points in the disease process and should be targeted by different disease modifying strategies.

In addition to these primary endpoints of microglial activation and BBB permeability, the MINERVA study should provide detailed assessments of the effect of this intervention on radiological measurements of SVD and the activation of the systemic immune response using conventional MRI markers of SVD and immunophenotyping

of peripheral blood respectively. Follow up after one year will allow assessment of any longer-term effects on brain structure/pathology and cognitive performance.

Inclusion and exclusion criteria were broadly the same as in the sporadic SVD arm of the observational study. White matter disease caused by CAA might have different pathological mechanisms, and participants with probable CAA defined using the modified Boston criteria³²¹ (2010 version, superseded after trial recruitment ended) were excluded. Patients with known or suspected monogenic forms of SVD, including CADASIL, were also excluded pending confirmatory genetic testing.

Figure 4.4 illustrates the MINERVA study design. The study protocol already been published³⁰⁷ and relevant parts of the methods are presented here.

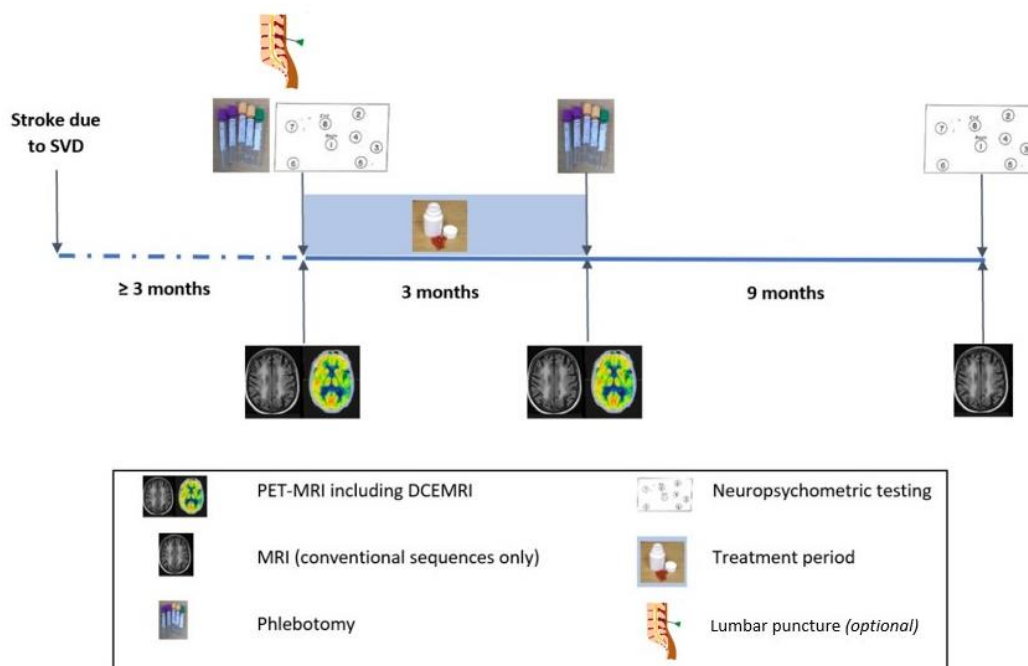


Figure 4.4. MINERVA study design and trial flowchart.

Trial procedures and interventions

Patients were randomised to intervention or placebo in the ratio 1:1 with a random permuted block randomisation design (block size of 2/4). Randomisation was performed via a web-based system managed by Sealed Envelope Ltd

(www.sealedenvelope.com). Participants in the intervention arm received minocycline 100mg orally twice daily; participants in the placebo arm took a matching cellulose capsule. Participants and investigators were blinded to treatment allocation.

Participants underwent visits at baseline (for PET-MRI using the imaging protocol as above in the observational phase, blood sampling and neuropsychometric testing), six weeks (for clinical check-up) and three months (for post-treatment data collection, phlebotomy and repeat PET-MRI). Participants will be followed up again at one year for non-contrast MRI and repeat neuropsychometry (data collection ongoing).

All participants were asked if they would consent to CSF sampling by lumbar puncture and if consenting this was also performed at the baseline appointment.

Patient selection

Participants were recruited from inpatient and outpatient stroke services at Cambridge University Hospitals NHS Foundation Trust. Figure 4.5 shows the inclusion and exclusion criteria for the study.

Imaging acquisition

The baseline neuroimaging protocol included identical sequences described above and given fully in Appendix B for the observational phase study, with the addition of a arterial spin-labelled sequence (ASL). This PET-MRI protocol was repeated on completion of treatment after three months. One year follow up includes the conventional MRI sequences only, again with the addition of an ASL sequence.

Image analysis

Image analysis was performed as described above in the observational phase.

Eligibility Criteria

Inclusion criteria

- Clinical evidence of cerebral small vessel disease as evidenced by one or more of:
 - a lacunar stroke syndrome (e.g. pure motor stroke, pure sensory stroke, sensorimotor stroke or ataxic hemiparesis, or clumsy hand-dysarthria syndrome) with a corresponding acute subcortical infarct on diffusion weighted imaging (DWI) for cases imaged (clinically) within three weeks of stroke or an anatomically compatible lacunar infarct on FLAIR/T1 MRI for cases imaged later after stroke (≤ 1.5 cm diameter).
 - Self-reported symptoms of cognitive impairment
 - Gait apraxia

AND

- Confluent white matter hyperintensities on T2 weighted MRI (Fazekas scale score ≥ 2)

Exclusion criteria

- Unable/unwilling to consent
- Recorded diagnosis of dementia for consent issues and to ensure cognitive testing is possible (or lack of capacity to consent and complete testing via clinician assessment)
- Age < 18
- Lacunar infarcts >1.5cm – as many of these are striatocapsular infarcts caused by embolism
- Evidence of cortical stroke
- Any stroke cause other than SVD including:
 - Cardioembolic source
 - Carotid or vertebral stenosis >50% measured on NASCET criteria
- Estimated glomerular filtration rate (eGFR) ≤ 59 ml/min/1.73m² within past three months. Estimated GFR will be calculated using the Modification of Diet in Renal Disease (MDRD) equation:
 $186 \times (\text{Creatinine} / 88.4)^{-1.154} \times (\text{Age})^{-0.203} \times (0.742 \text{ if female}) \times (1.210 \text{ if black})$
- No contraindications to taking part in MRI study, e.g. pacemaker
- Women of childbearing potential, pregnant or breastfeeding
- Concurrent inflammatory/autoimmune conditions or taking immunosuppressive or immunomodulatory medication
- Other neurological or neurodegenerative disorder
- Absolute or relative contraindications to treatment with minocycline:
 - Allergic to minocycline hydrochloride or other similar antibiotics
 - Suffer from myasthenia gravis, have impaired liver or kidney function, or systemic lupus erythematosus (SLE)
 - Sensitivity to sunlight or artificial light (e.g. sunbeds)
 - Taking medication contraindicated with minocycline

Figure 4.5. MINERVA inclusion and exclusion criteria

Blood sampling, processing, and analysis

10ml serum was collected and processed as above in the observational phase to be analysed for hsCRP and the Olink CVD-III proteomic panel, both pre- and post-treatment. A further aliquot was sent to the UK Dementia Research Institute Fluid Biomarkers Laboratory (University College London) for quantification of neurofilament light (NfL) and glial fibrillary acidic protein (GFAP) using the Simoa® platform (Quanterix, Billerica, MA, USA). This technology uses antibodies against a target bound to larger paramagnetic beads, in combination with a fluorescent detection antibody. At ultra-low concentrations, each bead binds one or no molecules of the target antigen and the sample is then loaded into a 200,000 microwell array where the fluorescence can be quantified.

6ml whole blood was collected in a sodium heparin tube and analysed with the CyTOF® mass cytometry platform using a Helios™ cytometer (Standard BioTools Inc, San Francisco, CA, USA), also both pre- and post-treatment. Mass cytometry allows high dimensional profiling of immune cells where antibodies against the key discriminatory surface antigens are conjugated with heavy metal cations, avoiding between-channel crosstalk that can be an issue for conventional fluorescence-based flow cytometry. I selected the Maxpar® Direct™ Immune Profiling assay which is a preconfigured and standardised 30 antibody channel analysis tube allowing identification of 37 cell lines including classical, non-classical and intermediate monocytes, B- and T-lymphocyte subsets, granulocytes, and NK cells (table 4.2; product literature available at <https://fluidigm.com/area-of-interest/immune-profiling/>).

Neuropsychometric testing

Participants underwent the same neuropsychometric test battery as those included in the observational phase study; additionally they were asked to complete the Geriatric Depression Scale and Fatigue Severity Scale questionnaires (table 4.3).

Cell surface markers	Cell lines identified
<ul style="list-style-type: none"> • CD3 • CD4 • CD8 • CD11c • CD14 • CD16 CD19 • CD20 • CD25 • CD27 • CD28 • CD38 CD45 • CD45RA • CD45RO 	<ul style="list-style-type: none"> • CD56 • CD57 • CD66b • CD123 • CD127 • CD161 • CD294 • CCR4 • CCR6 CCR7 • CXCR3 • CXCR5 • HLA-DR • IgD • TCR$\gamma\delta$
	<ul style="list-style-type: none"> • Naïve, central memory, effector memory, terminal effector CD4+ T cells • TH1, TH2, TH17 T cells • Regulatory T cells • $\gamma\delta$ T cells • Naïve, central memory, effector memory, terminal effector CD8+ T cells • NK T cells • Early and late NK cells • Naïve, memory and plasmoblast B cells • Classical, intermediate and non-classical monocytes • Myeloid and plasmacytoid dendritic cells • Neutrophils, basophils, eosinophils

Table 4.2. (A) Antibody panel used in Maxpar® Direct™ Immune Profiling assay and cell line profile identified.

Cerebrospinal fluid sampling

All patients enrolled in the trial were asked if they would additionally give a sample of cerebrospinal fluid (CSF), taken via a lumbar puncture (LP). If they consented, LP was performed at the baseline appointment (after the MRI scan, to avoid any spurious increases in BBB permeability introduced by the procedure) or the day after. Imaging was reviewed to ensure that there were no contraindications to the procedure (including raised intracranial pressure) and participants who were normally taking clopidogrel for stroke secondary prevention prescribed aspirin instead for seven days prior to the procedure in accordance with guidance from the Association of British Neurologists.³²²

Neuropsychometric domain	Assessments used
Working memory	Digit span
Episodic (long term) memory	Logical memory I & II and visual reproduction I & II from the Wechsler Memory Scale-IV (www.pearsonclinical.co.uk)
Processing speed	Digit symbol substitution, Brain Injury Rehabilitation Trust Memory and Information Processing Battery (www.thedtgroup.org/research/bmipb), and the grooved pegboard task (https://www.advys.be/docs/)
Executive function	Trail-making test (part B, Reitan, R. M., & Wolfson, D. (1985). <i>The Halstead-Reitan Neuropsychological Test Battery: Therapy and clinical interpretation</i> . Tucson, AZ: Neuropsychological Press), single letter verbal fluency, and the Wisconsin card sort test (Grant, D. A., Berg, E. (1948). A behavioral analysis of degree of reinforcement and ease of shifting to new responses in a Weigl-type card-sorting problem. <i>Journal of Experimental Psychology</i> , 38, 404-411)
Mood assessment (apathy and depression)	Geriatric Depression Scale (http://www.stanford.edu/~yesavage/GDS.html)
Fatigue severity assessment	Fatigue severity scale (Krupp, L. B., LaRocca, N. G., Muir-Nash, J., & Steinberg, A. D. (1989). The fatigue severity scale. Application to patients with multiple sclerosis and systemic lupus erythematosus. <i>Archives of Neurology</i> , 46, 1121-1123)

Table 4.3. Cognitive domains assessed and specific neuropsychometric tests and questionnaires used in each domain in the MINERVA trial

Patients were positioned in the left lateral decubitus position and 4-5ml 1% lidocaine was infiltrated at the L3/4 or L4/5 spinal level. A 22G atraumatic spinal needle was inserted and 30ml CSF withdrawn. Participants were advised to lie flat for 30-60 minutes after the procedure to minimise the risk of lumbar puncture associated headache.

10ml CSF was centrifuged at 2000g for 10 minutes. The supernatant was aliquoted into 2ml Eppendorf tubes and stored at -80°C for *en bloc* analysis. CSF albumin was measured at the University of Cambridge Core Biochemical Assay Laboratory by ELISA using a Siemens Dimension EXL auto-analyser . To allow calculation of the CSF/serum albumin ratio, CSF samples were sent with a matching sample of serum from the same patient as collected above which was also quantified using ELISA by the same method.

CSF samples were also sent to the UK Dementia Research Institute Fluid Biomarkers Laboratory (University College London) to measure NfL and GFAP using the Simoa® platform as above.

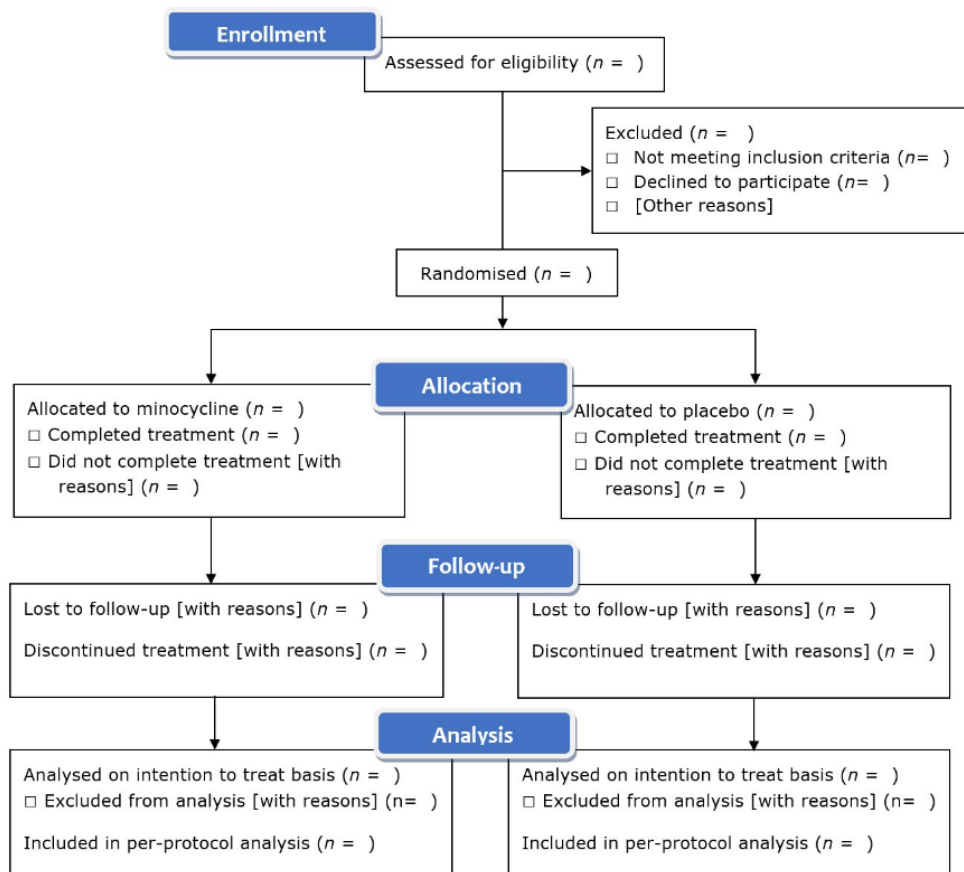


Figure 4.6. MINERVA study CONSORT reporting diagram template.

Statistical analysis and power calculations

Participant recruitment is reported in a Consolidated Standards of Reporting Trials (CONSORT) diagram (template shown in figure 4.6). Differences between the treatment and placebo groups will be tested using χ^2 tests (categorical data) and one way ANOVA or Mann-Whitney U tests (for normal or non-normal continuous data) as appropriate.

Primary outcome analysis will be performed on an intention-to-treat basis, including all randomised participants. As the MINERVA trial primary outcomes consider the treatment with minocycline as an experimental probe rather than a clinical endpoint, intention-to-treat analysis might bias the results towards the null hypothesis and so per-protocol analysis will also be performed including only participants who complete the treatment course. Outcomes will be tested using standard regression models both unadjusted and adjusted for age, sex and demographic or clinical variables that are significantly different between groups.

Using the data from the observational phase study²¹³, I calculated that in order to show a 20% reduction in ¹¹C-PK11195 binding metrics with power of 80% and $\alpha = 0.05$, we require 17 participants in each arm. To demonstrate a 20% reduction in BBB permeability with these constraints, 21 participants per arm are required. The sample size of 22 per arm encompasses these requirements.

Safety and adverse event reporting

The radiation dose during PET imaging is approximately 2.6mSv (the equivalent of one year of background environmental radiation). Participant information states that this confers a small additional lifetime risk of developing cancer, and patients consent explicitly to this level of radiation exposure. 3T MRI does not have any adverse clinical effects, but as gadolinium contrast usage can lead to nephrogenic systemic fibrosis in participants with renal dysfunction, only patients with an estimated glomerular filtration rate of 60ml/min/1.73m² were recruited.

Minocycline is a safe and well-tolerated medication but potential side effects include gastrointestinal disturbance, dizziness, and skin rashes/discoloration. Patients are provided with an alert card and emergency contact details for the study clinician in case of any possible side effects. Data are collected on adverse reactions in keeping with the Summary of Product Characteristics for minocycline during the treatment period. Additional safety outcomes include recurrent stroke or other cardiovascular events during the treatment period and at one year, and change in neuropsychometric test performance.

Data capture / data access

Data were recorded electronically using an online research data management tool (REDCap) hosted at the University of Cambridge.³²³ REDCap (Research Electronic Data Capture) is a secure, web-based software platform designed to support data capture for research studies, providing validated data capture, audit trails for tracking data manipulation and export procedures, and procedures for importing data from external sources. After study completion, cleaning and database finalisation and our pre-specified analyses, anonymised data will be made available for secondary uses to the wider scientific community subject to reasonable request.

Ethical and regulatory approval

The MINERVA study was approved by the East of England – Cambridge Central Research Ethics Committee (reference 18/EE/0237) and was classified as a non-CTIMP (clinical trial of investigational medical product) by the Medicines and Healthcare products Regulatory Authority. The use of ¹¹C-PK11195 was approved by the UK Administration of Radioactive Substances Advisory Committee (ARSAC, Research ID 176; 19/09/2018). The study was registered prospectively on the International Clinical Trials Registry Portal (reference ISRCTN15483452).

The cerebrospinal fluid sampling was approved by the East of England – Cambridge Central Research Ethics Committee (reference 19/EE/0008).

Potential limitations

The MINERVA study was There are potential limitations to this trial. The PET radioligand used is known to have off-target binding³²⁴ and its receptor is expressed in multiple cell lines in addition to microglia²³⁰; the application of a reference tissue kinetic model described above aims to mitigate this by increasing the specificity for brain parenchyma. In addition, the resolution of PET imaging is not as high as the 3T MR images and this may provide less anatomically specific details about the resolution of any areas of increased signal.

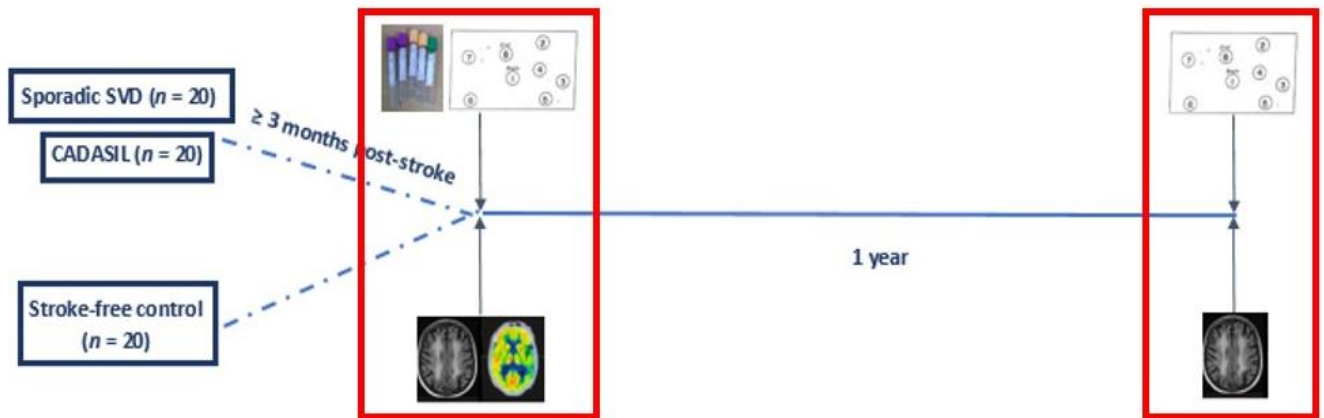
A further consideration is that the dose of minocycline that was effective in the rodent model²³⁴ may not translate to a human study. Minocycline has previously been tested unsuccessfully in neurodegenerative conditions such as Parkinson's disease,³²⁵ and Alzheimer's disease³²⁶, as well in neurological disorders with a less obvious inflammatory or degenerative component such as traumatic brain injury³²⁷ and schizophrenia.³²⁸ Issues with adverse effects, compliance and equivalent dosing might impact translatability; particularly the latter as doses used in preclinical studies are generally significantly higher than the licensed dose in humans. However, this mechanistic study using advanced neuroimaging markers might provide proof-of-concept level evidence even if clinical benefit is not demonstrated. If positive, the results might inform sample size calculations for future trials powered to detect clinical efficacy and support the testing of alternative pharmacological agents to dampen the innate immune response.

Pooled PET-MRI cohort

For the purposes of assessing baseline associations between demographic variables and cardiovascular risk factors and measurements of BBB permeability, ¹¹C-PK11195 binding and markers of inflammation in peripheral blood, patients with SVD from the observational phase study were pooled with unique patients recruited to the MINERVA trial. Figure 4.7 shows which elements of the study procedures are

analogous; as the treatment in the MINERVA could potentially affect one year outcomes, and the study is ongoing, the data in the remainder of this thesis is from the baseline visits only (pooled cohort) or from the observational phase patients at baseline and follow-up.

OBSERVATIONAL PET-MRI STUDY



MINERVA TRIAL

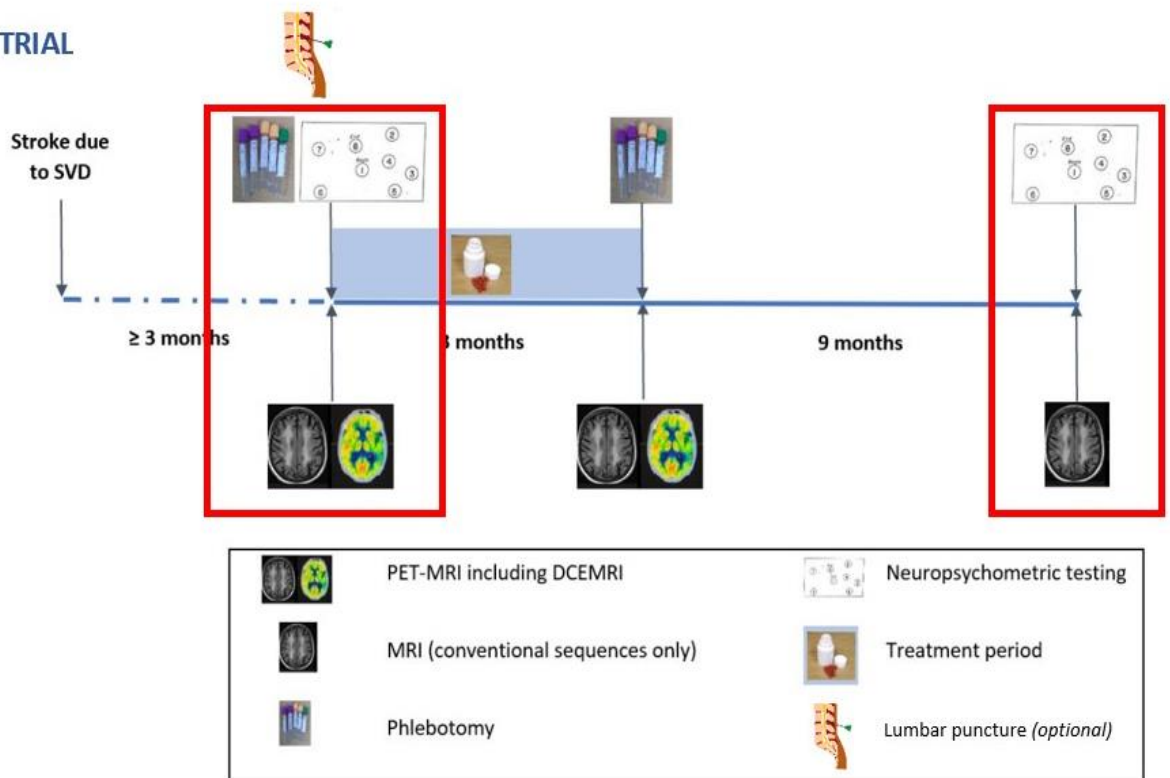


Figure 4.7. Schematic study diagrams of the observational phase cohort and the MINERVA trial with common study interventions highlighted in red.

CHAPTER FIVE

Participant demographics, conventional MRI and DTI results, and neuropsychometric testing

I recruited the participants to the interventional study, collected demographic data, performed neuropsychometric testing, performed follow-up neuropsychometric testing for the observational phase participants, analysed the imaging and analysed the results. Jessica Walsh recruited the participants to the observational phase, and performed baseline neuropsychometric testing. Daniel Tozer assisted with the image analysis.

Introduction

This chapter summarises the recruitment to the observational and interventional phase studies. Details of the observational cohort and differences between the sporadic SVD, CADASIL and control subgroups have previously been presented^{213,329}; here I discuss only the sporadic SVD subgroup and the control participants. I present the recruitment and demographic details of the MINERVA study and test for any differences in demographics and comorbidities between this cohort and the sporadic SVD subgroup in the observational study. Finally I present the baseline neuropsychometric testing results, comparing both the pooled patient group to control participants and the patients with sporadic SVD from the observational cohort to those in the MINERVA trial.

As the MINERVA study is ongoing, data presented include only those collected at baseline (i.e. prior to commencement of treatment).

Of note, seven patients participated in both the observational and interventional phases of the study. For the purposes of comparing the relationships between their baseline demographics, comorbidities and neuroimaging measurements, the baseline was taken to be the first visit of the observational study. For the purposes of comparing the observational and interventional cohorts, these participants were included in both groups.

I hypothesised that the patient group would have a higher burden of comorbidity and more severe radiological markers of SVD than the control population, and that neuropsychometric test scores would be correspondingly lower. I further hypothesised that the age of the trial participants would be older and there would be a longer gap from stroke to recruitment, as some participants overlapped in both and were by definition older at the point of enrolment into the trial phase. However, given that the interventional phase required significantly more participant commitment and was significantly more intensive, an alternative hypothesis would be that younger and less frail participants were more likely to participate in the trial.

Methods

Participants were recruited as described in chapter four. At the baseline appointment, demographic details, and medical history including comorbidities and medications were collected. Participants underwent DCE-MRI and neuropsychometric testing as described above.

Statistical analysis

Demographic data included categorical and continuous data. Between group differences were tested using χ^2 or Fisher's exact tests (in case of group sizes of five or less) for categorical data and unpaired Student's *t*-test or Mann-Whitney U tests (for normal or non-normal continuous data defined using the Shapiro-Wilk test). False discovery rate correction was applied to account for multiple comparisons.

Logistic regression models for neuropsychometric test score were constructed to test the difference in performance between patient and control groups, including as covariates sex, and baseline IQ which are known to predict performance in patients with SVD on a similarly constructed battery of cognitive tests.³⁹ Age was not included in the model as the neuropsychometric test results are already age-corrected.

Results

Observational phase recruitment

40 participants were recruited between 2017 and 2019; 20 in the sporadic SVD subgroup and 20 stroke-free control participants. Technical issues with the PET-MRI scanner, the intravenous access line for gadolinium contrast injection and ¹¹C-PK11195 production activity or quality control resulted in the following numbers of participants having complete data collected (table 5.1):

	Sporadic SVD (<i>n</i> = 20)	Control (<i>n</i> = 20)	Total (<i>n</i> = 40)
Non-contrast MRI	20	19	59
DCE-MRI	19	19	57
PET	17	17	48
Phlebotomy	20	20	60
Neuropsychometric testing	20	20	60

Table 5.1. Number of participants in each subgroup with complete images for non-contrast MRI, DCE-MRI and PET respectively.

Serum samples were taken and neuropsychometric testing performed in all participants.

MINERVA trial recruitment

44 participants with sporadic SVD were recruited between 2019 and 2022. In the event of technical issues compromising radioligand production or DCE-MRI acquisition, every attempt was made to reschedule the appointment to maximise the data collected in these domains.

Three participants were unable to tolerate the MRI scanner due to claustrophobia, and one further participant was unable to rearrange the appointment after radioligand production failure, leaving 40 participants who completed the PET imaging. Four participants were found to have $eGFR < 60\text{ml}/\text{min}/1.73\text{m}^2$ on the day of the scan appointment; this ordinarily would have been checked before the scan appointment but this was not possible at times in 2020-2021 due to the Covid-19 pandemic; these patients underwent non-contrast MRI and PET imaging but not DCE-MRI sequences. One participant was recruited while still an inpatient after stroke and did not complete the neuropsychometric testing due to the severity of ongoing physical disability.

Sporadic SVD (n = 44)			
Non-contrast MRI	41	Phlebotomy - serum	43
DCE-MRI	37	Phlebotomy - CyTOF	25
PET	40	CSF	18
Neuropsychometric testing	43		

Table 5.2. Number of MINERVA participants completing each aspect of the trial protocol (baseline appointment).

Comparison of patient groups and control

After merging the cohorts as above, I included 57 individual patients with sporadic SVD and 20 stroke-free control participants. Figure 5.1 displays the merged cohort graphically, plotted by age and baseline WMH volume and stratified by group (patient vs control) and sex.

The patient cohort was slightly older than the control group (mean age 69.8 ± 10.5 compared to 66.3 ± 6.7 years respectively, $p = 0.14$) and had a slightly lower proportion of male participants (59.6% compared to 65%, $p = 0.88$). There were no significant differences in ethnic background between the two populations (defined as proportion identifying as White British) or years in education. Regarding vascular risk factors, the patient cohort was significantly more likely to have hypertension (87.7% versus 30.0%, $p = 2.6 \times 10^{-6}$) and hypercholesterolaemia (73.7% versus 35.0%, $p = 0.0047$) and had a significantly higher BMI (29.9 ± 8.4 kg/m² compared to 26.3 ± 3.3 kg/m², $p = 0.014$). There were no significant differences in proportion with diabetes, systolic / diastolic blood pressure or smoking status. Regarding comorbidities, there was no significant difference in the prevalence of depression or migraine. The comparison of demographics, vascular risk factors and comorbidities is presented in

table 5.3. No participants in either phase of the study were prescribed regular immunomodulatory, immunosuppressive or anti-inflammatory medications.

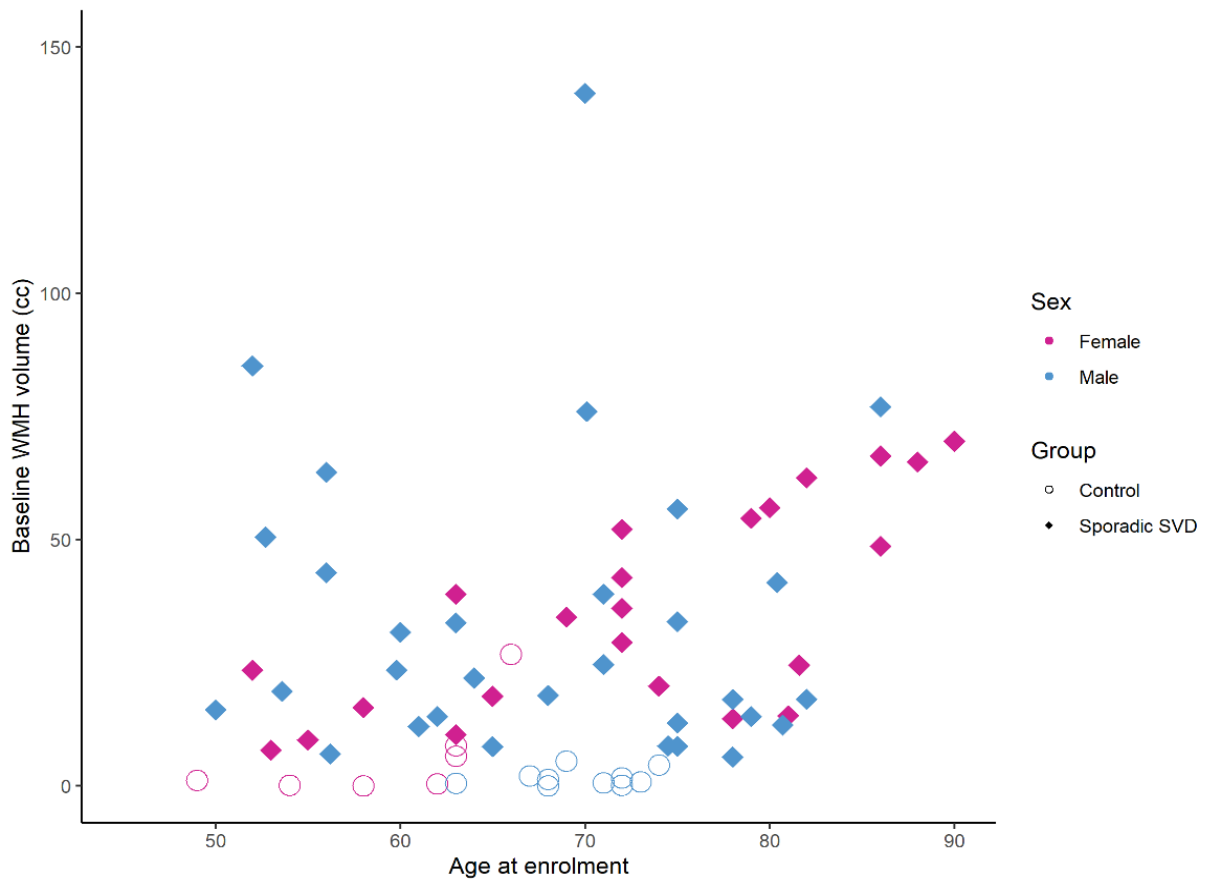


Figure 5.1. Combined PET-MRI cohort plotted by age and baseline WMH volume, stratified by sex and participant group.

Baseline conventional neuroimaging findings differed significantly between the patient and control groups. As expected, indices of SVD burden were more severe in the patient group, with higher WMH volume (29.9 ± 24.5 cc compared to 3.1 ± 6.10 cc, $p < 1 \times 10^{-6}$), lacune count (2.6 ± 2.0 compared to 0.05 ± 0.22 , $p < 1 \times 10^{-6}$), number of microbleeds (3.5 ± 11.6 compared to 0.15 ± 0.49 , $p < 1 \times 10^{-6}$) and lower total brain volume (1413.9 ± 81.7 cc compared to 1448.9 ± 44.1 cc, $p = 0.026$). MRI markers of SVD are presented in table 5.4.

		Sporadic SVD (n = 57)	Control (n = 20)	p value
Demographics				
Age (years)		69.9 ± 10.5	66.3 ± 6.7	0.08
Sex	Male	34 (59.6)	13 (65.0)	0.88
	Female	23 (40.4)	7 (35.0)	
Ethnicity				
	White British	48 (84.2)	19 (95.0)	0.40
	White Irish	4 (7.0)	1 (5.0)	
	White other	4 (7.0)		
	Asian (Pakistani)	1 (1.8)		
Years in education		13.6 ± 2.9	13.4 ± 3.8	0.80
Vascular risk factors				
Hypertension		50 (87.7)	6 (30.0)	2.6 × 10⁻⁶
SBP (mmHg)		146.6 ± 22.6	142.1 ± 17.7	0.41
DBP (mmHg)		76.3 ± 13.1	81.2 ± 9.0	0.11
Ischaemic heart disease		<i>Data only collected in trial cohort</i>		
Hypercholesterolaemia		42 (73.7)	7 (35.0)	0.0047
Diabetes mellitus		11 (19.3)	1 (5.0)	0.17
Smoking (current)		26 (45.6)	8 (40.0)	0.97
BMI (kg/m²)		29.9 ± 8.4	26.3 ± 3.3	0.014
Co-morbidities				
Depression		17 (29.8)	7 (35.0)	0.88
Migraine		17 (29.8)	5 (25.0)	0.90
Time since last stroke (months)		12.3 (5.1-20.5)	n/a	n/a

Table 5.3. Comparison of demographic and clinical factors between sporadic SVD cohort and control group. Values are number of patients (%) for categorical variables and mean ± SD or median (IQR) for continuous variable. *SBP systolic blood pressure; DBP diastolic blood pressure; BMI body mass index; * significant at FDR corrected $p < 0.05$;*

	Sporadic SVD (n = 57)	Control (n = 20)	p value
Conventional MRI markers of SVD severity			
WMH volume (cc)	29.9 ± 24.5	3.1 ± 6.1	* < 1 × 10⁻⁶
Lacunae	2.6 ± 2.0	0.05 ± 0.22	* < 1 × 10⁻⁶
CMBs	3.5 ± 11.6	0.15 ± 0.49	*0.003
Brain volume (cc)	1413.9	1448.9	*0.026

Table 5.4. Comparison of radiological markers between sporadic SVD cohort and control group. Values are mean ± SD. *WMH* white matter hyperintensities; *CMBs* cortical microbleeds; * significant at FDR corrected $p < 0.05$

Comparison of observational cohort with MINERVA trial interventional cohort

To assess for any differences between the observational phase participants and the trial patients, we tested for any differences in the above clinical and radiological variables between the two cohorts.

Figure 5.2 shows the sporadic SVD group from the observational phase together with the trial population, again presented as age versus baseline WMH volume and stratified by sex and study phase.

The trial participants were not significantly older than the observational patient cohort (mean age 69.1 ± 11.2 compared to 70.9 ± 9.0 years respectively, $p = 0.52$) and had a non-significantly higher proportion of male participants (65.9% compared to 50%, $p = 0.35$). There were no significant differences in ethnic background or years in education between the two cohorts; neither were there are significant differences in the prevalence of hypertension, hypercholesterolaemia, diabetes mellitus, BMI or smoking status. The observational cohort had a slightly higher systolic blood pressure on entry at the baseline visit than the MINERVA participants (153.2 ± 26.6 mmHg compared to 140.8 ± 16.6 mmHg, $p = 0.08$). There were no differences in the rates of depression

or migraine. The observational cohort were enrolled in the study somewhat later after stroke than the MINERVA participants (median 31.2 compared to 13.0 months, $p = 0.28$). The comparison of demographics, vascular risk factors and comorbidities is presented in table 5.5.

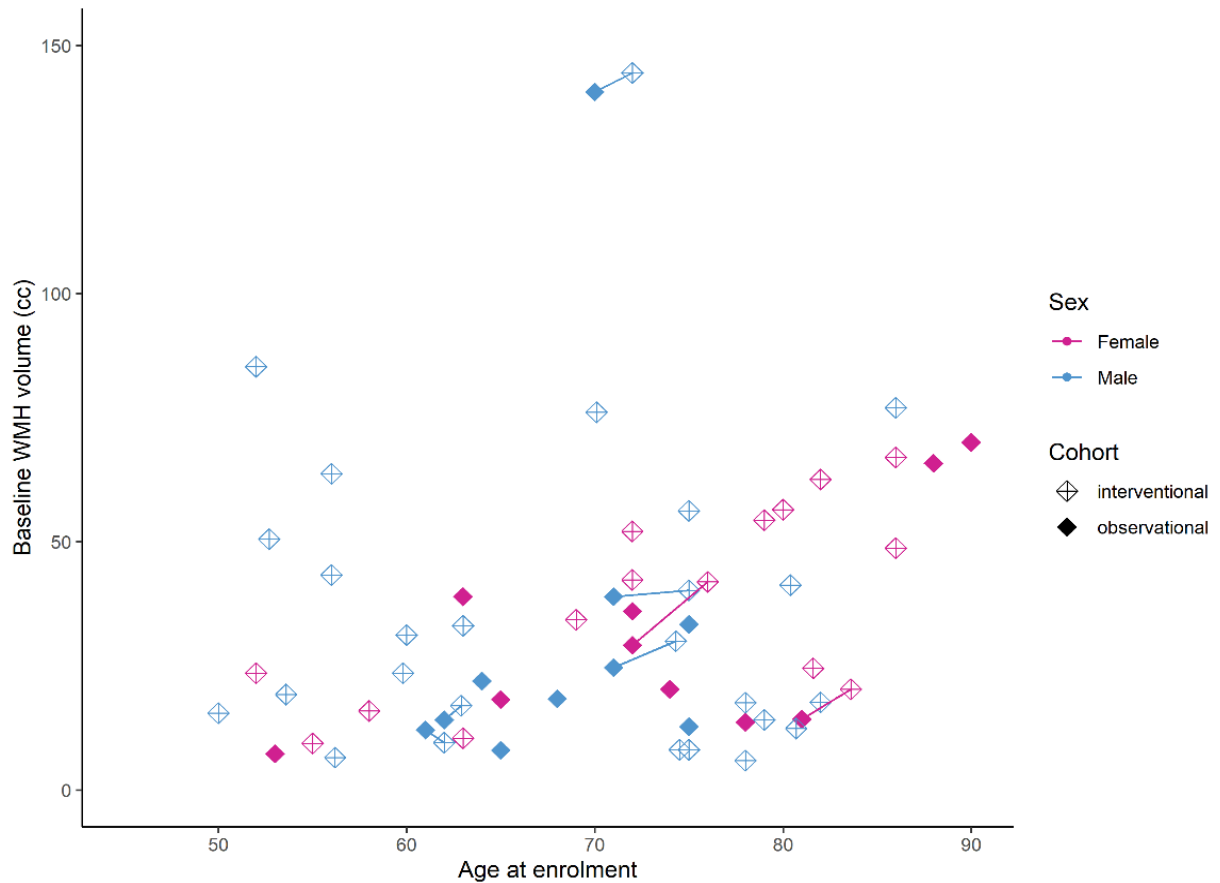


Figure 5.2. Observational and interventional cohorts plotted by age and baseline WMH volume, stratified by sex and cohort. Connected points indicate participants who participated in both phases.

	Observational (n = 20)	MINERVA (n = 44)	p value
Demographics			
Age (years)	70.9 ± 9.0	69.1 ± 11.2	0.52
Sex			
Male	10 (50.0)	29 (65.9)	0.35
Female	10 (50.0)	15 (34.1)	
Ethnicity			
White British	14 (70)	39 (88.6)	0.14
White Irish	3 (15)	3 (6.8)	
White other	3 (0.15)	1 (2.3)	
Asian	– 0	1 (2.3)	
Pakistani			
Years in education	13.0 ± 2.9	14.1 ± 2.7	0.16
Vascular risk factors			
Hypertension	18 (90.0)	38 (86.4%)	0.99
SBP (mmHg)	153.2 ± 26.6	140.8 ± 16.6	0.08
DBP (mmHg)	76.9 ± 14.0	75.4 ± 12.0	0.71
Ischaemic heart disease	<i>Data not collected</i>	4 (9.1)	
Hypercholesterolaemia	11 (55.0)	33 (75.0)	0.19
Diabetes mellitus	4 (25.0)	8 (18.2)	0.99
Smoking (current)	11 (55.0)	19 (43.2)	0.83
BMI (kg/m²)	27.9 ± 5.9	30.5 ± 8.8	0.18
Co-morbidities			
Depression	5 (25.0)	13 (29.6)	0.99
Migraine	5 (25.0)	13 (29.6)	0.99
Time since last stroke (months)	31.2 (7.5 – 29.5)	13.0 (5.2 – 22.5)	0.28

Table 5.5. Comparison of demographic and clinical factors between observational phase sporadic SVD cohort and MINERVA trial cohort. Values are number of patients (%) or mean ± SD. *SBP* systolic blood pressure; *DBP* diastolic blood pressure; *BMI* body mass index

Baseline conventional neuroimaging parameters were very well matched between the observational phase patient cohorts and the MINERVA cohort, with similar WMH volume ($31.9 \pm 30.9\text{cc}$ compared to $31.3 \pm 26.0\text{cc}$, $p = 0.94$) and lacune count (2.5 ± 2.1 compared to 2.6 ± 1.9 , $p = 0.92$). The MINERVA cohort had slightly larger brain volumes which approached statistical significance ($1428.0 \pm 76.3\text{cc}$ compared to $1386.0 \pm 77.5\text{cc}$, $p = 0.060$) and a slightly higher number of microbleeds that was not significant (3.8 ± 12.9 compared to 2.75 ± 4.9). Comparison of these MRI parameters between the two patient cohorts is presented in table 5.6.

	Observational (n = 20)	MINERVA (n = 44)	p value
Conventional MRI markers of SVD severity			
WMH volume (cc)	31.9 ± 30.9	31.3 ± 26.0	0.94
Lacunae	2.5 ± 2.1	2.6 ± 1.9	0.92
CMBs	2.75 ± 4.9	3.8 ± 12.9	0.65
Brain volume (cc)	1386.0 ± 77.5	1428.0 ± 76.3	0.060

Table 5.6. Comparison of radiological markers between observational cohort and MINERVA trial cohort. Values are mean \pm SD. *WMH white matter hyperintensities; CMBs cortical microbleeds;*

Baseline neuropsychiatric test performance

The mean IQ calculated in the pooled patient cohort was 114.5 ± 7.6 , which was not significantly different to that in the control participants (113.3 ± 6.5 , $p = 0.51$). Processing speed was significantly lower in the pooled patient cohort than controls (z-score -0.60 ± 1.23 compared to 0.42 ± 0.43 , $p = 3.9 \times 10^{-6}$). There were no significant differences in scores in the executive function (EF), working memory (WoM) or long-term memory domains (LTM), or in global cognition (GC; table 5.7); the patient group performed worse in all domains except executive function.

	Control (n = 20)	Pooled patients with SVD (n = 57)	p value
IQ (NART)	113.3 ± 6.5	114.5 ± 7.6	0.51
EF	0.15 ± 0.87	0.45 ± 1.18	0.25
PS	0.42 ± 0.43	-0.60 ± 1.23	3.9 × 10⁻⁶
WoM	-0.0083 ± 0.76	-0.23 ± 0.82	0.30
LTM	0.30 ± 0.75	0.34 ± 0.91	0.87
GC	0.22 ± 0.52	-0.01 ± 0.74	0.16

Table 5.7. Comparison of neuropsychometric test scores between control participants and pooled SVD patients (observational phase / MINERVA trial). Scores are estimated IQ (NART), *z*-scores in specific cognitive domains and averaged over all domains to estimate global cognition. IQ intelligence quotient; EF executive function; *PS* processing speed; *WoM* working memory; *LTM* long-term memory; *GC* global cognition.

Within the patient cohort, there was a significant difference in executive function sub-scores with the MINERVA trial group scoring higher than average (0.97 ± 0.95) and the patients in the observational phase study performing slightly worse than average (-0.28 ± 1.09 , $p = 0.00019$). There were no significant differences between the groups in any of the other domains or in estimated global cognition (table 5.8).

	Observational phase patients (n = 20)	MINERVA trial patients (n = 37)	p value
IQ (NART)	112.5 ± 7.9	116.2 ± 7.0	0.11
EF	-0.28 ± 1.09	0.97 ± 0.95	0.00019
PS	-0.58 ± 1.12	-0.61 ± 1.34	0.94
WoM	-0.09 ± 0.95	-0.32 ± 0.72	0.36
LTM	0.31 ± 0.71	0.36 ± 1.04	0.83
GC	-0.16 ± 0.8	0.10 ± 0.69	0.24

Table 5.8. Comparison of neuropsychometric test scores between observational phase and MINERVA trial patients. Scores are estimated IQ (NART), *z*-scores in specific cognitive domains and averaged over all domains to estimate global cognition. IQ intelligence quotient; EF executive function; *PS* processing speed; *WoM* working memory; *LTM* long-term memory; *GC* global cognition.

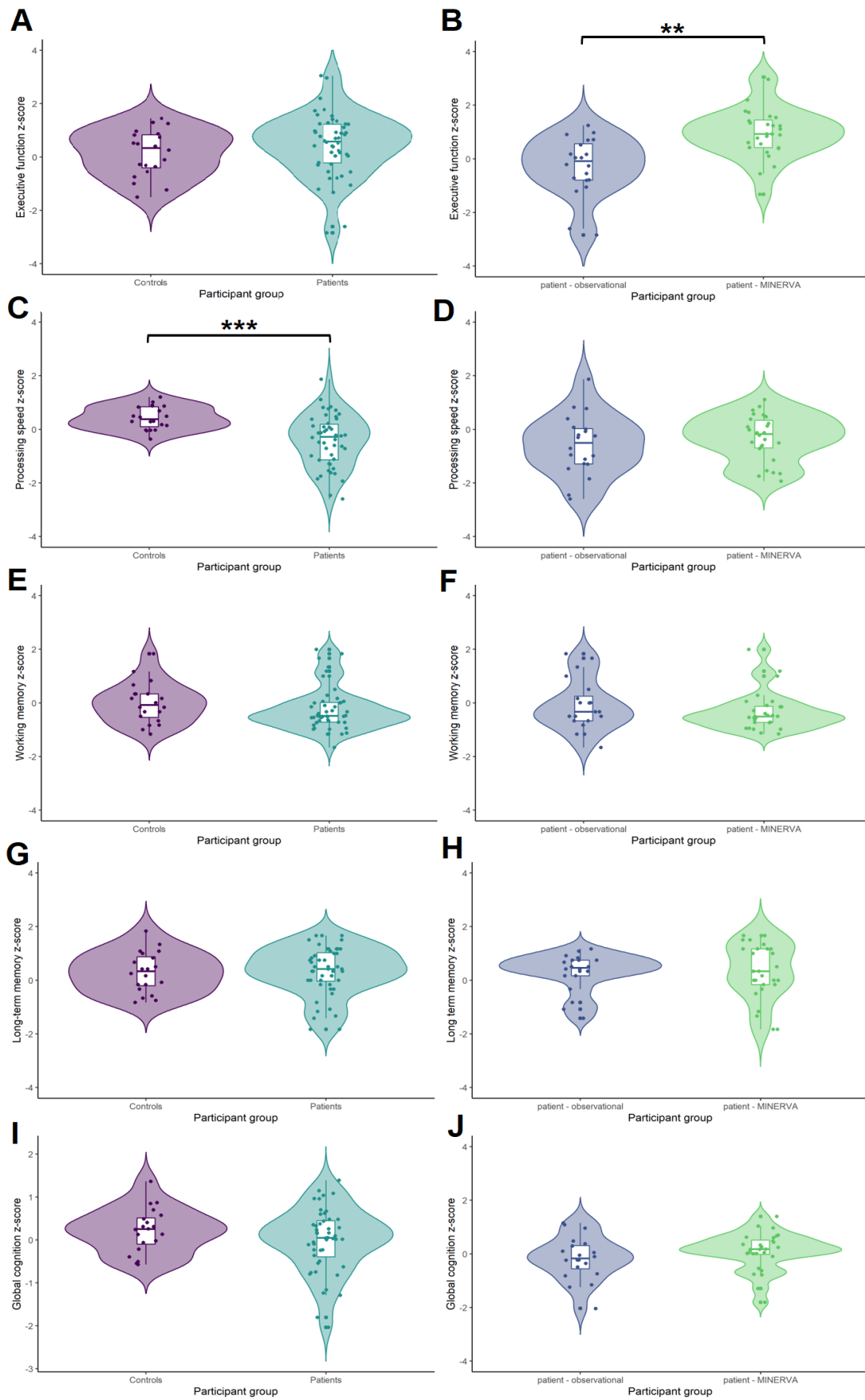


Figure 5.3. Plots of baseline executive function, processing speed, working memory, long-term memory and global cognition z-scores comparing control and pooled patient groups (A,C,E,G,I) and observational phase cohort to MINERVA trial (respectively B,D,F,H,J). * $p < 0.05$; ** $p < 0.01$; *** $p < 0.0001$

In univariate logistic regression models, SVD patient status did not significantly predict executive function z -score ($\beta = 0.304$, $SE = 0.293$, $p = 0.30$), working memory z -score ($\beta = -0.219$, $SE = 0.214$, $p = 0.31$) or long-term memory z -score ($\beta = 0.035$, $SE = 0.230$, $p = 0.88$) but did significantly predict performance in processing speed ($\beta = -1.024$, $SE = 0.285$, $p = 0.00062$). SVD patient status did not predict global cognition score ($\beta = -0.226$, $SE = 0.183$, $p = 0.22$).

In the multivariate logistic regression models, SVD patient status significantly predicted the performance in processing speed ($\beta = -1.127$, $SE = 0.297$, $p = 0.00039$) and global cognition ($\beta = -0.328$, $SE = 0.157$, $p = 0.041$, not significant when corrected for multiple comparisons). Results of these models are given in table 5.9.

Predictor	Sex (male)			NART			SVD patient vs control		
	β	SE	p value	β	SE	p value	β	SE	p value
EF: univariate model							0.305	0.293	0.30
EF: multivariate model	-0.241	0.250	0.34	0.082	0.017	0.00014	0.136	0.264	0.61
PS: univariate model							-1.024	0.285	0.00061
PS: multivariate model	-0.327	0.282	0.25	0.025	0.019	0.21	-1.117	0.297	0.00039
WoM: univariate model							-0.219	0.214	0.31
WoM: multivariate model	0.085	0.175	0.63	0.060	0.012	5.1×10⁻⁶	-0.296	-0.184	0.11
LTM: univariate model							0.035	0.230	0.88
LTM: multivariate model	-0.220	0.193	0.26	0.054	0.013	0.00013	-0.035	0.204	0.86
GC: univariate model							-0.226	0.183	0.22
GC: multivariate model	-0.176	0.149	0.24	0.055	0.010	1.3×10⁻⁶	-0.328	0.157	0.041

Table 5.9. Results of univariate and multivariate regression models showing predictors for neuropsychometric scores in each domain. NART National Adult Reading Test; EF executive function; PS processing speed; WoM working memory; LTM long-term memory; GC global cognition; SE standard error.

Discussion

This chapter summarises the recruitment details and demographics of 57 patients with SVD, pooled from two phases of an ongoing study, and 20 healthy control participants. The patient and control groups were reasonably well matched, though the patient cohorts included participants with a significantly higher burden of cardiovascular risk factors. The patient cohorts from the observational phase study and the MINERVA trial were very well matched on demographic details, comorbidities and neuroimaging markers of SVD.

This is a large group of participants to have undergone such a detailed neuroimaging protocol, blood and CSF sampling and neuropsychometric profiling. The relative lack of ethnic diversity likely reflects the Cambridge / Cambridgeshire population and may limit the applicability of study results to non-White populations; the preponderance of male patients is also typical for stroke research studies which on average include only 40% female participants.³³⁰ This may be the case because female patients are approximately five years older at the time of first stroke and become more disabled by it³³¹, and should also be taken into account when discussing results.

As hypothesised, the patient cohort was significantly more likely to have vascular risk factors including hypertension and hypercholesterolaemia, and had a significantly higher BMI. These factors are well known to be associated with SVD prevalence in large community based studies.^{18-21,220} The patient cohort also showed significantly more severe neuroimaging findings on every marker of SVD tested; this was not an unexpected finding given that recruitment was based on evidence of moderate to severe white matter damage pre-baseline but is reassuring that the cohorts were well segregated.

There were no significant differences in demographic details or comorbidities and vascular risk factors between the MINERVA trial participants and the patient group recruited to the observation phase study; again this was expected as the MINERVA inclusion criteria were somewhat more restrictive due potential contraindications to

the medication, and all MINERVA participants would have been de facto eligible for the observational phase. The MINERVA participants were recruited sooner after the index stroke than those in the observational phase, although this wasn't statistically significant; this may have been a consequence of my having a clinical role and recruiting some patients for whom I had provided medical care, including during the acute stroke phase itself, whereas the recruitment to the observational phase was led by a non-clinician (JW). The Covid-19 pandemic may also have influenced recruitment by impeding contact with patients who were in the chronic phase of stroke, such that the majority of eligible participants screened were those who had required emergency treatment during the pandemic. In any case, it seems reasonable that the brain changes of SVD are in a stable phase in both patient subgroups as acute inflammatory changes after stroke likely resolved within three months^{308,309} and further analysis will test whether the delay is relevant for both the ¹¹C-PK11195 binding and the BBB permeability. The baseline neuroimaging parameters are very well matched between patients in the observational and interventional studies.

Neuropsychometric test scores were reasonably well-matched between the control and pooled patient cohorts, with the main significant difference shown in processing speed, a domain which is well known to reflect SVD severity. Contrary to my hypothesis, the patient group demonstrated higher scores in executive function, which was driven by significantly higher scores in the MINERVA subgroup. This may reflect a recruitment bias if only patients with preserved executive function tended to be interested in the interventional trial and maintained the capacity to consent (quite aside from the statistical paradox in finding significance in subgroups that is not present in the population).

Further work will assess the effect of other demographics and other cardiovascular risk factors or comorbidities on cognition in this pooled sample of patients with SVD, and will also investigate the extent to which deficits are mediated by neuroimaging findings; conventional markers of SVD such as WMHs^{39,69,72}, lacunes^{39,332}, CMBs^{39,102} and PVSs^{114,117} are known to be associated with cognitive deficits, but this cohort will allow

assessment of geographically-specific markers of microglial signal and BBB breakdown in addition, which are discussed in chapters six and seven respectively. In chapter eight, I present data from the one year follow-up of patients with SVD in the observational study, including changes in radiological markers of disease and in cognition.

CHAPTER SIX

Association of central and peripheral inflammation with baseline SVD severity and neuropsychometric performance

I recruited the participants for the MINERVA trial, arranged neuroimaging, collected and processed blood samples, performed cognitive testing, segmented the image masks, and analysed the data. Jessica Walsh recruited the participants to the observational phase study and performed baseline cognitive testing. Young Hong and Tim Fryer performed pre-processing of the images. Daniel Tozer performed image registration and hotspot identification. Malin Overmars assisted with calculation of the biomarker cluster scores.

Introduction

This chapter examines the role of inflammation, both systemic (i.e. in peripheral blood) and local (i.e. within the CNS) in SVD and its association with both radiological markers of disease severity and cognition. There is growing evidence to suggest that the immune system has a role in both cardiovascular³³³ and neurological disease³³⁴, and therefore worthy of investigation in cerebrovascular disease specifically. The evidence that it is relevant in SVD is observational; this is discussed below with reference to the central and peripheral compartments.

Evidence for central inflammation

Early evidence for immune activation came from post-mortem brain samples in patients with SVD, which show areas of demyelination and the co-localisation of inflammatory cells.⁷⁵ Immune cells seen are typically microglia, myeloid-derived phagocytic cells that reside in brain and scavenge extracellular debris. Much of the work in pre-clinical models of SVD / stroke inflammation has focused on microglia as they are a common endpoint of the activation of diverse pathways in the innate immune system;³³⁵ recently it has also been established that they have a role in maintaining the BBB³³⁶ and promoting healing and tissue repair.^{337,338} Microglia have also recently been shown to have a role in myelination.³³⁹

As post-mortem samples can be collected some time after SVD symptoms (in some cases years or decades), *in vivo* methods of investigation are necessary to demonstrate contemporaneous evidence of neuroinflammation or microglial activation. Pre-clinical models are useful in this regard, and a rodent model of SVD suggests that immune activation leads to ECM degradation mediated by matrix metalloproteases as discussed above.²³⁴

In humans, neuroimaging can provide this evidence either indirectly (for example, using texture analysis of conventional FLAIR images to infer additional information about brain tissue not visible by eye²⁷³) or directly, leveraging the specificity of microglial cell surface markers by using a positron-emitting radioligand in a PET scan. The

targets for such ligands are generally markers of the M1 pro-inflammatory phase and the majority of the literature is based on targeting TSPO (discussed in the introduction), although other targets of interest include the cannabinoid receptor-2, the P2X₇ receptor and cyclooxygenase-2.³⁴⁰ Previous PET studies imaging microglia have shown clearly elevated signal in symptomatic SVD compared to control participants²¹³ and that ¹¹C-PK11195 binding is associated with SVD burden in patients with MCI/AD.²²⁹

A second method for assessing immune activation *in vivo* is to sample CSF. This has previously been done to look for associations with isolated biomarkers, for example MMPs associated with extracellular matrix degradation.^{201,227} No studies have yet reported data from panels of biomarkers tested in the CSF of patients with SVD, nor of any cytometric analysis to assess CNS cell populations. The advent of proteomics and transcriptomics has made it possible to interrogate CSF in much greater detail.

Evidence for peripheral inflammation

In contrast, many studies have investigated potential inflammatory biomarkers relevant for SVD in the peripheral compartment. This literature has been reviewed in detail²²¹, the authors noting 82 studies that tested combinations of associations between systemic inflammatory markers (such as IL-6, C-reactive protein and fibrinogen), vascular-specific inflammatory markers (such as homocysteine, E-selectin, ICAM-1, thrombomodulin, VEGF, and von Willebrand factor) and individual radiological markers of disease. The authors conclude that while systemic inflammatory markers have a more robust association with CAA, it is vascular-specific inflammation that is of interest in sporadic SVD. This is likely to provide more informative data about the mechanism of disease and offer more realistic therapeutic targets.

In addition to individual biomarkers, some authors have applied compound biomarker panels to investigate peripheral inflammation in SVD. This has been employed both with a hypothesis-driven panel of markers including IL-6, C-reactive protein, TNF- α , P-selectin, ICAM-1 and homocysteine, which predicted WMH progression and incident

lacunes at two year follow-up,³⁴¹ and using the same commercially available proteomics panel used in this study.²²² The authors of the latter identified a subcluster of proteins predominantly reflecting coagulation that were associated with disease severity and mediated the relationship between WMH volume and both age and hypertension.

Detailed peripheral immunophenotyping has not been used extensively in SVD, but early studies have suggested that the phenotype and behaviour of monocytes, circulating myeloid cells also involved in the innate immune response, may be relevant in SVD.²²⁶ The authors built on evidence from atherosclerotic cardiovascular disease that oxidised phospholipids from atherosclerotic plaque are associated with enhanced monocyte response²²⁴ which is mediated by epigenetic modification²²⁵ and show that cytokine production capacity is enhanced in peripheral blood mononuclear cells of patients with SVD and predicted WMH progression, as well as identifying an association between an intermediate subtype of monocytes with SVD burden. Intermediate (CD14⁺/CD16⁺) monocytes represent around 2-8% of circulating monocytes and are involved in reactive oxygen species production and angiogenesis,³⁴² so may be relevant in any immune response to vascular disease; they there are also known to be associated with unstable atherosclerotic plaque in coronary artery disease.³⁴³

Interaction between peripheral and central compartments

Activation of immune cells in the peripheral and central compartments as discussed above may be relevant for SVD through mechanisms that are either independent or inter-related; if the processes are related, this may be mediated by cytokine signalling or direct invasion of peripheral immune cells into the CNS. The CNS is traditionally considered to have immune privilege due to the protection from cells and large molecules afforded by the BBB³⁴⁴; however more recent evidence suggest that this is not the case and that meningeal and border-associated macrophages (BAMs) resident within perivascular spaces can facilitate cytokine signalling that activates parenchymal immune cells³⁴⁵ and promote the direct infiltration of mononuclear cells from blood.³⁴⁶ Particular focus has been placed on BAMs, which promote the infiltration of other

myeloid cells after ischaemia,³⁴⁷ enhance parenchymal microglial phagocytic activity³⁴⁸ and are expanded in ageing.³⁴⁹

Hypotheses and study design

I hypothesised that immune activation is associated with SVD pathology both in the central compartment (as a consequence of tissue damage / ischaemia), and in the peripheral compartment (likely as a consequence of overlapping cardiovascular risk factors that predispose to SVD). I tested these associations by assessing the correlation of MRI markers of SVD severity and neuropsychometric test scores with parameters derived from ¹¹C-PK11195 PET imaging as a marker of central inflammation, and the results of peripheral blood proteomics analysis and populations of monocytes measured using mass cytometry as markers of peripheral inflammation. To do this, I also derived the optimal parameters from PET imaging to discriminate between patients and control participants. As activated microglia are present throughout the whole brain,⁷⁵ and the NAWM is thought to be most at risk for disease progression^{92,288}, an additional hypothesis was that the volume of hotspots in the NAWM would be the optimal discriminant between groups.

I further hypothesised that peripheral immune activation directly influences immune cells in the CNS, and further tested the association between markers of inflammation in these two compartments and whether any effects of peripheral inflammation were mediated by markers of central inflammation.

Methods

For this analysis I used data from the pooled cohort of 57 unique patients with SVD that had baseline PET-MRI, phlebotomy and neuropsychometric testing as described in chapter five. Inclusion and exclusion criteria are presented in chapter four, as are details of the neuroimaging protocol (with full sequence details in Appendix B).

Image analysis

WMH were marked semi-automatically using Jim version 8.0 (<http://xinapse.com/jim-software/>) using the blind-to-timepoint method outlined in chapters three and four; baseline WMH volumes were calculated from analysis of the baseline and one year follow-up FLAIR images (observational cohort) and baseline and three-month follow-up FLAIR images (MINERVA cohort). Lacunes were outlined using a similar method, also including visual inspection of T1 and T2 sequences to exclude other lesions which can be difficult to discriminate on FLAIR alone such as PVSs. CMBs were dotted on SWAN images and counted automatically. Brain volumes were calculated using SIENA (<https://fsl.fmrib.ox.ac.uk/fsl/fslwiki/SIENA>).

PET images were pre-processed by YH and TF as described in chapter four, and registered to T1 MR images by DT. As several parameters of interest can be generated from the maps of ^{11}C -PK11195 binding (including volume of hotspot tissue and hotspot volume scaled for tissue class across all the tissue class masks defined above), I first aimed to establish which parameters were optimal markers of disease activity. To do this, I assessed which of these potential metrics was the best discriminant between the sporadic SVD and patient groups and selected this as a single readout value from the PET images.

Blood processing

Blood was collected from each participant and processed as described in chapter four. C-reactive protein was measured by ELISA in the Core Biochemical Analysis Laboratory, University of Cambridge. Aliquots were sent to Olink Analysis Service, Uppsala, Sweden in two batches (corresponding to the observational cohort and

MINERVA trial cohort participants). The output of this data is Normalised Protein eXpression (NPX), an arbitrary unit of protein expression for each of the panel components. *A priori* markers of interest from within the panel were chosen to highlight in results based on previous literature discussed above: E-selectin, MMP-2, MMP-3, MMP-9, TIMP-4, P-selectin and vWF.

In the MINERVA participants only, an additional blood sample was taken to the NIHR Cambridge BRC Cell Phenotyping Hub for CyTOF® mass cytometry as discussed above using the Maxpar® Direct™ Immune Profiling assay. Proportions of classical, non-classical and intermediate monocytes were extracted from the cytometric output file using the Maxpar® PathSetter™ software, using the proprietary gating strategy which identifies as monocytes cells which are CD3/CD19 negative and positive for CD45 (a pan-leucocyte marker) and either CD14 or CD16.

Neuropsychometric testing

Neuropsychometric testing was performed as above in chapter four. JW tested all participants in the observational phase; I tested the participants in the MINERVA trial. To minimise the risk of bias or discrepancy, the tests were administered in a standardised order according to a prepared script and JW provided training (during the one year follow-up testing of the observational phase patients, discussed further in chapter eight) involving observation of test administration and performing several batteries under observation until consensus was reached that the administration of the tests was as reproducible as possible.

Statistical analysis

To derive the optimal output from the PET scans, I performed multivariate logistic regression to assess the extent to which each candidate metric predicted participant group (patient versus control), including as covariates age and sex, and selected the metric that minimised the Akaike Information Criteria (AIC) in this model. All analysis was performed in the R project for statistical computing²⁶⁰ version 4.2.1.

Univariate linear regression was used to test the correlation of this output marker with radiological markers of SVD severity (WMHs, lacunes, CMBs and brain volume). The Kolmogorov-Smirnov test was used to test the normality of these distributions and any non-normally distributed variables were transformed until normal. The association of other key demographic and cardiovascular risk factor variables was also tested.

I next performed multivariate linear regression to assess the relationship between PET binding and the above markers of SVD, including as covariates age and sex. If any pairs of predictors showed a correlation coefficient >0.8 , only one variable was taken forward to the final multivariate model. I used a combination of stepwise forward selection of any predictors with $p < 0.05$ on univariate analysis and backward selection of predictors that lost this significance in the multivariate model. In all regression models, results are presented as unstandardised estimated β coefficients and standard errors where the independent and dependent variables are biologically meaningful, and standardised β coefficients where the units of either variable are arbitrary.

Similar regression models were constructed to test the correlation of PET binding with each specific cognitive domain based on the z -scores from each subset of tests.

C-reactive protein and the 92 biomarkers from the Olink CVD-III proteomic panel were first treated individually and entered into linear regression models as predictors for each radiological SVD marker and for each cognitive domain, including age and sex as covariates. Correlations were considered significant at false discovery rate-corrected $p < 0.05$ in view of multiple comparisons. To pool results from the observational cohort and the MINERVA trial, samples from eight of the observational phase were chosen to maximise the range of expression across all biomarkers and re-tested as bridging samples alongside serum from the MINERVA patients. NPX values were then normalised to the median for each assay individually, applying an additional correction factor calculated from the bridging samples using a proprietary but open-source package in *R* (*OlinkAnalyse*³⁵⁰).

I then performed principal component analysis of the CVD-III panel data and tested the association of the first principal component with markers of SVD severity in the same way. Finally with the assistance of MO I calculated biomarker cluster scores for each participant according to the weighted NPX values of the subset of proteins from the panel that were found to be related to WMH severity.²²² I tested the correlation of the biomarker cluster score with radiological markers of SVD as above, corrected for age, sex and diagnosis of hypertension in the same way as these were the covariates used by the authors who defined the subset of interest.

Proportions of classical, non-classical and intermediate monocytes were entered into linear regression models to test associations with MRI markers, also corrected for age and sex.

Finally significant associations between measurements of peripheral inflammation and radiological/neuropsychometric outcomes were taken forward for causal mediation analysis, a statistical technique used to determine whether a relationship between two variables is explained by a third variable. Here, to determine whether inflammation in the CNS mediates the relationship between inflammation in the periphery and SVD severity, I used the PET imaging summary readout values as the potential mediating factor. This analysis was conducted in *R* using the *mediation* package.³⁵¹

Results

Data were included from 20 control participants and 20 patients with sporadic SVD who were enrolled in the observational phase study between October 2017 and January 2019, and 44 participants who were enrolled in the MINERVA trial between October 2019 and June 2022. Demographics, cardiovascular risk factors and comorbidities are discussed in chapter five (see table 5.5).

Determination of optimal PET marker

The optimal ¹¹C-PK11195 binding metric for discriminating groups was the NAWM hotspot volume as a proportion of NAWM ($\beta = 0.33$, $p = 0.027$). These measurements also discriminated better between groups than the voxelwise mean ¹¹C-PK11195

binding. Figure 6.1 shows the between group comparisons for metrics of ^{11}C -PK11195 binding and results from the logistic regression models from possible candidate metrics of ^{11}C -PK11195 binding and BBB permeability are shown in table 6.1. Accordingly, NAWM percentage hotspot value was selected for use in subsequent analysis (henceforth termed ^{11}C -PK11195 hotspot proportion).

Candidate predictor metric	β	SE	z-statistic	p value	AIC
PK11195 binding					
Hotspot volume (NAWM)	0.11	0.10	1.06	0.29	45.67
Hotspot percentage (NAWM)	0.33	0.15	2.21	0.027	39.77
Hotspot volume (all WM)	0.13	0.12	1.06	0.29	44.98
Hotspot percentage (all WM)	0.23	0.15	1.57	0.12	44.31

Table 6.1. Logistic regression model results for candidate metrics of PK11195 binding. *WM white matter; NAWM normal appearing white matter*

Relationship of PET binding to MRI markers of SVD

WMHs

On univariate analysis, the ^{11}C -PK11195 hotspot proportion was a significant predictor of WMH volume ($\beta = 2.644$, $\text{SE} = 0.398$, $p = 5.9 \times 10^{-8}$). Other significant predictors were years in education ($\beta = -2.868$, $\text{SE} = 1.114$, $p = 0.013$) and time since stroke ($\beta = 0.421$, $\text{SE} = 0.140$, $p = 0.0044$). In the multivariate analysis, only ^{11}C -PK11195 hotspot proportion remained a significant predictor of WMH volume ($\beta = 2.591$, $\text{SE} = 0.397$, $p = 1.1 \times 10^{-7}$). Results of these models are shown in table 6.2; figure 6.2 shows the relationship between WMH volume and ^{11}C -PK11195 hotspot proportion.

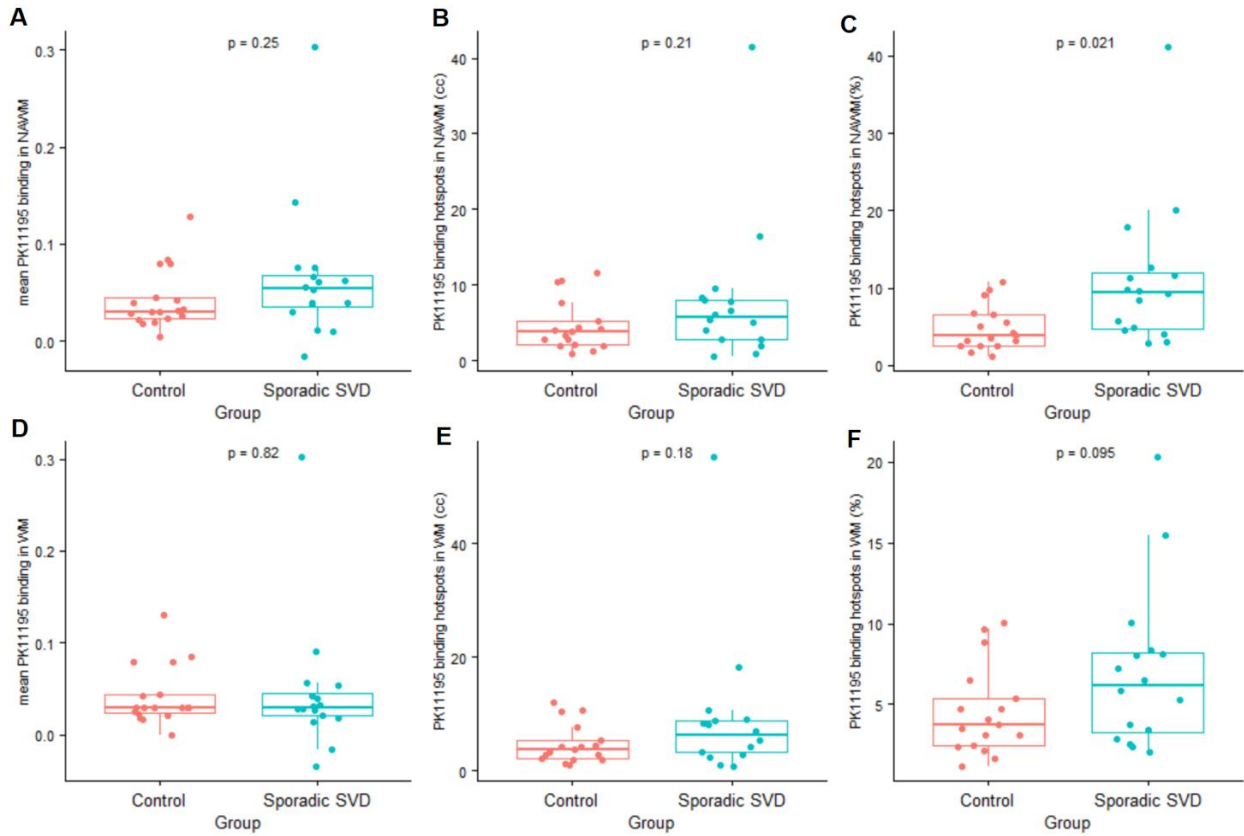


Figure 6.1 . Boxplots showing comparisons between control group and sporadic SVD patients for candidate metrics of ¹¹C-PK11195 binding: (A) mean binding in NAWM; (B) hotspot volume in NAWM; (C) NAWM hotspots as percentage of NAWM; (D) mean binding in all white matter; (E) hotspot volume in all white matter; (F) white matter hotspots as percentage of all white matter. *WM white matter; NAWM normal appearing white matter*

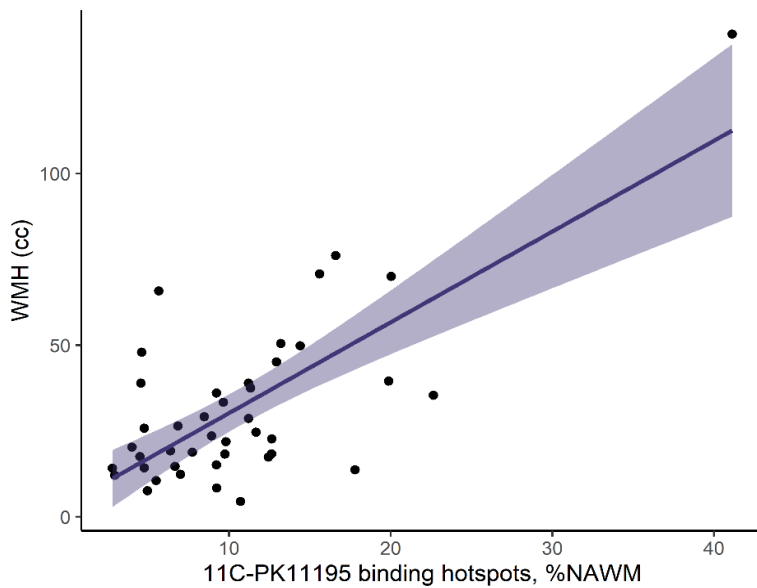


Figure 6.2 . Scatter plot showing relationship between WMH and 11C-PK11195 binding hotspots as percentage of NAWM. *%NAWM percentage of normal appearing white matter*

	Univariate analysis			Multivariate analysis			
	β	SE	<i>p</i> value	β	SE	<i>p</i> value	
Demographics							
Age (years)	0.466	0.316	0.15	0.445	0.269	0.11	
Sex	Male	3.547	6.800	0.60	0.386	5.668	0.95
Ethnicity	White	9.150	24.49	0.29			
	British						
Years in education	-2.868	1.114	0.013				
Vascular risk factors							
Hypertension	-13.053	9.866	0.19				
SBP (mmHg)	-0.039	0.206	0.85				
DBP (mmHg)	-0.381	0.364	0.30				
Ischaemic heart disease	-12.397	10.773	0.26				
Hyper-cholesterolaemia	5.290	7.486	0.48				
Diabetes mellitus	1.245	8.672	0.89				
Smoking (current)	7.383	6.679	0.27				
BMI (kg/m ²)	-0.366	0.480	0.45				
Comorbidities							
Depression	9.454	7.261	0.20				
Migraine	7.298	7.309	0.32				
Time since last stroke (months)	0.421	0.140	0.0044				
Central nervous system inflammation							
¹¹ C-PK11195 hotspots, %NAWM	2.644	0.398	5.9 × 10⁻⁸	2.591	0.397	<1 × 10⁻⁶	

Table 6.2. Linear regression model results univariate and multivariate models of candidate predictors of WMH volume. Values are unstandardised β coefficients and standard errors. *SBP* systolic blood pressure; *DBP* diastolic blood pressure; *BMI* body mass index); %NAWM percentage of normal appearing white matter, values in percentage points.

	Univariate analysis			Multivariate analysis			
	β	SE	<i>p</i> value	β	SE	<i>p</i> value	
Demographics							
Age (years)	-0.014	0.007	0.049	-0.014	0.008	0.07	
Sex	Male	0.105	0.151	0.49	-0.0004	0.161	0.99
Ethnicity	White	0.038	0.535	0.94			
	British						
Years in education		-0.024	0.026	0.36			
Vascular risk factors							
Hypertension		0.360	0.213	0.098			
SBP (mmHg)		0.002	0.004	0.65			
DBP (mmHg)		-0.001	0.007	0.99			
Ischaemic heart disease		-0.083	0.333	0.81			
Hyper-cholesterolaemia		0.296	0.160	0.071			
Diabetes mellitus		0.085	0.207	0.68			
Smoking (current)		-0.051	0.151	0.74			
BMI (kg/m ²)		-0.005	0.011	0.68			
Comorbidities							
Depression		0.065	0.165	0.70			
Migraine		0.102	0.164	0.54			
Time since last stroke (months)		0.007	0.004	0.10			
Central nervous system inflammation							
¹¹ C-PK11195 hotspots, %NAWM		1.064	1.137	0.36	1.222	1.126	0.28

Table 6.3. Linear regression model results univariate and multivariate models of candidate predictors of lacune count. Values are unstandardised β coefficients and standard errors. *SBP* systolic blood pressure; *DBP* diastolic blood pressure; *BMI* body mass index); *%NAWM* percentage of normal appearing white matter, values in percentage points.

Lacunae

The lacune count was non-normally distributed and natural logarithm-transformed to create a normal distribution. The ^{11}C -PK11195 hotspot proportion was not significantly related to lacune count on univariate analysis ($\beta = 1.064$, $\text{SE} = 1.137$, $p = 0.36$). No other predictors reached significance on univariate analysis, nor in the multivariate analysis (table 6.3). Figure 6.3 shows a scatter plot of raw lacune count versus the ^{11}C -PK11195 hotspot proportion.

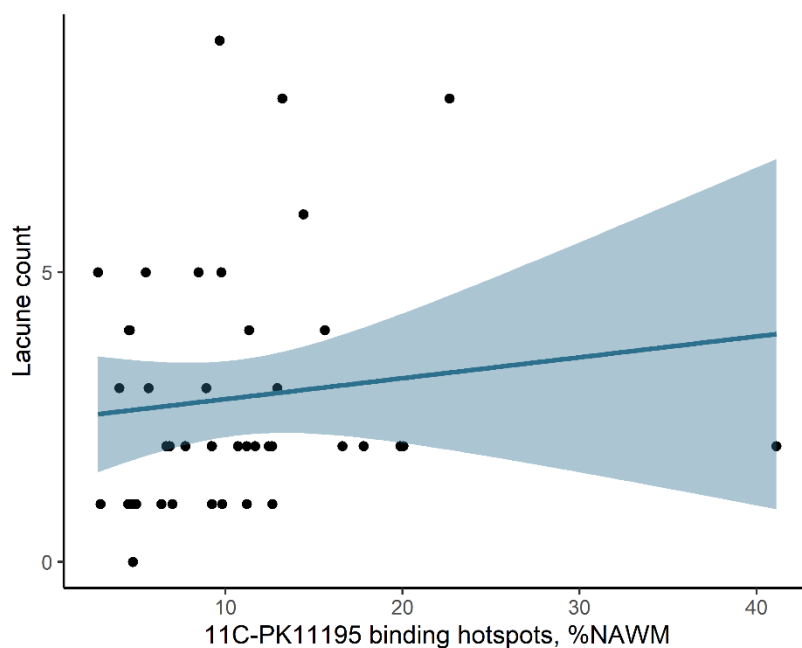


Figure 6.3 . Scatter plot showing relationship between lacune count and ^{11}C -PK11195 binding hotspots as percentage of NAWM. *%NAWM percentage of normal appearing white mater*

CMBs

The CMB count was also non-normally distributed and natural logarithm-transformed; neither the ^{11}C -PK11195 hotspot proportion ($\beta = 1.064$, $\text{SE} = 1.137$, $p = 0.36$) nor any other predictor was significantly associated with the CMB count. No predictors reached significance in the multivariate model (table 6.4). Figure 6.4 shows the association between raw CMB count and ^{11}C -PK11195 hotspot proportion.

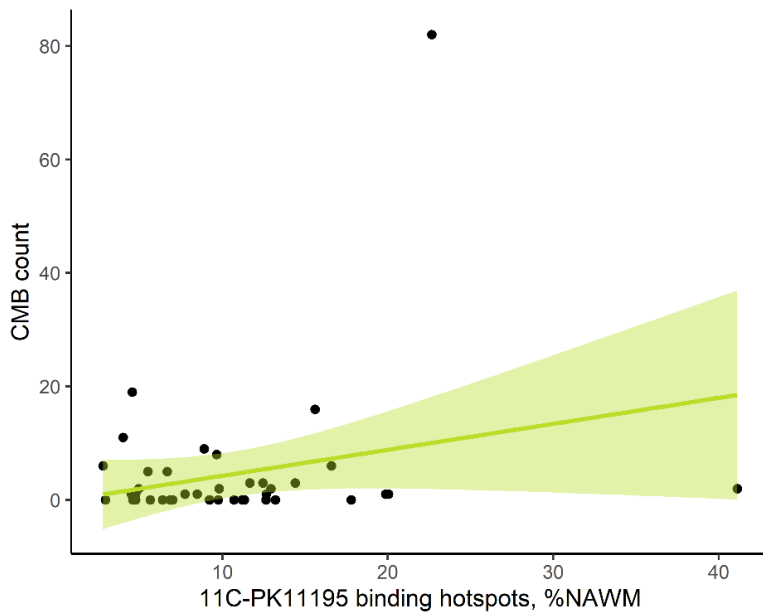


Figure 6.4. Scatter plot showing relationship between CMB count and 11C-PK11195 binding hotspots as percentage of NAWM. *%NAWM percentage of normal appearing white mater*

Brain volume

Age ($\beta = -3.155$, $SE = 1.018$, $p = 0.003$) and time since stroke ($\beta = -1.427$, $SE = 0.631$, $p = 0.029$) were the only significant predictors of brain volume. The $^{11}\text{C-PK11195}$ hotspot proportion was non-significantly associated with lower brain volume ($\beta = -278.0$, $SE = 187.0$, $p = 0.14$). In the multivariable model only age predicted brain volume ($\beta = -3.94$, $SE = 1.18$, $p = 0.002$; table 6.5). Figure 6.5 shows the association between brain volumes and $^{11}\text{C-PK11195}$ hotspot proportion.

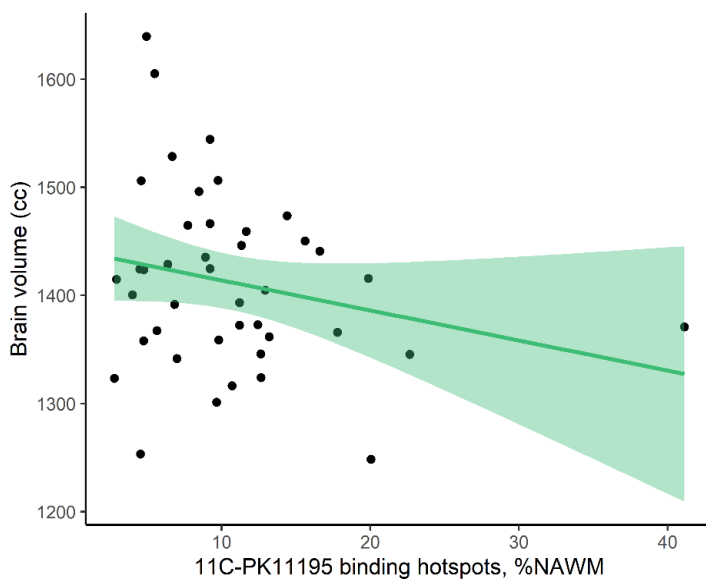


Figure 6.5. Scatter plot showing relationship between brain volume and 11C-PK11195 binding hotspots as percentage of NAWM. *%NAWM percentage of normal appearing white*

	Univariate analysis			Multivariate analysis			
	β	SE	p value	β	SE	p value	
Demographics							
Age (years)	-0.023	0.0127	0.072	-0.030	0.016	0.08	
Sex	Male	-0.099	0.277	0.72	-0.341	0.342	0.33
Ethnicity	White	0.010	1.039	0.99			
	British						
Years in education	0.013	0.148	0.79				
Vascular risk factors							
Hypertension	0.660	0.398	0.10				
SBP (mmHg)	0.007	0.006	0.26				
DBP (mmHg)	0.003	0.012	0.81				
Ischaemic heart disease	-0.161	0.559	0.77				
Hyper-cholesterolaemia	0.012	0.306	0.97				
Diabetes mellitus	0.130	0.353	0.72				
Smoking (current)	0.068	0.275	0.81				
BMI (kg/m ²)	-0.012	0.020	0.56				
Comorbidities							
Depression	-0.389	0.296	0.19				
Migraine	-0.126	0.300	0.68				
Time since last stroke (months)	0.010	0.006	0.11				
Central nervous system inflammation							
¹¹ C-PK11195 hotspots, %NAWM	2.483	2.425	0.31	3.051	2.402	0.21	

Table 6.4. Linear regression model results univariate and multivariate models of candidate predictors of CMB count. Values are unstandardised β coefficients and standard errors. *SBP* systolic blood pressure; *DBP* diastolic blood pressure; *BMI* body mass index); *%NAWM* percentage of normal appearing white matter, values in percentage points.

	Univariate analysis			Multivariate analysis			
		β	SE	p value	β	SE	p value
Demographics							
Age (years)		-3.155	1.018	0.003	-3.94	1.18	0.002
Sex	Male	-25.10	23.22	0.29	-41.53	24.59	0.10
Ethnicity	White	-47.93	75.80	0.53			
	British						
Years in education		-2.244	2.989	0.58			
Vascular risk factors							
Hypertension		-9.271	33.597	0.78			
SBP (mmHg)		-0.566	0.564	0.32			
DBP (mmHg)		0.003	1.029	0.98			
Ischaemic heart disease		25.04	49.57	0.62			
Hyper-cholesterolaemia		-26.40	25.70	0.31			
Diabetes mellitus		-11.02	31.78	0.73			
Smoking (current)		-4.686	23.49	0.84			
BMI (kg/m²)		-2.038	1.538	0.19			
Comorbidities							
Depression		28.03	25.14	0.27			
Migraine		20.64	25.28	0.42			
Time since last stroke (months)		-1.427	0.631	0.029			
Central nervous system inflammation							
¹¹C-PK11195 hotspots, %NAWM		-278.0	187.0	0.14	-152.65	284.1	0.59

Table 6.5. Linear regression model results univariate and multivariate models of candidate predictors of brain volume. Values are unstandardised β coefficients and standard errors. *SBP* systolic blood pressure; *DBP* diastolic blood pressure; *BMI* body mass index; *%NAWM* percentage of normal appearing white matter, values in percentage points.

Relationship of PET binding to cognition

On univariate analysis, ^{11}C -PK11195 hotspot proportion was significantly associated with lower neuropsychometric scores in executive function ($\beta = -5.920$, $\text{SE} = 2.55$, $p = 0.026$), and global cognition ($\beta = -4.452$, $\text{SE} = 1.59$, $p = 0.0079$) domains.

Other significant predictors of performance in the executive function domain included years of education ($\beta = 0.159$, $\text{SE} = 0.053$, $p = 0.0043$), NART score ($\beta = 0.079$, $\text{SE} = 0.021$, $p = 0.00075$), time since stroke ($\beta = -0.019$, $\text{SE} = 0.008$, $p = 0.031$), WMH volume ($\beta = -0.016$, $\text{SE} = 0.006$, $p = 0.019$) and FA median ($\beta = -18.16$, $\text{SE} = 5.161$, $p = 0.002$). In the multivariate model, FA median ($\beta = -8.401$, $\text{SE} = 3.000$, $p = 0.0082$) and ^{11}C -PK11195 hotspot proportion ($\beta = -7.560$, $\text{SE} = 2.456$, $p = 0.0040$) remained significant.

Significant predictors of processing speed included lacune count ($\beta = -0.238$, $\text{SE} = 0.081$, $p = 0.0052$), CMB count ($\beta = -0.044$, $\text{SE} = 0.013$, $p = 0.0020$), brain volume ($\beta = 0.005$, $\text{SE} = 0.002$, $p = 0.03$), FA median ($\beta = 17.45$, $\text{SE} = 5.468$, $p = 0.0051$) and MD peak height ($\beta = -0.016$, $\text{SE} = 0.006$, $p = 0.019$). WMH volume negatively predicted performance at a level approaching statistical significance ($\beta = -0.014$, $\text{SE} = 0.007$, $p = 0.059$). In the multivariate model, age ($\beta = 0.062$, $\text{SE} = 0.019$, $p = 0.002$) and brain volume ($\beta = 0.006$, $\text{SE} = 0.002$, $p = 0.0088$) remained significant.

Significant predictors of long-term memory included years of education ($\beta = 0.104$, $\text{SE} = 0.042$, $p = 0.017$), NART score ($\beta = 0.046$, $\text{SE} = 0.016$, $p = 0.007$), lacune count ($\beta = -0.150$, $\text{SE} = 0.061$, $p = 0.018$) and FA median ($\beta = 11.030$, $\text{SE} = 3.455$, $p = 0.005$). In the multivariate model, only age predicted performance with borderline statistical significance and positive correlation ($\beta = 0.029$, $\text{SE} = 0.014$, $p = 0.048$).

Other significant predictors of global cognitive performance included years of education ($\beta = 0.085$, $\text{SE} = 0.034$, $p = 0.018$), NART score ($\beta = 0.051$, $\text{SE} = 0.013$, $p = 0.00037$), WMH volume ($\beta = -0.013$, $\text{SE} = 0.004$, $p = 0.0031$) lacune count ($\beta = -0.125$, $\text{SE} = 0.049$, $p = 0.016$), CMB count ($\beta = -0.023$, $\text{SE} = 0.008$, $p = 0.007$), and FA median ($\beta = 14.87$, $\text{SE} = 3.43$, $p = 0.00040$). In the multivariate model, NART score ($\beta = 0.052$,

SE = 0.125, $p = 0.0002$) and CMB count ($\beta = -0.024$, SE = 0.007, $p = 0.0026$) remained significantly associated with GC s -score; ^{11}C -PK11195 hotspot proportion was associated with worse performance and approached statistical significance ($\beta = -2.607$, SE = 1.39, $p = 0.060$). Figure 6.6 shows the univariate relationships between ^{11}C -PK11195 hotspot proportion and each cognitive domain domains while tables 6.6, 6.7, 6.8 and 6.9 outline the results of the linear regression models respectively.

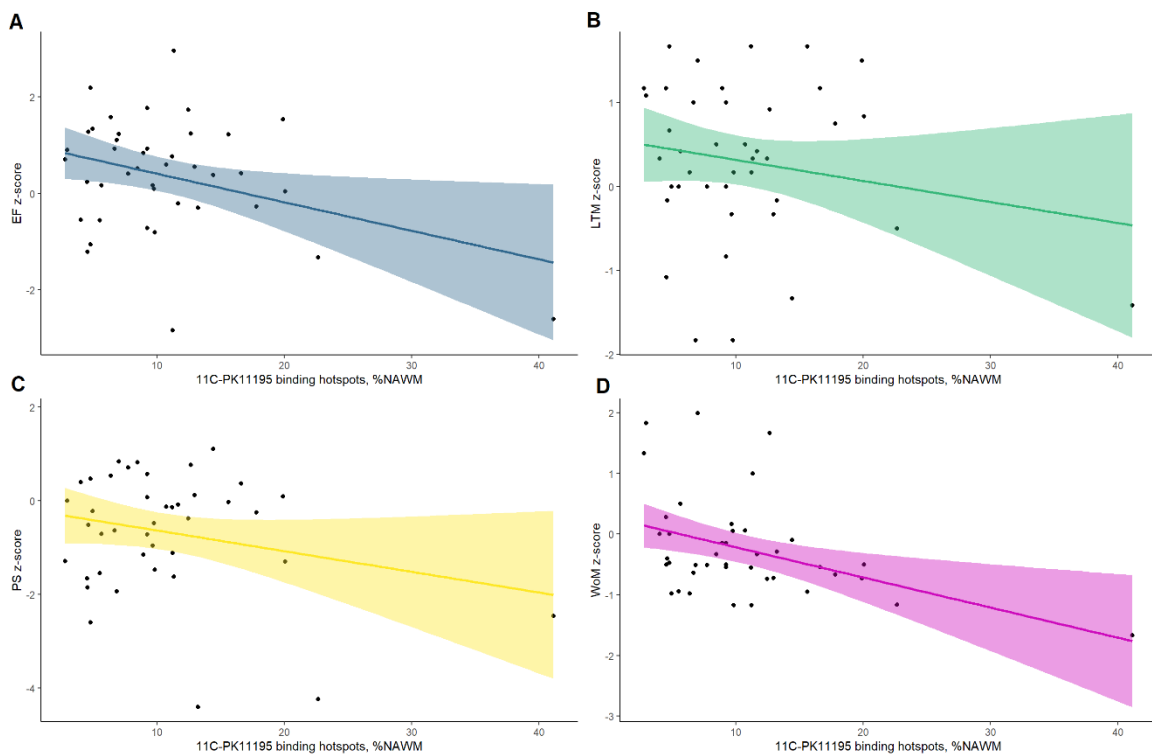


Figure 6.6. Scatter plot showing correlation of ^{11}C -PK11195 hotspot proportion to (A) executive function z-score; (B) processing speed z-score; (C) long-term memory z-score and (D) global cognition z-score.

		Univariate analysis			Multivariate analysis		
		β	SE	<i>p</i> value	β	SE	<i>p</i> value
Demographics							
Age (years)		0.012	0.016	0.46	0.023	0.017	0.19
Sex	Male	-0.131	0.346	0.71	0.305	0.352	0.39
Ethnicity	White British	0.255	1.093	0.82			
Years in education		0.159	0.053	0.0043			
IQ (NART)		0.079	0.021	0.00075			
Vascular risk factors							
Hypertension		-0.694	0.4763	0.152			
SBP (mmHg)		-0.007	0.009	0.43			
DBP (mmHg)		-0.004	0.015	0.79			
Ischaemic heart disease		-0.161	0.588	0.7			
Hypercholesterolaemia		0.280	0.369	0.45			
Diabetes mellitus		-0.398	0.458	0.39			
Smoking (current)		-0.654	0.332	0.056			
BMI (kg/m ²)		-0.020	0.032	0.53			
Comorbidities							
Depression		-0.504	0.363	0.17			
Migraine		0.148	0.370	0.69			
Time since stroke (months)		-0.019	0.008	0.031			
Conventional MRI markers							
WMH (cc)		-0.016	0.006	0.019			
Lacunes		-0.110	0.082	0.19			
CMBs		-0.026	0.014	0.06			
Brain volume (cc)		0.004	0.002	0.09			
FA median		18.16	5.161	0.002	-8.401	3.000	0.0082
MD PH (mm ² /s)		112.5	144.9	0.45			
Central nervous system inflammation							
¹¹ C-PK11195 hotspots, %NAWM		-5.920	2.550	0.026	-7.560	2.456	0.0040

Table 6.6. Unstandardised β coefficients and standard errors of univariate and multivariate models of candidate predictors of executive function *z*-score. *SBP* systolic blood pressure; *DBP* diastolic blood pressure; *BMI* body mass index; *FA* fractional anisotropy; *MDPH* mean diffusivity peak height; *%NAWM* percentage of normal appearing white matter, values in percentage points.

		Univariate analysis			Multivariate analysis		
		β	SE	<i>p</i> value	β	SE	<i>p</i> value
Demographics							
Age (years)		0.023	0.0170	0.18	0.063	0.019	0.002
Sex	Male	-0.298	0.361	0.41	0.144	0.370	0.70
Ethnicity	White British	-1.150	2.232	0.31			
Years in education		-0.0335	0.060	0.58			
IQ (NART)		0.022	0.026	0.40			
Vascular risk factors							
Hypertension		-0.016	0.512	0.97			
SBP (mmHg)		-0.016	0.009	0.08			
DBP (mmHg)		-0.006	0.017	0.74			
Ischaemic heart disease		-0.600	0.824	0.47			
Hypercholesterolaemia		-0.252	0.388	0.52			
Diabetes mellitus		-0.360	0.482	0.46			
Smoking (current)		-0.133	0.364	0.72			
BMI (kg/m ²)		-0.005	0.033	0.87			
Comorbidities							
Depression		-0.360	0.386	0.36			
Migraine		-0.397	0.385	0.31			
Time since stroke (months)		-0.004	0.009	0.66			
Conventional MRI markers							
WMH (cc)		-0.014	0.007	0.059			
Lacunae		-0.238	0.081	0.0052			
CMBs		-0.044	0.013	0.0020			
Brain volume (cc)		0.005	0.002	0.03	0.006	0.002	0.0088
FA median		17.45	5.468	0.0051			
MD PH (mm ² /s)		404.5	116.3	0.0027			
Central nervous system inflammation							
¹¹ C-PK11195 hotspots, %NAWM		-4.412	2.831	0.12	-3.414	2.561	0.19

Table 6.7. Unstandardised β coefficients and standard errors of univariate and multivariate models of candidate predictors of processing speed *z*-score. *SBP* systolic blood pressure; *DBP* diastolic blood pressure; *BMI* body mass index; *FA* fractional anisotropy; *MDPH* mean diffusivity peak height; *%NAWM* percentage of normal appearing white matter, values in percentage points.

		Univariate analysis			Multivariate analysis		
		β	SE	<i>p</i> value	β	SE	<i>p</i> value
Demographics							
Age (years)		0.023	0.012	0.06	0.029	0.014	0.048
Sex	Male	-0.272	0.264	0.31	-0.212	0.294	0.47
Ethnicity	White British	0.383	0.955	0.69			
Years in education		0.104	0.042	0.017			
IQ (NART)		0.046	0.016	0.007			
Vascular risk factors							
Hypertension		-0.249	0.374	0.51			
SBP (mmHg)		0.004	0.006	0.51			
DBP (mmHg)		-0.006	0.011	0.58			
Ischaemic heart disease		-0.338	0.645	0.60			
Hypercholesterolaemia		-0.135	0.285	0.64			
Diabetes mellitus		-0.065	0.356	0.86			
Smoking (current)		-0.045	0.270	0.87			
BMI (kg/m ²)		0.031	0.024	0.20			
Comorbidities							
Depression		-0.011	0.286	0.97			
Migraine		0.531	0.275	0.06			
Time since stroke (months)		0.003	0.007	0.97			
Conventional MRI markers							
WMH (cc)		-0.010	0.05	0.060			
Lacunes		-0.150	0.061	0.018			
CMBs		-0.010	0.011	0.37			
Brain volume (cc)		0.00031	0.0017	0.86			
FA median		11.030	3.455	0.005			
MD PH (mm ² /s)		37.97	94.60	0.69			
Central nervous system inflammation							
¹¹ C-PK11195 hotspots, %NAWM		-2.507	2.111	0.24	-2.661	2.022	0.20

Table 6.8. Unstandardised β coefficients and standard errors of univariate and multivariate models of candidate predictors of long-term memory *z*-score. *SBP* systolic blood pressure; *DBP* diastolic blood pressure; *BMI* body mass index); *FA* fractional anisotropy; *MDPH* mean diffusivity peak height; *%NAWM* percentage of normal appearing white matter, values in percentage points.

		Univariate analysis			Multivariate analysis		
		β	SE	<i>p</i> value	β	SE	<i>p</i> value
Demographics							
Age (years)		0.013	0.010	0.20	0.010	0.011	0.35
Sex	Male	-0.084	0.218	0.70	-0.052	0.191	0.79
Ethnicity	White British	-0.033	0.711	0.96			
Years in education		0.085	0.034	0.018			
IQ (NART)		0.051	0.013	0.00037	0.052	0.125	0.0002
Vascular risk factors							
Hypertension		-0.250	0.305	0.42			
SBP (mmHg)		-0.004	0.005	0.45			
DBP (mmHg)		-0.003	0.010	0.75			
Ischaemic heart disease		-0.037	0.433	0.93			
Hypercholesterolaemia		-0.032	0.234	0.89			
Diabetes mellitus		-0.306	0.288	0.29			
Smoking (current)		-0.351	0.213	0.11			
BMI (kg/m ²)		-0.0002	0.020	0.99			
Comorbidities							
Depression		-0.353	0.228	0.13			
Migraine		-0.044	0.234	0.85			
Time since stroke (months)		-0.007	0.005	0.13			
Conventional MRI markers							
WMH (cc)		-0.013	0.004	0.0031			
Lacunes		-0.125	0.049	0.016			
CMBs		-0.023	0.008	0.007	-0.024	0.007	0.0026
Brain volume (cc)		0.002	0.001	0.23			
FA median		14.87	3.43	0.00040			
MD PH (mm ² /s)		158.4	101.1	0.14			
Central nervous system inflammation							
¹¹ C-PK11195 hotspots, %NAWM		-4.452	1.59	0.0079	-2.607	1.369	0.060

Table 6.9 Unstandardised β coefficients and standard errors of univariate and multivariate models of candidate predictors of global cognition *z*-score. *SBP* systolic blood pressure; *DBP* diastolic blood pressure; *BMI* body mass index); *FA* fractional anisotropy; *MDPH* mean diffusivity peak height; *%NAWM* percentage of normal appearing white matter, values in percentage points.

Relationship of peripheral blood proteomic panel with markers of SVD severity

Proteomics data were available for 56 participant. All samples passed quality control based on the deviation from the median value of pooled serum internal control samples for each protein below a threshold of 0.3 NPX. All plates passed quality control based on a standard deviation of the values for the pooled internal control samples below a threshold of 0.2 NPX. The mean intra-assay coefficient of variance was 8%, and the mean inter-assay coefficient of variance was 13%. Details of the intra- and inter-assay coefficient of variance distributions are provide in Appendix C.

On univariate analysis, neither C-reactive protein nor any of the 92 biomarkers in the Olink CVD III panel was significantly associated with any SVD marker (WMH volume, lacune count, CMB count or brain volume) when false discovery rate-corrected. The most significant predictors of WMH volumes were BLM hydrolase ($\beta = 0.402$, FDR-corrected $p = 0.14$), Galectin-4 ($\beta = 0.390$, $p = 0.14$) and myoglobin ($\beta = 0.387$, $p = 0.14$). The most significant predictor of CMBs was IGFBP-1 ($\beta = -0.414$, $p = 0.67$). The best predictors of lacune count and brain volume were on the borderline of statistical significance uncorrected. Results for individual biomarkers are presented in Appendix D. Of the pre-specified panel components, there were no statistically significant associations with radiological SVD markers; TIMP-4 correlated positively with WMH volume, lacune count and CMBs and negatively with brain volume, whereas P-selectin showed the opposite associations (table 6.10).

	WMHs		Lacunes		CMBs		Brain volume	
	β	p value	β	p value	β	p value	β	p value
CRP	0.064	0.96	-0.118	0.27	-0.739	0.22	0.461	0.91
MMP-2	0.086	0.54	-0.081	0.57	-0.145	0.28	0.146	0.27
MMP-3	-0.029	0.83	-0.024	0.86	-0.098	0.46	-0.132	0.30
MMP-9	-0.145	0.30	-0.167	0.23	-0.207	0.12	0.008	0.96
E-selectin	-0.187	0.18	-0.079	0.57	-0.028	0.84	-0.183	0.20
P-selectin	-0.184	0.20	-0.128	0.36	-0.157	0.24	0.051	0.72
TIMP-4	0.217	0.12	0.131	0.35	0.147	0.27	-0.009	0.95
vWF	0.124	0.40	-0.055	0.71	0.047	0.74	-0.052	0.71

Table 6.10. Results from univariate linear regression models of C-reactive protein and pre-specified biomarkers from the Olink CVD III panel as predictors for WMHs (cc), lacune count, CMB count and brain volume (cc).

Principal component analysis of the Olink biomarker panel results did not satisfactorily reduce the dimension of the data, with the first two principal components accounting for 9.96% and 9.11% of the inter-subject variance respectively (figure 6.7A). 21 dimensions were required to account for 85% of the variance, the figure at which principal components are considered to be sufficiently representative to take forward for further analysis (figure 6.7B). This was considered analytically intractable and unlikely to provide biologically meaningful results from more detailed analysis.

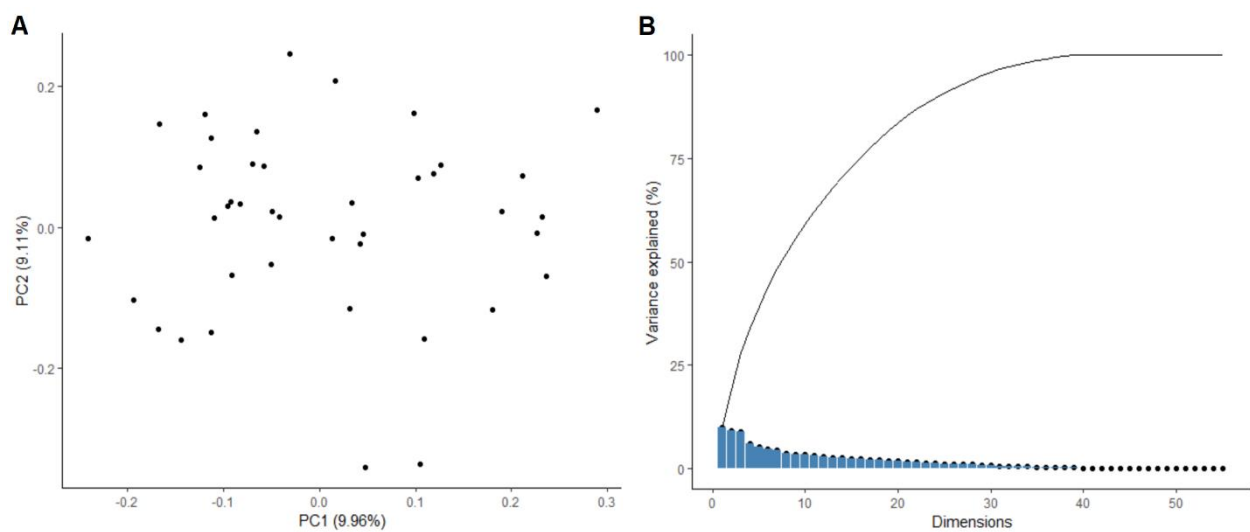


Figure 6.7. Principal component analysis results of Olink CVD III panel data. (A) Scatter plot showing association of principal components 1 and 2. (B) Scree plot showing variance explained by each dimension and cumulative variance explained across all dimensions (black line).

Compound biomarker cluster scores were calculated as described above. The mean for the pooled patient cohort was significantly higher than the control population (5.48 compared to 4.74, $p < 1 \times 10^{-6}$). On univariate analysis, biomarker cluster score was not significantly associated with any markers of SVD severity, with the strongest correlation shown with brain volume (standardised $\beta = -0.24$, $p = 0.08$). Figure 6.8 shows the relationship between the biomarker cluster scores and radiological SVD markers.

On multivariate analysis, corrected for age, sex and diagnosis of hypertension, the biomarker cluster score had a negative correlation with brain volume at borderline

statistical significance (standardised $\beta = -0.262$, $p = 0.043$). No other markers reached statistical significance, though the prediction effect size for this score was similar to that demonstrated by Kuipers et al.²²² ($\beta = 0.205$, $p = 0.14$; results for each marker are presented in table 6.11).

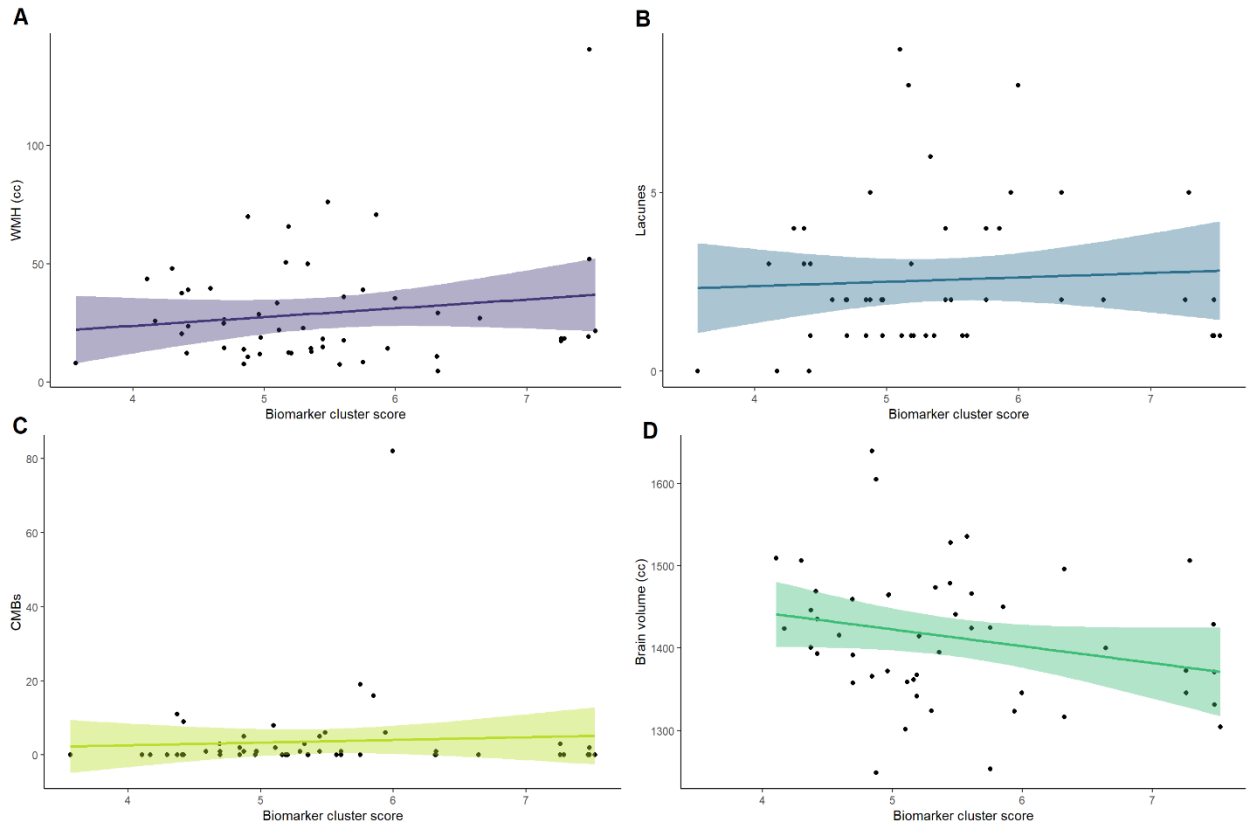


Figure 6.8. Scatter plot showing correlation of compound biomarker cluster score to (A) WMHs (B) lacune count (C) CMB count and (D) brain volume.

Marker	β (standardised)	p value
WMH	0.205	0.14
Lacunes	-0.009	0.95
CMBs	0.021	0.88
Brain volume	-0.262	0.043
FA median	-0.027	0.85
MD PH	-0.11	0.41

Table 6.11. Results from multivariate linear regression of biomarker cluster score versus radiological markers of SVD, corrected for age, sex and diagnosis of hypertension.

Relationship of circulating monocytes to radiological SVD markers

Mass cytometry data were available for the final 25 participants in the MINERVA trial. Proportions of classical ($3.57 \pm 1.58\%$ of intact live cells) and non-classical ($0.41 \pm 0.22\%$) monocytes were broadly as expected from population reference ranges; there was a slightly larger population of intermediate monocytes ($0.30 \pm 0.16\%$).

Within this subgroup of the MINERVA trial participants, neither the proportion of classical monocytes (standardised $\beta = 0.188$, $p = 0.14$) nor intermediate monocytes ($\beta = 0.216$, $p = 0.08$) were associated with WMH. However both classical and intermediate subsets negatively predicted FA median and MD peak height (classical/FA: $\beta = -0.564$, $p = 0.034$; classical/MDPH: $\beta = -0.720$, $p = 0.0062$; intermediate/FA: $\beta = -0.665$, $p = 0.0041$; intermediate/MDPH: $\beta = -0.611$, $p = 0.013$). These results are displayed in table 6.12.

	Classical		Non-classical		Intermediate	
	β	p value	β	p value	β	p value
WMH	0.188	0.14	0.049	0.69	0.216	0.08
Lacunae	0.391	0.12	0.177	0.52	0.427	0.06
CMBs	0.254	0.46	0.142	0.65	0.473	0.15
Brain volume	0.019	0.93	0.125	0.58	0.108	0.59
FA median	-0.564	0.034	-0.187	0.54	-0.665	0.0041
MD PH	-0.720	0.0062	-0.060	0.85	-0.611	0.013

Table 6.12. Results from multivariate linear regression of monocyte subset (percentage of live cells) versus radiological markers of SVD, corrected for age and sex.

Interactions between peripheral and central compartments

The biomarker cluster score was positively correlated with ^{11}C -PK11195 binding proportion (standardised $\beta = 0.317$, $p = 0.05$) and statistically significant when corrected for age, sex, and diagnosis of hypertension ($\beta = 0.359$, $p = 0.034$). Figure 6.9 shows this relationship.

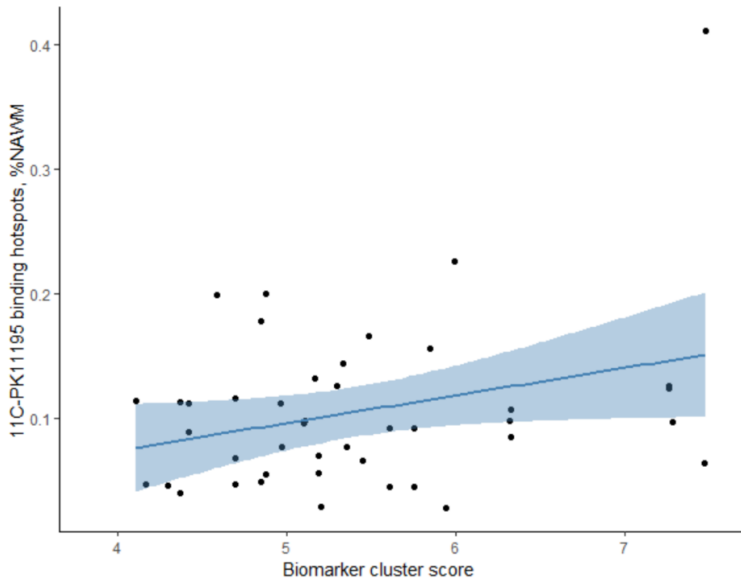


Figure 6.9. Scatter plot showing relationship between biomarker cluster score and ^{11}C -PK11195 binding hotspots as percentage of NAWM. *%NAWM percentage of normal appearing white matter*

Proportions of both circulating classical ($\beta = 0.501$, $p = 0.12$) and intermediate ($\beta = 0.513$, $p = 0.11$) were positively correlated with ^{11}C - PK11195 binding proportion, though did not reach statistical significance (figure 6.10).

According to these results and their relationships with radiological markers, compound biomarker cluster score, proportion of classical and intermediate monocytes were taken forward to causal mediation analysis (the putative mediator being ^{11}C - PK11195 binding and the outcomes radiological markers of SVD).

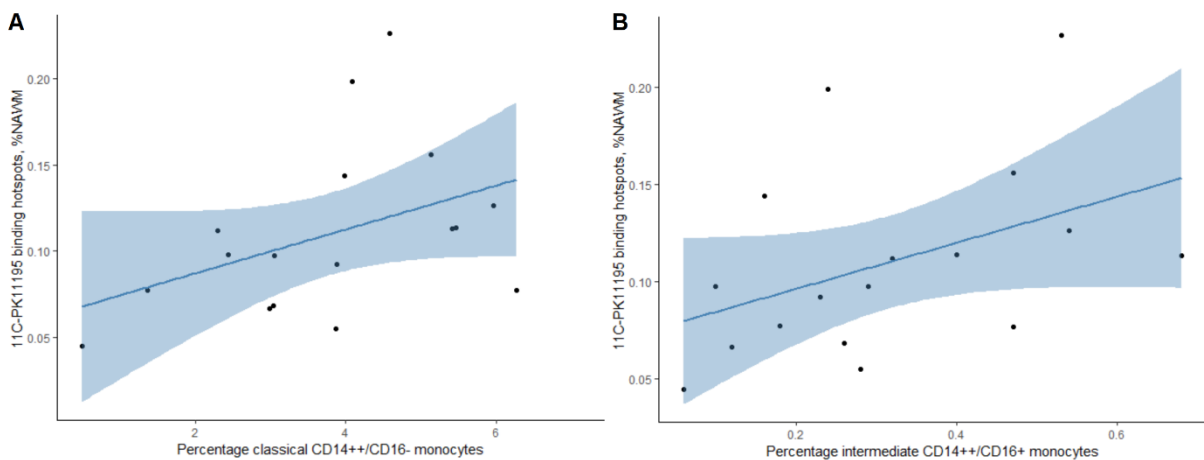


Figure 6.10. Scatter plots showing relationship between proportion of (A) CD14++/CD16- classical monocytes and (B) CD14++/CD16+ intermediate monocytes and ^{11}C -PK11195 binding hotspots as percentage of NAWM. *%NAWM percentage of normal appearing white matter*

In the causal mediation analyses, there were no significant partially mediating effects found for the relationship between any of these peripheral metrics of inflammation and either WMH volume, lacune count, CMB count or brain volume. However, there were some significant partial mediation effects shown between each of the monocyte subsets and both FA median and MD peak height (figure 6.11).

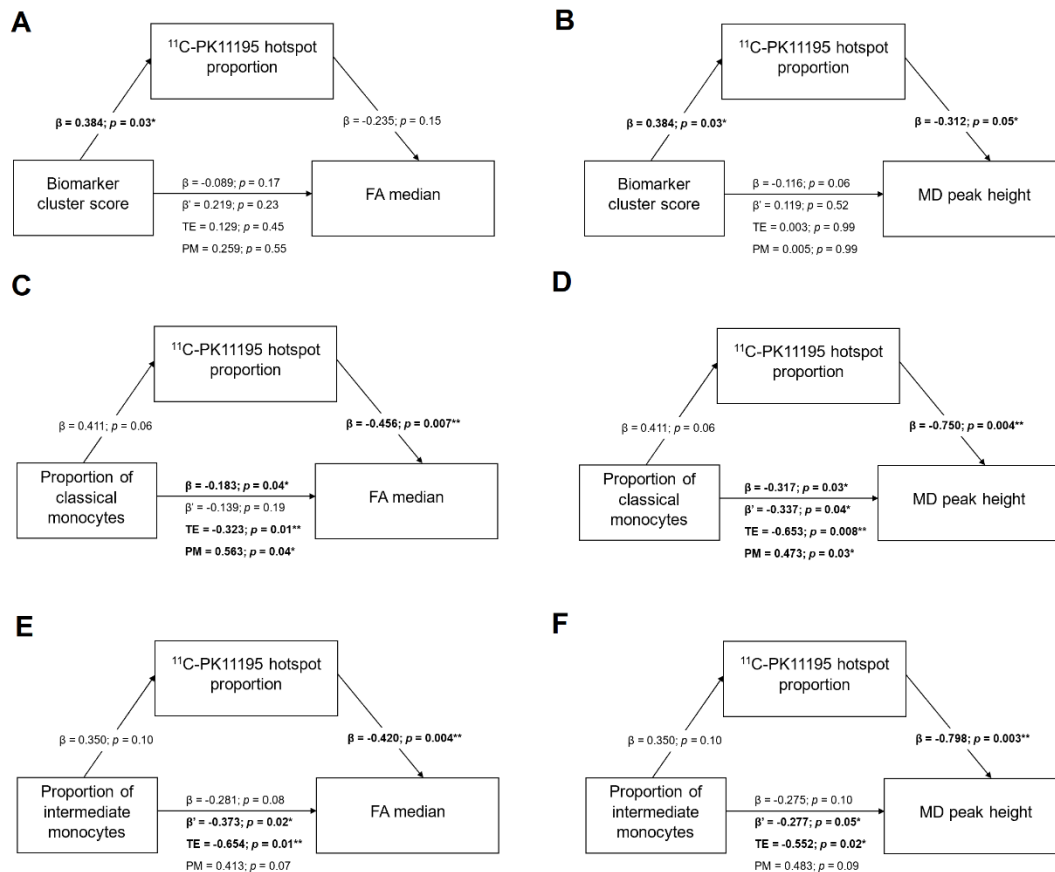


Figure 6.11. Models testing if ^{11}C -PK11195 binding proportion mediates association between measurements of peripheral inflammation and radiological outcomes. (A) Olink CVD III biomarker cluster score versus FA median (B) Olink CVD III biomarker cluster score versus MD PH (C) Proportion of classical monocytes versus FA median (D) Proportion of classical monocytes versus MD PH (E) Proportion of intermediate monocytes versus FA median (F) Proportion of intermediate monocytes versus MD PH. *FA* fractional anisotropy; *MD* mean diffusivity; β standardised β -coefficient for direct effect; β' standardised β -coefficient for indirect effect; *TE* treatment effect; *PM* proportion mediated

Discussion

These detailed results describe immune system activity in a cohort of patients with symptomatically-defined moderate-to-severe SVD, investigated using a range of experimental techniques to interrogate both peripheral (blood) and central (CNS) compartments. These demonstrated significant differences between the SVD patient and control groups, both in the CNS measuring ^{11}C -PK11195 binding in several exploratory metrics, and in a cluster of serum biomarkers. These findings support previous work using the Olink CVD III panel²²² and build on findings from the observational phase of this study alone.²¹³

I demonstrated a very clear relationship between the ^{11}C -PK11195 binding in the NAWM and the WMH lesion volume. As discussed in chapter two, WMHs are a key radiological marker of SVD severity due to their near ubiquitous presence and continuous distribution, and this finding provides further evidence that microglia may be relevant in their pathogenesis. There was no relationship to lacune count, CMB count or brain volume, which may reflect the discontinuous nature of these distributions and other overlapping disease processes such as neurodegeneration. Age significantly predicted a lower brain volume, as expected.

A further novel finding is that ^{11}C -PK11195 was associated with worse performance in the executive function cognitive domain. This suggests that microglia activity in white matter networks may be associated with impairment in this domain and supports previous studies showing that white matter network parameters measured using DTI and white matter free water also relate executive function performance.^{352,353} Importantly, although markers of white matter integrity contributed significantly to this model (in this case FA), the signal was independent from the relationship with ^{11}C -PK11195.

Neither C-reactive protein nor any of the individual biomarkers from the Olink CVD III panel were associated with radiological markers of SVD severity. This was unsurprising as previous studies that have found significant associations have been

larger by approximately an order of magnitude.^{217,219,222} However, it was noteworthy that I found no evidence to support the role of specific matrix metalloproteases (MMP-2, MMP-3, MMP-9 and TIMP-4) or markers of endothelial activation / coagulation (E-selection, P-selectin and vWF) on markers of SVD severity. It is not known to what extent values for these biomarkers vary over time or are subject to perturbation by illness or other medical factors. Principal component analysis of the Olink panel data was uninformative as there was weak covariance between the individual panel components; it has previously been applied to this panel in a much larger study investigating pulse pressure³⁵⁴ with broadly similar findings.

The biomarker cluster score was more informative. Although only associated with brain volume on multivariate analyses, it predicted ¹¹C-PK11195 binding in the central compartment and although this cannot be interpreted as proof of causation, it suggests that there may be a common pathophysiological process underlying both phenomena. The components of this compound score include GDF-15, a marker of cellular stress, cystatin B, an extracellular vesicle protein considered to represent BBB permeability, GP-VI, a platelet receptor, TIMP-4, and SPP-1, a pleiotropic cell surface marker that can be induced in activated macrophages.³⁵⁵ This suggests that diffuse cellular, endothelial and intravascular processes may be active in SVD. These may simply represent a response to the haemodynamic instability presented by cardiovascular risk factors rather than a direct risk for further tissue damage as there were no significant mediation effects identified by causal mediation analysis using the biomarker cluster score.

In contrast, there were clear associations between the proportions of circulating classical and intermediate monocyte subsets and DTI markers of white matter microstructure (FA median and MD PH). Although there was not a statistically significant relationship between these subsets and ¹¹C-PK11195 binding, the causal mediation analysis did reveal significant associations in the direct effect (classical monocytes on FA median and MD PH), indirect effect (classical monocytes on MD PH, intermediate monocytes on FA median and MD PH) and overall treatment effect

(both subsets on FA median and MD PH). This suggests that contemporaneous activation of blood monocytes and subtle early evidence of white matter damage may be mediated by microglia in the central compartment. It is interesting that this relationship was not shown for overtly damaged tissue as measured by either WMH volume or lacune count; recent analysis of the one-year follow-up data from the observational phase study showed that NAWM voxels that go on to become WMH at follow-up have significantly lower ^{11}C -PK11195 binding, suggesting that if microglial activity is a factor for disease progression, it is relevant at least a year prior to overt tissue injury.³⁵⁶ These results add further support to this study and suggest a model where peripheral monocyte activation stimulates microglia in the NAWM, which is then at risk of progression to WMH over a period of one year or longer. I included only raw cell counts from mass cytometry, but did not analysis functional markers of monocyte activity such as cytokine stimulation, and this work is planned in order to gain a deeper immunophenotype of this patient population.

As resident tissue phagocytes, activation of microglia is seen at the end-point of inflammatory pathways regardless of whether the initial injury is primarily immune (for example, in multiple sclerosis³⁵⁷), ischaemic or degenerative³⁵⁸; disentangling the role of primary microglial activity requires more detailed phenotyping of the CNS cell population itself (from animal models or CSF in patients) and longitudinal follow-up correcting for other demographic and cardiovascular risk factors and markers of disease severity. The summary metric for inflammation in the central compartment in this study was microglial signal as measured by ^{11}C -PK11195 binding hotspot proportion. This discriminated well between patients and control participants, but it may be less useful for mechanistic analysis within the patient group. I did not perform regional analysis (either voxelwise, which would be limited by the somewhat coarser resolution of the PET images, or by region of interest), which may offer more specific mechanistic insight into how the microglial signal relates to afferent blood supply and anatomical location.

Critically, the cells are dynamic and have the potential to demonstrate either pro-inflammatory (“M1” phase, defined by the expression of stimulatory surface molecules including CD86, and production of IL-1 β , and TNF- α) or anti-inflammatory (“M2” phase, characterised by anti-inflammatory surface markers such as CD206, and production of IL-10, and TGF- β) phenotypes.¹⁹¹ However, recent consensus is that these strict categories are insufficient to describe the range of functional behaviours exhibited by microglia³⁵⁹ and more detailed assessment of microglial phenotype via transcriptomic analysis might provide more accurate insight into their role in disease.

Strengths of this study included the number of participants included, which although significantly smaller than previous observational MRI-based studies of patients with SVD, was comparable in size and used more detailed central and peripheral inflammation metrics than similar immunophenotyping studies.^{214,226} A reasonably homogeneous patient population is likely to reflect the fact that this cohort is representative of patients with SVD in our area, and robust processing was included to harmonise data from the observational phase study and the MINERVA trial.

Despite the number of participants included, the study was nevertheless underpowered to detect certain associations and may not have detected relationships between the peripheral and central biomarkers or radiological markers of disease. Recruitment was limited by the number necessary for the MINERVA trial and associated funding for neuroimaging. A further potential limitation is that this relatively small participant cohort was used to test the relationship between a large number of variables, and although these were hypothesis-driven it is possible that some of the relationships identified were chance findings based on the number of experiments performed on this population.

Comparison of blood results measured at a single time point to radiological outcomes that reflect the accumulation of disease over many years also limits the interpretation of the role of these processes identified. Various patient factors including intercurrent illness or infection may affect these parameters and further work is needed to establish

how they fluctuate over time and what should be considered the normal range in patients with SVD. However, the clear separation between patient and control groups in all parameters measured supports the ongoing investigation of these processes.

Further work will test whether the MINERVA trial treatment has any differential effects in the central and peripheral compartments and also whether the markers of central and peripheral inflammation identified predict disease progression longitudinally (as would be necessary to demonstrate a causal effect). Initial longitudinal analysis using only data from the observational phase patients is discussed in chapter eight. Additional work is planned to perform more detailed immunophenotyping of CSF cells using single cell RNA sequencing of CSF from the MINERVA trial patients; this will provide additional evidence towards whether the signal identified in the PET images represents a discrete CSF myeloid cell profile. Finally the mass cytometry results include a large amount of data on other leucocyte cell lines and suggests a data-driven approach to investigate whether any additional cell populations may be relevant in SVD.

CHAPTER SEVEN

Association of blood-brain barrier permeability with baseline SVD severity, neuropsychometric performance and cerebrospinal fluid biomarkers

I recruited the participants for the MINERVA trial, arranged neuroimaging, collected and processed blood samples, performed cognitive testing, segmented the image masks, and analysed the data. Jessica Walsh recruited the participants to the observational phase study and performed baseline cognitive testing. Guy Williams assisted with pre-processing of the images. Daniel Tozer performed image registration and hotspot identification. Malin Overmars assisted with calculation of the biomarker cluster scores.

Introduction

This chapter examines the relationship between BBB permeability, measured both non-invasively and via invasive biomarker sampling, and both radiological markers of SVD and cognition. The role of the BBB has been well established in health and in neurological disease; evidence that is relevant in SVD has accumulated over several years and is summarised below. I go on to investigate the relationship between biomarkers of astrocytic activation and neuronal breakdown and SVD severity.

Evidence for the role of BBB permeability in SVD

The BBB is a network of cells and extracellular matrix around capillary endothelium in the brain which serves to maintain brain homeostasis and prevent exposure to potential toxins¹⁸⁸; details of the cellular structure are presented in the introduction.

Initial evidence for deficiency in the BBB in patients with SVD came from post-mortem brain samples; reasonably large molecules such as immunoglobulins^{194,360} and fibrinogen^{195,196}, which in healthy BBB states should not penetrate into brain parenchyma, are seen on immunohistochemical studies.

Due to the limitations with post-mortem sampling discussed in chapters one and six, *in vivo* experimental techniques to demonstrate an association between BBB permeability and SVD severity must either use pre-clinical animal models or measure flux across the BBB using neuroimaging techniques.

Rodent models of SVD do provide some evidence that the BBB is deficient, including in the spontaneously hypertensive / stroke-prone rat where white matter staining three weeks after carotid artery occlusion showed immunoglobulin staining in the white matter²²⁵, an indication of its permeability through the BBB, and in mice with bilateral carotid artery occlusion; in this paradigm, mice undergoing this procedure displayed significant leakage of Evans blue dye after 14 days and this was associated with significantly lower expression of occludin, a tight junction protein key for BBB integrity.³⁶¹ However, these models are necessarily limited by the invasiveness of the

interventions required to generate them and by subtle differences in BBB anatomy, physiology and neurogliovascular cell behaviour.

BBB permeability can be measured using neuroimaging techniques, typically using the administration of gadolinium-based contrast to shorten the T1 relaxation time and amplify the T1 image signal where it penetrates the CNS (DCE-MRI), though encouraging techniques are being developed to generate images based on applying a diffusion filter rather than using contrast agents.³⁶² DCE-MRI studies have shown increased area under curve across the whole brain of patients with SVD²⁰⁶ and focal areas of BBB breakdown by application of the Patlak tracer kinetic model.^{210,213} Similar results in a cohort of patients with minor stroke showed a significant negative correlation between voxels of increased BBB permeability and distance from WMH.²¹⁰ However, BBB permeability did not predict incident WMH voxels at one year follow-up.

The optimal method for measuring overall BBB permeability is comparison of concentration in blood and CSF of a large molecule to which the BBB ought to be impermeable. Albumin is most often used as an abundant serum protein that is practical to measure and increasing leaks through tight junctions as BBB permeability increases. The CSF/serum albumin ratio (or albumin quotient, Q_{alb}) has been suggested as the gold standard assessment of BBB function and is increased in populations with lacunar stroke or VCI/VaD¹⁹⁹, patients with vascular risk factors within a mixed dementia cohort²⁰⁰ and a cohort explicitly with subcortical VaD.²⁰¹

Other CSF markers of BBB integrity have been investigated, including Cystatin C²⁰⁴ (an extracellular vesicle protein, which was significantly associated with WMH progression, and several cardiovascular biomarkers that were found to be associated with BBB dysfunction in early Alzheimer's disease,³⁶³ including proinsulin and apolipoprotein A. A further marker of interest is platelet-derived growth factor receptor- β (PDGFR β), which is expressed by pericytes and shed when the BBB breaks down¹⁹³; this study found that CSF PDGFR β concentrations were independent of

vascular risk factor burden, but importantly that it correlated with early cognitive impairment. This suggests that BBB integrity may be important for cognition regardless of the aetiology of cognitive dysfunction.

Role of markers of neurogliovascular unit breakdown in SVD

The highly conserved architecture of the BBB described in chapter one (figure 1.6) and strictly regulated interactions between the perivascular cells and endothelium together with astrocytes and neurons has led to this structure being described as the neurogliovascular unit.³⁶⁴ As all components are required for intracerebral homeostasis and neuronal signalling, the idea has arisen that disruption of any one component of this unit may be responsible for neurological impairment in disease.³⁶⁵

Assessment of neurogliovascular unit dysfunction in a more general sense has been limited in SVD, though some pre-clinical studies have been informative. In mice undergoing bilateral carotid artery microcoil stenosis, histological analysis showed widespread disruption to vascular and astrocytic cytoarchitecture and relocation of astrocytic aquaporin-4 water channels³⁶⁶, and in a middle cerebral occlusion mouse model, neurons were found to express proteins previously only seen in astrocytes.³⁶⁷ Evidence in humans is less clear, but widespread changes in astrocyte morphology have been shown in CADASIL³⁶⁸, and it has been suggested that altered neurogliovascular function rather than structure may underlie some of the motor symptoms seen in SVD.³⁶⁹

An emerging marker of astrocytic dysfunction is glial fibrillary acidic protein (GFAP), a structural protein found predominantly in astrocytes that is upregulated when astrocytes are activated by immune challenge³⁷⁰ and can leak into blood in very low concentrations across the BBB and the blood-CSF barrier.³⁷¹ This low concentration makes measurement by conventional techniques challenging, but the development of single molecule detection assays has made it viable and raised serum GFAP levels have been found in neurodegenerative conditions where neuroinflammatory processes and

BBB breakdown are known to be relevant, including Alzheimer's disease and Lewy Body Dementia.³⁷²

A more general marker of neuronal breakdown is neurofilament light chain (NfL), a neuronal cytoplasmic structural protein that is expressed in large myelinated axons and increases in the CSF in proportion to the breakdown of these axons.³⁷³ The development of similar single molecule assays has allowed NfL to be measured accurately in the serum, and in addition to traditionally demyelinating conditions such as multiple sclerosis, recent studies have shown that NfL in blood rises proportion to SVD severity³⁷⁴ and predicts incident dementia in patients with SVD.³⁷⁵ It has not been established whether the serum NfL increases seen in these conditions represent increased concentrations in the CNS, increased BBB breakdown or a combination of the two; in addition to testing the relationship between NfL and disease severity, comparison with measures of BBB permeability allow me to evaluate this relationship.

Hypotheses and study design

I hypothesised that SVD pathology is associated with focal areas of BBB breakdown and tested these associations by assessing the correlation of MRI markers of SVD severity and neuropsychometric test scores with parameters derived from DCE-MRI images. To do this, I also derived the optimal parameters from DCE-MRI imaging to discriminate between patients and control participants similar to the derivation of these parameters for the PET images described in chapter six. I further testing the relationship of these markers with the CSF/serum albumin ratio, and compared the radiological and biomarker-based methods of assessing BBB permeability.

I further hypothesised that astrocytic activation represents a distinct pathological process in SVD,, and tested the association between GFAP in both serum and CSF with markers of disease severity. NfL was also tested in a similar manner to test the hypothesis that axonal breakdown is related to radiological markers of SVD.

Finally I hypothesised that the concentration of these proteins in blood is related to increased CNS turnover rather than increased leakage through the BBB.

Methods

For this analysis, I used data from the pooled cohort of 57 independent Patients with SVD that had baseline DCE-MRI, phlebotomy and neuropsychometric testing as described in chapter five. As CSF sampling and some of the serum assays were only implemented for the MINERVA trial participants, aspects of the analysis include only the trial cohort and this is highlighted where relevant. Inclusion and exclusion criteria are presented in chapter four, as are details of the neuroimaging protocol (with full sequence details in Appendix B).

Image analysis

WMHs, lacunes and CMBs were highlighted as described in chapter six. Brain volumes and DTI histograms were calculated as discussed in chapter four.

T1 maps were calculated using the standard radiofrequency spoiled-gradient echo signal equation. The Patlak model³¹⁰ was then fitted by GBW and DJT to produce maps of permeability constant (K_{in}). These maps were registered to the original T1 images and voxels of increased BBB permeability ('hotspots') defined as those with a K_{in} greater than the 95th percentile of permeability derived from control participants, analogous to the method used for calculating hotspots of ¹¹C-PK11195 binding in chapter six.

As several parameters can be produced from the BBB permeability mapping, I first aimed to establish the optimal metric for further testing using methods analogous to those employed for the ¹¹C-PK11195 binding maps in chapter six. I assessed which of these potential metrics (including volume of hotspot tissue and hotspot volume scaled for tissue class across all the tissue class masks) was the best discriminant between the sporadic SVD and patient groups and selected this as a single readout value from the DCE-MRI images.

Blood processing

Blood was collected from each participant and processed as described in chapter four. From the Olink CVD-III panel, *a priori* markers of interest were chosen to examine

specifically based on evidence from the literature: COL1A1, Cystatin B, Junctional Adhesion Molecule-A, MMP-2, MMP-3, MMP-9, and TIMP-4.

In the MINERVA patients, an additional blood sample was sent to the Dementia Research Institute Biomarker Laboratory, University College London for measurement of NfL and GFAP using the SIMOA platform as described in chapter four. In the subset of MINERVA patient who underwent CSF sampling, a serum aliquot was also sent to the Core Biochemical Research Laboratory, University of Cambridge for paired measurement of albumin by ELISA.

Cerebrospinal fluid processing

CSF was collected from a subset of the MINERVA participants as described in chapter four and albumin measured in the Core Biochemical Research Laboratory, University of Cambridge for paired measurement of albumin by ELISA as above. NfL and GFAP were measured in CSF using the SIMOA platform as above.

Neuropsychiatric testing

Neuropsychometric testing was performed as detailed in chapter six.

Statistical analysis

To derive the optimal output from the DCE-MRI images, I performed multivariate logistic regression to assess the extent to which each candidate metric predicted participant group, including as covariates age and sex, and selected the metric that minimised the Akaike Information Criteria (AIC) in this model. All statistical analysis was performed in the R project for statistical computing²⁶⁰ 4.2.1.

Univariate linear regression was performing to test the association of this BBB permeability metric with radiological markers of SVD (WMHs, lacunes, CMBs and brain volume). Any variables not normally distributed under the Shapiro-Wilk test were transformed until normal. Associations between potential covariates already tested in chapter five, including demographic details and comorbidities, are presented again to provide context for multiple linear regression analysis.

Multivariable linear regression models were then constructed to test the correlation of BBB permeability and radiological SVD markers, including as pre-specified covariates age and sex. Only one variable from any pairs of predictors with a correlation coefficient >0.8 was taken forward to the final model. I used a combination of stepwise forward selection of any predictors with $p < 0.05$ on univariate analysis and backward selection of predictors that lost this significance in the multivariate model. As in chapter five, results are presented as unstandardised β coefficients and standard errors except where the units of either independent or dependent variables are arbitrary, in which case standardised β coefficients are given.

Similar univariate and multivariable linear regression models were next constructed to test the relationship between BBB permeability and neuropsychometric test performance in each of the cognitive domains.

Each biomarker from the Olink CVD-III panel was first entered individually into linear regression models of WMHs, lacune count, CMB count and brain volume and considered significant at $p < 0.05$ (false discovery rate-corrected). Next, the biomarker cluster scores were also tested, corrected for age, sex and hypertension as was done in their derivation.²²²

The CSF/serum albumin quotient, Q_{alb} , was defined as the ratio of the serum albumin (g/L) to CSF albumin (mg/L). I next tested the relationship between Q_{alb} and both radiological markers of SVD and cognitive performance in each domain. As a post-hoc validation exercise, I assessed the correlation of Q_{alb} to average K_{in} in the slab of tissue under consideration using Pearson's product moment correlation; on an exploratory basis I also tested whether Q_{alb} was related to the BBB permeability hotspot metric that best discriminated patients from controls.

Finally, I tested the relationship of serum and CSF NfL and GFAP with markers of markers of disease severity using similar models and whether the relationship between serum and CSF values was mediated by the BBB permeability metrics using causal mediation analysis.

Results

Data were included from 20 control participants and 20 patients with sporadic SVD from the observational phase study, and 44 participants from the MINERVA trial. CSF was taken from 18 trial participants; in four of these, albumin concentrations were in an intermediate range and presumed to represent contamination with blood. These were excluded from analysis leaving CSF samples from 14 participants. Demographics, cardiovascular risk factors and comorbidities are discussed in chapter five (see table 5.5).

Determination of optimal DCE-MRI marker for BBB permeability

The optimal BBB permeability metric to differentiate patients from controls was the NAWM hotspot volume as proportion of NAWM ($\beta = 0.29$, $p = 0.008$). This also discriminated better between groups than the voxelwise mean K_{in} . Table 7.1 shows the results of the logistic regression models from possible candidate metrics.

Figure 7.1 shows the between group comparisons for the DCE-MRI metrics of BBB permeability. Accordingly, NAWM percentage hotspot was selected for use in subsequent analysis (henceforth termed BBB hotspot proportion).

Candidate predictor metric	β	SE	z-statistic	p value	AIC
DCE-MRI					
Hotspot volume (NAWM)	0.24	0.10	2.30	0.021	47.62
Hotspot percentage (NAWM)	0.29	0.11	2.64	0.008	42.02
Hotspot volume (all WM)	0.24	0.10	2.81	0.004	45.72
Hotspot percentage (all WM)	0.32	0.12	2.75	0.006	42.47

Table 7.1. Logistic regression model results for candidate metrics of BBB permeability. *DCE-MRI* dynamic contrast-enhanced MRI; *WM* white matter; *NAWM* normal appearing white matter

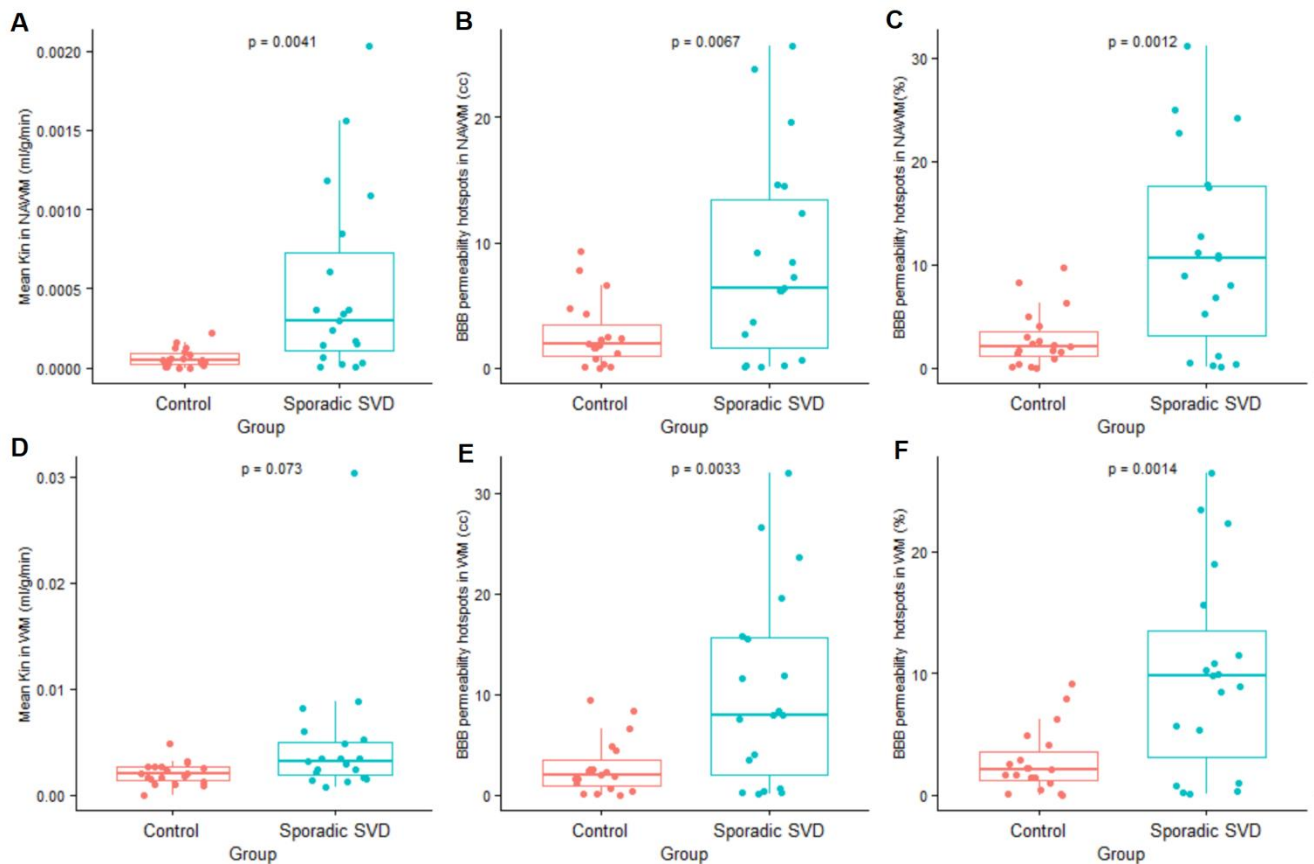


Figure 7.1 . Boxplots showing comparisons between control group and sporadic SVD patients for candidate metrics of BBB permeability: (A) mean K_{in} in NAWM; (B) hotspot volume in NAWM; (C) NAWM hotspots as percentage of NAWM; (D) mean K_{in} in all white matter; (E) hotspot volume in all white matter; (F) white matter hotspots as percentage of all white matter. *WM* white matter; *NAWM* normal appearing white matter

Relationship of BBB permeability to MRI markers of SVD

Univariate relationships between demographic factors/comorbidities and radiological SVD markers are discussed in chapter six and presented again in results tables.

WMHs

On univariate analysis, the BBB hotspot proportion was not a significant predictor of WMH volume ($\beta = -10.640$, $SE = 46.925$, $p = 0.82$). These results are shown in figure 7.2A. The BBB hotspot proportion did not predict WMH volume in the multivariate model. Table 7.2 shows the results of these models.

	Univariate analysis			Multivariate analysis			
	β	SE	<i>p</i> value	β	SE	<i>p</i> value	
Demographics							
Age (years)	0.466	0.316	0.15	0.548	0.368	0.14	
Sex	Male	3.547	6.800	0.60	6.112	7.953	0.45
Ethnicity	White	9.150	24.49	0.29			
	British						
Years in education	-2.868	1.114	0.013	-3.074	1.298	0.023	
Vascular risk factors							
Hypertension	-13.053	9.866	0.19				
SBP (mmHg)	-0.039	0.206	0.85				
DBP (mmHg)	-0.381	0.364	0.30				
Ischaemic heart disease	-12.397	10.773	0.26				
Hyper-cholesterolaemia	5.290	7.486	0.48				
Diabetes mellitus	1.245	8.672	0.89				
Smoking (current)	7.383	6.679	0.27				
BMI (kg/m ²)	-0.366	0.480	0.45				
Comorbidities							
Depression	9.454	7.261	0.20				
Migraine	7.298	7.309	0.32				
Time since last stroke (months)	0.421	0.140	0.0044				
BBB permeability							
K _{in} hotspots, %NAWM	-10.640	46.925	0.82	-23.341	46.31	0.62	

Table 7.2. Linear regression model results univariate and multivariate models of candidate predictors of WMH volume. Values are unstandardised β coefficients and standard errors. *SBP* systolic blood pressure; *DBP* diastolic blood pressure; *BMI* body mass index); *%NAWM* percentage of normal appearing white matter, values in percentage points.

	Univariate analysis			Multivariate analysis			
		β	SE	p value	β	SE	p value
Demographics							
Age (years)		-0.014	0.007	0.049	-0.013	0.008	0.11
Sex	Male	0.105	0.151	0.49	-0.078	0.169	0.65
Ethnicity	White British	0.038	0.535	0.94			
Years in education		-0.024	0.026	0.36			
Vascular risk factors							
Hypertension		0.360	0.213	0.098			
SBP (mmHg)		0.002	0.004	0.65			
DBP (mmHg)		-0.001	0.007	0.99			
Ischaemic heart disease		-0.083	0.333	0.81			
Hyper-cholesterolaemia		0.296	0.160	0.071			
Diabetes mellitus		0.085	0.207	0.68			
Smoking (current)		-0.051	0.151	0.74			
BMI (kg/m ²)		-0.005	0.011	0.68			
Comorbidities							
Depression		0.065	0.165	0.70			
Migraine		0.102	0.164	0.54			
Time since last stroke (months)		0.007	0.004	0.10			
BBB permeability							
K _{in} hotspots, %NAWM		-0.873	0.999	0.39	-1.156	1.007	0.26

Table 7.3. Linear regression model results univariate and multivariate models of candidate predictors of log lacune count. Values are unstandardised β coefficients and standard errors. *SBP* systolic blood pressure; *DBP* diastolic blood pressure; *BMI* body mass index); *%NAWM* percentage of normal appearing white matter, values in percentage points.

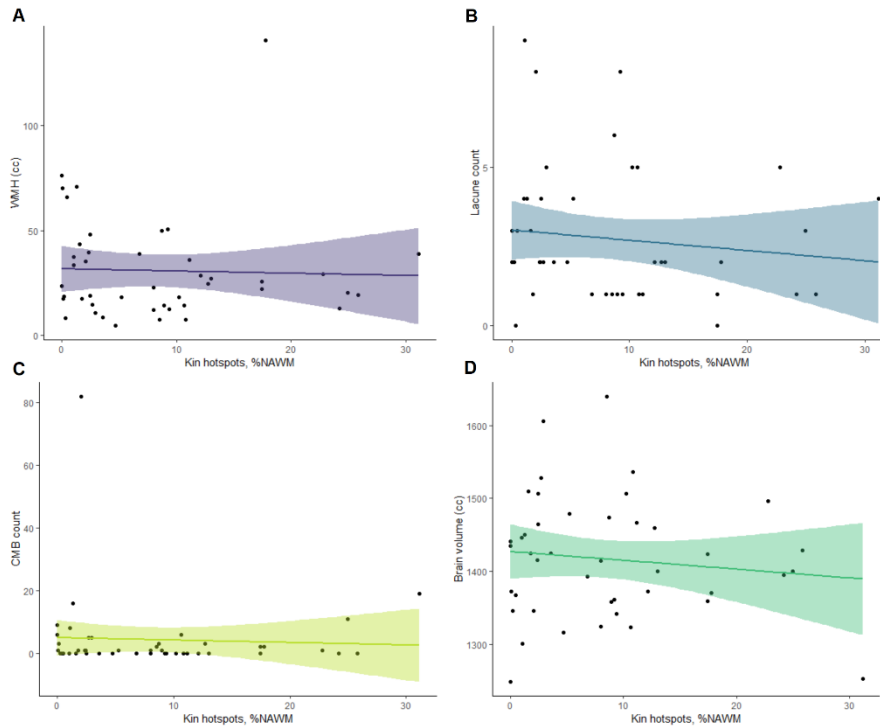


Figure 7.2. Scatter plots showing correlation of BBB permeability hotspot proportion to (A) WMHs (B) lacune count (C) CMB count and (D) brain volume.

Lacunae

The logarithm of the lacune count was tested as lacune count was not normally distributed. The BBB hotspot proportion did not predict lacune count on univariate analysis ($\beta = -0.873$, $SE = 0.999$, $p = 0.39$) not in the multivariate model. These results are shown in figure 7.2B and table 7.3.

CMBs

The CMB count was also non-normally distributed and natural logarithm-transformed; the BBB permeability hotspot proportion did not predict this value on univariate ($\beta = 0.0358$, $SE = 1.992$, $p = 0.98$) or multivariate analysis. These results are shown in table 7.4 and figure 7.2C.

Brain volume

BBB permeability hotspot did not predict brain volume on univariate analysis ($\beta = -120.89$, $SE = 158.17$, $p = 0.45$). On the multivariate analysis, only age was a significant predictor of brain volume with a negative correlation ($\beta = -3.732$, $SE = 1.168$, $p = 0.0028$). These results are shown in table 7.5 and figure 7.2D.

	Univariate analysis			Multivariate analysis			
	β	SE	p value	β	SE	p value	
Demographics							
Age (years)	-0.023	0.0127	0.072	-0.026	0.016	0.12	
Sex	Male	-0.099	0.277	0.72	-0.334	0.336	0.33
Ethnicity	White	0.010	1.039	0.99	[Redacted]		
	British						
Years in education	0.013	0.148	0.79	[Redacted]			
Vascular risk factors							
Hypertension	0.660	0.398	0.10	[Redacted]			
SBP (mmHg)	0.007	0.006	0.26				
DBP (mmHg)	0.003	0.012	0.81				
Ischaemic heart disease	-0.161	0.559	0.77				
Hyper-cholesterolaemia	0.012	0.306	0.97				
Diabetes mellitus	0.130	0.353	0.72				
Smoking (current)	0.068	0.275	0.81				
BMI (kg/m ²)	-0.012	0.020	0.56	[Redacted]			
Comorbidities							
Depression	-0.389	0.296	0.19	[Redacted]			
Migraine	-0.126	0.300	0.68				
Time since last stroke (months)	0.010	0.006	0.11				
BBB permeability							
K _{in} hotspots, %NAWM	0.0358	1.992	0.98	-0.567	2.003	0.78	

Table 7.4. Linear regression model results univariate and multivariable models of candidate predictors of log CMB count. Values are unstandardised β coefficients and standard errors. *SBP* systolic blood pressure; *DBP* diastolic blood pressure; *BMI* body mass index; *%NAWM* percentage of normal appearing white matter, values in percentage points.

	Univariate analysis			Multivariate analysis			
	β	SE	p value	β	SE	p value	
Demographics							
Age (years)	-3.155	1.018	0.003	-3.732	1.168	0.0028	
Sex	Male	-25.10	23.22	0.29	-44.043	24.202	0.08
Ethnicity	White	-47.93	75.80	0.53			
	British						
Years in education		-2.244	2.989	0.58			
Vascular risk factors							
Hypertension		-9.271	33.597	0.78			
SBP (mmHg)		-0.566	0.564	0.32			
DBP (mmHg)		0.003	1.029	0.98			
Ischaemic heart disease		25.04	49.57	0.62			
Hyper-cholesterolaemia		-26.40	25.70	0.31			
Diabetes mellitus		-11.02	31.78	0.73			
Smoking (current)		-4.686	23.49	0.84			
BMI (kg/m²)		-2.038	1.538	0.19			
Comorbidities							
Depression		28.03	25.14	0.27			
Migraine		20.64	25.28	0.42			
Time since last stroke (months)		-1.427	0.631	0.029			
BBB permeability							
K_{in} hotspots, %NAWM		-120.89	158.17	0.45	-207.49	145.23	01.6

Table 7.5. Linear regression model results univariate and multivariable models of candidate predictors of brain volume. Values are unstandardised β coefficients and standard errors. *SBP* systolic blood pressure; *DBP* diastolic blood pressure; *BMI* body mass index); *%NAWM* percentage of normal appearing white matter, values in percentage points.

Relationship of BBB permeability to cognition

On univariate analysis, BBB permeability hotspot percentage was not significantly related to neuropsychometric scores in executive function ($\beta = -4.206$, $SE = 2.132$, $p = 0.055$), processing speed ($\beta = 1.158$, $SE = 2.430$, $p = 0.63$), long-term memory ($\beta = -2.265$, $SE = 1.563$, $p = 0.15$) or global cognition ($\beta = -1.634$, $SE = 1.430$, $p = 0.26$). Univariate relationships are shown in figure 7.3.

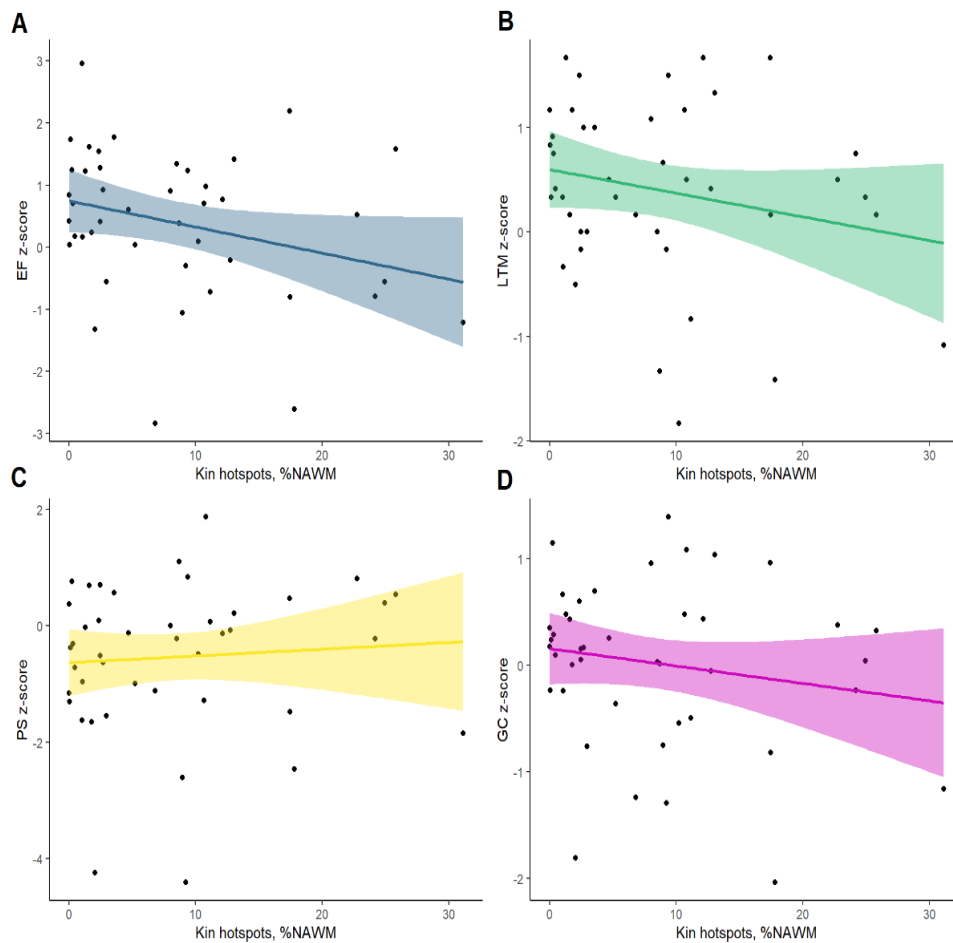


Figure 7.3. Scatter plots showing correlation of BBB permeability hotspot proportion to (A) executive function; (B) long-term memory; (C) processing speed and (D) global cognition. Outcomes are age-corrected z-scores. *EF* executive function; *LTM* long-term memory; *PS* processing speed; *GC* global cognition.

BBB permeability hotspot was not related to executive function score on multivariate analysis; significant predictors in this model were WMH volume ($\beta = -0.022$, $SE = 0.007$, $p = 0.0034$) and FA median ($\beta = 6.511$, $SE = 2.761$, $p = 0.024$). These results are presented in table 7.6.

		Univariate analysis			Multivariate analysis		
		β	SE	<i>p</i> value	β	SE	<i>p</i> value
Demographics							
Age (years)		0.012	0.016	0.46	0.018	0.017	0.31
Sex	Male	-0.131	0.346	0.71	0.003	0.339	0.99
Ethnicity	White British	0.255	1.093	0.82			
Years in education		0.159	0.053	0.0043			
IQ (NART)		0.079	0.021	0.00075			
Vascular risk factors							
Hypertension		-0.694	0.4763	0.152			
SBP (mmHg)		-0.007	0.009	0.43			
DBP (mmHg)		-0.004	0.015	0.79			
Ischaemic heart disease		-0.161	0.588	0.7			
Hypercholesterolaemia		0.280	0.369	0.45			
Diabetes mellitus		-0.398	0.458	0.39			
Smoking (current)		-0.654	0.332	0.056			
BMI (kg/m ²)		-0.020	0.032	0.53			
Comorbidities							
Depression		-0.504	0.363	0.17			
Migraine		0.148	0.370	0.69			
Time since stroke (months)		-0.019	0.008	0.031			
Conventional MRI markers							
WMH (cc)		-0.016	0.006	0.019	-0.022	0.007	0.0034
Lacunae		-0.110	0.082	0.19			
CMBs		-0.026	0.014	0.06			
Brain volume (cc)		0.004	0.002	0.09			
FA median		18.16	5.161	0.002	6.511	2.761	0.024
MD PH (mm ² /s)		112.5	144.9	0.45			
BBB permeability							
K _{in} hotspots, %NAWM		-4.206	2.132	0.055	-3.421	1.999	0.10

Table 7.6. Unstandardised β coefficients and standard errors of univariate and multivariate models of candidate predictors of executive function *z*-score. *SBP* systolic blood pressure; *DBP* diastolic blood pressure; *BMI* body mass index; *FA* fractional anisotropy; *MDPH* mean diffusivity peak height; *%NAWM* percentage of normal appearing white matter, values in percentage points.

		Univariate analysis			Multivariate analysis		
		β	SE	<i>p</i> value	β	SE	<i>p</i> value
Demographics							
Age (years)		0.023	0.0170	0.18	0.041	0.021	0.057
Sex	Male	-0.298	0.361	0.41	0.037	0.375	0.92
Ethnicity	White British	-1.150	2.232	0.31			
Years in education		-0.0335	0.060	0.58			
IQ (NART)		0.022	0.026	0.40			
Vascular risk factors							
Hypertension		-0.016	0.512	0.97			
SBP (mmHg)		-0.016	0.009	0.08			
DBP (mmHg)		-0.006	0.017	0.74			
Ischaemic heart disease		-0.600	0.824	0.47			
Hypercholesterolaemia		-0.252	0.388	0.52			
Diabetes mellitus		-0.360	0.482	0.46			
Smoking (current)		-0.133	0.364	0.72			
BMI (kg/m ²)		-0.005	0.033	0.87			
Comorbidities							
Depression		-0.360	0.386	0.36			
Migraine		-0.397	0.385	0.31			
Time since stroke (months)		-0.004	0.009	0.66			
Conventional MRI markers							
WMH (cc)		-0.014	0.007	0.059			
Lacunae		-0.238	0.081	0.0052	-0.184	0.090	0.050
CMBs		-0.044	0.013	0.0020			
Brain volume (cc)		0.005	0.002	0.03	0.007	0.002	0.007
FA median		17.45	5.468	0.0051			
MD PH (mm ² /s)		404.5	116.3	0.0027			
BBB permeability							
K _{in} hotspots, %NAWM		1.158	2.430	0.64	2.209	2.269	0.34

Table 7.7. Unstandardised β coefficients and standard errors of univariate and multivariate models of candidate predictors of processing speed *z*-score. *SBP* systolic blood pressure; *DBP* diastolic blood pressure; *BMI* body mass index; *FA* fractional anisotropy; *MDPH* mean diffusivity peak height; *%NAWM* percentage of normal appearing white matter, values in percentage points.

		Univariate analysis			Multivariate analysis		
		β	SE	<i>p</i> value	β	SE	<i>p</i> value
Demographics							
Age (years)		0.023	0.012	0.06	0.016	0.011	0.18
Sex	Male	-0.272	0.264	0.31	-0.335	0.237	0.17
Ethnicity	White British	0.383	0.955	0.69			
Years in education		0.104	0.042	0.017	0.108	0.038	0.008
IQ (NART)		0.046	0.016	0.007			
Vascular risk factors							
Hypertension		-0.249	0.374	0.51			
SBP (mmHg)		0.004	0.006	0.51			
DBP (mmHg)		-0.006	0.011	0.58			
Ischaemic heart disease		-0.338	0.645	0.60			
Hypercholesterolaemia		-0.135	0.285	0.64			
Diabetes mellitus		-0.065	0.356	0.86			
Smoking (current)		-0.045	0.270	0.87			
BMI (kg/m ²)		0.031	0.024	0.20			
Comorbidities							
Depression		-0.011	0.286	0.97			
Migraine		0.531	0.275	0.06			
Time since stroke (months)		0.003	0.007	0.97			
Conventional MRI markers							
WMH (cc)		-0.010	0.05	0.060			
Lacunes		-0.150	0.061	0.018	-0.152	0.053	0.007
CMBs		-0.010	0.011	0.37			
Brain volume (cc)		0.00031	0.0017	0.86			
FA median		11.030	3.455	0.005			
MD PH (mm ² /s)		37.97	94.60	0.69			
BBB permeability							
K _{in} hotspots, %NAWM		-2.265	1.563	0.15	-1.951	1.376	0.16

Table 7.8. Unstandardised β coefficients and standard errors of univariate and multivariate models of candidate predictors of long-term memory *z*-score. *SBP* systolic blood pressure; *DBP* diastolic blood pressure; *BMI* body mass index; *FA* fractional anisotropy; *MDPH* mean diffusivity peak height; *%NAWM* percentage of normal appearing white matter, values in percentage points.

		Univariate analysis			Multivariate analysis		
		β	SE	<i>p</i> value	β	SE	<i>p</i> value
Demographics							
Age (years)		0.013	0.010	0.20	0.024	0.011	0.040
Sex	Male	-0.084	0.218	0.70	0.025	0.221	0.91
Ethnicity	White British	-0.033	0.711	0.96			
Years in education		0.085	0.034	0.018			
IQ (NART)		0.051	0.013	0.00037			
Vascular risk factors							
Hypertension		-0.250	0.305	0.42			
SBP (mmHg)		-0.004	0.005	0.45			
DBP (mmHg)		-0.003	0.010	0.75			
Ischaemic heart disease		-0.037	0.433	0.93			
Hypercholesterolaemia		-0.032	0.234	0.89			
Diabetes mellitus		-0.306	0.288	0.29			
Smoking (current)		-0.351	0.213	0.11			
BMI (kg/m ²)		-0.0002	0.020	0.99			
Comorbidities							
Depression		-0.353	0.228	0.13			
Migraine		-0.044	0.234	0.85			
Time since stroke (months)		-0.007	0.005	0.13			
Conventional MRI markers							
WMH (cc)		-0.013	0.004	0.0031	-0.015	0.004	0.0012
Lacunes		-0.125	0.049	0.016			
CMBs		-0.023	0.008	0.007			
Brain volume (cc)		0.002	0.001	0.23			
FA median		14.87	3.43	0.00040			
MD PH (mm ² /s)		158.4	101.1	0.14			
BBB permeability							
K _{in} hotspots, %NAWM		-1.634	1.430	0.26	-1.332	1.291	0.31

Table 7.9 Unstandardised β coefficients and standard errors of univariate and multivariate models of candidate predictors of global cognition *z*-score. *SBP* systolic blood pressure; *DBP* diastolic blood pressure; *BMI* body mass index); *FA* fractional anisotropy; *MDPH* mean diffusivity peak height; *%NAWM* percentage of normal appearing white matter, values in percentage points.

Significant predictors of processing speed in the multivariate analysis were lacune count ($\beta = -0.238$, $SE = 0.081$, $p = 0.050$) and brain volume ($\beta = 0.007$, $SE = 0.002$, $p = 0.007$). These results are shown in table 7.7. Table 7.8 shows the univariate and multivariate results for predictors of long-term memory; in this model years of education ($\beta = 0.108$, $SE = 0.038$, $p = 0.008$) and lacune count ($\beta = -0.150$, $SE = 0.061$, $p = 0.007$) were significant predictors. Significant predictors of global cognition in the final multivariable model were age ($\beta = 0.024$, $SE = 0.011$, $p = 0.040$) and WMH volume ($\beta = -0.015$, $SE = 0.004$, $p = 0.0012$); see table 7.9. The BBB permeability hotspot proportion was not significantly associated with performance in any of these domains.

Relationship of peripheral blood proteomic panel with BBB permeability

On univariate analysis, none of the individual biomarkers from the Olink CVD III panel were associated with BBB hotspot proportion when false discovery rate-corrected. Full results for each individual biomarker are presented in Appendix D. Of the pre-specified panel components, there were no statistically significant associations with either radiological BBB permeability measurement or Q_{alb} ; (table 7.10).

	BBB hotspot proportion		Q_{alb}	
	β	p value	β	p value
COL1A1	-0.010	0.95	-0.068	0.85
Cystatin B	-0.042	0.79	-0.018	0.96
JAM-A	-0.155	0.32	-0.112	0.688
MMP-2	0.003	0.99	0.015	0.95
MMP-3	0.009	0.95	-0.010	0.98
MMP-9	-0.024	0.87	0.396	0.30
TIMP-4	0.102	0.52	-0.466	0.26

Table 7.10. Results from univariate linear regression models of pre-specified biomarkers from the Olink CVD III panel as predictors for BBB permeability hotspot proportion and Q_{alb} .

The compound biomarker cluster score was positively but non-significantly related to both BBB hotspot proportion and Q_{alb} (figure 7.4). On linear regression, BCS did not predict BBB hotspot proportion or Q_{alb} in either univariate models ($\beta = 0.019$, $SE = 0.013$, $p = 0.15$; $\beta = 9.192$, $SE = 6.361$, $p = 0.17$ respectively) or in multivariate models corrected for age and sex. (table 7.11).

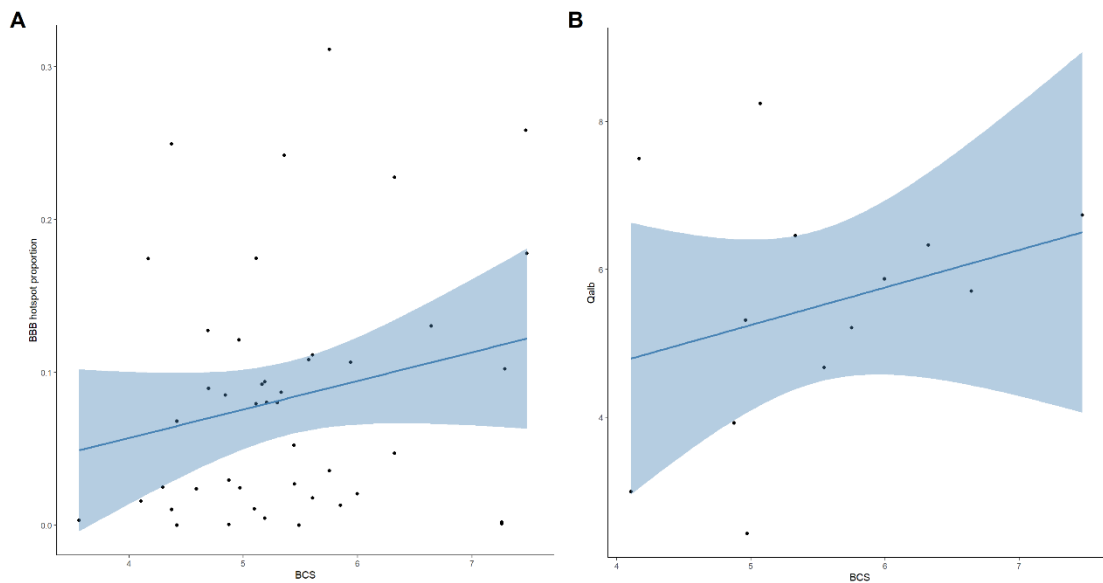


Figure 7.4. Scatter plots showing correlation of BCS to (A) Q_{alb} and (B) BBB permeability hotspot proportion, NAWM; *BCS* biomarker compound score; Q_{alb} CSF/serum albumin quotient.

	Predictor	β	SE	<i>p</i> value
<i>BBB hotspot proportion</i>	Age (y)	-0.001	0.001	0.44
	Sex (male)	-0.018	0.025	0.48
	BCS (NPX)	0.017	0.014	0.21
<i>Q_{alb}</i>	Age (y)			
	Sex (male)	-9.407	19.405	0.64
	BCS (NPX)	17.806	11.374	0.15

Table 7.11. Results multivariable linear regression showing association of BCS with BBB hotspot proportion and Q_{alb} , corrected for age and sex.

Relationship of Q_{alb} to radiological SVD markers and cognition

There was a weak and statistically insignificant positive correlation between the Q_{alb} and WMH volume, and a statistically insignificant negative correlation between Q_{alb} and brain volume. There was no relationship between Q_{alb} and either the lacune or CMB count (figure 7.5). When corrected for age and sex, Q_{alb} did not predict any of these radiological parameters (table 7.12). The number of participants precluded more detailed multivariate regression modelling.

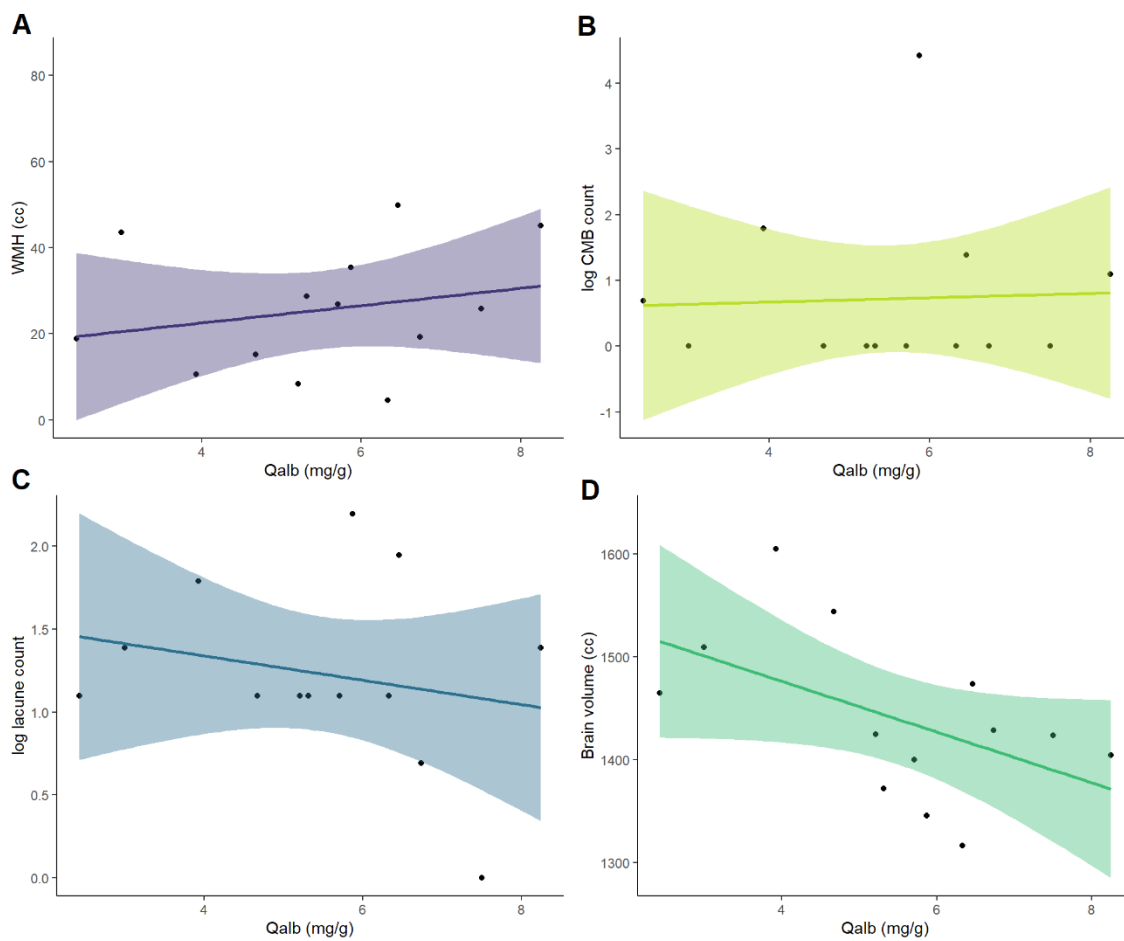


Figure 7.5. Scatter plots showing correlation of Q_{alb} to (A) WMHs (B) lacune count (C) CMB count and (D) brain volume.

There was no relationship between Q_{alb} and any of the individual cognitive domain z -scores (figure 7.6); regression models corrected for age, sex and pre-morbid IQ

revealed no significant predictive effect of Q_{alb} and these results are shown in table 7.13.

	Predictor	β	SE	p value
WMHs	Age	0.222	0.459	0.64
	Sex (male)	1.029	11.727	0.93
	Q_{alb}	1.605	3.614	0.67
Lacune count	Age	-0.013	0.015	0.40
	Sex	0.530	0.378	0.20
	Q_{alb}	-0.156	0.117	0.21
CMB count	Age	-0.054	0.036	0.17
	Sex	0.329	0.923	0.73
	Q_{alb}	0.027	0.284	0.93
Brain volume	Age	-2.615	1.1881	0.20
	Sex	-83.482	48.081	0.12
	Q_{alb}	-6.990	14.816	0.65

Table 7.12 Unstandardised β coefficients and standard errors of regression models testing relationship between Q_{alb} and radiological markers of SVD, corrected for age and sex.

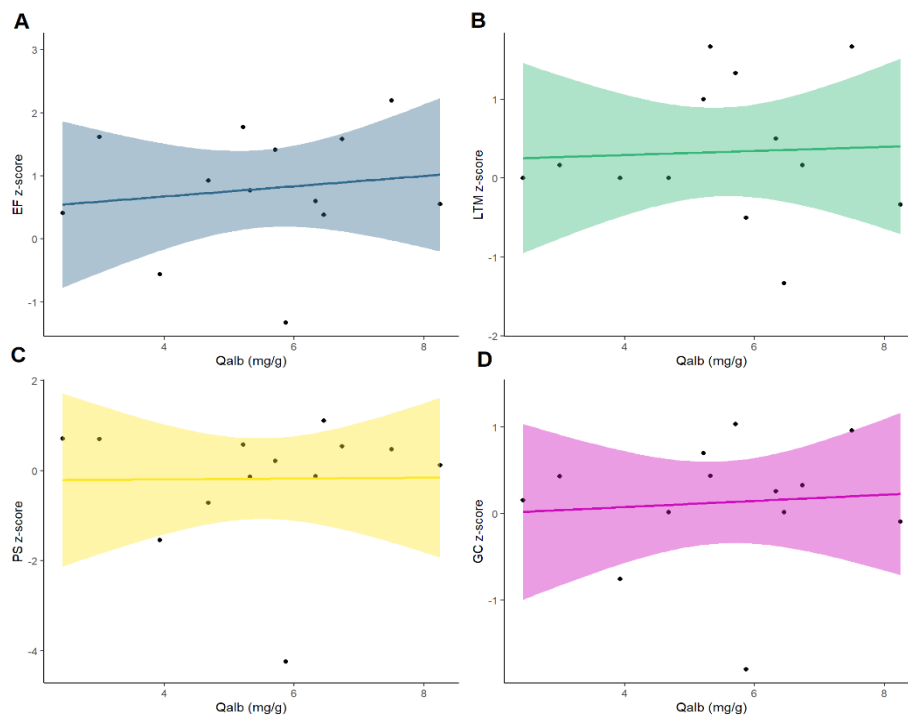


Figure 7.6. Scatter plots showing correlation of Q_{alb} to (A) executive function; (B) long-term memory; (C) processing speed and (D) global cognition. Outcomes are age-corrected z-scores. *EF* executive function; *LTM* long-term memory; *PS* processing speed; *GC* global cognition.

	Predictor	β	SE	<i>p</i> value
EF	Age	0.027	0.036	0.44
	Sex (male)	-0.071	0.672	0.92
	NART	-0.017	0.034	0.63
	Q _{alb}	0.126	0.215	0.58
PS	Age	0.030	0.026	0.29
	Sex	0.842	0.523	0.15
	NART	0.014	0.027	0.61
	Q _{alb}	-0.157	0.168	0.38
LTM	Age	0.048	0.032	0.18
	Sex	-0.847	0.650	0.23
	NART	-0.057	0.033	0.13
	Q _{alb}	0.257	0.208	0.26
GC	Age	0.031	0.019	0.15
	Sex	0.058	0.385	0.89
	NART	-0.023	0.019	0.27
	Q _{alb}	0.066	0.123	0.61

Table 7.13 Unstandardised β coefficients and standard errors of regression models testing relationship between Q_{alb} and neuropsychometric performance in each domain, corrected for age, sex, and pre-morbid IQ measured by NART.. *EF* executive function; *LTM* long-term memory; *PS* processing speed; *GC* global cognition; *NART* National Adult Reading Test.

Relationship of Q_{alb} to DCE-MRI markers

Q_{alb} was highly correlated with radiological measurements of BBB permeability, including both the overall mean permeability constant K_{in} and the BBB permeability hotspot proportion in the NAWM (Pearson's r correlation coefficients 0.599, $p = 0.04$, and 0.756, $p = 0.004$ respectively). To verify this relationship, I further tested the relationship between Q_{alb} and the overall mean permeability constant K_{in} and the BBB permeability hotspot proportion in the entirety of the white matter; these were also significantly correlated (correlation coefficients 0.626, $p = 0.03$, and 0.709, $p = 0.010$ respectively). These data are shown in figure 7.7.

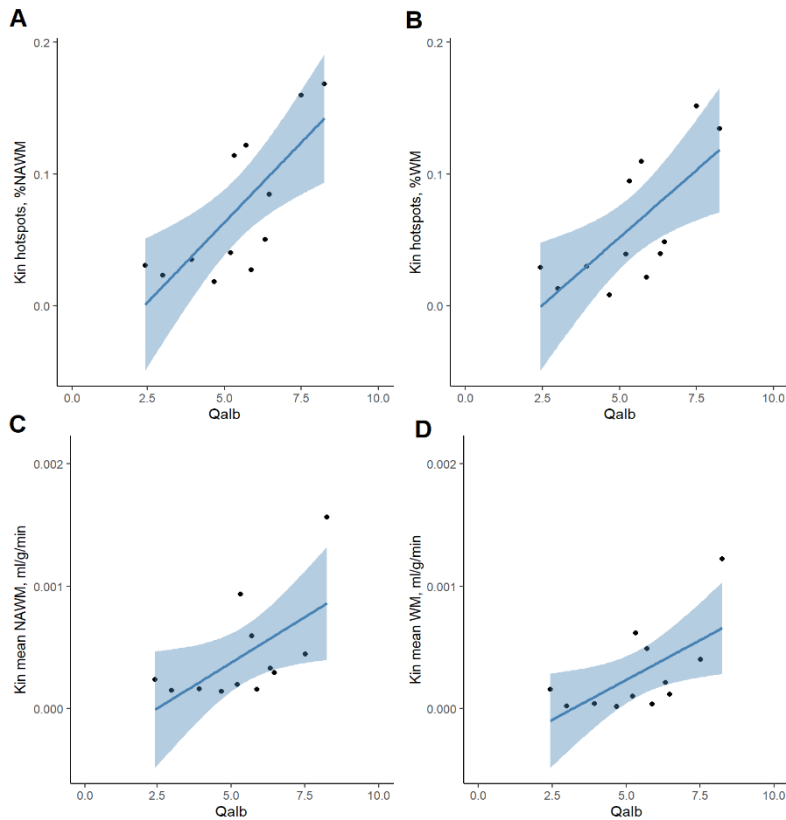


Figure 7.7. Scatter plots showing correlation of Q_{alb} to (A) mean BBB permeability, NAWM; (B) BBB permeability hotspot proportion, NAWM; (C) mean BBB permeability, WM; (D) BBB permeability hotspot proportion, WM. K_{in} permeability constant; NAWM normal appearing white matter; WM all white matter.

Association of GFAP with SVD severity

The intra-plate coefficient of variance for the GFAP SIMOA assay was 7.6% in serum and 10.4% in CSF. The mean inter-plate coefficient of variance was 5.8% in serum and 11.4% in CSF.

Mean serum GFAP was 191.77 ± 122.77 pg/mL, and was non-normally distributed (Shapiro-Wilk $W = 0.899$, $p = 0.002$). The median and IQR were 144.86 pg/mL and 108.11 – 255.64 pg/mL respectively). Mean and median values were considerably higher than the expected value in healthy individuals of 61 ± 44 pg/mL detected by the same assay.³⁷⁶ CSF GFAP was normally distributed ($W = 0.895$, $p = 0.11$) with mean 9397.34 ± 7477.68 pg/mL; reference values in asymptomatic individuals are unclear for this assay but the CSF values are considerably lower than in patients with traumatic brain injury which ranged from 284,000 to 816,000 pg/mL.

Serum GFAP was not related to WMH volume, lacune count, CMB count or brain volume (figure 7.8) and in multivariate regression models was not a significant predictor for any of these radiological markers (table 7.14). CSF GFAP was not significantly associated with any of these markers (figure 7.9 and table 7.15).

In multivariate models, serum GFAP was a significant predictor only of processing speed with minimal negative effect size ($\beta = -0.006$, $SE = 0.002$, $p = 0.0029$). These data are presented in figure 7.10 and table 7.16. CSF GFAP did not predict cognitive performance in any domain (figure 7.11 and table 7.17).

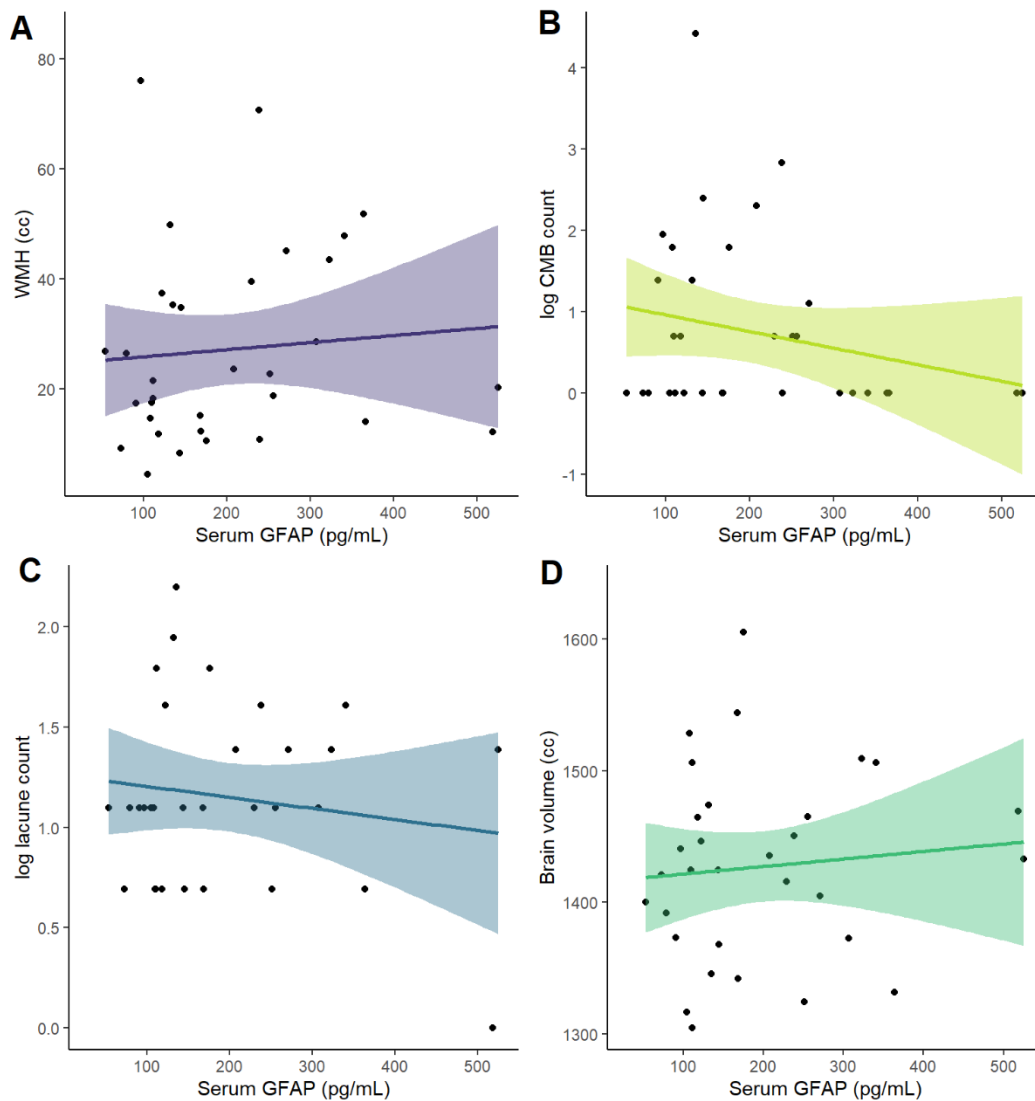


Figure 7.8. Scatter plots showing correlation of serum GFAP to (A) WMHs (B) lacune count (C) CMB count and (D) brain volume.

	Predictor	β	SE	p value
WMHs	Age (y)	0.179	0.396	0.66
	Sex (male)	3.267	7.311	0.66
	GFAP (pg/mL)	0.009	0.038	0.82
Lacune count	Age (y)	-0.029	0.010	0.006
	Sex (male)	0.209	0.181	0.256
	GFAP (pg/mL)	0.001	0.0009	0.15
CMB count	Age (y)	-0.036	0.023	0.13
	Sex (male)	-0.034	0.420	0.94
	GFAP (pg/mL)	-0.0001	0.002	0.95
Brain volume	Age (y)	-4.476	1.355	0.003
	Sex (male)	-38.684	25.492	0.14
	GFAP (pg/mL)	0.220	0.133	0.11

Table 7.14. Unstandardised β coefficients and standard errors of regression models testing relationship between serum GFAP and radiological markers of SVD, corrected for age and sex.

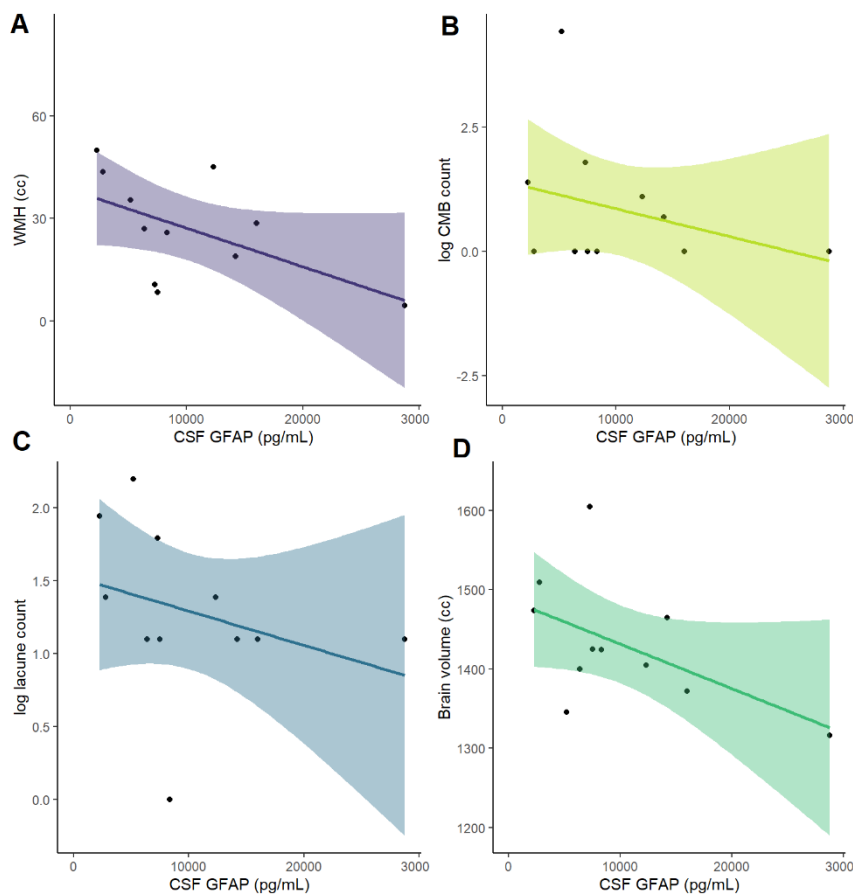


Figure 7.9. Scatter plots showing correlation of CSF GFAP to (A) WMHs (B) lacune count (C) CMB count and (D) brain volume.

	Predictor	β	SE	p value
WMHs	Age (y)	0.575	0.467	0.26
	Sex (male)	5.921	8.568	0.51
	GFAP (pg/mL)	-0.001	0.0006	0.06
Lacune count	Age (y)	-0.034	0.016	0.08
	Sex (male)	0.280	0.298	0.38
	GFAP (pg/mL)	-7.2×10^{-6}	2.2×10^{-5}	0.75
CMB count	Age (y)	-0.088	0.037	0.05
	Sex (male)	0.345	0.685	0.63
	GFAP (pg/mL)	-1.2×10^{-5}	5.0×10^{-5}	0.81
Brain volume	Age (y)	-1.319	2.182	0.56
	Sex (male)	-8.257	4.002	0.08
	GFAP (pg/mL)	-0.005	0.003	0.15

Table 7.15. Unstandardised β coefficients and standard errors of regression models testing relationship between CSF GFAP and radiological markers of SVD, corrected for age and sex.

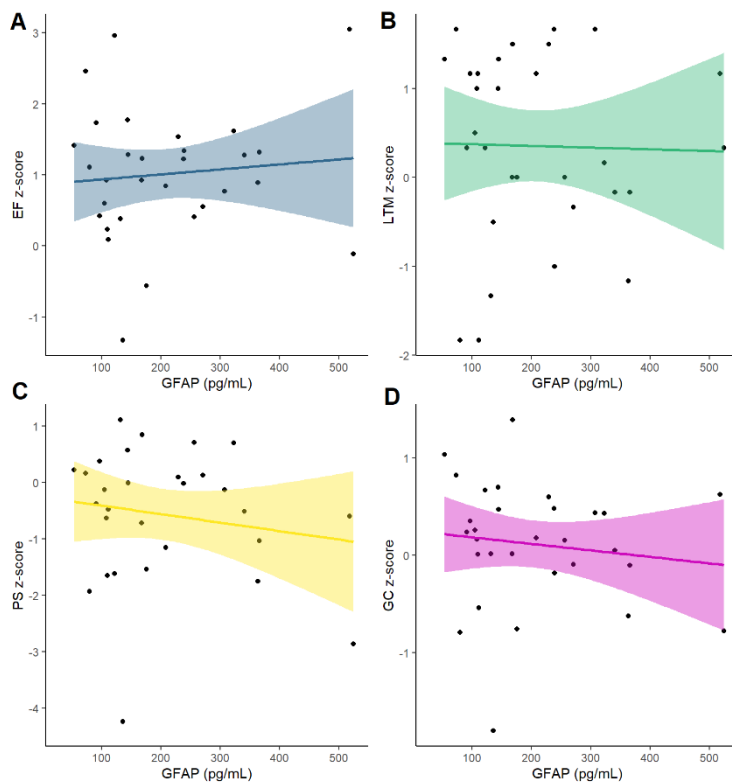


Figure 7.10. Scatter plots showing correlation of serum GFAP to (A) executive function; (B) long-term memory; (C) processing speed and (D) global cognition. Outcomes are age-corrected z-scores. *EF* executive function; *LTM* long-term memory; *PS* processing speed; *GC* global cognition.

	Predictor	β	SE	p value
EF	Age	0.018	0.026	0.49
	Sex (male)	0.124	0.401	0.76
	NART	0.002	0.018	0.93
	GFAP (pg/mL)	-0.001	0.002	0.80
PS	Age	0.061	0.031	0.06
	Sex	-0.267	0.458	0.57
	NART	-0.008	0.020	0.69
	GFAP (pg/mL)	-0.006	0.002	0.029
LTM	Age	-0.002	0.031	0.95
	Sex	0.015	0.483	0.98
	NART	0.014	0.022	0.53
	GFAP (pg/mL)	-0.0006	0.002	0.82
GC	Age	0.017	0.016	0.28
	Sex	0.122	0.244	0.62
	NART	0.002	0.011	0.87
	GFAP (pg/mL)	-0.002	0.001	0.17

Table 7.16. Unstandardised β coefficients and standard errors of regression models testing relationship between serum GFAP and neuropsychometric performance in each domain, corrected for age, sex, and pre-morbid IQ measured by NART.. *EF* executive function; *LTM* long-term memory; *PS* processing speed; *GC* global cognition; *NART* National Adult Reading Test.

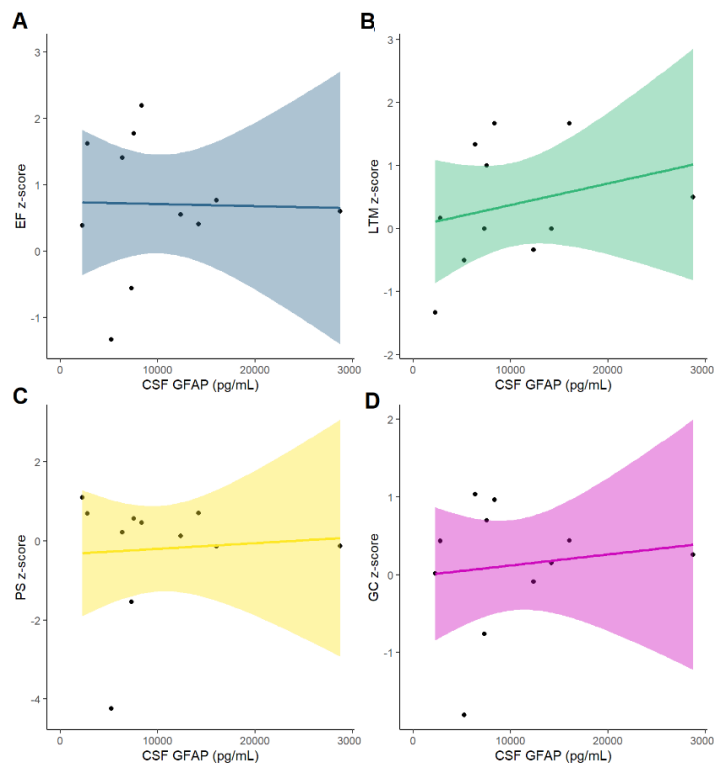


Figure 7.11. Scatter plots showing correlation of CSF GFAP to (A) executive function; (B) long-term memory; (C) processing speed and (D) global cognition. Outcomes are age-corrected z-scores. *EF* executive function; *LTM* long-term memory; *PS* processing speed; *GC* global cognition.

	Predictor	β	SE	<i>p</i> value
EF	Age	0.095	0.038	0.05
	Sex (male)	0.178	0.450	0.71
	NART	-0.034	0.27	0.26
	GFAP (pg/mL)	-5.6×10^{-5}	3.3×10^{-5}	0.15
PS	Age	0.067	0.033	0.10
	Sex	0.445	0.395	0.31
	NART	-0.009	0.023	0.70
	GFAP (pg/mL)	-5.1×10^{-5}	2.9×10^{-5}	0.13
LTM	Age	0.054	0.058	0.39
	Sex	-0.478	0.691	0.52
	NART	-0.043	0.041	0.35
	GFAP (pg/mL)	1.5×10^{-5}	5.0×10^{-5}	0.79
GC	Age	0.056	0.029	0.11
	Sex	0.193	0.340	0.60
	NART	-0.029	0.020	0.22
	GFAP (pg/mL)	-2.3×10^{-5}	2.4×10^{-5}	0.29

Table 7.17. Unstandardised β coefficients and standard errors of regression models testing relationship between CSF GFAP and neuropsychometric performance in each domain, corrected for age, sex, and pre-morbid IQ measured by NART.. *EF* executive function; *LTM* long-term memory; *PS* processing speed; *GC* global cognition; *NART* National Adult Reading Test.

Association of NfL with SVD severity

The intra-plate coefficient of variance for the NfL SIMOA assay was 5.9% in serum and 32.4% in CSF. The mean inter-plate coefficient of variance was 4.0% in serum and 39.1% in CSF.

Mean serum NfL was 44.59 ± 58.04 pg/mL, with median 28.561 pg/mL and IQR 16.75 – 44.51 pg/mL. The distribution was non-normal ($W = 0.529$, $p < 1 \times 10^{-6}$). The normal range for NfL levels using this assay is 34.69 ± 13.09 pg/mL for age 60–70, and 45.85 ± 15.31 pg/mL above age 70.³⁷⁷

Mean CSF NfL was 1885.01 ± 2320.63 pg/mL, with median 999.17 pg/mL and IQR 665.39 – 1784.92 pg/mL. CSF NfL was also non-normally distributed ($W = 0.708$, $p = 0.0007$). These are broadly similar to a population of patients with vascular dementia

and subcortical white matter disease, presumed to reflect SVD (who had CSF NfL levels 1316 ± 1218 pg/mL).³⁷⁸

Serum NfL was not related to WMH volume, lacune count, CMB count or brain volume (figure 7.12) and in multivariate regression models was not a significant predictor for any of these radiological markers (table 7.18). Serum NfL was a significant predictor only of long-term memory with minimal negative effect size ($\beta = -0.008$, $SE = 0.003$, $p = 0.012$). These data are presented in figure 7.13 and table 7.19).

In multivariate models, CSF NfL was a significant negative predictor of brain volume ($\beta = -0.017$, $SE = 0.007$, $p = 0.048$). These data are presented in figure 7.14 and table 7.20. CSF NfL did not predict cognitive performance in any domain (figure 7.15 and table 7.21).

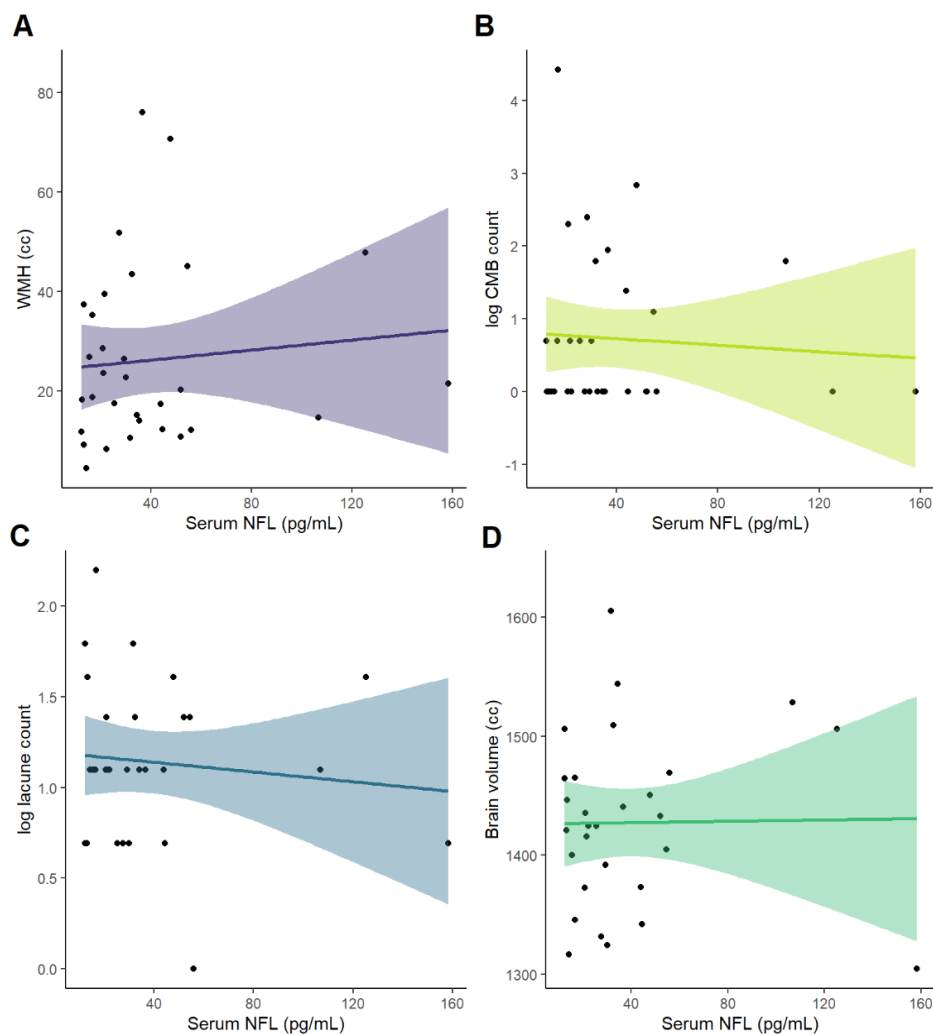


Figure 7.12. Scatter plots showing correlation of serum NfL to (A) WMHs (B) lacune count (C) CMB count and (D) brain volume.

	Predictor	β	SE	p value
WMHs	Age (y)	0.234	0.302	0.45
	Sex (male)	2.010	6.639	0.76
	NfL (pg/mL)	0.064	0.054	0.25
Lacune count	Age (y)	-0.017	0.007	0.04
	Sex (male)	0.039	0.165	0.81
	NfL (pg/mL)	0.002	0.001	0.11
CMB count	Age (y)	-0.032	0.018	0.09
	Sex (male)	-0.081	0.391	0.84
	NfL (pg/mL)	0.002	0.003	0.51
Brain volume	Age (y)	-3.106	1.061	0.007
	Sex (male)	-64.084	22.862	0.009
	NfL (pg/mL)	0.278	0.180	0.14

Table 7.18. Unstandardised β coefficients and standard errors of regression models testing relationship between serum NfL and radiological markers of SVD, corrected for age and sex.

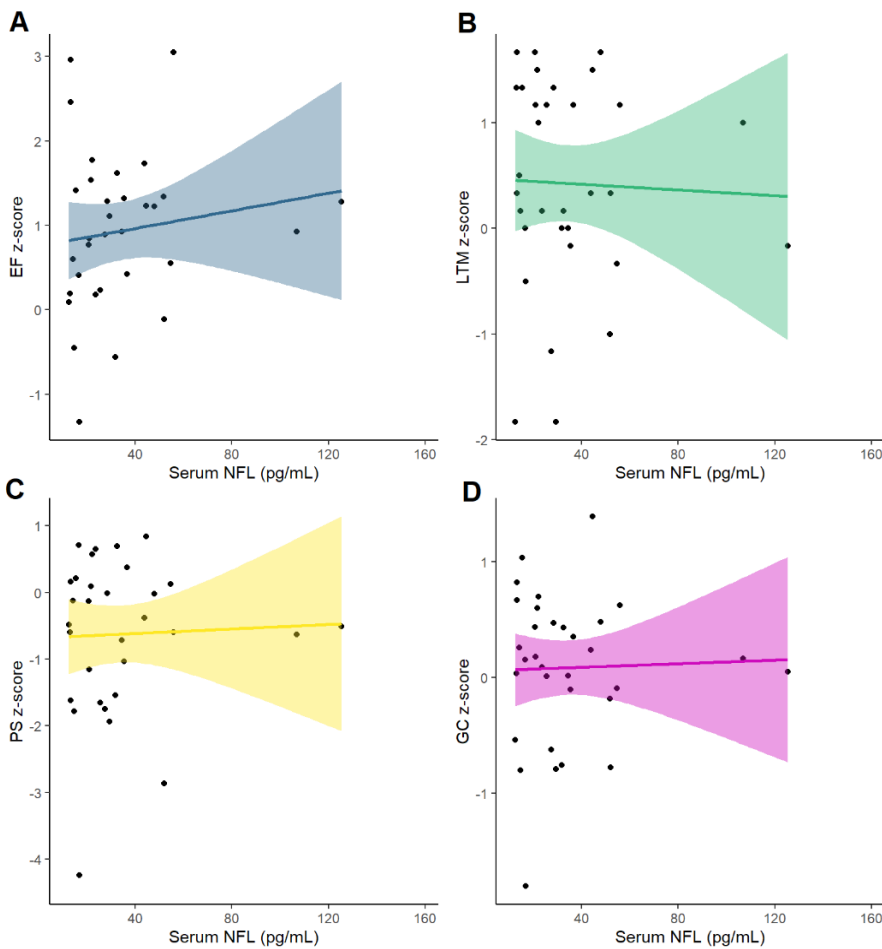


Figure 7.13. Scatter plots showing correlation of serum NfL to (A) executive function; (B) long-term memory; (C) processing speed and (D) global cognition. Outcomes are age-corrected z-scores. *EF* executive function; *LTM* long-term memory; *PS* processing speed; *GC* global cognition.

	Predictor	β	SE	p value
EF	Age	0.024	0.018	0.20
	Sex (male)	0.233	0.237	0.51
	NART	0.009	0.018	0.61
	NfL (pg/mL)	-0.003	0.002	0.33
PS	Age	-0.003	0.021	0.88
	Sex	-0.026	0.406	0.95
	NART	-0.009	0.023	0.69
	NfL (pg/mL)	0.004	0.003	0.20
LTM	Age	0.001	0.018	0.97
	Sex	0.194	0.343	0.58
	NART	0.026	0.018	0.16
	NfL (pg/mL)	-0.008	0.003	0.013
GC	Age	0.005	0.010	0.64
	Sex	0.179	0.203	0.39
	NART	0.006	0.011	0.61
	NfL (pg/mL)	-0.001	0.002	0.42

Table 7.19. Unstandardised β coefficients and standard errors of regression models testing relationship between serum NfL and neuropsychometric performance in each domain, corrected for age, sex, and pre-morbid IQ measured by NART.. *EF executive function; LTM long-term memory; PS processing speed; GC global cognition; NART National Adult Reading Test.*

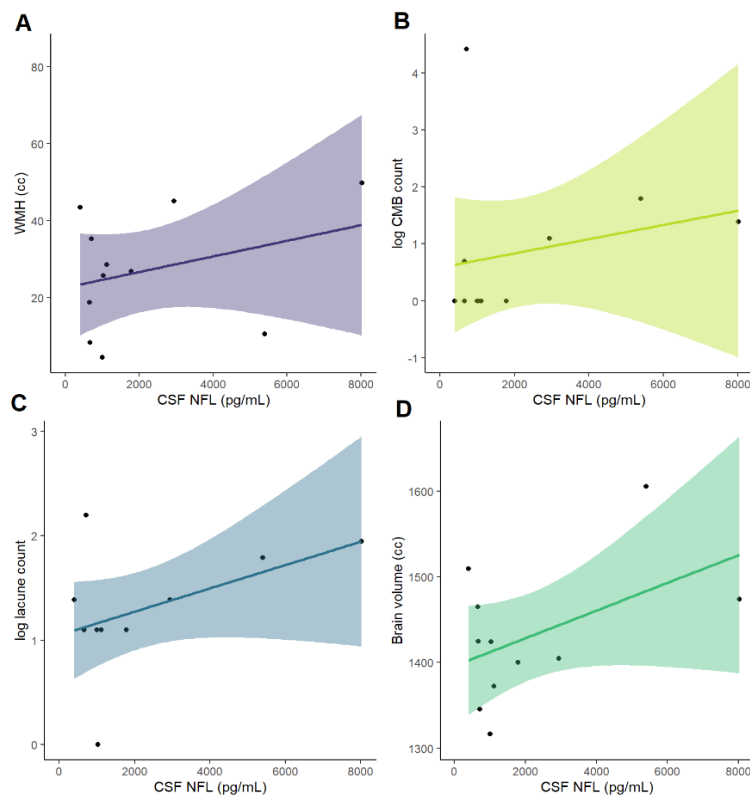


Figure 7.14. Scatter plots showing correlation of CSF NfL to (A) WMHs (B) lacune count (C) CMB count and (D) brain volume.

	Predictor	β	SE	p value
WMHs	Age (y)	0.302	0.462	0.53
	Sex (male)	2.033	9.894	0.84
	NfL (pg/mL)	0.002	0.002	0.30
Lacune count	Age (y)	-0.018	0.015	0.27
	Sex (male)	0.122	0.325	0.72
	NfL (pg/mL)	0.0001	0.0001	0.18
CMB count	Age (y)	-0.061	0.036	0.13
	Sex (male)	0.086	0.772	0.91
	NfL (pg/mL)	8.6×10^{-5}	0.0002	0.61
Brain volume	Age (y)	-2.079	1.567	0.22
	Sex (male)	-97.18	33.18	0.02
	NfL (pg/mL)	0.017	0.007	0.048

Table 7.20. Unstandardised β coefficients and standard errors of regression models testing relationship between CSF NfL and radiological markers of SVD, corrected for age and sex.

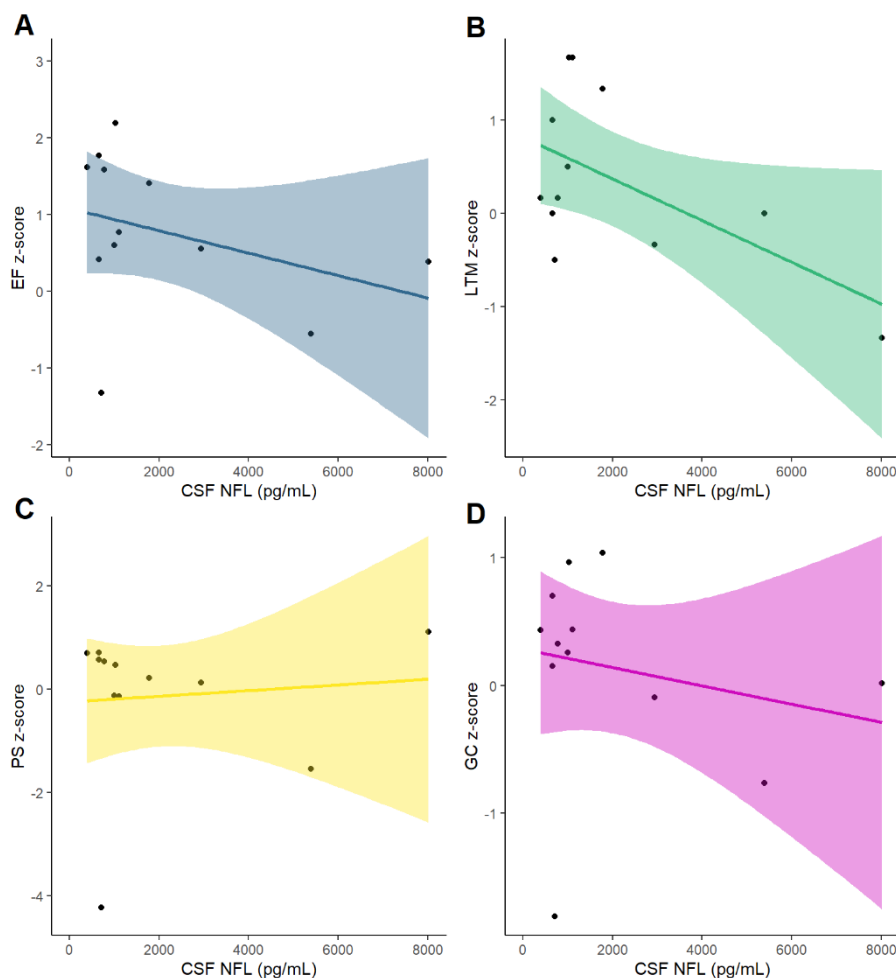


Figure 7.15. Scatter plots showing correlation of CSF NfL to (A) executive function; (B) long-term memory; (C) processing speed and (D) global cognition. Outcomes are age-corrected z-scores. *EF* executive function; *LTM* long-term memory; *PS* processing speed; *GC* global cognition.

	Predictor	β	SE	p value
EF	Age	-0.012	0.037	0.75
	Sex (male)	0.367	0.456	0.45
	NART	0.027	0.032	0.43
	NfL (pg/mL)	-0.0003	0.0001	0.08
PS	Age	0.013	0.039	0.75
	Sex	0.481	0.476	0.35
	NART	0.016	0.033	0.65
	NfL (pg/mL)	6.4×10^{-5}	0.0001	0.64
LTM	Age	0.006	0.043	0.90
	Sex	-0.282	0.534	0.62
	NART	-0.007	0.038	0.87
	NfL (pg/mL)	-0.0002	0.0001	0.17
GC	Age	0.013	0.025	0.61
	Sex	0.259	0.304	0.43
	NART	-0.004	0.023	0.87
	NfL (pg/mL)	-0.0001	8.2×10^{-5}	0.23

Table 7.21. Unstandardised β coefficients and standard errors of regression models testing relationship between CSF NfL and neuropsychometric performance in each domain, corrected for age, sex, and pre-morbid IQ measured by NART.. *EF* executive function; *LTM* long-term memory; *PS* processing speed; *GC* global cognition; *NART* National Adult Reading Test.

Relationship between CSF/serum GFAP and NfL

The CSF/serum ratio for GFAP was negatively correlated with both the overall white matter BBB permeability (mean K_{in}) and with Q_{alb} (Pearson's r correlation coefficients -0.31, $p = 0.36$ and -0.39, $p = 0.23$ respectively). The CSF/serum ratio for NfL was similarly negatively correlated with white matter mean K_{in} and Q_{alb} ($r = -0.23$, $p = 0.48$ and $r = -0.39$, $p = 0.24$ respectively). These data are shown in figure 7.16.

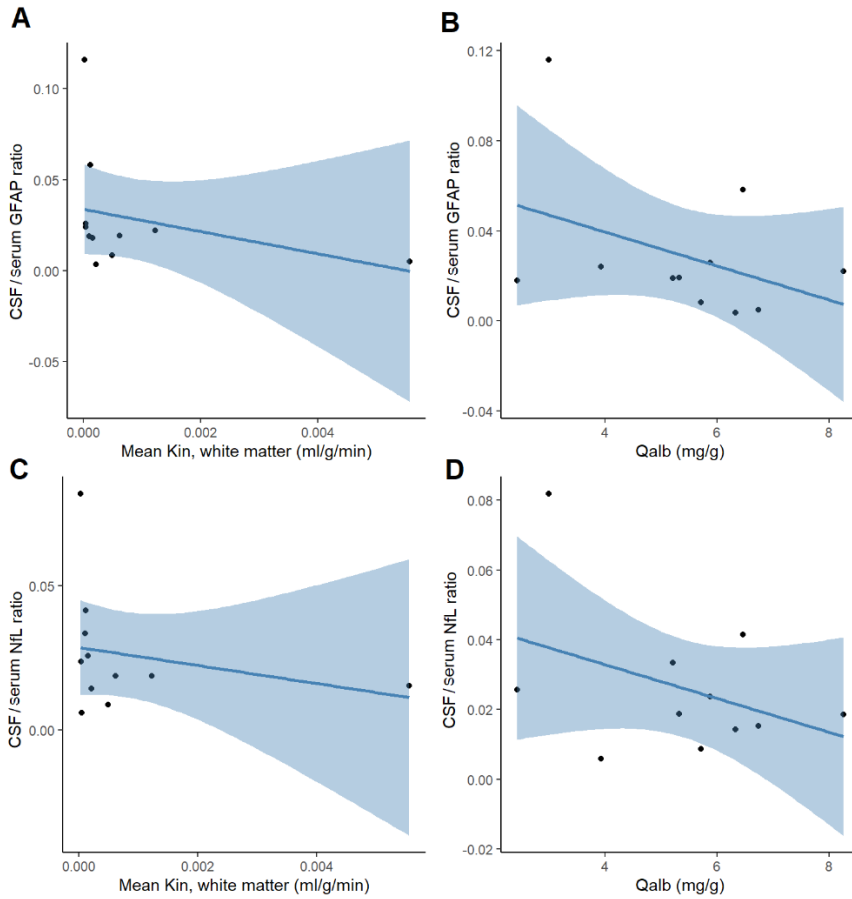


Figure 7.16. Scatter plots showing correlation of CSF/serum GFAP ratio to (A) mean BBB permeability in the white matter and (B) Q_{alb} . (C) shows scatter plot of CSF/serum NfL ratio and BBB permeability in the white matter and (D) shows scatter plot of CSF/serum NfL ratio and Q_{alb} .

Discussion

This detailed examination of BBB permeability in a cohort of patient with moderately severe symptomatic SVD used both radiological and functional measurements to assess the integrity of the BBB and the function of its components. I identified significant differences between the SVD patient and control groups based on DCE-MRI, and these differences were robust to the various ways that outcome metrics can be calculated from the images. Interestingly, the BBB hotspot proportion was the most effective metric for discriminating between the patient and control groups, and this mirrors the

most effective metric found for the co-acquired ^{11}C -PK1195 PET images discussed in chapter six.

The relationship between BBB permeability and markers of SVD severity were however less secure than the markers of microglial signal; BBB permeability hotspot proportion did not correlate well with any specific radiological marker of SVD or dysfunction in any cognitive domain. Previous studies have found that DCE-MRI imaging is not highly reproducible,²¹⁴ and studies in mice suggest that BBB permeability can be induced and recover over timescales in the range of hours³⁷⁹; it may simply be that BBB permeability changes are too dynamic to be able to accurately capture the relationship with other demographic and radiological variables.

Individual biomarkers in the Olink CVD III panel did not suggest a relationship between vascular inflammation and BBB permeability, nor did the compound biomarker score show any association with markers of BBB permeability. This may be partly due to the sample size (the cohort used to derive the BCS being ten-fold larger than this study population) or partly that a different subset of serum biomarkers might be required to capture a relationship with BBB permeability.

There was no significant relationship between Q_{alb} and radiological or neuropsychometric markers of SVD severity, and this is not surprising given the small subset of participants who consented to have CSF sampling. However, it is reassuring that the Q_{alb} correlated significantly with all possible DCE-MRI metrics that I tested and this suggests that the radiological measurements used in the full participant cohort are likely to be accurate and meaningful.

The identification of serum GFAP levels above the expected reference range suggest that astrocytic activation is a further relevant disease process to study in SVD. Imaging techniques are being developed to study this, including PET using a novel radioligand specific for astrocytic cell surface proteins (^{11}C -BU990008)³⁸⁰ and using non-irradiating modified diffusion-weighted MRI.³⁸¹ This is some way from becoming a therapeutic option as there are no safe and tolerable astrocyte inhibitors available.

NfL levels were raised in both serum and CSF in this cohort; this is expected in SVD³⁷⁴ and predicts cognitive impairment and incident dementia.³⁷⁵ It is noteworthy that the only significant associations found in this study between NfL and radiological or neuropsychometric markers of disease were between serum NfL and long-term memory and between CSF NfL and brain volume. These might be considered radiological evidence and impaired cognitive domains more consistent with Alzheimer's disease or other neurodegenerative disorders than with SVD, in which the relationship with NfL is probably more secure.³⁷² Although the overlap between cerebrovascular disease and Alzheimer's disease is significant, and the clinical distinction can be difficult, the exclusion criteria for this study prohibited participants with additional neurological or neurodegenerative conditions from being recruited.

By comparison of serum and CSF levels of NfL and GFAP with BBB permeability markers, I tested the hypothesis that these proteins that represent CNS dysfunction are only detectable in peripheral blood due to increased transit across the BBB. However, as the relationship was negative for both radiological and functional measurements of BBB permeability in both proteins, this suggests that detection in serum reflects a genuine increase production in the CNS compartment.

Strengths of this study include the range of radiological and functional metrics used to interrogate BBB dysfunction, and the relatively large number of participants who underwent advanced neuroimaging. Nevertheless, the study was likely underpowered to ascertain associations between the BBB permeability and clinic-radiological features of SVD severity, particularly given the small number of participants who gave CSF samples. Comparison of anatomically specific markers of permeability based on MRI may carry provide different information than a single numerical output representative of the entire CNS, and further work will aim to determine if hotspots of BBB permeability are in proximity to WMHs (and other overt SVD lesions) and also whether hotspots of increased permeability in NAWM are likely to progress to lesions.

Similar to the limitations discussed in chapter six, this chapter leveraged a relatively small cohort of participants to test a number of hypotheses involving complex high-dimensional data, and there remains a risk that any significant findings were due to chance. This is less of a concern in the BBB permeability studies as no major significant relationships were identified.

Measurements of GFAP and NfL were compared to reference data from healthy participants, but their role in SVD would be better tested by the inclusion of control participants in these experiments. The CSF NfL assay in particular was less reliable as evidenced by the relative high coefficient of variance, and this limits interpretability particularly in this small sample.

Additionally, longitudinal data from the pooled observational and MINERVA trial cohorts will allow me to test whether BBB permeability predicts disease progression (or indeed if it is protective), and the repeat imaging included in the trial protocol will provide a large dataset in which to investigate fluctuation in BBB permeability (i.e. whether the mean permeability constant and hotspot volume are stable over a three month time period, and whether focal areas of increased permeability continue to show dysfunction from baseline to follow-up). Finally as minocycline, the trial intervention, has been suggested as a BBB stabiliser³¹⁸, the MINERVA results will include testing of whether intervention can in fact decrease permeability of the BBB and whether this has a beneficial effect in the longer term.

CHAPTER EIGHT

Blood-brain barrier permeability and markers of central and peripheral inflammation: associations with one year imaging and neuropsychometric performance

Content from this chapter has been published as :

Tozer DJ, **Brown, RB**, Walsh J, Hong YT, Fryer TD, Williams GB, O'Brien JT, Fryer TJ & Markus HS. *Stroke* 2023; 54: 549-557³⁵⁶

and presented as:

Brown, RB, Walsh J, Tozer, DJ, Hong YT, Fryer TD, Williams GB, Graves MJ, O'Brien JT & Markus HS. *European Molecular Biology Organization Stroke Immunology Workshop [oral presentation from submitted abstract]* (09.03.2022)

I designed the study, performed follow-up neuropsychometric testing and analysed the imaging. Jessica Walsh recruited the participants, and performed blood sampling and baseline. neuropsychometric testing. Daniel Tozer, Young Hong and Tim Fryer assisted with the image analysis.

Introduction

Chapters six and seven examined the relationship between neuroinflammation (measured using ^{11}C -PK11195 PET), BBB permeability (measured using DCE-MRI) and radiological measures of SVD severity at baseline, and demonstrated associations between these metrics similar to those found in the observational phase of our study alone.²¹³ However, this association at a single timepoint is not necessarily causative; to prove that these processes are responsible for SVD progression, it would be necessary to demonstrate both that they correlate with disease severity and that they independently predict clinical or radiological outcome in the longer term (in addition to the effect of intervention as discussed in chapter five).

The evidence for the effect of neuroinflammation and BBB permeability in the longer term is sparse in human populations, likely due to the resources required to gather this data and follow up large enough cohorts for sufficient time. Markers of endothelial function may represent the intersection between haemodynamic compromise and inflammation³⁸² but few have been tested; one observational community cohort study found that ICAM-1, responsible for lymphocyte adhesion and migration, predicted both WMH progression over three and six years.²¹⁹ Individual markers of systemic inflammation have been tested with mixed results, particularly focusing on the IL-6 / CRP pathway; one study³⁸³ found that CRP was associated with WMH progression over 3.3 years in a cohort of over 1000 community-dwelling participants, particularly in the tertile with highest CRP at baseline, while Gu et al.³⁸⁴ found that IL-6 (but not CRP) was associated with WMH progression over 4.5 years in a similar population based cohort. Other authors have failed to demonstrate any association with WMH progression^{220,290}.

One longitudinal study performed has included more detailed immunophenotyping.²²⁶ The authors calculated change in WMH volume in 51 patients with SVD over nine years, and found that baseline IL-6 predicted progression with moderate effect size (correlation coefficient = 0.294, $p < 0.05$). In addition, WMH growth was also

predicted by the proportion of intermediate CD14⁺⁺ CD16⁺ monocytes and their capacity for IL-17 production. It was also negatively correlated with IFN- γ production on exposure to *C. albicans*. These results do provide some evidence in humans that inflammation relates to disease progression. However, key acute inflammatory markers fluctuate over a timescale of days and vary significantly with intercurrent illness, and it is likely that all these studies are limited by the measurement of inflammatory markers at a single timepoint.

The longitudinal effect of alterations in BBB permeability has only been assessed in two human studies to date. Wardlaw et al.¹⁸⁷ applied the Patlak model to DCE-MRI data in a cohort of patients with mild stroke, and found that although the BBB permeability was related to WMH severity, it did not predict progression after one year. Further analysis of this cohort data did not find evidence that BBB permeability predicts progression in other markers of SVD individually or using a composite SVD severity score, though it did predict performance.³⁸⁵ This study was limited by the inclusion of other stroke subtypes which may have affected the robustness of the conclusions for SVD markers specifically. The second study by Huisa et al.²¹⁴ examined a cohort of 22 patients felt to have VCI due to Binswanger's disease (defined as severe SVD characterised by inflammation/demyelination and relatively quick progression to dementia), and found that BBB permeability at baseline using the Patlak model did not predict WMH progression or incident lacunes over ten months.

Pre-clinical models have provided further limited evidence of both neuroinflammatory processes and BBB leakage contributing to disease progression. In a spontaneously hypertensive / stroke-prone rat model, unilateral carotid occlusion led to typical WMH lesions developing and this was accompanied by an MMP-9 associated leakage of IgG into parenchyma on serial histological sampling²³⁴; in a similar rodent model, fibrinogen staining (a further marker of BBB permeability) was only present late in the disease.³⁸⁶ Further evidence is needed to elucidate the time course of both the inflammatory response and the permeability of the BBB in SVD in order to target the timing of any intervention appropriately in the course of the disease.

This accumulated evidence informs three possible models of the relationship between inflammatory processes, increased permeability of the BBB and tissue damage in SVD (figure 8.1). One model, broadly following the structure outlined by Rosenberg et al.²²⁷, proposes that inflammatory mediators are produced as a response to haemodynamic upset and initial ischaemia, followed sequentially by BBB opening and further tissue damage. In an alternative model, the inflammation described above is purely a response to the initial injury and does not drive further tissue damage; authors proposing the latter have even suggested that microglial activation may even be protective, leading to resolution of tissue damage and restoration of local homeostasis.²³² A final model suggests that these processes are independent downstream results of a common primary injury. Ascertaining which of these models best describes the relationship between the novel disease processes identified and long term SVD progression is critical for determining whether intervention is likely to be meaningful.

I aimed to test which of these models best described the relationship between inflammation (using ¹¹C-PK11195 PET as a proxy for central inflammation, and serum inflammatory proteins as peripheral markers), BBB permeability (using DCE-MRI) and the progression of SVD. I hypothesised that if the sequential model shown in figure 8.1(A) is most accurate, inflammation and BBB permeability would independently predict worsening of radiological SVD severity and cognitive performance, when corrected for other known factors that predict disease progression. I aimed to answer the following questions:

- (1) Do baseline measurements of inflammation predict disease progression based on MRI or neuropsychometric testing?
- (2) Do baseline measurements of BBB permeability predict disease progression in the same way?

To answer these questions, I performed one year follow-up appointments for participants in the observational phase of our PET/DCE-MRI study, which included repeat MRI (conventional sequences only) and neuropsychometric testing.

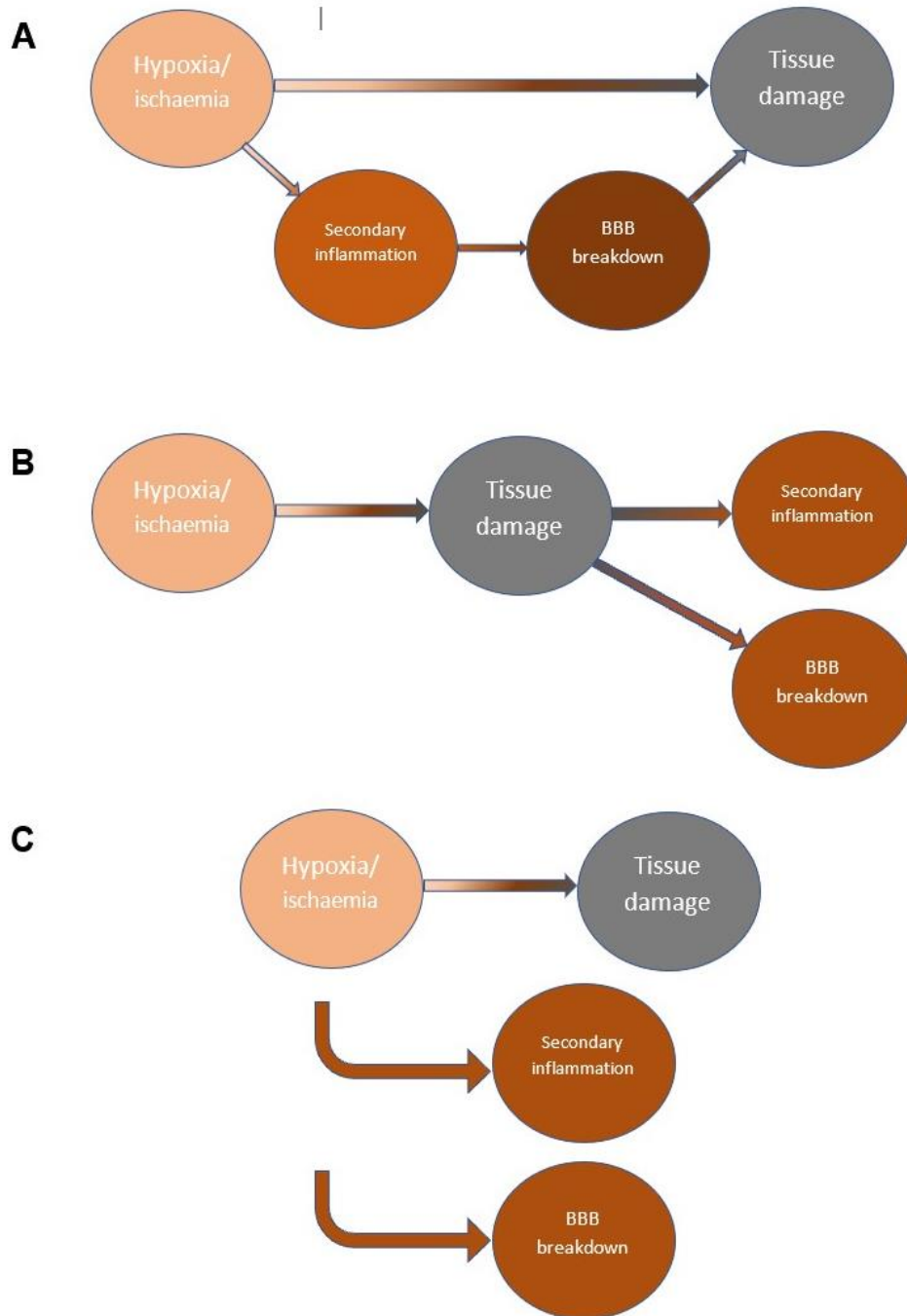


Figure 8.1. Alternative models for the relationship between initial cerebrovascular injury, inflammation / BBB permeability and parenchymal damage. (A) The model discussed in chapter one. Hypoxia / ischaemia leads to direct tissue damage, and also results in a parallel inflammatory cascade and BBB opening that exacerbates this damage. (B) Hypoxia / ischaemia leads to direct tissue damage, and this causes both BBB opening and local inflammation. (C) Inflammation and BBB permeability occur unrelated to tissue damage, either as a consequence of the initial hypoxia / ischaemia or secondary to other related factors such as cardiac risk factors, lifestyle factors, linked genetic factors or medications.

Methods

Patients with sporadic SVD were recruited as described in chapter four and underwent baseline appointment at which demographic details, and medical history including comorbidities and medications were collected. Participants underwent co-acquired PET and DCE-MRI as described above, as well as baseline neuropsychiatric testing.

All participants were invited back one year after the baseline appointment for a repeat MRI including conventional / structural sequences only on the same MRI scanner (T1, T2, FLAIR, SWI and DTI; full sequence details are provided in Appendix B).

Image analysis

Baseline PET and DCE-MRI images were analysed using the methods described in chapter four. Volumes of ‘hotspot’ areas of increased ^{11}C -PK11195 binding and of K_{in} in the NAWM as defined in chapter five were taken as the primary indicator metrics from the PET and DCE-MRI scans respectively.

SPM12 was used to segment the tissue in grey and white matter, and WMHs were marked semi-automatically using Jim version 8.0 (<http://xinapse.com/j-im-software/>). I employed a similar blind-to-timepoint method discussed in chapter three where the baseline and follow-up images were marked in parallel and displayed in a random order to the rater. Lacunes were marked on baseline and FLAIR images with parallel visual inspection of T1 and T2-weighted sequences to confirm any lesions, and the masked using the ‘Masker’ tool in Jim to confirm the number of discrete regions of interest (ROI). CMBs were marked on SWI images and were also counted automatically using the Masker tool. DTI data were converted to histograms as above.

Neuropsychiatric test scoring

The neuropsychiatric tests were scored at baseline and at one year according to the method described in chapter six. The difference in z -scores in EF (ΔEF), PS (ΔPS), LTM (ΔLTM) and GC (ΔGC) were taken as outcome indicators for cognitive performance.

Statistical analysis

Within the data collected, demographic factors (age, sex, premorbid IQ and years in education), participant comorbidities (hypertension, hypercholesterolaemia, diabetes and smoking history) and baseline imaging parameters (WMHs, lacunar infarcts, CMBs, brain volume and DTI metrics) were identified as potential variables that might predict radiological progression and/or cognitive deterioration. Univariate linear regression was used to test the effect of each of these predictors individually on continuous radiological markers of SVD progression (WMH expansion) and metrics of change in cognition (Δ EF, Δ PS, Δ LTM and Δ GC). Logistic regression was used to test the effect of these predictors on subjects developing incident lacunes or CMBs.

I next performed multiple linear or logistic regression to assess the effects of the predictor variables on these outcomes as above. This was limited by the number of patients with SVD included ($n = 20$); conventionally it has been suggested that a minimum of ten subjects-per-predictor is required to allow a linear regression model to predict outcomes correctly in subsequent subjects³⁸⁷, and although other authors have challenged this assumptions, calculating the required subject-per-variable as low as two³⁸⁸, the area remains controversial. Logistic regression also likely requires ten subjects-per-variable.³⁸⁹ I created models to test the effect of ¹¹C-PK11195 binding and BBB permeability that included as covariates age, sex, baseline severity for radiological markers and pre-morbid IQ for cognitive markers. These models were considered exploratory.

All analysis was performed in the R project for statistical computing²⁶⁰ version 4.2.1.

Results

20 participants with moderate to severe SVD were recruited; demographic and comorbidity data were available from 20 patients, as were conventional MRI data at baseline and follow-up and baseline serum samples. 16 participants had available PET

data and 19 had successful DCE-MRI that could be analysed. 19 patients completed baseline and follow-up neuropsychometric testing.

Predictors of radiological disease progression

WMH progression

The mean change in WMH volume over one year was $3.6\text{cc} \pm 3.9\text{cc}$. Table 8.1 shows the results of univariate and multivariate linear regression models.

On univariate analysis, the only significant predictor of WMH progression was age at enrolment (unstandardised β value 0.23, standard error 0.084, $p = 0.013$). ^{11}C -PK11195 binding and BBB permeability hotspots were not significantly associated with WMH progression (figure 8.2).

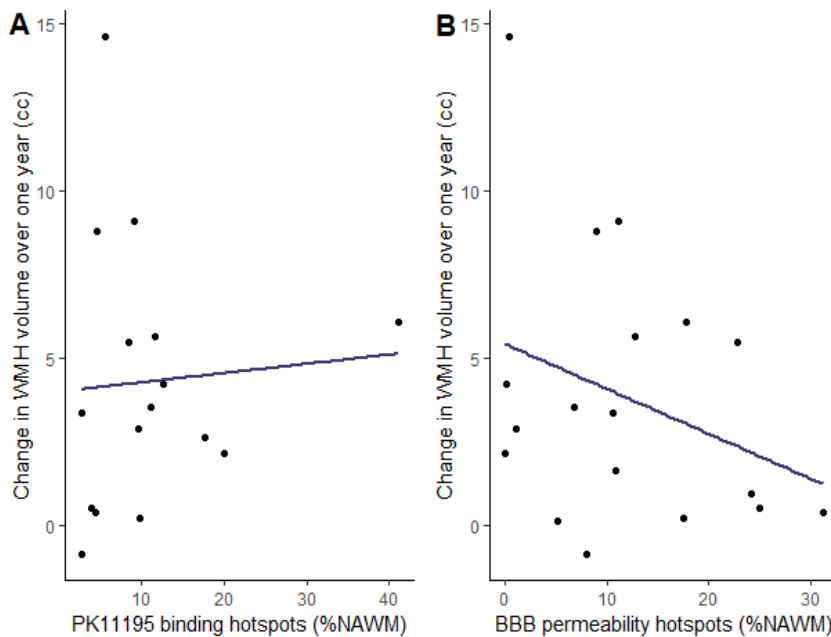


Figure 8.2. Scatter plots of (A) ^{11}C -PK11195 binding hotspots versus change in WMH and (B) BBB permeability hotspots versus change in WMH over one year.

Predictor variables	Univariate models			Multivariate model		
	β	SE	p value	β	SE	p value
Demographics						
Age (years)	0.23	0.084	0.013	0.055	0.28	0.85
Sex (male vs female)	-1.94	1.72	0.27	-0.20	0.44	0.66
Comorbidities						
Hypertension (yes/ no)	0.054	2.96	0.98			
Hypercholesterolaemia (yes/no)	1.28	1.76	0.48			
Diabetes (yes/no)	-2.13	2.16	0.34			
Smoking (yes/no)	1.32	1.76	0.46			
BMI	-1.91	1.56	0.24			
Radiological features						
Baseline WMH (cc)	0.049	0.027	0.091	0.077	0.078	0.35
Brain volume (cc)	0.0024	0.0044	0.58			
Lacunes (count)	0.073	0.456	0.87			
Microbleeds (count)	0.236	0.180	0.20			
FA median	10.43	23.46	0.55			
MD peak height (mm ² /s)	-370.25	513.38	0.48			
Novel pathophysiological markers						
¹¹ C-PK11195 binding hotspots	9.8×10^{-6}	1.1×10^{-4}	0.93	-0.018	0.028	0.53
K_{in} hotspots	-8.3×10^{-5}	1.2×10^{-4}	0.49	-0.016	0.020	0.45

Table 8.1. Unstandardised β values, standard errors and p values from univariate linear regression models and multivariate (exploratory) model measuring effect of predictors on WMH progression (cc). *FA fractional anisotropy; MD mean diffusivity; SE standard error.*

In the multivariate model, none of the predictors was significantly associated with WMH progression; of note, although the effect sizes were small, the values for both ¹¹C-PK11195 binding and BBB permeability were negative i.e. associated with less progression.

Incident lacunes

Five participants (25%) showed incident lacunes during the one year follow-up. These were all single infarcts; multiple incident lacunes were not observed in any of the participants. In four of the participants (20%), the one lacune had become invisible at follow-up. Table 8.2 shows the results of univariate and multivariate logistic regression models.

On univariate analysis, the only significant predictor of incident lacunes was the presence of diabetes (unstandardised β value 2.97, standard error 1.38, $p = 0.032$). ¹¹C-PK11195 binding and BBB permeability hotspots were not significantly associated with incident lacunes (figure 8.3).

Predictor variables	Univariate models			Multivariate model		
	β	SE	<i>p</i> value	β	SE	<i>p</i> value
Demographics						
Age (years)	0.034	0.059	0.56	0.48	0.31	0.12
Sex (male vs female)	-0.41	1.06	0.70	6.79	4.94	0.17
Comorbidities						
Hypertension (yes/ no)	16.7	279	0.99			
Hypercholesterolaemia (yes/no)	1.39	1.24	0.26			
Diabetes (yes/no)	2.97	1.38	0.032			
Smoking (yes/no)	0.41	1.06	0.70			
BMI	0.17	0.10	0.10			
Radiological features						
Baseline WMH (cc)	-0.017	0.026	0.51			
Brain volume (cc)	-0.004	0.003	0.19			
Lacunae (count)	0.30	0.26	0.25	0.080	0.30	0.79
Microbleeds (count)	0.068	0.099	0.50			
FA median	-4.09	13.2	0.76			
MD peak height (mm ² /s)	-74.7	305.5	0.81			
Novel pathophysiological markers						
¹¹ C-PK11195 binding hotspots	-0.11	0.12	0.39	-0.24	0.20	0.21
<i>K</i> _{in} hotspots	-0.045	0.063	0.48	-0.34	0.30	0.26

Table 8.2. Unstandardised β values, standard errors and *p* values from univariate logistic regression models and multivariate (exploratory) model measuring effect of predictors on likelihood of incident lacunes. *FA* fractional anisotropy; *MD* mean diffusivity; *SE* standard error.

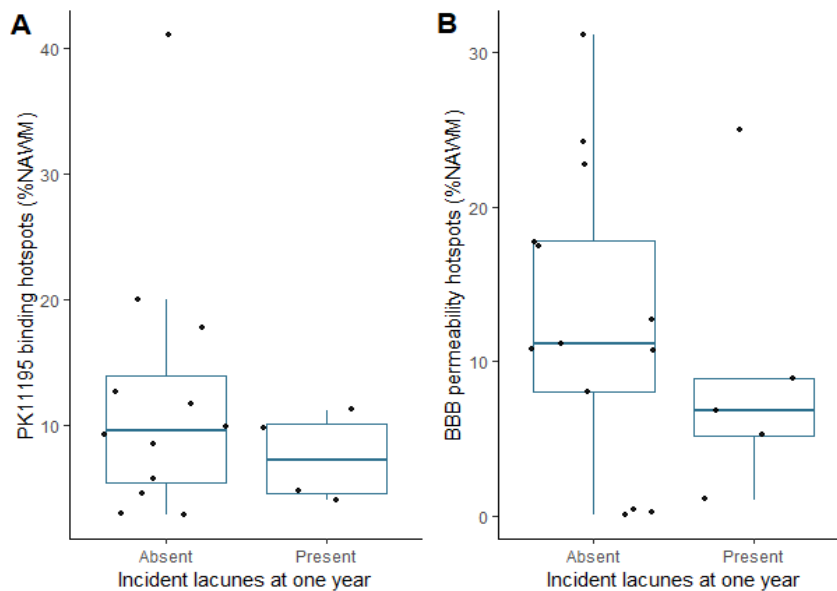


Figure 8.3. Boxplots of (A) ¹¹C-PK11195 binding hotspots and (B) BBB permeability hotspots, stratified by incident lacunes.

Incident cerebral microbleeds

Seven participants (35%) had incident CMBs during the one year follow-up. The number of new CMBs ranged from one to seven and these were only present in participants who had CMBs at baseline. CMBs did not disappear in any participant.

Table 8.3 shows the results of univariate and multivariate logistic regression models.

Predictor variables	Univariate models			Multivariate model		
	β	SE	<i>p</i> value	β	SE	<i>p</i> value
Demographics						
Age (years)	-0.053	0.058	0.36	0.18	0.15	0.26
Sex (male vs female)	1.61	1.04	0.12	3.11	2.30	0.21
Comorbidities						
Hypertension (yes/ no)	-0.61	1.5	0.69			
Hypercholesterolaemia (yes/no)	-0.98	0.98	0.32			
Diabetes (yes/no)	0.69	1.14	0.54			
Smoking (yes/no)	1.25	1.02	0.22			
BMI	0.017	0.085	0.84			
Radiological features						
Baseline WMH (cc)	0.0097	0.015	0.53			
Brain volume (cc)	0.0012	0.0023	0.62			
Lacunae (count)	0.50	0.33	0.12			
Microbleeds (count)	0.12	0.11	0.26	0.07	0.14	0.61
FA median	-3.2	12.4	0.80			
MD peak height (mm ² /s)	-303.4	311.7	0.33			
Novel pathophysiological markers						
¹¹ C-PK11195 binding hotspots	0.040	0.058	0.70	0.019	0.075	0.81
K _{in} hotspots	0.018	0.053	0.73	0.18	0.12	0.16

Table 8.3. Unstandardised β values, standard errors and *p* values from univariate logistic regression models and multivariate (exploratory) model measuring effect of predictors on likelihood of incident microbleeds. *FA fractional anisotropy; MD mean diffusivity; SE standard error.*

On univariate analysis no predictors were significantly associated with incident CMBs, including ¹¹C-PK11195 binding and BBB permeability hotspots. Figure 8.4 shows the distribution of these values stratified by the presence or absence of incident CMBs. In the multivariate model, none of the predictors was significantly associated with incident CMBs.

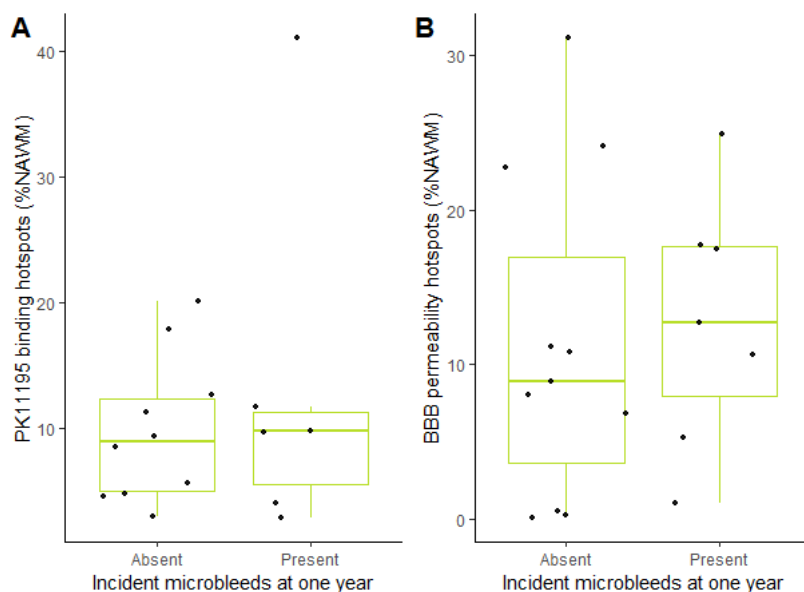


Figure 8.4. Boxplots of (A) ^{11}C -PK11195 binding hotspots and (B) BBB permeability hotspots, stratified by new CMBs.

Change in DTI parameters

Mean FA was 0.343 at baseline and 0.331 at follow-up (a difference of -0.011 ± 0.04 , $p = 0.34$). Mean MD peak height was $0.0110\text{mm}^2/\text{s}$ at baseline and $0.0103\text{mm}^2/\text{s}$ at follow-up (A difference of $-0.0007 \pm 0.0008\text{mm}^2/\text{s}$, $p = 0.19$). Table 8.4 shows the results of univariate and multivariate logistic regression models for factors that predict change in FA, and table 8.5 shows the results of similarly constructed models to predict change in MD. On univariate analysis, the only significant predictor of change in FA was baseline FA ($\beta = -0.547$, $\text{SE} = 0.209$, $p = 0.018$); no predictors were significant in the final model. Similarly on univariate analysis the only significant predictor of change in MD was baseline MD ($\beta = -0.264$, $\text{SE} = 0.0897$, $p = 0.0091$) and no predictors were significant in the multivariate model.

Predictor variables	Univariate models			Multivariate model		
	β	SE	<i>p</i> value	β	SE	<i>p</i> value
Demographics						
Age (years)	-0.000749	0.00104	0.48	-0.00116	0.00396	0.78
Sex (male vs female)	0.0121	0.0187	0.53	0.00221	0.0654	0.97
Comorbidities						
Hypertension (yes/ no)	-0.0232	0.0303	0.46			
Hypercholesterolaemia (yes/no)	0.0273	0.0178	0.14			
Diabetes (yes/no)	0.00886	0.0231	0.71			
Smoking (yes/no)	0.00712	0.0189	0.71			
BMI	-0.000256	0.00175	0.89			
Radiological features						
Baseline WMH (cc)	0.000249	0.000301	0.42			
Brain volume (cc)	1.09×10^{-5}	4.60×10^{-5}	0.82			
Lacunae (count)	0.00374	0.00451	0.41			
Microbleeds (count)	0.00361	0.00175	0.055			
FA median	-0.547	0.209	0.018	-0.521	0.393	0.22
MD peak height (mm ² /s)	-0.401	5.42	0.94			
Novel pathophysiological markers						
11C-PK11195 binding hotspots	0.000668	0.00123	0.54	0.000126	0.00181	0.78
K _{in} hotspots	0.00183	0.000949	0.07	0.000515	0.00285	0.97

Table 8.4. Unstandardised β values, standard errors and *p* values from univariate logistic regression models and multivariate (exploratory) model measuring effect of predictors on change in FA. *FA fractional anisotropy; MD mean diffusivity; SE standard error.*

Predictor variables	Univariate models			Multivariate model		
	β	SE	<i>p</i> value	β	SE	<i>p</i> value
Demographics						
Age (years)	1.91×10^{-5}	2.08×10^{-5}	0.37	5.71×10^{-5}	7.46×10^{-5}	0.47
Sex (male vs female)	0.000138	0.000384	0.72	0.000888	0.00123	0.49
Comorbidities						
Hypertension (yes/ no)	0.000272	0.000624	0.67			
Hypercholesterolaemia (yes/no)	0.000458	0.000369	0.23			
Diabetes (yes/no)	-2.62×10^{-5}	0.00472	0.96			
Smoking (yes/no)	0.000578	0.000359	0.13			
BMI	1.23×10^{-5}	3.18×10^{-5}	0.70			
Radiological features						
Baseline WMH (cc)	4.26×10^{-6}	6.16×10^{-6}	0.49			
Brain volume (cc)	1.78×10^{-7}	9.35×10^{-7}	0.85			
Lacunae (count)	0.000138	8.73×10^{-5}	0.13			
Microbleeds (count)	2.08×10^{-5}	3.95×10^{-5}	0.61			
FA median	-0.00359	0.00500	0.48			
MD peak height (mm ² /s)	-0.264	0.0897	0.0091	-0.245	0.181	0.21
Novel pathophysiological markers						
11C-PK11195 binding hotspots	-2.20×10^{-6}	2.23×10^{-5}	0.92	-2.7×10^{-5}	3.35×10^{-5}	0.45
K _{in} hotspots	-4.60×10^{-6}	2.09×10^{-5}	0.83	5.40×10^{-5}	5.32×10^{-5}	0.34

Table 8.5. Unstandardised β values, standard errors and *p* values from univariate logistic regression models and multivariate (exploratory) model measuring effect of predictors on change in MD. *FA fractional anisotropy; MD mean diffusivity; SE standard error.*

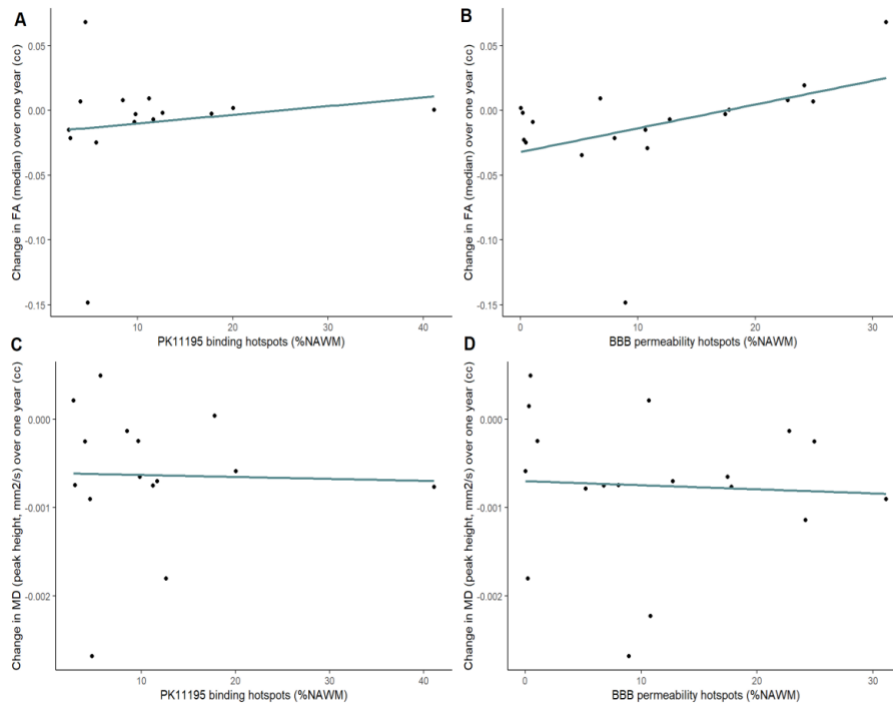


Figure 8.5. Scatter plots of (A) ^{11}C -PK11195 binding hotspots versus change in FA; (B) BBB permeability hotspots versus change in FA; (C) ^{11}C -PK11195 binding hotspots versus change in MD; and (D) BBB permeability hotspots versus change in MD over one year;

Predictors of change in cognition

The mean scores in all cognitive domains increased between baseline and follow-up appointments, particularly in executive function (mean change in z -score 1.14, $p = 8.51 \times 10^{-6}$). The mean change in z -score in processing speed and long-term memory were 0.11 ($p = 0.35$) and 0.069 ($p = 0.52$) respectively. The mean score for global cognition increased significantly (mean change in z -score 0.26, $p = 0.0047$). Figure 8.6 shows the distribution of scores in these domains at baseline and one year follow-up.

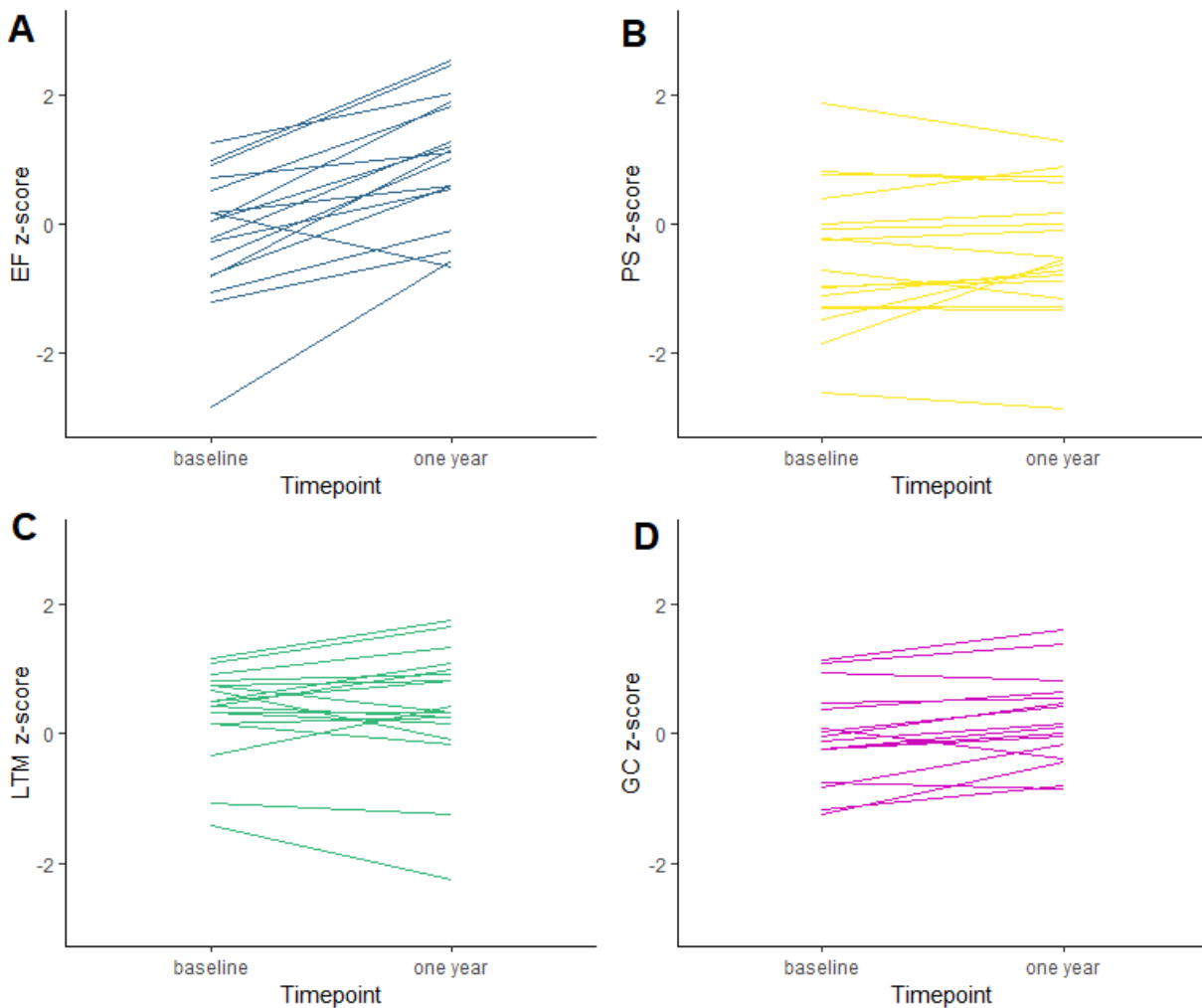


Figure 8.6. Baseline and follow-up distribution of z-scores in (A) executive function – EF; (B) processing speed – PS; (C) long-term memory – LTM; and (D) global cognition – GC.

Figure 8.7 shows the relationship between baseline microglial signal (measured as volume of ^{11}C -PK11195 binding hotspots) and change in neuropsychometric performance; figure 8.8 shows the relationship between baseline BBB permeability (measured as volume of permeability hotspots) and change in neuropsychometric performance as above. The results of univariate and multivariate linear regression models are presented below.

Change in executive function

Pre-morbid IQ as measured by NART was the only significant predictor of change in executive function z-score (unstandardised β value -0.059, standard error 0.020, $p = 0.0089$). This was not significant when false discovery rate corrected. In the multivariate model, no predictors were significantly associated with executive function change (table 8.6).

Predictor variables	Univariate models			Multivariate model		
	β	SE	<i>p</i> value	β	SE	<i>p</i> value
Demographics						
Age (years)	-0.033	0.018	0.083	0.014	0.06	0.83
Sex (male vs female)	0.27	0.36	0.46	0.38	1.05	0.73
Years of education	-0.026	0.062	0.68			
Baseline IQ	-0.059	0.020	0.0089	-0.042	0.034	0.26
Comorbidities						
Hypertension (yes/ no)	-0.25	0.78	0.76			
Hypercholesterolaemia (yes/no)	-0.32	0.36	0.39			
Diabetes (yes/no)	0.44	0.42	0.31			
Smoking (yes/no)	0.054	0.37	0.88			
BMI	0.028	0.032	0.40			
Radiological features						
Baseline WMH (cc)	-0.015	0.0096	0.12			
Brain volume (cc)	-0.00024	0.0010	0.81			
Lacunes (count)	-0.14	0.080	0.095			
Microbleeds (count)	-0.021	0.036	0.58			
FA median	0.32	4.74	0.95			
MD peak height (mm ² /s)	168.9	90.1	0.081			
Novel pathophysiological markers						
11C-PK11195 binding hotspots	0.022	0.041	0.59	0.047	0.055	0.43
K_{in} hotspots	0.022	0.019	0.29	0.028	0.050	0.59

Table 8.6. Unstandardised β values, standard errors and *p* values from univariate linear regression models and multivariate (exploratory) model measuring effect of predictors on change in executive function domain z-score. *FA* fractional anisotropy; *MD* mean diffusivity; *SE* standard error.

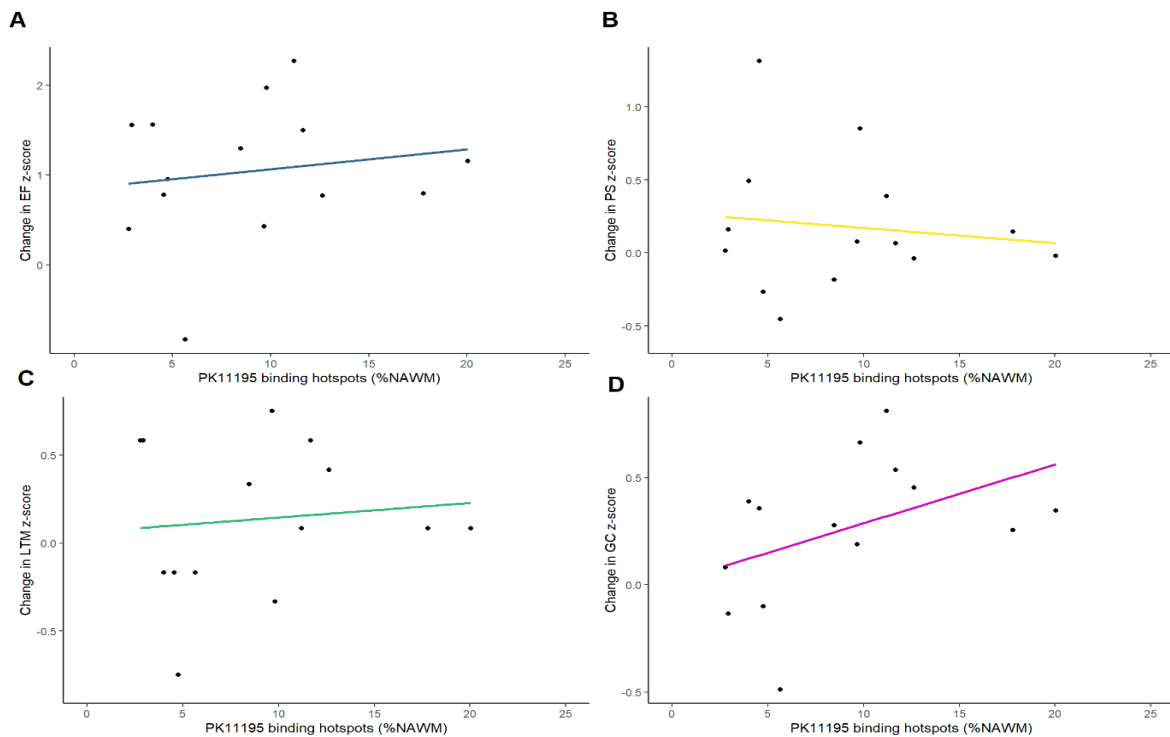


Figure 8.7. Scatter plots showing relationship between baseline ¹¹C-PK11195 binding hotspots and one year change in z-score in (A) executive function – EF; (B) processing speed – PS; (C) long-term memory – LTM; and (D) global cognition – GC.

Change in processing speed

On univariate analysis, number of CMBs was negatively correlated with change in processing speed z -score ($\beta = -0.059$, $SE = 0.020$, $p = 0.0089$). FA was positively correlated ($\beta = 9.20$, $SE = 1.89$, $p = 0.00021$). In the multivariate model, no predictors were significantly associated with change in processing speed (table 8.7).

Predictor variables	Univariate models			Multivariate model		
	β	SE	p value	β	SE	p value
Demographics						
Age (years)	-0.012	0.012	0.33	-0.34	0.032	0.33
Sex (male vs female)	0.081	0.23	0.73	-0.27	0.55	0.64
Years of education	0.0066	0.040	0.87			
Baseline IQ	-0.025	0.015	0.11	-0.024	0.018	0.22
Comorbidities						
Hypertension (yes/ no)	0.44	0.49	0.38			
Hypercholesterolaemia (yes/no)	0.20	0.23	0.40			
Diabetes (yes/no)	-0.025	0.28	0.93			
Smoking (yes/no)	0.024	0.24	0.92			
BMI	-0.0034	0.020	0.87			
Radiological features						
Baseline WMH (cc)	0.0015	0.0067	0.82			
Brain volume (cc)	0.00026	0.00063	0.68			
Lacunae (count)	0.020	0.056	0.73			
Microbleeds (count)	-0.062	0.017	0.0021	0.0559	0.0528	0.34
FA median	9.20	1.89	0.00021	1.399	8.26	0.87
MD peak height (mm ² /s)	55.0	62.6	0.39			
Novel pathophysiological markers						
11C-PK11195 binding hotspots	-0.010	0.025	0.68	0.014	0.029	0.64
K _{in} hotspots	0.023	0.012	0.065	0.011	0.026	0.70

Table 8.7. Unstandardised β values, standard errors and p values from univariate linear regression models and multivariate (exploratory) model measuring effect of predictors on change in processing speed domain z -score. FA fractional anisotropy; MD mean diffusivity; SE standard error.

Change in long term memory

On univariate analysis, hypertension was positively associated with change in long-term memory z -score ($\beta = 0.792$, $SE = 0.299$, $p = 0.0017$). WMH was negatively correlated ($\beta = -0.00677$, $SE = 0.00313$, $p = 0.045$). In the multivariate model, no predictors were significantly associated with change in long-term memory (table 8.8).

Predictor variables	Univariate models			Multivariate model		
	β	SE	<i>p</i> value	β	SE	<i>p</i> value
Demographics						
Age (years)	-0.0175	0.0113	0.14	-0.00369	0.0366	0.92
Sex (male vs female)	0.194	0.213	0.38	0.877	0.67	0.24
Years of education	0.0603	0.0342	0.096			
Baseline IQ	0.0260	0.0131	0.065	0.0375	0.0221	0.14
Comorbidities						
Hypertension (yes/ no)	0.792	0.299	0.017	0.322	0.563	0.07
Hypercholesterolaemia (yes/no)	0.0880	0.217	0.69			
Diabetes (yes/no)	0.0263	0.267	0.92			
Smoking (yes/no)	-0.158	0.215	0.47			
BMI	0.0267	0.0183	0.17			
Radiological features						
Baseline WMH (cc)	-0.00677	0.00313	0.045	-0.00127	0.00106	0.28
Brain volume (cc)	-0.000139	0.000529	0.80			
Lacunae (count)	0.0744	0.0497	0.15			
Microbleeds (count)	-0.00225	0.0225	0.92			
FA median	4.776	2.600	0.083			
MD peak height (mm ² /s)	4.149	62.333	0.95			
Novel pathophysiological markers						
¹¹ C-PK11195 binding hotspots	0.0194	0.0126	0.15	0.0237	0.0338	0.51
K _{in} hotspots	-0.0185	0.0112	0.12	0.0209	0.0312	0.53

Table 8.8. Unstandardised β values, standard errors and *p* values from univariate linear regression models and multivariate (exploratory) model measuring effect of predictors on change in long-term memory domain *z*-score. *FA* fractional anisotropy; *MD* mean diffusivity; *SE* standard error.

Change in global cognition

On univariate analysis, baseline IQ as measured by NART was negatively correlated with change in global cognition *z*-score ($\beta = -0.0246$, $SE = 0.00870$, $p = 0.013$). In the multivariate model, ¹¹C-PK11195 binding hotspot volume was significantly associated with change in global cognition *z*-score ($\beta = 0.0501$, $SE = 0.147$, $p = 0.011$ (table 8.9).

Predictor variables	Univariate models			Multivariate model		
	β	SE	p value	β	SE	p value
Demographics						
Age (years)	-0.00964	0.00816	0.26	-0.00356	0.0164	0.83
Sex (male vs female)	0.188	0.156	0.25	0.409	0.278	0.18
Years of education	-0.0131	0.0279	0.65			
Baseline IQ	-0.0246	0.00870	0.013	-0.00676	0.00899	0.48
Comorbidities						
Hypertension (yes/ no)	0.0184	0.338	0.96			
Hypercholesterolaemia (yes/no)	0.0297	0.164	0.72			
Diabetes (yes/no)	0.188	0.203	0.37			
Smoking (yes/no)	0.0968	0.163	0.56			
BMI	0.0124	0.0142	0.39			
Radiological features						
Baseline WMH (cc)	-0.00215	0.00451	0.64			
Brain volume (cc)	-0.000201	0.000437	0.65			
Lacunae (count)	-0.0232	0.0382	0.55			
Microbleeds (count)	0.00678	0.0160	0.67			
FA median	-1.774	1.999	0.39			
MD peak height (mm ² /s)	39.463	42.113	0.37			
Novel pathophysiological markers						
11C-PK11195 binding hotspots	0.0274	0.0164	0.12	0.0501	0.0147	0.011
K_{in} hotspots	0.00847	0.00870	0.35	0.0274	0.0132	0.077

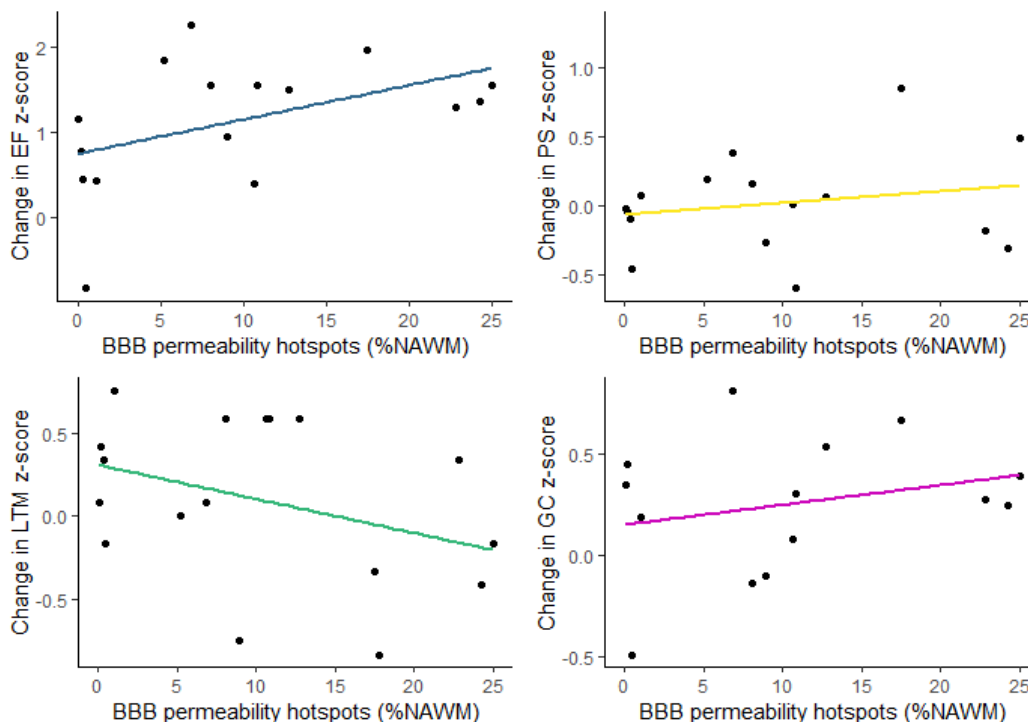


Figure 8.8. Scatter plots showing relationship between baseline BBB permeability hotspots and one year change in z-score in (A) executive function – EF; (B) processing speed – PS; (C) long-term memory – LTM; and (D) global cognition – GC.

Discussion

Longitudinal data from this cohort of patients with SVD do not show that either BBB permeability or microglial signal measured by PET imaging predict disease progression. The only significant relationship was that the ^{11}C -PK11195 binding hotspot volume predicted improved global cognition at one year. This study suggests that these disease processes do not predict disease progression in SVD and raise the possibility that microglia in particular may rather be protective.

Radiological progression

At one year follow-up, I found radiological progression of disease in this cohort of patients with moderate to severe SVD that is broadly in keeping with existing literature. WMHs increased by $3.6 \pm 3.9\text{cc}$ which is similar to the expected value of 2.5cc calculated in chapter two and previously published²⁵⁴; the incidence of lacunar infarcts (25% in one year) was also broadly similar to previous estimates of between 9.5% - 36.6%.³⁹⁰ 35% of this cohort showed incident CMBs, which is considerably higher than the 2.2% documented previously in an SVD cohort²⁶⁸, albeit in a population with less severe disease. This may be related to the increased sensitivity of our neuroimaging sequences (i.e. using a SWAN sequence at 3T compared to a T2*-weighted sequence at 1.5T).³⁹¹ As expected, we found decreases in both MD peak height and median FA, indicating a deterioration in microstructural integrity in this population that was also similar to previously published values.^{268,289}

I identified few associations between demographic variables and cardiovascular risk factors that predicted radiological SVD progression. Age was significantly associated with WMH progression, a finding that has previously been well documented^{153,254,262}, and diabetes with incident lacunar infarction, which is less clear in previous literature from observational cohorts.^{266,293} The DTI parameters median FA and normalised peak height MD at baseline were the only significant predictors of progression in each case. Multivariate regression models revealed no significant predictors among possible predictors.

Although baseline ^{11}C -PK11195 binding did not predict progression in any of the radiological markers of SVD, it was noteworthy that in multivariate models the volume of hotspot tissue in NAWM predicted less WMH growth, fewer incident lacunes and higher FA/MD (i.e. less deterioration in white matter microarchitecture). This was unexpected and although not statistically significant, the finding was quite consistent across outcome measurements. There are several possible explanations for this observation:

- 1) It is a chance finding and not representative of a true biological process; or the association is correlative rather than causative. It may be the case that inflammation (if relevant) causes irreversible cellular and tissue changes over a much longer time period than the one year follow-up in this study, and the association is driven by participants in whom inflammation peaked at a previous timepoint but set in motion an irreversible cascade leading to further damage. Evidence towards this is supported by findings from this cohort that NAWM voxels that become WMH at follow-up have a significantly lower ^{11}C -PK11195 binding potential than the remainder of the white matter.³⁵⁶
- 2) Aspects of the pathophysiological processes influencing the PET signal resolve over time and this causes apparent improvement in some markers in specific areas of the brain, for example, oedema.⁷⁶
- 3) The PET signal is representative of a process that is reparative or regenerative rather than destructive.

Microglial function has previously been split somewhat crudely into two polar phenotypes; a pro-inflammatory “M1” phase characterised by expression of surface proteins including CD86, IL-1 β , and TNF- α , and an anti-inflammatory “M2” phase characterised by expression different markers than include CD206, IL-10, and TGF- β .³³⁸ This is likely to be an oversimplification, and TSPO itself mediates the polarisation between microglial M1 and M2 phenotypes in rat models³⁹²; as this process is dynamic, PET imaging may not distinguish between populations of pro-

inflammatory microglia becoming less activated or vice versa. Some authors have even argued (contentiously) against the existence of M1 and M2 phenotypes altogether.³⁹³

Ageing may add additional complexity as aged microglia are known to have an altered transcriptome compared to earlier life³⁹⁴; in this extensive transcriptomic atlas, TSPO is identified as one of the genes significantly upregulated in ageing and this may be an important confounder when leveraging it to image microglia. It has been proposed that TSPO does not indicate microglial activation in humans as in rodent and non-human primates based on analysis of multiple transcriptomic studies across a range of preclinical models of neuroinflammation and data from cohorts of patients with both Alzheimer's disease and multiple sclerosis.³⁹⁵ It is therefore possible that the microglial signal identified using ¹¹C-PK11195 PET imaging represents a protective phenomenon, and various mechanisms by which this could happen have been investigated including direct repair of myelin, clearance of toxic proteins such as β -amyloid and the preservation of synaptic function.³⁹⁵ Further data from participants in the MINERVA trial will allow this hypothesis to be tested, albeit in a small number of subjects: if the intervention reduces microglial signal from the PET images, follow-up imaging at one year and clinical outcome/neuropsychometric performance can be used to test whether this is positive or deleterious. Additionally, future experiments to perform single cell RNA sequencing on stored CSF from these participants will allow me to test whether any cell populations in the CNS are associated with the imaging signal.

Hotspots of increased BBB permeability did not significantly predict progression in any of the markers of BBB tested, though the indicative relationship suggest an association with lower WMH progression, fewer incident lacunes and improved DTI markers. The potential explanations for this are similar to those for the findings from the PET imaging as discussed above; the study may have been insufficiently powered or the follow-up at too short an interval to detect changes over the relevant timescale. These findings are similar to the two previous longitudinal studies investigating DCE-MRI in SVD.^{187,214}

It is less obvious to conjecture that opening of the BBB could be beneficial; the BBB is ubiquitously held to be a critical regulator of homeostasis and prevention of toxins. However, there are suggestions in mouse models of Alzheimer's disease that focused transcranial ultrasound used to temporarily open the BBB can expose the brain to circulating endogenous antibodies against β -amyloid and alter the phenotype of cortical microglia³⁹⁶; this technique may also induce a neuroprotective phenotype in astrocytes at the BBB³⁹⁷ and other authors have suggested that this is both safe and desirable in the treatment of certain neuro-inflammatory or neuro-oncological conditions.³⁹⁸

Progression of cognition

Measures of cognitive performance in the executive function domain and global cognition increased significantly between baseline and one year follow-up. This "practice effect" is a well-described phenomenon across nearly all cognitive tests in every neuropsychometric domain, typically affecting the z -score in the range of between 0-0.5.³⁹⁹ These values are comparable to the practice effect I found in this cohort (though executive function was somewhat higher with an improvement of 1.14). Values were also consistent with the results of a previous study in a specific SVD population.²⁴⁵

Given that cognitive performance improved throughout the study, any associations identified may represent a higher ability to learn the task rather than the preservation of cognition per se. However, some authors have suggested that an inability to demonstrate a practice effect is itself a predictor of cognitive impairment⁴⁰⁰ and so it may be relevant to consider which factors predict greater cognitive improvement.

On univariate analysis, baseline IQ was significantly associated with worsening of executive function z -score. This is counter-intuitive and may represent statistical artefact or a "floor" effect in participants who performed worse (although cognitive impairment/dementia were exclusion criteria for the study and deterioration was likely possible in all participants). Cerebral microbleeds were associated with lower processing speed, consistent with previous analyses in patients with SVD,¹⁰² although the mechanism of this association has yet to be elucidated. Baseline WMH was

associated with worsening of long term memory, consistent with previous meta-analysis.⁶⁹ However hypertension was associated with improved cognitive performance; this is unlikely to be plausible and likely reflects the very low numbers of participants without hypertension.

On multivariate analysis, the only statistically significant association identified was that ¹¹C-PK11195 binding hotspot volume predicted favourable cognitive performance. This finding was reasonably robust ($p = 0.011$), although the effect size was small (correlation coefficient for each percentage point increase in hotspot volume to z-score in cognition = 0.0501). Neuroinflammation is common across several neurodegenerative conditions and has a clear association with neuropsychometric performance.⁴⁰¹ Analogous to the possible explanations for association between the PET findings and radiological progression, there are three possible explanations for this longitudinal finding:

- 1) It is a statistical artefact and not representative of a true biological phenomenon
- 2) The apparent improvement is indicative of a process or factor causing compromise at baseline that resolves by follow-up, for example either the inflammation due to an acute infarct or the cognitive sequelae caused by new onset disability that improves by follow-up. As the median time between stroke and enrolment in this study was 12 months, it is unlikely that the index stroke is relevant to the time course of cognitive performance during this study.
- 3) Neuroinflammation represented by the PET signal is beneficial and promotes regeneration, as has been suggested above.

Conclusions and further directions

I did not find evidence that either the innate inflammatory response or increased permeability of the BBB seen in patients with SVD was related to progression of disease, either clinically or radiologically. This was a small study and likely underpowered to detect such associations; in addition, to the sample size, the follow-up period was short and although in SVD populations there is typically enough change in

WMHs over one year to detect associations,²⁵⁴ there were few incident lacunes and CMBs and associations may have been missed. Cognitive impairment develops over considerably longer than the duration of this study and so although significant changes in cognition were detected, this may not have been clinically relevant. Similar to the limitations discussed in chapters six and seven, I performed a large number of experiments on this small sample of patients and if they were not representative of the condition this may have introduced bias to the results.

Strengths of this study include that the image analysis was performed by the same rater, blind to timepoint and that the cognitive test battery was comprehensive and examined the specific domains affected in vascular cognitive impairment.

Further studies will interrogate the baseline immunophenotype in more detail to examine whether serum inflammatory markers relate to disease progression and if so whether this is mediated by the BBB permeability and microglial signal; peripheral immune challenge with LPS was shown to affect the phenotype of microglia and disrupt BBB tight junctions in mice³³⁶, and one day after this challenge microglia were found to express claudin-5 (an endothelial cell tight junction component) at the BBB itself. This time course and the nature of the challenge are unlikely to be representative of the response to microglia in chronic ischaemia, but the experiment illustrates the potential for microglia to interact with the BBB in different ways at different timepoints.

I have also secured ethical approval to collect longer-term follow-up data from this cohort of patients, including neuropsychometric testing at two and four years after enrolment and data on diagnosis of dementia or cognitive impairment. When combined with the participants from the MINERVA trial, this will provide longitudinal data in 57 patients with SVD and 20 control participants who had identical neuroimaging and serum analysis, and will be better powered to detect any significant relationships between these disease processes.

CHAPTER NINE
Conclusions and further directions

Summary: Part I

Part I of the thesis includes a review of existing literature concerning WMH progression, and a meta-analysis of the expected annual WMH growth across different populations, with implications for clinical trial design. I calculated that WMH progression is highest in cohorts of patients selected on the basis of existing and symptomatic SVD, and in such populations is expected to grow at a mean rate of 2.50 cc per year. This is informative for future clinical trial design, as are calculated requisite sample sizes on which to measure a significantly slower progression when WMH are used as an outcome. The sample sizes I calculated based on baseline WMH volume and participant characteristics match well with a significant and positive recent clinical trial, the SPRINT-MIND study.²⁴⁰

I further investigated WMH regression in several cohorts of participants with SVD, and found a relatively small proportion of participants who exhibited this phenomenon. Those who did showed only a very modest reduction in WMH volume between timepoints. These findings are significantly lower than in other studies including community dwelling participants or unselected stroke patients, and further work would need to demonstrate the method I used could also be applied to patients at a much earlier stage of SVD with significantly lower WMH lesion burdens.

In part I, I focused on WMHs as a biomarker of SVD severity. WMHs are a key radiological hallmark of SVD⁶⁸ and are well correlated with evidence of small vessel pathology at post-mortem examination.¹⁹⁶ However, there are multiple categories of biomarker (i.e., biological measurements that relate to the underlying disease process but distinct from clinical outcomes) that can be used not only for diagnosis, but also for prognostication and treatment response. There is excellent evidence that WMHs are associated with stroke and cognitive impairment⁶⁹; some individual studies have also reported evidence that WMH progression is associated with a worsening of these outcomes.²⁹⁴ No study has yet shown that treatment to reduce the risk of stroke or dementia has done so explicitly by reducing WMH progression or reversing it; however

it is noteworthy that the SPRINT-MIND study showed a beneficial treatment effect of intensive blood pressure control on both WMH progression²⁴⁰ and dementia risk.²⁴¹

The ultimate aim of Part I was to provide data on which future interventional studies might be based. There have been some suggestions that DTI markers are more sensitive to subtle white matter damage⁴⁰² and so this may be a more appropriate biomarker to use for monitoring in clinical trials; however, one longitudinal study showed approximately equivalent sample sizes needed to demonstrate a treatment effect²⁸⁹ and it is likely that upcoming clinical trials will continue to use WMH volume as a biomarker for therapeutic effect.

Summary: Part II

Part II of the thesis includes data from the two analogous cohorts of patients with SVD who have undergone advanced neuroimaging and immunophenotyping. 57 patients and 20 stroke-free control participants were included, making this a relatively large population to have had such detailed investigation. Metrics of microglial signal and BBB permeability discriminated very well between the patient and control groups, particularly the volume of hotspot tissue in the NAWM, and this provides further observational evidence that these processes are associated with SVD. I showed for the first time that SVD severity as evidenced by WMH volume is correlated with ¹¹C-PK11195 binding in patients with SVD, consistent with findings in patients with clinical⁴⁰³ or high risk genotypes for Alzheimer's disease.⁴⁰⁴ It is possible that DTI measures of white matter ultrastructure are more informative for this relationship and work is underway to assess the relationship between DTI markers and the ¹¹C-PK11195 binding in this cohort.

I found no significant relationships between any of the candidate inflammatory biomarkers and conventional markers of SVD severity. These studies were likely underpowered to detect such associations (previous studies finding significant relationship having around ten times as many participants²²²) and work is ongoing to

recruit a considerably larger population for deep immunophenotyping. Within a subpopulation of this cohort, there was evidence that classical and intermediate monocytes may relate to SVD severity via an association with microglial. This is an important finding and suggests a possible mechanism for the interaction between the central nervous system immune compartment and the periphery. Further data-driven analysis of this mass cytometry data, as well as stimulation assays of peripheral blood mononuclear cells, should provide further details on the cell populations involved in this interaction.

BBB permeability measured using DCE-MRI was not well correlated with markers of SVD severity or cognition, though it correlated well with Q_{alb} . This is important as subsequent analysis (Robin Brown & Hugh Markus, *under review*) using the pre- and post-treatment DCE-MRI data from the MINERVA cohort demonstrated that the BBB metrics are not well reproduced between timepoints. Taken together, these findings suggest that BBB permeability is a highly dynamic process and this has significant implications for any interventions targeted at manipulating the BBB.

Outstanding research questions and further directions

Establishment of microglial signal and BBB permeability as causative factors for disease progression

The studies detailed in this thesis do not conclusively answer the questions as to whether microglial activation and permeability of the BBB have a causal role in SVD progression, and this is one of the major outstanding questions to be addressed. While these experiments endorse several of the key criteria for a biological relationship to be considered causative,⁴⁰⁵ particularly concerning immune activation, I was not able to satisfy all of them. There is a clear statistical relationship between ^{11}C -PK11195 binding and clinicoradiological markers of SVD severity, with an effect size that is meaningful, and a plausible mechanistic interpretation as to how this interaction may be deleterious; however, the key criterion that is unsupported by these data is the

relationship in time between measures of inflammation and severity of SVD, and if anything, the data in chapter eight suggest that microglial signal may be protective against SVD progression. Power will be added to this study by incorporating analogous one year follow up data from the MINERVA trial to analyse one year clinical and radiological outcomes of the entire pooled PET-MRI cohort, though this analysis will have to correct for any treatment effect in the trial population.

Overlap between BBB permeability and microglial signal

Another aspect of the disease processes investigated in part II of the thesis that has not been fully explored is the relationship between the two novel processes, either in space, or in time. If both are relevant for SVD progression, then to fully describe the pathophysiological mechanisms involved it would be necessary to elucidate whether these processes co-occur at the same anatomical location, and whether this happens contemporaneously or if one precedes the other.

Spatial overlap has already been considered in the 20 patients with SVD from the observational phase study³²⁹; there was no significant anatomical overlap between hotspots of ¹¹C-PK11195 signal and BBB permeability in this cohort. I will repeat this analysis in the pooled participant cohort to verify that there is no topological relationship that may have been missed in a smaller study that was not powered to detect such correlations.

Further detailed analysis of the relationship between these disease processes and conventional clinical/radiological measurements of SVD severity might be achieved by complex multivariate mediation analysis such as structured equation modelling. In this context, the underlying pathophysiological processes could be modelled as latent variables affected by cardiovascular risk factors and genotype, with outcomes based on conventional MRI metrics and neuropsychometric performance. Structural equation modelling likely requires at least 100 observations (and more if there are many degrees of freedom introduced by multiple dependent variables)⁴⁰⁶ and it may not be feasible to undertake advanced neuroimaging in enough participants to support this analysis;

however, if serum biomarkers can be found that represent CNS inflammation and BBB permeability, it would become much more tractable. Deep immunophenotyping of a further 200 participants with SVD is underway and additional studies to explore this possibility will be performed. The recruitment of a larger sample for detailed immunophenotyping will help to address the issue presented by the large number of comparisons tested in this thesis using the same reasonably small cohort of participants.

Interaction between central and peripheral inflammation

Another key outstanding mechanistic questions is to fully describe the relationship between the CNS and peripheral immune compartments. These compartments might plausibly be related in either direction, either by recruitment of peripheral bone-marrow derived myeloid cells as a response to intra-parenchymal damage and release of damage-associated molecular patterns within the CNS³⁴⁹ or by the peripheral immunophenotype responding to vascular risk factors/comorbidities to produce cytokines that affect brain homeostasis.²²⁶ Further experiments to delineate these processes further will be performed using comparative transcriptomic studies of mononuclear cells from CSF and peripheral blood already biobanked from the MINERVA trial participants to determine the origin and phenotype/behaviour of these cells.

Periventricular versus deep white matter disease

Several authors have found radiological or histological differences between deep WMHs and periventricular WMHs,⁴⁰⁷ and there are suggestions that different disease mechanisms might be responsible for their formation and progression, with the inflammatory response particularly related to WMHs in deep white matter territories.^{408,409} Data from the PET-MRI studies described in part II will allow the differential relationships between these processes and other conventional radiological hallmarks of SVD to be investigated.

MINERVA trial results and future therapeutic targets

A final significant further direction of research from this thesis is the analysis of the MINERVA trial results, which will test whether treatment with minocycline is associated with a reduction in neuroinflammation as measured by ¹¹C-PK11195 binding or BBB permeability as measured using DCE-MRI. One year follow up neuropsychometric testing and repeat MRI will allow analysis of whether this treatment has any protective or deleterious effect on SVD progression, and if so, whether the treatment response is mediated by the effect on either of these disease processes. I have secured ethical approval to continue to follow-up this cohort for six years after trial enrolment; this will involve collecting data from electronic and General Practice records in order to ascertain time to dementia (although the sample size may be too small to be able to detect a meaningful predictive effect).

The disease processes identified in this work and other studies suggest several potential novel therapeutic strategies that might be tried if treatment with minocycline is ineffective. These include cilostazol, a weak antiplatelet agent that had some beneficial effect on dependence after lacunar stroke and in combination with isosorbide mononitrate may reduce the risk of recurrent stroke or cognitive impairment²⁴⁷; cilostazol may inhibit pro-inflammatory transcription factors in microglia.⁴¹⁰ Another licensed drug that may be repurposed is colchicine, a microtubule inhibitor that is effective in reducing recurrent cardiovascular events in ischaemic heart disease^{411,412} and is currently under investigation in unselected stroke.²⁴⁹ Small molecules targeting immune cell recruitment such as CSF1R (a microglial receptor that drives proliferation) and MCP-1 (a monocyte adhesion molecule) have had promising initial results in pre-clinical studies in rodent models of SVD⁴¹³ and atheromatous disease⁴¹⁴ respectively, but are not yet licensed in human participants. Results of these studies may inform future mechanistic trials in SVD.

References

- 1 Pantoni L. Cerebral small vessel disease: from pathogenesis and clinical characteristics to therapeutic challenges. *Lancet Neurol* 2010; 9: 689–701.
- 2 Wardlaw JM, Smith C, Dichgans M. Small vessel disease: mechanisms and clinical implications. *Lancet Neurol* 2019; 4422: 1–13.
- 3 Ornello R, Degan D, Tiseo C, Di Carmine, Caterina Perciballi L, Pistoia F, Carolei A *et al.* Distribution and Temporal Trends From 1993 to 2015 of Ischemic Stroke Subtypes. A Systematic Review and Meta-Analysis. *Stroke* 2018; 49: 814–819.
- 4 Gorelick PB, Counts SE, Nyenhuis D. Vascular cognitive impairment and dementia. *Biochim Biophys Acta - Mol Basis Dis* 2016; 1862: 860–868.
- 5 Iadecola C, Duering M, Hachinski V, Joutel A, Pendlebury ST, Schneider JA *et al.* Vascular Cognitive Impairment and Dementia: JACC Scientific Expert Panel. *J. Am. Coll. Cardiol.* 2019; 73: 3326–3344.
- 6 Lo RY, Jagust WJ. Vascular burden and Alzheimer disease pathologic progression Supplemental data at www.neurology.org. *Neurology* 2012; 79: 1349–1355.
- 7 Collaborators G 2019 S. Global, regional, and national burden of stroke and its risk factors, 1990-2019: a systematic analysis for the Global Burden of Disease Study 2019. *Lancet Neurol* 2019; 29: 795–820.
- 8 Wittenberg R, Hu B, Barraza-Araiza L, Rehill A. Projections of older people with dementia and costs of dementia care in the United Kingdom, 2019–2040. 2019www.modem-dementia.org.uk (accessed 30 Jun2022).
- 9 Smith EE, Markus HS. New Treatment Approaches to Modify the Course of Cerebral Small Vessel Diseases. *Stroke* 2020; 51: 38–46.
- 10 Charidimou A, Pantoni L, Love S. The concept of sporadic cerebral small vessel disease: A road map on key definitions and current concepts. *Int J Stroke* 2016; 11: 6–18.
- 11 Thompson CS, Hakim AM. Living beyond our physiological means: Small vessel disease of the brain is an expression of a systemic failure in arteriolar function: A unifying hypothesis. *Stroke*. 2009; 40: e322–e330.
- 12 Silva GS, Koroshetz WJ, González RG, Schwamm LH. Causes of acute ischaemic stroke. In: Silva GS, Koroshetz WJ, González RG, Schwamm LH (eds). *Acute Ischemic Stroke: Imaging and Intervention*. Springer, Berlin, Germany, 2011, pp 25–42.
- 13 Greenberg SM, Bacskai BJ, Hernandez-Guillamon M, Pruzin J, Sperling R, van Veluw SJ. Cerebral amyloid angiopathy and Alzheimer disease — one peptide, two pathways. *Nat. Rev. Neurol.* 2020; 16: 30–42.
- 14 Jakel L, De Kort AM, Klijn CJM, Schreuder FHBM, Verbeek MM. Prevalence of cerebral amyloid angiopathy: A systematic review and meta-analysis. *Alzheimer's Dement* 2022; 18: 10–28.
- 15 Tanskanen M, Lindsberg PJ, Tienari PJ, Polvikoski T, Sulkava R, Verkkoniemi A *et al.* Cerebral amyloid angiopathy in a 95 + cohort: complement activation and apolipoprotein E (ApoE) genotype. *Neuropathol Appl Neurobiol* 2005; 31: 589–599.
- 16 Van Broeckhoven C, Haan J, Bakker E, Hardy JA, Van Hul W, Wehnert A *et al.* Amyloid β

- Protein Precursor Gene and Hereditary Cerebral Hemorrhage with Amyloidosis (Dutch). *Science* (80-) 1990; 248: 1120–1122.
- 17 Banerjee G, Adams ME, Jaunmuktane Z, Lammie GA, Turner B, Wani M *et al.* Early onset cerebral amyloid angiopathy following childhood exposure to cadaveric dura. *Ann Neurol* 2019; 85: 284–290.
 - 18 Liao D, Cooper L, Cai J, Toole J, Bryan N, ... GB- *et al.* The prevalence and severity of white matter lesions, their relationship with age, ethnicity, gender, and cardiovascular disease risk factors: the ARIC Study. *karger.com*<https://www.karger.com/Article/Abstract/368814> (accessed 1 Jul2022).
 - 19 Longstreth WT, Manolio TA, Arnold A, Burke GL, Bryan N, Jungreis CA *et al.* Clinical correlates of white matter findings on cranial magnetic resonance imaging of 3301 elderly people: The cardiovascular health study. *Stroke* 1996; 27: 1274–1282.
 - 20 Jeerakathil T, Wolf PA, Beiser A, Massaro J, Seshadri S, D'Agostino RB *et al.* Stroke risk profile predicts white matter hyperintensity volume: the Framingham Study. *Stroke* 2004; 35: 1857–1861.
 - 21 Basile AM, Pantoni L, Pracucci G, Asplund K, Chabriat H, Erkinjuntti T *et al.* Age, Hypertension, and Lacunar Stroke Are the Major Determinants of the Severity of Age-Related White Matter Changes. *Cerebrovasc Dis* 2006; 21: 315–322.
 - 22 Staals J, Makin SDJ, Doubal FN, Dennis MS, Wardlaw JM. Stroke subtype, vascular risk factors, and total MRI brain small-vessel disease burden. *Neurology* 2014; 83: 1228–34.
 - 23 Ikram MA, van der Lugt A, Niessen WJ, Koudstaal PJ, Krestin GP, Hofman A *et al.* The Rotterdam Scan Study: design update 2016 and main findings. *Eur J Epidemiol* 2015 3012 2015; 30: 1299–1315.
 - 24 Brundel M, Kappelle LJ, Biessels GJ. Brain imaging in type 2 diabetes. *Eur Neuropsychopharmacol* 2014; 24: 1967–1981.
 - 25 Liu J, Rutten-Jacobs L, Liu M, Markus HS, Traylor M. Causal impact of type 2 diabetes mellitus on cerebral small vessel disease: A mendelian randomization analysis. *Stroke* 2018; 49: 1325–1331.
 - 26 Warsch JRL, Wright CB. The Aging Mind: Vascular Health in Normal Cognitive Aging. *J Am Geriatr Soc* 2010; 58: S319–S324.
 - 27 Joutel A, Corpechot C, Ducros A, Vahedi K, Chabriat H, Mouton P *et al.* Notch3 mutations in CADASIL, a hereditary adult-onset condition causing stroke and dementia. *Nat* 1996 3836602 1996; 383: 707–710.
 - 28 Di Donato I, Bianchi S, De Stefano N, Dichgans M, Dotti MT, Duering M *et al.* Cerebral Autosomal Dominant Arteriopathy with Subcortical Infarcts and Leukoencephalopathy (CADASIL) as a model of small vessel disease: update on clinical, diagnostic, and management aspects. *BMC Med* 2017; 15: 1–12.
 - 29 Cho BPH, Nannoni S, Harshfield EL, Tozer D, Gra¨f S, Bell S *et al.* NOTCH3 variants are more common than expected in the general population and associated with stroke and vascular dementia: an analysis of 200 000 participants. *J Neurol Neurosurg Psychiatry* 2021; 92: 694–701.
 - 30 Dichgans M, Mayer M, Uttner I, Brüning R, Müller-Höcker J, Rungger G *et al.* The phenotypic spectrum of CADASIL: Clinical findings in 102 cases. *Ann Neurol* 1998; 44: 731–739.

- 31 Donnan GA, Norrving B. Lacunes and lacunar syndromes. In: *Handbook of Clinical Neurology*. Elsevier, 2008, pp 559–575.
- 32 Camps-Renom P, Delgado-Mederos R, Martínez-Domeño A, Prats-Sánchez L, Cortés-Vicente E, Simón-Talero M *et al*. Clinical characteristics and outcome of the capsular warning syndrome: A multicenter study. *Int J Stroke* 2015; 10: 571–575.
- 33 Nadarajan V, Adesina T. Capsular warning syndrome. *BMJ Case Rep* 2013. doi:10.1136/bcr-2013-010503.
- 34 Gorelick PB, Scuteri A, Black SE, DeCarli C, Greenberg SM, Iadecola C *et al*. Vascular Contributions to Cognitive Impairment and Dementia: A Statement for Healthcare Professionals From the American Heart Association/American Stroke Association. *Stroke* 2011; 42: 2672.
- 35 Skrobot OA, Love S, Kehoe PG, O’Brien J, Black S, Chen C *et al*. The Vascular Impairment of Cognition Classification Consensus Study. *Alzheimers Dement* 2017; 13: 624–633.
- 36 Román GC, Tatemichi TK, Erkinjuntti T, Cummings JL, Masdeu JC, Garcia JH *et al*. Vascular dementia: Diagnostic criteria for research studies: Report of the ninds-airen international workshop*. *Neurology* 1993; 43: 250–260.
- 37 Hachinski VC, Lassen NA, Marshall J. Multi-infarct dementia. A cause of mental deterioration in the elderly. *Lancet (London, England)* 1974; 2: 207–209.
- 38 Wardlaw JM, Smith C, Dichgans M. Small vessel disease: mechanisms and clinical implications. *Lancet Neurol* 2019. doi:10.1016/S1474-4422(19)30079-1.
- 39 Lawrence AJ, Patel B, Morris RG, MacKinnon AD, Rich PM, Barrick TR *et al*. Mechanisms of Cognitive Impairment in Cerebral Small Vessel Disease: Multimodal MRI Results from the St George’s Cognition and Neuroimaging in Stroke (SCANS) Study. *PLoS One* 2013; 8. doi:10.1371/journal.pone.0061014.
- 40 Zhou A, Jia J. Different cognitive profiles between mild cognitive impairment due to cerebral small vessel disease and mild cognitive impairment of Alzheimer’s disease origin. *J Int Neuropsychol Soc* 2009; 15: 898–905.
- 41 Lawrence AJ, Brookes RL, Zeestraten EA, Barrick TR, Morris RG, Markus HS. Pattern and rate of cognitive decline in cerebral small vessel disease: A prospective study. *PLoS One* 2015; 10. doi:10.1371/JOURNAL.PONE.0135523.
- 42 Godin O, Dufouil C, Maillard P, Delcroix N, Mazoyer B, Crivello F *et al*. White Matter Lesions as a Predictor of Depression in the Elderly: The 3C-Dijon Study. *Biol Psychiatry* 2008; 63: 663–669.
- 43 Taylor WD, Aizenstein HJ, Alexopoulos GS. The vascular depression hypothesis: mechanisms linking vascular disease with depression. *Mol Psychiatry* 2013 189 2013; 18: 963–974.
- 44 Lohner V, Brookes RL, Hollocks MJ, Morris RG, Markus HS. Apathy, but not depression, is associated with executive dysfunction in cerebral small vessel disease. *PLoS One* 2017; 12. doi:10.1371/JOURNAL.PONE.0176943.
- 45 Tay J, Lisiecka-Ford DM, Hollocks MJ, Tuladhar AM, Barrick TR, Forster A *et al*. Network neuroscience of apathy in cerebrovascular disease. *Prog Neurobiol* 2020; 188: 1–12.
- 46 Tay J, Morris RG, Tuladhar AM, Husain M, De Leeuw FE, Markus HS. Apathy, but not depression, predicts all-cause dementia in cerebral small vessel disease. *J Neurol Neurosurg Psychiatry* 2020; 91: 953–959.

- 47 Starr JM, Leaper SA, Murray AD, Lemmon HA, Staff RT, Deary IJ *et al.* Brain white matter lesions detected by magnetic resonance imaging are associated with balance and gait speed. *J Neurol Neurosurg Psychiatry* 2003; 74: 94–98.
- 48 Cavallari M, Moscufo N, Skudlarski P, Meier D, Panzer VP, Pearlson GD *et al.* Mobility impairment is associated with reduced microstructural integrity of the inferior and superior cerebellar peduncles in elderly with no clinical signs of cerebellar dysfunction. *NeuroImage Clin* 2013; 2: 332–40.
- 49 De Laat KF, Tuladhar AM, Van Norden AGW, Norris DG, Zwiers MP, De Leeuw FE. Loss of white matter integrity is associated with gait disorders in cerebral small vessel disease. *Brain* 2011; 134: 73–83.
- 50 Callisaya M, Beare R, Phan T, Blizzard L, Thrift A, Chen J *et al.* Brain Structural Change and Gait Decline: A Longitudinal Population-Based Study. *J Am Geriatr Soc* 2013; 61: 1074–1079.
- 51 Moscufo N, Wolfson L, Meier D, Liguori M, Hildenbrand PG, Wakefield D *et al.* Mobility decline in the elderly relates to lesion accrual in the splenium of the corpus callosum. *Age (Omaha)* 2011; 34: 405–414.
- 52 Srikanth V, Phan TG, Chen J, Beare R, Stapleton JM, Reutens DC. The location of white matter lesions and gait-A voxel-based study. *Ann Neurol* 2010; 67: 265–269.
- 53 Baezner H, Hennerici M. From trepidant abasia to motor network failure—gait disorders as a consequence of subcortical vascular encephalopathy (SVE): Review of historical and contemporary concepts. *J Neurol Sci* 2005; 229–230: 81–88.
- 54 Van Zagten M, Lodder J, Kessels F. Gait disorder and parkinsonian signs in patients with stroke related to small deep infarcts and white matter lesions. *Mov Disord* 1998; 13: 89–95.
- 55 Zijlmans JCM, Daniel SE, Hughes AJ, Révész T, Lees AJ. Clinicopathological investigation of vascular parkinsonism, including clinical criteria for diagnosis. *Mov Disord* 2004; 19: 630–640.
- 56 Duering M, Biessels GJ, Brodtmann A, Chen C, Cordonnier C, de Leeuw FE *et al.* Neuroimaging standards for research into small vessel disease—advances since 2013. *Lancet Neurol* 2023; 22: 602–618.
- 57 Duering M, Biessels GJ, Brodtmann A, Chen C, Cordonnier C, de Leeuw FE *et al.* Neuroimaging standards for research into small vessel disease—advances since 2013. *Lancet Neurol* 2023; 22: 602–618.
- 58 Harteveld AA, De Cocker LJJ, Dieleman N, van der Kolk AG, Zwanenburg JJM, Robe PA *et al.* High-Resolution Postcontrast Time-of-Flight MR Angiography of Intracranial Perforators at 7.0 Tesla. *PLoS One* 2015; 10: e0121051.
- 59 Koch S, McClendon MS, Bhatia R. Imaging evolution of acute lacunar infarction: Leukoariosis or lacune? *Neurology* 2011; 77: 1091–1095.
- 60 Moreau F, Patel S, Lauzon ML, McCreary CR, Goyal M, Frayne R *et al.* Cavitation after acute symptomatic lacunar stroke depends on time, location, and MRI sequence. *Stroke* 2012; 43: 1837–1842.
- 61 Gesierich B, Duchesnay E, Jouvent E, Chabriat H, Schmidt R, Mangin JF *et al.* Features and Determinants of Lacune Shape: Relationship With Fiber Tracts and Perforating Arteries. *Stroke* 2016; 47: 1258–1264.
- 62 Duering M, Csanadi E, Gesierich B, Jouvent E, Herve D, Seiler S *et al.* Incident lacunes

- preferentially localize to the edge of white matter hyperintensities: insights into the pathophysiology of cerebral small vessel disease. *Brain* 2013; 136: 2717–2726.
- 63 del C. Valdés Hernández M, Maconick LC, Muñoz Maniega S, Wang X, Wiseman S, Armitage PA *et al.* A Comparison of Location of Acute Symptomatic vs. ‘Silent’ Small Vessel Lesions. *Int J Stroke* 2015; 10: 1044–1050.
- 64 Chen X, Wen W, Anstey KJ, Sachdev PS. Prevalence, incidence, and risk factors of lacunar infarcts in a community sample. *Neurology* 2009; 73: 266–272.
- 65 Wardlaw JM, DeBette S, Jokinen H, De Leeuw FE, Pantoni L, Chabriat H *et al.* ESO Guideline on covert cerebral small vessel disease. *Eur Stroke J* 2021; 6: CXI–CLXII.
- 66 Jokinen H, Gouw AA, Madureira S, Ylikoski R, Van Straaten ECW, Van Der Flier WM *et al.* Incident lacunes influence cognitive decline. *Neurology* 2011; 76: 1872–1878.
- 67 Fernando J, Brown RB, Edwards H, Egle M, Markus HS, Tay J. Individual markers of cerebral small vessel disease and domain-specific quality of life deficits. *Brain Behav* 2021; 11: 1–7.
- 68 Wardlaw JM, Smith EE, Biessels GJ, Cordonnier C, Fazekas F, Frayne R *et al.* Neuroimaging standards for research into small vessel disease and its contribution to ageing and neurodegeneration. *Lancet Neurol* 2013; 12: 822–838.
- 69 DeBette S, Schilling S, Duperron M-G, Larsson SC, Markus HS. Clinical Significance of Magnetic Resonance Imaging Markers of Vascular Brain Injury. *JAMA Neurol* 2018; 76: 81–94.
- 70 Gouw AA, van der Flier WM, van Straaten EC., Pantoni L, Bastos-Leite AJ, Inzitari D *et al.* Reliability and Sensitivity of Visual Scales versus Volumetry for Evaluating White Matter Hyperintensity Progression. *Cerebrovasc Dis* 2008; 25: 247–253.
- 71 Fazekas F, Chawluk JB, Alavi A, Hurtig HI, Zimmerman RA. MR signal abnormalities at 1.5 T in Alzheimer’s dementia and normal aging. *Am J Roentgenol* 1987; 149: 351–356.
- 72 Gouw AA, Van Der Flier WM, Van Straaten ECW, Barkhof F, Ferro JM, Baezner H *et al.* Simple versus complex assessment of white matter hyperintensities in relation to physical performance and cognition: The LADIS study. *J Neurol* 2006; 253: 1189–1196.
- 73 Maillard P, Carmichael O, Harvey D, Fletcher E, Reed B, Mungas D *et al.* FLAIR and Diffusion MRI Signals Are Independent Predictors of. *Am J Neuroradiol* 2013; 34: 54–61.
- 74 Fernando MS, Simpson JE, Matthews F, Brayne C, Lewis CE, Barber R *et al.* White matter lesions in an unselected cohort of the elderly: Molecular pathology suggests origin from chronic hypoperfusion injury. *Stroke* 2006; 37: 1391–1398.
- 75 Gouw AA, Seewann A, Van Der Flier WM, Barkhof F, Rozemuller AM, Scheltens P *et al.* Heterogeneity of small vessel disease: A systematic review of MRI and histopathology correlations. *J Neurol Neurosurg Psychiatry* 2011; 82: 126–135.
- 76 Wardlaw JM, Valdés Hernández MC, Muñoz-Maniega S. What are white matter hyperintensities made of? Relevance to vascular cognitive impairment. *J Am Heart Assoc* 2015; 4: 1–19.
- 77 Black S, Gao F, Bilbao J. Understanding White Matter Disease. *Stroke* 2009; 40: S48–S52.
- 78 Habes M, Erus G, Toledo J, Zhang T, Bryan N, Launer L *et al.* White matter hyperintensities and imaging patterns of brain ageing in the general population. *Brain* 2016; 139: 1164–1179.

- 79 Smith SM, Douaud G, Chen W, Hanayik T, Alfaro-Almagro F, Sharp K *et al.* An expanded set of genome-wide association studies of brain imaging phenotypes in UK Biobank. *Nat Neurosci* 2021; 24: 737–745.
- 80 DeCarli C, Fletcher E, Ramey V, Harvey D, Jagust WJ. Anatomical Mapping of White Matter Hyperintensities (WMH). *Stroke* 2005; 36: 50–55.
- 81 Blanco PJ, Müller LO, Spence JD. Blood pressure gradients in cerebral arteries: A clue to pathogenesis of cerebral small vessel disease. *Stroke Vasc Neurol* 2017; 2: 108–117.
- 82 van der Veen PH, Muller M, Vincken KL, Hendrikse J, Mali WPTM, van der Graaf Y *et al.* Longitudinal Relationship Between Cerebral Small-Vessel Disease and Cerebral Blood Flow: The Second Manifestations of Arterial Disease-Magnetic Resonance Study. *Stroke* 2015; 46: 1233–1238.
- 83 Firbank MJ, Wiseman RM, Burton EJ, Saxby BK, O'Brien JT, Ford GA. Brain atrophy and white matter hyperintensity change in older adults and relationship to blood pressure: Brain atrophy, WMH change and blood pressure. *J Neurol* 2007; 254: 713–721.
- 84 Sachdev P, Wen W, Chen X, Brodaty H. Progression of white matter hyperintensities in elderly individuals over 3 years. *Neurology* 2007; 68: 214–222.
- 85 Pico F, Dufouil C, Lévy C, Besançon V, De Kersaint-Gilly A, Bonithon-Kopp C *et al.* Longitudinal Study of Carotid Atherosclerosis and White Matter Hyperintensities: The EVA-MRI Cohort. *Cerebrovasc Dis* 2002; 14: 109–115.
- 86 Armstrong NJ, Mather KA, Sargurupremraj M, Knol MJ, Malik R, Satizabal CL *et al.* Common genetic variation indicates separate causes for periventricular and deep white matter hyperintensities. *Stroke* 2020; 51: 2112–2121.
- 87 Gottesman RF, Coresh J, Catellier DJ, Sharrett R, Rose KM, Coker LH *et al.* Blood pressure and white matter disease progression in a biethnic cohort: the Atherosclerosis Risk in Communities (ARIC) study. *Stroke* 2010; 41: 3–8.
- 88 Godin O, Dufouil C, Maillard P, Delcroix N, Mazoyer B, Crivello F *et al.* White Matter Lesions as a Predictor of Depression in the Elderly: The 3C-Dijon Study. *Neurology* 2013; 73: 687–694.
- 89 Maillard P, Fletcher E, Lockhart SN, Roach AE, Reed B, Mungas D *et al.* White matter hyperintensities and their penumbra lie along a continuum of injury in the aging brain. *Stroke* 2014; 45: 1721–1726.
- 90 Bellenguez C, Küçükali F, Jansen IE, Kleindam L, Moreno-Grau S, Amin N *et al.* New insights into the genetic etiology of Alzheimer's disease and related dementias. *Nat Genet* 2022; 54: 412–436.
- 91 Promjunyakul N, Lahna D, Kaye JA, Dodge HH, Erten-Lyons D, Rooney WD *et al.* Characterizing the white matter hyperintensity penumbra with cerebral blood flow measures. *NeuroImage Clin* 2015; 8: 224–229.
- 92 Promjunyakul N, Dodge HH, Lahna D, Boespflug EL, Kaye JA, Rooney WD *et al.* Baseline NAWM structural integrity and CBF predict periventricular WMH expansion over time. *Neurology* 2018; 90: e2119–e2126.
- 93 Wardlaw JM, Chappell FM, Valdés Hernández MDC, Makin SDJ, Staals J, Shuler K *et al.* White matter hyperintensity reduction and outcomes after minor stroke. *Neurology* 2017; 89: 1003–1010.

- 94 Jochems ACC, Arteaga C, Chappell F, Ritakari T, Hooley M, Doubal F *et al.* Longitudinal Changes of White Matter Hyperintensities in Sporadic Small Vessel Disease: A Systematic Review and Meta-analysis. *Neurology* 2022; 99: E2454–E2463.
- 95 Shoamanesh A, Kwok CS, Benavente O. Cerebral microbleeds: Histopathological correlation of neuroimaging. *Cerebrovasc Dis* 2011; 32: 528–534.
- 96 Greenberg SM, Vernooij MW, Cordonnier C, Viswanathan A, Al-Shahi Salman R, Warach S *et al.* Cerebral microbleeds: a guide to detection and interpretation. *Lancet Neurol* 2009; 8: 165–174.
- 97 Charidimou A, Boulouis G, Frosch MP, Baron J-C, Pasi M, Albucher JF *et al.* The Boston criteria version 2.0 for cerebral amyloid angiopathy: a multicentre, retrospective, MRI–neuropathology diagnostic accuracy study. *Lancet Neurol* 2022; 21: 714–725.
- 98 Nylander R, Fahlström M, Rostrup E, Kullberg J, Damangir S, Ahlström H *et al.* Quantitative and qualitative MRI evaluation of cerebral small vessel disease in an elderly population: a longitudinal study. *Acta radiol* 2018; 59: 612–618.
- 99 Smith EE, Charidimou A, Ayata C, Werring DJ, Greenberg SM. Cerebral Amyloid Angiopathy–Related Transient Focal Neurologic Episodes. *Neurology* 2021; 97: 231–238.
- 100 Li L, Wu D-H, Li H-Q, Tan L, Xu W, Dong Q *et al.* Association of Cerebral Microbleeds with Cognitive Decline: A Longitudinal Study. *J Alzheimer's Dis* 2020; 75: 1–9.
- 101 Werring DJ, Frazer DW, Coward LJ, Losseff NA, Watt H, Cipolotti L *et al.* Cognitive dysfunction in patients with cerebral microbleeds on T2*-weighted gradient-echo MRI. *Brain* 2004; 127: 2265–2275.
- 102 Nannoni S, Ohlmeier L, Brown RB, Morris RG, MacKinnon AD, Markus HS. Cognitive impact of cerebral microbleeds in patients with symptomatic small vessel disease. *Int J Stroke* 2022; 17: 415–424.
- 103 Gregoire SM, Scheffler G, Jäger HR, Yousry TA, Brown MM, Kallis C *et al.* Strictly lobar microbleeds are associated with executive impairment in patients with ischemic stroke or transient ischemic attack. *Stroke* 2013; 44: 1267–1272.
- 104 Wardlaw JM, Benveniste H, Nedergaard M, Zlokovic B V., Mestre H, Lee H *et al.* Perivascular spaces in the brain: anatomy, physiology and pathology. *Nat Rev Neurol* 2020 163 2020; 16: 137–153.
- 105 Weller RO, Hawkes CA, Kalaria RN, Werring DJ, Carare RO. White Matter Changes in Dementia: Role of Impaired Drainage of Interstitial Fluid. *Brain Pathol* 2015; 25: 63–78.
- 106 Benjamin P, Trippier S, Lawrence AJ, Lambert C, Zeestraten E, Williams OA *et al.* Lacunar infarcts, but not perivascular spaces, are predictors of cognitive decline in cerebral small-vessel disease. *Stroke* 2018; 49: 586–593.
- 107 Bouvy WH, Zwanenburg JJM, Reinink R, Wisse LEM, Luijten PR, Kappelle LJ *et al.* Perivascular spaces on 7 Tesla brain MRI are related to markers of small vessel disease but not to age or cardiovascular risk factors. *J Cereb Blood Flow Metab* 2016; 36: 1708–1717.
- 108 Del Brutto OH, Mera RM. Enlarged perivascular spaces in the basal ganglia are independently associated with intracranial atherosclerosis in the elderly. *Atherosclerosis* 2017; 267: 34–38.
- 109 Best JG, Barbato C, Ambler G, Du H, Banerjee G, Wilson D *et al.* Association of enlarged perivascular spaces and anticoagulant-related intracranial hemorrhage. *Neurology* 2020; 95: E2192–E2199.

- 110 Carare RO, Bernardes-Silva M, Newman TA, Page AM, Nicoll JAR, Perry VH *et al.* Solutes, but not cells, drain from the brain parenchyma along basement membranes of capillaries and arteries: significance for cerebral amyloid angiopathy and neuroimmunology. *Neuropathol Appl Neurobiol* 2008; 34: 131–144.
- 111 Pizzo ME, Wolak DJ, Kumar NN, Brunette E, Brunnuquell CL, Hannocks MJ *et al.* Intrathecal antibody distribution in the rat brain: surface diffusion, perivascular transport and osmotic enhancement of delivery. *J Physiol* 2018; 596: 445–475.
- 112 Asgari M, De Zélicourt D, Kurtcuoglu V. Glymphatic solute transport does not require bulk flow. *Sci Reports* 2016 61 2016; 6: 1–11.
- 113 Hladky SB, Barrand MA. Elimination of substances from the brain parenchyma: Efflux via perivascular pathways and via the blood-brain barrier 11 Medical and Health Sciences 1109 Neurosciences. *Fluids Barriers CNS*. 2018; 15: 1–73.
- 114 Bown CW, Carare RO, Schrag MS, Jefferson AL. Physiology and Clinical Relevance of Enlarged Perivascular Spaces in the Aging Brain. *Neurology* 2022; 98: 107–117.
- 115 Ding J, Sigurdsson S, Jonsson P V, Eiriksdottir G, Charidimou A, Lopez OL *et al.* Large MRI-visible perivascular spaces, cerebral small vessel disease progression and risk of dementia: the AGES-Reykjavik Study. *JAMA Neurol* 2017; 74: 1105–1112.
- 116 Arba F, Quinn TJ, Hankey GJ, Lees KR, Wardlaw JM, Ali M *et al.* Enlarged perivascular spaces and cognitive impairment after stroke and transient ischemic attack. *Int J Stroke* 2018; 13: 47–56.
- 117 Hurford R, Charidimou A, Fox Z, Cipolotti L, Jager R, Werring DJ. MRI-visible perivascular spaces: Relationship to cognition and small vessel disease MRI markers in ischaemic stroke and TIA. *J Neurol Neurosurg Psychiatry* 2014; 85: 522–525.
- 118 Scheltens P, Kuiper M, Ch Wolters E, Barkhof F, Valk J, Weinstein HC *et al.* Atrophy of medial temporal lobes on MRI in ‘probable’ Alzheimer’s disease and normal ageing: diagnostic value and neuropsychological correlates. *J Neurol Neurosurg Psychiatry* 1992; 55: 967.
- 119 Habes M, Sotiras A, Erus G, Toledo JB, Janowitz D, Wolk DA *et al.* White matter lesions spatial heterogeneity, links to risk factors, cognition, genetics, and atrophy. *Neurology* 2018; 91: E964–E975.
- 120 Godin O, Tzourio C, Maillard P, Alperovitch A, Mazoyer B, Dufouil C. Apolipoprotein E genotype is related to progression of white matter lesion load. *Stroke* 2009; 40: 3186–3190.
- 121 Kloppenborg RP, Geerlings MI, Visseren FL, Nederkoorn PJ. Homocysteine and progression of generalized small-vessel disease. The SMART-MR Study. *Neurology* 2014; 82: 777–783.
- 122 Jokinen H, Scheltens P, Inzitari D, Wallin A, Madureira S, Verdelho A *et al.* White Matter Lesion Progression in LADIS. *Stroke* 2012; 43: 2643–2647.
- 123 Aribisala BS, Valdés Hernández MC, Royle NA, Morris Z, Muñoz Maniega S, Bastin ME *et al.* Brain atrophy associations with white matter lesions in the ageing brain: The Lothian Birth Cohort 1936. *Eur Radiol* 2013; 23: 1084–1092.
- 124 Shi Y, Wardlaw JM. Update on cerebral small vessel disease: a dynamic whole-brain disease. *Stroke Vasc Neurol* 2016; 1: 83–92.
- 125 Blair GW, Maria Valdez Hernandez M, Thrippleton MJ, Doubal FN, Wardlaw JM. Advanced Neuroimaging of Cerebral Small Vessel Disease. *Curr Treat Options Cardio Med* 1936; 19: 56.
- 126 Sen PN, Basser PJ. A Model for Diffusion in White Matter in the Brain. *Biophys J* 2005; 89:

- 2927–2938.
- 127 Tuladhar AM, van Norden AGW, de Laat KF, Zwiers MP, van Dijk EJ, Norris DG *et al.* White matter integrity in small vessel disease is related to cognition. *NeuroImage Clin* 2015; 7: 518–524.
- 128 Zeestraten EA, Lawrence AJ, Lambert C, Benjamin P, Brookes RL, Mackinnon AD *et al.* Change in multimodal MRI markers predicts dementia risk in cerebral small vessel disease. *Neurology* 2017; 89: 1869–1876.
- 129 Vernooij MW, Ikram MA, Vrooman HA, Wielopolski PA, Krestin GP, Hofman A *et al.* White Matter Microstructural Integrity and Cognitive Function in a General Elderly Population. *Arch Gen Psychiatry* 2009; 66: 545–553.
- 130 Croall ID, Lohner V, Moynihan B, Khan U, Hassan A, O'brien JT *et al.* Using DTI to assess white matter microstructure in cerebral small vessel disease (SVD) in multicentre studies. *Clin Sci* 2017; 131: 1361–1373.
- 131 Egle M, Hilal S, Tuladhar AM, Pirpamer L, Hofer E, Duering M *et al.* Prediction of dementia using diffusion tensor MRI measures: the OPTIMAL collaboration. *J Neurol Neurosurg Psychiatry* 2022; 93: 14–23.
- 132 Van Veluw SJ, Zwanenburg JJM, Engelen-Lee J, Spliet WGM, Hendrikse J, Luijten PR *et al.* In vivo detection of cerebral cortical microinfarcts with high-resolution 7T MRI. *J Cereb Blood Flow Metab* 2013; 33: 322–329.
- 133 Zwartbol MHT, Rissanen I, Ghaznawi R, de Bresser J, Kuijf HJ, Blom K *et al.* Cortical cerebral microinfarcts on 7T MRI: Risk factors, neuroimaging correlates and cognitive functioning – The Medea-7T study. *J Cereb Blood Flow Metab* 2021; 41: 3127–3138.
- 134 van den Brink H, Ferro DA, Bresser J de, Bron EE, Onkenhout LP, Kappelle LJ *et al.* Cerebral cortical microinfarcts in patients with internal carotid artery occlusion. *J Cereb Blood Flow Metab* 2021; 41: 2690–2698.
- 135 Smith EE, Greenberg SM. β -Amyloid, blood vessels, and brain function. *Stroke* 2009; 40: 2601–2606.
- 136 Van Veluw SJ, Shih AY, Smith EE, Chen C, Schneider JA, Wardlaw JM *et al.* Detection, risk factors, and functional consequences of cerebral microinfarcts HHS Public Access. *Lancet Neurol* 2017; 16: 730–740.
- 137 Hilal S, Baaij LGA, De Groot M, Niessen WJ, Kamran Ikram M, Ikram A *et al.* Prevalence and clinical relevance of diffusion-weighted imaging lesions: The Rotterdam study. *Neurology* 2019; 93: e1058–e1067.
- 138 Ii Y, Ishikawa H, Shindo A, Matsuyama H, Matsuura K, Matsuda K *et al.* Association between cortical microinfarcts and total small vessel disease burden in cerebral amyloid angiopathy on 3-Tesla magnetic resonance imaging. *Eur J Neurol* 2021; 28: 794–799.
- 139 Sadaghiani S, Dolui S, Tisdall DM, Tackett W, Wolk DA, Detre JA. Associations between cortical microinfarcts and MRI markers of neurodegeneration and cerebrovascular disease in aging. *Alzheimer's Dement* 2021; 17: 1–3.
- 140 Kapasi A, Leurgans SE, Arvanitakis Z, Barnes LL, Bennett DA, Schneider JA. $A\beta$ (Amyloid Beta) and Tau Tangle Pathology Modifies the Association between Small Vessel Disease and Cortical Microinfarcts. *Stroke* 2021; : 1012–1021.
- 141 Ter Telgte A, Wiegertjes K, Gesierich B, Baskaran BS, Marques JP, Kuijf HJ *et al.* Temporal

- Dynamics of Cortical Microinfarcts in Cerebral Small Vessel Disease. *JAMA Neurol* 2020; 77: 643–647.
- 142 Rudilosso S, Chui E, Stringer MS, Thrippleton M, Chappell F, Blair GW *et al.* Prevalence and Significance of the Vessel-Cluster Sign on Susceptibility-Weighted Imaging in Patients With Severe Small Vessel Disease. *Neurology* 2022; 99: E440–E452.
- 143 Ferrand J. *Essai sur l'hémiplégie des vieillards, les lacunes de désintégration cérébrale.* Hachette Livre, 1902.
- 144 Miller Fisher C. Lacunes: Small, deep cerebral infarcts. *Neurology* 1965; 15: 774–784.
- 145 Fisher CM. The Arterial Lesions Underlying Lacunes*. 1969.
- 146 Fisher CM. Lacunar strokes and infarcts: A review. *Neurology* 1982; 32: 871–876.
- 147 Masuda J, Tanaka K, Omae T, Ueda K, Sadoshima S. Cerebrovascular diseases and their underlying vascular lesions in hisayama, japan—A pathological study of autopsy cases. *Stroke* 1983; 14: 934–940.
- 148 Bailey EL, Smith C, Sudlow CLM, Wardlaw JM. Pathology of Lacunar Ischemic Stroke in Humans—A Systematic Review. *Brain Pathol* 2012; 22: 583–591.
- 149 Blevins BL, Harry ·, Vinters V, Love S, Wilcock DM, Lea · *et al.* Brain arteriolosclerosis. *Acta Neuropathol* 2021; 141: 1–24.
- 150 Kuwabara Y, Ichiya Y, Sasaki M, Yoshida T, Fukumura T, Masuda K *et al.* Cerebral blood flow and vascular response to hypercapnia in hypertensive patients with leukoaraiosis. *Ann Nucl Med* 1996 103 1996; 10: 293–298.
- 151 Sun Y, Cao W, Ding W, Wang Y, Han X, Zhou Y *et al.* Cerebral blood flow alterations as assessed by 3D ASL in cognitive impairment in patients with subcortical vascular cognitive impairment: A marker for disease severity. *Front Aging Neurosci* 2016; 8: 211.
- 152 Jochemsen HM, Muller M, Bots ML, Scheltens P, Vincken KL, Mali WPTM *et al.* Arterial stiffness and progression of structural brain changes: The SMART-MR study. *Neurology* 2015; 84: 448–455.
- 153 Lee W, Jung K, Ryu Y, Lee K, Kim J, Lee S *et al.* Progression of Cerebral White Matter Hyperintensities and the Associated Sonographic Index. *Radiology* 2017; 284: 824–833.
- 154 Maeda H, Matsumoto M, Handa N, Hougaku H, Ogawa S, Itoh T *et al.* Reactivity of Cerebral Blood Flow to Carbon Dioxide in Various Types of Ischemic Cerebrovascular Disease: Evaluation by the Transcranial Doppler Method. *Stroke* 1993; 24: 670–675.
- 155 Bernbaum M, Menon BK, Fick G, Smith EE, Goyal M, Frayne R *et al.* Reduced blood flow in normal white matter predicts development of leukoaraiosis. *J Cereb Blood Flow Metab* 2015; 35: 1610–1615.
- 156 Promjunyakul N, Lahna D, Kaye JA, Dodge HH, Erten-Lyons D, Rooney WD *et al.* Characterizing the white matter hyperintensity penumbra with cerebral blood flow measures. *NeuroImage Clin* 2015; 8: 224–229.
- 157 Shi Y, Thrippleton MJ, Makin SD, Marshall I, Geerlings MI, De Craen AJM *et al.* Cerebral blood flow in small vessel disease: A systematic review and meta-analysis. *J Cereb Blood Flow Metab* 2016; 36: 1653–1667.
- 158 Brown WR, Moody DM, Challa VR, Thore CR, Anstrom JA. Venous collagenosis and arteriolar tortuosity in leukoaraiosis. *J Neurol Sci* 2002; 203–204: 159–163.

- 159 Shaaban CE, Aizenstein HJ, Jorgensen DR, MacCloud RL, Meckes NA, Erickson KI *et al.* In Vivo Imaging of Venous Side Cerebral Small-Vessel Disease in Older Adults: An MRI Method at 7T. *Am J Neuroradiol* 2017; 38: 1923–1928.
- 160 Kester M, Goos J, Teunissen C, Benedictus M, Bouwman F, Wattjes M *et al.* Associations Between Cerebral Small-Vessel Disease and Alzheimer Disease Pathology as Measured by Cerebrospinal Fluid Biomarkers. *JAMA Neurol* 2014; 71: 855.
- 161 Kress BT, Iliff JJ, Xia M, Wang M, Wei Bs HS, Zeppenfeld D *et al.* Impairment of paravascular clearance pathways in the aging brain. *Ann Neurol* 2014; 76: 845–861.
- 162 Lodder J, Bamford JM, Sandercock PAG, Jones LN, Warlow CP. Are hypertension or cardiac embolism likely causes of lacunar infarction? *Stroke* 1990; 21: 375–381.
- 163 Breteler MMB, Van Gijn J, Witteman JCM, Oudkerk M, Hofman A, De Groot JC *et al.* A follow-up study of blood pressure and cerebral white matter lesions. *Ann Neurol* 2004; 46: 827–833.
- 164 Ammirati E, Moroni F, Magnoni M, Rocca MA, Anzalone N, Cacciaguerra L *et al.* Progression of brain white matter hyperintensities in asymptomatic patients with carotid atherosclerotic plaques and no indication for revascularization. *Atherosclerosis* 2019; 287: 171–178.
- 165 Van Veluw SJ, Hilal S, Kuijf HJ, Ikram MK, Xin X, Yeow TB *et al.* Cortical microinfarcts on 3T MRI: Clinical correlates in memory-clinic patients. *Alzheimers Dement* 2015; 11: 1500–1509.
- 166 Dufouil C, Chalmers J, Coskun O, Besançon V, Bousser M-G, Guillon P *et al.* Effects of Blood Pressure Lowering on Cerebral White Matter Hyperintensities in Patients With Stroke. *Circulation* 2005; 112: 1644–1650.
- 167 ten Dam VH, van Buchem MA, Westendorp RGJ, Ford I, de Craen AJM, van den Heuvel DMJ *et al.* Effect of pravastatin on cerebral infarcts and white matter lesions. *Neurology* 2006; 64: 1807–1809.
- 168 Peila R, Rodriguez BL, Launer LJ. Type 2 Diabetes, APOE Gene, and the Risk for Dementia and Related Pathologies The Honolulu-Asia Aging Study. *Diabetes* 2002; 51: 1256–1262.
- 169 Luo X, Jiaerken Y, Yu X, Huang P, Qiu T, Jia Y *et al.* Associations between APOE genotype and cerebral small-vessel disease: A longitudinal study. *Oncotarget* 2017; 8: 44477–44489.
- 170 Cox SR, Ritchie SJ, Dickie DA, Pattie A, Royle NA, Corley J *et al.* Interaction of APOE e4 and poor glycemic control predicts white matter hyperintensity growth from 73 to 76. *Neurobiol Aging* 2017; 54: 54–58.
- 171 Wang R, Fratiglioni L, Laukka E, Lovden M, Kalpouzos G, Keller L *et al.* Effects of vascular risk factors and APOE 4 on white matter integrity and cognitive decline. *Neurology* 2015; 84: 1–8.
- 172 Visscher PM, Wray NR, Zhang Q, Sklar P, McCarthy MI, Brown MA *et al.* 10 Years of GWAS Discovery: Biology, Function, and Translation. *Am J Hum Genet* 2017; 101: 5–22.
- 173 Choi SW, Mak TSH, O'Reilly PF. Tutorial: a guide to performing polygenic risk score analyses. *Nat Protoc* 2020 159 2020; 15: 2759–2772.
- 174 Traylor M, Malik R, Nalls MA, Cotlarciuc I, Radmanesh F, Thorleifsson G *et al.* Genetic variation at 16q24.2 is associated with small vessel stroke. *Ann Neurol* 2017; 81: 383–394.
- 175 Traylor M, Persyn E, Tomppo L, Klasson S, Abedi V, Bakker MK *et al.* Genetic basis of lacunar stroke: a pooled analysis of individual patient data and genome-wide association

- studies. *Lancet Neurol* 2021; 20: 351–61.
- 176 Traylor M, Zhang CR, Adib-Samii P, Devan WJ, Parsons OE, Lanfranconi S *et al.* Genome-wide meta-analysis of cerebral white matter hyperintensities in patients with stroke. *Neurology* 2016; 86: 146–53.
- 177 Traylor M, Tozer DJ, Croall ID, Lisiecka Ford DM, Olorunda AO, Boncoraglio G *et al.* Genetic variation in PLEKHG1 is associated with white matter hyperintensities (n = 11,226). *Neurology* 2019; 92: e749–e757.
- 178 Persyn E, Hanscombe KB, Howson JMM, Lewis CM, Traylor M, Markus HS. Genome-wide association study of MRI markers of cerebral small vessel disease in 42,310 participants. *Nat Commun* 2020; 11: 1–12.
- 179 Knol MJ, Lu D, Traylor M, Adams HHH, Romero JRJ, Smith A V. *et al.* Association of common genetic variants with brain microbleeds. *Neurology* 2020; 95: e3331–e3343.
- 180 Debette S, Duperron M-G, Knol M, Le Grand Q, Evans T, Konuma T *et al.* Genomics of perivascular space burden unravels early mechanisms of cerebral small vessel disease. *Res Sq* 2021; : doi: 10.21203/rs.3.rs-963149/v1.
- 181 Dubois B, Villain N, Frisoni GB, Rabinovici GD, Sabbagh M, Cappa S *et al.* Clinical diagnosis of Alzheimer’s disease: recommendations of the International Working Group. *Lancet Neurol* 2021; 20: 484–496.
- 182 Janelidze S, Mattsson N, Stomrud E, Lindberg O, Palmqvist S, Zetterberg H *et al.* CSF biomarkers of neuroinflammation and cerebrovascular dysfunction in early Alzheimer disease. *Neurology* 2018; 91: e867–e877.
- 183 Toledo JB, Arnold SE, Raible K, Brettschneider J, Xie SX, Grossman M *et al.* Contribution of cerebrovascular disease in autopsy confirmed neurodegenerative disease cases in the National Alzheimer’s Coordinating Centre. *Brain* 2013; 136: 2697–2706.
- 184 Burton EJ, Mckeith IG, Burn DJ, Firbank MJ, Brien JTO. Progression of White Matter Hyperintensities in Alzheimer Disease , Dementia W ... *Am J Geriatr Psychiatry* 2006; 14: 842–849.
- 185 Ramirez J, McNeely AA, Berezuk C, Gao F, Black SE. Dynamic progression of white matter hyperintensities in Alzheimer’s disease and normal aging: Results from the Sunnybrook dementia study. *Front Aging Neurosci* 2016; 8: 1–9.
- 186 Low A, Mak E, Malpetti M, Passamonti L, Nicastro N, Stefaniak JD *et al.* In vivo neuroinflammation and cerebral small vessel disease in mild cognitive impairment and Alzheimer’s disease Neuro-inflammation. *J Neurol Neurosurg Psychiatry* 2021; 92: 45–52.
- 187 Wardlaw JM, Doubal FN, Valdes-Hernandez M, Wang X, Chappell FM, Shuler K *et al.* Blood-brain barrier permeability and long-term clinical and imaging outcomes in cerebral small vessel disease. *Stroke* 2013; 44: 525–527.
- 188 Abbott NJ, Patabendige AAK, Dolman DEM, Yusof SR, Begley DJ. Structure and function of the blood-brain barrier. *Neurobiol. Dis.* 2010; 37: 13–25.
- 189 Abbott NJ, Rönnbäck L, Hansson E. Astrocyte-endothelial interactions at the blood-brain barrier. *Nat Rev Neurosci* 2006; 7: 41–53.
- 190 Perea G, Navarrete M, Araque A. Tripartite synapses: astrocytes process and control synaptic information. *Trends Neurosci* 2009; 32: 421–431.
- 191 Kabba JA, Xu Y, Christian H, Ruan W, Chenai K, Xiang Y *et al.* Microglia: Housekeeper of

- the Central Nervous System. *Cell Mol Neurobiol* 2018; 38: 53–71.
- 192 Banks WA, Reed MJ, Logsdon AF, Rhea EM, Erickson MA. Healthy aging and the blood–brain barrier. *Nat Aging* 2021 13 2021; 1: 243–254.
- 193 Nation DA, Sweeney MD, Montagne A, Sagare AP, D’Orazio LM, Pachicano M *et al.* Blood–brain barrier breakdown is an early biomarker of human cognitive dysfunction. *Nat Med* 2019; 25: 270–276.
- 194 Tomimoto H, Akiguchi I, Suenaga T, Nishimura M, Wakita H, Nakamura S *et al.* Alterations of the blood-brain barrier and glial cells in white-matter lesions in cerebrovascular and Alzheimer’s disease patients. *Stroke* 1996; 27: 2069–2074.
- 195 Akiguchi I, Tomimoto H, Suenaga T, Wakita H, Budka H. Blood-brain barrier dysfunction in Binswanger’s disease; An immunohistochemical study. *Acta Neuropathol* 1997; 95: 78–84.
- 196 Hainsworth AH, Minett T, Andoh J, Forster G, Bhide I, Barrick TR *et al.* Neuropathology of white matter lesions, blood-brain barrier dysfunction, and dementia. *Stroke* 2017; 48: 2799–2804.
- 197 Wharton SB, Simpson JE, Brayne C, Ince PG. Age-Associated white matter lesions: The MRC cognitive function and ageing study. In: *Brain Pathology*. Blackwell Publishing Ltd, 2015, pp 35–43.
- 198 Jickling GC, Ander BP, Zhan X, Stamova B, Hull H, DeCarli C *et al.* Progression of cerebral white matter hyperintensities is related to leucocyte gene expression. *Brain* 2022; 145: 3179–3186.
- 199 Taheri S, Gasparovic C, Huisa BN, Adair JC, Edmonds E, Prestopnik J *et al.* Blood-brain barrier permeability abnormalities in vascular cognitive impairment. *Stroke* 2011; 42: 2158–2163.
- 200 Hermann P, Romero C, Schmidt C, Reis C, Zerr I. CSF Biomarkers and Neuropsychological Profiles in Patients with Cerebral Small-Vessel Disease. *PLoS One* 2014; 9: e105000.
- 201 Bjerke M, Zetterberg H, Edman Å, Blennow K, Wallin A, Andreasson U. Cerebrospinal fluid matrix metalloproteinases and tissue inhibitor of metalloproteinases in combination with subcortical and cortical biomarkers in vascular dementia and Alzheimer’s disease. *J Alzheimer’s Dis* 2011; 27: 665–676.
- 202 Bowman G, Kaye J, Moore M, Waichunas D, Carlson N, Quinn J. Blood–brain barrier impairment in Alzheimer disease. *Neurology* 2007; 68: 1809–1814.
- 203 Jonsson M, Zetterberg H, Van Straaten E, Lind K, Syversen S, Edman Å *et al.* Cerebrospinal fluid biomarkers of white matter lesions - cross-sectional results from the LADIS study. *Eur J Neurol* 2010; 17: 377–382.
- 204 Kanhai DA, De Kleijn DPV, Kappelle LJ, Uiterwaal CSPM, Van Der Graaf Y, Pasterkamp G *et al.* Extracellular vesicle protein levels are related to brain atrophy and cerebral white matter lesions in patients with manifest vascular disease: The SMART-MR study. *BMJ Open* 2014; 4: 1–7.
- 205 Lee WJ, Jung KH, Ryu YJ, Kim JM, Lee ST, Chu K *et al.* Cystatin C, a potential marker for cerebral microvascular compliance, is associated with white-matter hyperintensities progression. *PLoS One* 2017; 12: 1–12.
- 206 Topakian R, Barrick TR, Howe FA, Markus HS. Blood-brain barrier permeability is increased in normal-appearing white matter in patients with lacunar stroke and leucoaraiosis. *J Neurol*

- Neurosurg Psychiatry* 2010; 81: 192–197.
- 207 Wardlaw JM, Doubal F, Armitage P, Chappell F, Carpenter T, Muñoz Maniega S *et al.* Lacunar stroke is associated with diffuse Blood-Brain barrier dysfunction. *Ann Neurol* 2009; 65: 194–202.
- 208 Thrippleton MJ, Backes WH, Sourbron S, Ingrisch M, van Osch MJP, Dichgans M *et al.* Quantifying blood-brain barrier leakage in small vessel disease: Review and consensus recommendations. *Alzheimer's Dement.* 2019; 15: 840–858.
- 209 Stringer MS, Heye AK, Armitage PA, Chappell F, Valdés Hernández M del C, Makin SDJ *et al.* Tracer kinetic assessment of blood–brain barrier leakage and blood volume in cerebral small vessel disease: Associations with disease burden and vascular risk factors. *NeuroImage Clin* 2021; 32: 102883.
- 210 Wardlaw JM, Makin SJ, Valdés Hernández MC, Armitage PA, Heye AK, Chappell FM *et al.* Blood-brain barrier failure as a core mechanism in cerebral small vessel disease and dementia: evidence from a cohort study. *Alzheimer's Dement* 2017; 13: 634–643.
- 211 Li Y, Li M, Zuo L, Shi Q, Qin W, Yang L *et al.* Compromised blood-brain barrier integrity is associated with total magnetic resonance imaging burden of cerebral small vessel disease. *Front Neurol* 2018; 9: 1–8.
- 212 Li Y, Li M, Yang L, Qin W, Yang S, Yuan J *et al.* The relationship between blood-brain barrier permeability and enlarged perivascular spaces: a cross-sectional study. 2019. doi:10.2147/CIA.S204269.
- 213 Walsh J, Tozer DJ, Sari H, Hong YT, Drazyk A, Williams G *et al.* Microglial activation and blood-brain barrier permeability in cerebral small vessel disease. *Brain* 2021; 144: 1361–1371.
- 214 Huisa BN, Caprihan A, Thompson J, Prestopnik J, Qualls CR, Rosenberg GA. Long-Term Blood-Brain Barrier Permeability Changes in Binswanger Disease. *Stroke* 2015; 46: 2413–2418.
- 215 Simpson JE, Ince PG, Higham CE, Gelsthorpe CH, Fernando MS, Matthews F *et al.* Microglial activation in white matter lesions and nonlesional white matter of ageing brains. *Neuropathol Appl Neurobiol* 2007; 33: 670–683.
- 216 Waller R, Narramore R, Simpson JE, Heath PR, Verma N, Tinsley M *et al.* Heterogeneity of cellular inflammatory responses in ageing white matter and relationship to Alzheimer's and small vessel disease pathologies. *Wiley Online Libr* 2021; 31: 12928.
- 217 Fornage M, Chiang YA, O'Meara ES, Psaty BM, Reiner AP, Siscovick DS *et al.* Biomarkers of inflammation and MRI-defined small vessel disease of the brain: The cardiovascular health study. *Stroke* 2008; 39: 1952–1959.
- 218 Hassan A, Hunt BJ, O'Sullivan M, Parmar K, Bamford JM, Briley D *et al.* Markers of endothelial dysfunction in lacunar infarction and ischaemic leukoaraiosis. *Brain* 2003; 126: 424–432.
- 219 Markus HS, Hunt B, Palmer K, Enzinger C, Schmidt H, Schmidt R. Markers of Endothelial and Hemostatic Activation and Progression of Cerebral White Matter Hyperintensities. *Stroke* 2005; 36: 1410–1414.
- 220 Satizabal CL, Zhu YC, Mazoyer B, Tzourio C, Dufouil C. Circulating IL-6 and CRP are associated with MRI findings in the elderly: The 3C-Dijon Study. *Neurology* 2012; 78: 720–727.
- 221 Low A, Mak E, Rowe JB, Markus HS, O'Brien JT. Inflammation and cerebral small vessel disease: A systematic review. *Ageing Res Rev* 2019; 53: 100916.

- 222 Kuipers S, Overmars LM, van Es B, de Bresser J, Bron EE, Hofer IE *et al.* A cluster of blood-based protein biomarkers reflecting coagulation relates to the burden of cerebral small vessel disease. *J Cereb Blood Flow Metab* 2022; 42: 1282–1293.
- 223 Libby P, Loscalzo J, Ridker PM, Farkouh ME, Hsue PY, Fuster V *et al.* Inflammation, Immunity, and Infection in Atherothrombosis: JACC Review Topic of the Week. *J Am Coll Cardiol* 2018; 72: 2071–2081.
- 224 Van Der Valk FM, Bekkering S, Kroon J, Yeang C, Van Den Bossche J, Van Buul JD *et al.* Oxidized phospholipids on Lipoprotein(a) elicit arterial wall inflammation and an inflammatory monocyte response in humans. *Circulation* 2016; 134: 611–624.
- 225 Bekkering S, van den Munckhof I, Nielen T, Lamfers E, Dinarello C, Rutten J *et al.* Innate immune cell activation and epigenetic remodeling in symptomatic and asymptomatic atherosclerosis in humans in vivo. *Atherosclerosis* 2016; 254: 228–236.
- 226 Noz MP, ter Telgte A, Wiegertjes K, Joosten LAB, Netea MG, de Leeuw F-E *et al.* Trained Immunity Characteristics Are Associated With Progressive Cerebral Small Vessel Disease. *Stroke* 2018; 49: 2910–2917.
- 227 Rosenberg GA, Bjerke M, Wallin A. Multimodal Markers of Inflammation in the Subcortical Ischemic Vascular Disease Type of Vascular Cognitive Impairment. *Stroke* 2014; 45: 1531–1538.
- 228 Werry EL, Bright FM, Piguet O, Ittner LM, Halliday GM, Hodges JR *et al.* Recent Developments in TSPO PET Imaging as A Biomarker of Neuroinflammation in Neurodegenerative Disorders. *Int J Mol Sci* 2019; 20: 3161.
- 229 Low A, Mak E, Malpetti M, Passamonti L, Nicastro N, Stefaniak JD *et al.* In vivo neuroinflammation and cerebral small vessel disease in mild cognitive impairment and Alzheimer’s disease. *J Neurol Neurosurg Psychiatry* 2021; 92: 45–52.
- 230 Nutma E, Ceyzériat K, Amor S, Tsartsalis S, Millet P, Owen DR *et al.* Cellular sources of TSPO expression in healthy and diseased brain. *Eur J Nucl Med Mol Imaging* 2021 491 2021; 49: 146–163.
- 231 Nutma E, Fancy N, Weinert M, Marzin MC, Tsartsalis S, Muirhead RCJ *et al.* Translocator protein is a marker of activated microglia in rodent models but not human neurodegenerative diseases. *bioRxiv* 2022; : 2022.05.11.491453.
- 232 Kettenmann H, Ransom BR. *Neuroglia*. 2nd ed. Oxford University Press: New York, 2005.
- 233 Taheri S, Gasparovic C, Huisa BN, Adair JC, Edmonds E, Prestopnik J *et al.* Blood-brain barrier permeability abnormalities in vascular cognitive impairment. *Stroke* 2011; 42: 2158–2163.
- 234 Jalal FY, Yang Y, Thompson JF, Roitbak T, Rosenberg GA. Hypoxia-induced neuroinflammatory white-matter injury reduced by minocycline in SHR/SP. *J Cereb Blood Flow Metab* 2015; 35: 1145–1153.
- 235 Kwok CS, Shoamanesh A, Copley HC, Myint PK, Loke YK, Benavente OR. Efficacy of Antiplatelet Therapy in Secondary Prevention Following Lacunar Stroke: Pooled Analysis of Randomized Trials. *Stroke* 2015; 46: 1014–1023.
- 236 Investigators TS. Effects of Clopidogrel Added to Aspirin in Patients with Recent Lacunar Stroke. *N Engl J Med* 2012; 367: 817–825.
- 237 Wardlaw JM, DeBette S, Jokinen H, De Leeuw F-E, Pantoni L, Chabriat H *et al.* ESO

- Guideline on covert cerebral small vessel disease. *journals.sagepub.com* 2021; : 239698732110121.
- 238 Mok VCT, Lam WWM, Fan YH, Wong A, Ng PW, Tsoi TH *et al.* Effects of statins on the progression of cerebral white matter lesion. *J Neurol* 2009; 256: 750–757.
- 239 Van Dalen JW, Moll Van Charante EP, Caan MWA, Scheltens P, Majoie CBLM, Nederveen AJ *et al.* Effect of Long-Term Vascular Care on Progression of Cerebrovascular Lesions. *Stroke* 2017; 48: 1842–1848.
- 240 Nasrallah IM, Pajewski NM, Auchus AP, Chelune G, Cheung AK, Cleveland ML *et al.* Association of Intensive vs Standard Blood Pressure Control With Cerebral White Matter Lesions. *JAMA* 2019; 322: 524.
- 241 Williamson J, Pajewski N, Auchus A, Jama RB-, 2019 U. Effect of intensive vs standard blood pressure control on probable dementia: a randomized clinical trial. *JAMA* 2019; 321: 553–561.
- 242 Blood-pressure targets in patients with recent lacunar stroke: the SPS3 randomised trial. *Lancet* 2013; 382: 507–515.
- 243 Kitagawa K, Yamamoto Y, Arima H, Maeda T, Sunami N, Kanzawa T *et al.* Effect of Standard vs Intensive Blood Pressure Control on the Risk of Recurrent Stroke: A Randomized Clinical Trial and Meta-analysis. *JAMA Neurol* 2019; 76: 1309–1318.
- 244 Pflanz CP, Egle MS, O'Brien JT, Morris RG, Barrick TR, Blamire AM *et al.* Association of Blood Pressure Lowering Intensity With White Matter Network Integrity in Patients With Cerebral Small Vessel Disease. *Neurology* 2022; 99: e1945–e1953.
- 245 Markus HS, Egle M, Croall ID, Sari H, Khan U, Hassan A *et al.* PRESERVE: Randomized Trial of Intensive Versus Standard Blood Pressure Control in Small Vessel Disease. *Stroke* 2021; : 2484–2493.
- 246 NICE. Hypertension in adults: diagnosis and management. NICE guideline 136. 2019.
- 247 Wardlaw JM, Woodhouse LJ, Mhlanga II, Oatey K, Heye AK, Bamford J *et al.* Isosorbide Mononitrate and Cilostazol Treatment in Patients With Symptomatic Cerebral Small Vessel Disease The Lacunar Intervention Trial-2 (LACI-2) Randomized Clinical Trial Visual Abstract Supplemental content. *JAMA Neurol* 2023; 80: 682–692.
- 248 Dawson J, Robertson M, Dickie DA, Bath P, Forbes K, Quinn T *et al.* Xanthine oxidase inhibition and white matter hyperintensity progression following ischaemic stroke and transient ischaemic attack (XILO-FIST): a multicentre, double-blinded, randomised, placebo-controlled trial. 2023. doi:10.1016/j.eclinm.2023.101863.
- 249 Kelly P, Weimar C, Lemmens R, Murphy S, Purroy F, Arsovska A *et al.* Colchicine for prevention of vascular inflammation in Non-CardioEmbolic stroke (CONVINCE) – study protocol for a randomised controlled trial. *Eur Stroke J* 2021; 6: 222–228.
- 250 Cavalieri M, Schmidt R, Chen C, Mok V, De Freitas GR, Song S *et al.* B vitamins and magnetic resonance imaging-detected ischemic brain lesions in patients with recent transient ischemic attack or stroke: The VITamins to prevent stroke (VITATOPS) MRI-substudy. *Stroke* 2012; 43: 3266–3270.
- 251 Liu-Ambrose T, Best JR, Davis JC, Eng JJ, Lee PE, Jacova C *et al.* Aerobic exercise and vascular cognitive impairment. *Neurology* 2016; 87: 2082–2090.
- 252 Bolandzadeh N, Tam R, Handy TC, Nagamatsu LS, Liang Hsu C, Davis JC *et al.* Resistance Training and White Matter Lesion Progression in Older Women: Exploratory Analysis of a 12-

- Month Randomized Controlled Trial From the. *J Am Geriatr Soc* 2015; 63: 2052–2060.
- 253 O'Brien JT, Thomas A. Vascular dementia. *Lancet* 2015; 386: 1698–1706.
- 254 Brown R, Low A, Markus HS. Rate of, and risk factors for, white matter hyperintensity growth: A systematic review and meta-analysis with implications for clinical trial design. *J Neurol Neurosurg Psychiatry* 2021; 92: 1271–1277.
- 255 Breteler MM, van Swieten JC, Bots ML, Grobbee DE, Claus JJ, van den Hout JH *et al.* Cerebral white matter lesions, vascular risk factors, and cognitive function in a population-based study: the Rotterdam Study. *Neurology* 1994; 44: 1246–52.
- 256 Liao D, Cooper L, Cai J, Toole J, Bryan N, Hutchinson R *et al.* Presence and severity of cerebral white matter lesions and hypertension, its treatment, and its control. *Stroke* 1996; 27: 2262–2270.
- 257 Moher D, Liberati A, Tetzlaff J, Altman DG, Group TP. Preferred Reporting Items for Systematic Reviews and Meta-Analyses: The PRISMA Statement. *PLoS Med* 2009; 6: e1000097.
- 258 Knapp G, Hartung J. Improved tests for a random effects meta-regression with a single covariate. *Stat Med* 2003; 22: 2693–2710.
- 259 Borenstein M, Hedges L, Higgins J, Rothstein H. Meta-regression. In: *Introduction to Meta-Analysis*. John Wiley & Sons, Ltd, 2009.
- 260 The R Core Team, R Foundation for Statistical Computing, Vienna A. R: A language and environment for statistical computing. R URL <https://www.R-project.org/>. 2019.
- 261 Balduzzi S, Rücker G, Schwarzer G. How to perform a meta-analysis with R: A practical tutorial. *Evid Based Ment Health* 2019; 22: 153–160.
- 262 Chappell FM, del Carmen Valdés Hernández M, Makin SD, Shuler K, Sakka E, Dennis MS *et al.* Sample size considerations for trials using cerebral white matter hyperintensity progression as an intermediate outcome at 1 year after mild stroke: Results of a prospective cohort study. *Trials* 2017; 18: 1–10.
- 263 Chen Y, Gurol M, Rosand J, Viswanathan A, Rakich S, Groover T *et al.* Progression of white matter lesions and hemorrhages in cerebral amyloid angiopathy. *Neurology* 2006; 67: 83–87.
- 264 Markus HS, Hunt B, Palmer K, Enzinger C, Schmidt H, Schmidt R. Markers of Endothelial and Hemostatic Activation and Progression of Cerebral White Matter Hyperintensities. *Stroke* 2005; 36: 1410–1414.
- 265 Taylor WD, Steffens DC, Ashley-Koch A, Payne ME, MacFall JR, Potocky CF *et al.* Angiotensin receptor gene polymorphisms and two-year changes in hyperintense lesion volume in men. *Mol Psychiatry* 2010; 15: 816–822.
- 266 Van Dijk EJ, Prins ND, Vrooman HA, Hofman A, Koudstaal PJ, Breteler MMB. Progression of cerebral small vessel disease in relation to risk factors and cognitive consequences: Rotterdam scan study. *Stroke* 2008; 39: 2712–2719.
- 267 Whitman GT, Tang T, Lin A, Baloh RW. A prospective study of cerebral white matter abnormalities in older people with gait dysfunction. *Neurology* 2001; 57: 990–994.
- 268 Van Leijsen EMC, Van Uden IWM, Ghafoorian M, Bergkamp MI, Lohner V, Kooijmans ECM *et al.* Nonlinear temporal dynamics of cerebral small vessel disease. *Neurology* 2017; 89: 1569–1577.

- 269 Taylor WD, MacFall JR, Provenzale JM, Payne ME, McQuoid DR, Steffens DC *et al.* Serial MR Imaging of Volumes of Hyperintense White Matter Lesions in Elderly Patients: Correlation with Vascular Risk Factors. *Am J Roentgenol* 2003; 181: 571–576.
- 270 Cho A-H, Kim H-R, Kim W, Yang DW. White Matter Hyperintensity in Ischemic Stroke Patients: It May Regress Over Time. *J Stroke* 2015; 17: 60.
- 271 Raz N, Rodrigue KM, Kennedy KM, Acker JD. Vascular health and longitudinal changes in brain and cognition in middle-aged and older adults. *Neuropsychology* 2007; 21: 149–157.
- 272 Van Den Heuvel DMJ, Ten Dam VH, De Craen AJM, Admiraal-Behloul F, Olofsen H, Bollen ELEM *et al.* Increase in periventricular white matter hyperintensities parallels decline in mental processing speed in a non-demented elderly population. *J Neurol Neurosurg Psychiatry* 2006; 77: 149–153.
- 273 Shu Z, Xu Y, Shao Y, Pang P, Gong X. Radiomics from magnetic resonance imaging may be used to predict the progression of white matter hyperintensities and identify associated risk factors. *Eur Radiol* 2020; 30: 3046–3058.
- 274 Dickie DA, Karama S, Ritchie SJ, Cox SR, Sakka E, Royle NA *et al.* Progression of White Matter Disease and Cortical Thinning Are Not Related in Older Community-Dwelling Subjects. *Stroke* 2016; 47: 410–416.
- 275 Debette S, Seshadri S, Beiser A, Au R, Himali JJ, Palumbo C *et al.* Midlife vascular risk factor exposure accelerates structural brain aging and cognitive decline. *Neurology* 2011; 77: 461–8.
- 276 Godin O, Tzourio C, Maillard P, Mazoyer B, Dufouil C. Antihypertensive treatment and change in blood pressure are associated with the progression of white matter lesion volumes: The three-city (3C)-Dijon magnetic resonance imaging study. *Circulation* 2011; 123: 266–273.
- 277 Goldstein IB, Bartzokis G, Guthrie D, Shapiro D. Ambulatory blood pressure and the brain. *Neurology* 2005; 64: 1846–1852.
- 278 Johnson AD, McQuoid DR, Steffens DC, Payne ME, Beyer JL, Taylor WD. Effects of stressful life events on cerebral white matter hyperintensity progression. *Int J Geriatr Psychiatry* 2016; 32: e10–e17.
- 279 Leung LY, Bartz TM, Rice K, Floyd J, Psaty B, Gutierrez J *et al.* Blood Pressure and Heart Rate Measures Associated with Increased Risk of Covert Brain Infarction and Worsening Leukoaraiosis in Older Adults. *Arterioscler Thromb Vasc Biol* 2017; 37: 1579–1586.
- 280 Liu Z, Zhao Y, Zhang H, Chai Q, Cui Y, Diao Y *et al.* Excessive variability in systolic blood pressure that is self-measured at home exacerbates the progression of brain white matter lesions and cognitive impairment in the oldest old. *Hypertens Res* 2016; 39: 245–253.
- 281 Kuriyama N, Mizuno T, Ohshima Y, Yamada K, Ozaki E, Shigeta M *et al.* Intracranial deep white matter lesions (DWLs) are associated with chronic kidney disease (CKD) and cognitive impairment: A 5-year follow-up magnetic resonance imaging (MRI) study. *Arch Gerontol Geriatr* 2013; 56: 55–60.
- 282 Peng J, Hu N, Zhong M, Lu F, Wang Z, Liu Z *et al.* Excessive Lowering of Blood Pressure Is Not Beneficial for Progression of Brain White Matter Hyperintensive and Cognitive Impairment in Elderly Hypertensive Patients: 4-Year Follow-Up Study. *J Am Med Dir Assoc* 2014; 15: 904–910.
- 283 Sedaghat S, Ding J, Eiriksdottir G, van Buchem MA, Sigurdsson S, Ikram MA *et al.* The AGES-Reykjavik Study suggests that change in kidney measures is associated with subclinical brain pathology in older community-dwelling persons. *Kidney Int* 2018; 94: 608–615.

- 284 Shu ZY, Shao Y, Xu YY, Ye Q, Cui SJ, Mao DW *et al.* Radiomics nomogram based on MRI for predicting white matter hyperintensity progression in elderly adults. *J Magn Reson Imaging* 2020; 51: 535–546.
- 285 Verhaaren BFJ, Vernooij MW, De Boer R, Hofman A, Niessen WJ, Van Der Lugt A *et al.* High blood pressure and cerebral white matter lesion progression in the general population. *Hypertension* 2013; 61: 1354–1359.
- 286 Moon S, Barreto P de S, Chupin M, Mangin J, Bouyahia A, Fillon L *et al.* Red Blood Cells Omega-3 Polyunsaturated Fatty Acids & White Matter Hyperintensities. *J Nutr Heal Aging* 2017; 22: 174–179.
- 287 Ronneberger O, Fischer P, Brox T. U-net: Convolutional networks for biomedical image segmentation. *Lect Notes Comput Sci (including Subser Lect Notes Artif Intell Lect Notes Bioinformatics)* 2015; 9351: 234–241.
- 288 Maillard P, Fletcher E, Harvey D, Carmichael O, Reed B, Mungas D *et al.* White Matter Hyperintensity Penumbra. *Stroke* 2011; 42: 1917–1922.
- 289 Benjamin P, Zeestraten E, Lambert C, Chis Ster I, Williams OA, Lawrence AJ *et al.* Progression of MRI markers in cerebral small vessel disease: Sample size considerations for clinical trials. *J Cereb Blood Flow Metab* 2016; 36: 228–240.
- 290 Schmidt R, Enzinger C, Ropele S, Schmidt H, Fazekas F. Progression of cerebral white matter lesions: 6-Year results of the Austrian Stroke Prevention Study. *Lancet* 2003; 361: 2046–2048.
- 291 Maltais M, de Souto Barreto P, Moon SY, Rolland Y, Vellas B. Prospective association of white matter hyperintensity volume and frailty in older adults. *Exp Gerontol* 2019; 118: 51–54.
- 292 Wardlaw JM. Blood-brain barrier and cerebral small vessel disease. *J Neurol Sci* 2010; 299: 66–71.
- 293 Knopman DS, Penman AD, Catellier DJ, Coker LH, Shibata DK, Sharrett AR *et al.* Vascular risk factors and longitudinal changes on brain MRI: The ARIC study. *Neurology* 2011; 76: 1879–1885.
- 294 Van Der Veen PH, Muller M, Vincken KL, Witkamp TD, Mali WPTM, Van Der Graaf Y *et al.* Longitudinal changes in brain volumes and cerebrovascular lesions on MRI in patients with manifest arterial disease: The SMART-MR study. *J Neurol Sci* 2014; 337: 112–118.
- 295 Al-Janabi OM, Bauer CE, Goldstein LB, Murphy RR, Bahrani AA, Smith CD *et al.* White Matter Hyperintensity Regression: Comparison of Brain Atrophy and Cognitive Profiles with Progression and Stable Groups. *Brain Sci* 2019; 9: 170.
- 296 Mayer C, Nägele FL, Petersen M, Frey BM, Hanning U, Pasternak O *et al.* Free-water diffusion MRI detects structural alterations surrounding white matter hyperintensities in the early stage of cerebral small vessel disease. *J Cereb Blood Flow Metab* 2022; 42: 1707–1718.
- 297 Bahrani AA, Al-Janabi OM, Abner EL, Bardach SH, Kryscio RJ, Wilcock DM *et al.* Post-acquisition processing confounds in brain volumetric quantification of white matter hyperintensities. *J Neurosci Methods* 2019; 327: 108391.
- 298 van Norden AG, de Laat KF, Gons RA, van Uden IW, van Dijk EJ, van Oudheusden LJ *et al.* Causes and consequences of cerebral small vessel disease. The RUN DMC study: a prospective cohort study. Study rationale and protocol. *BMC Neurol* 2011; 11: 1–8.
- 299 Croall ID, Tozer DJ, Moynihan B, Khan U, O'Brien JT, Morris RG *et al.* Effect of Standard vs Intensive Blood Pressure Control on Cerebral Blood Flow in Small Vessel Disease. *JAMA*

- Neurol* 2018; 75: 720–727.
- 300 Lambert C, Benjamin P, Zeestraten E, Lawrence AJ, Barrick TR, Markus HS. Longitudinal patterns of leukoaraiosis and brain atrophy in symptomatic small vessel disease. *Brain* 2016; 139: 1136–1151.
- 301 Lambert C, Lutti A, Helms G, Frackowiak R, Ashburner J. Multiparametric brainstem segmentation using a modified multivariate mixture of Gaussians. *NeuroImage Clin* 2013; 2: 684–694.
- 302 Zwiers MP. Patching cardiac and head motion artefacts in diffusion-weighted images. *Neuroimage* 2010; 53: 565–575.
- 303 Croall ID, Lohner V, Moynihan B, Khan U, Hassan A, O'Brien JT *et al.* Using DTI to assess white matter microstructure in cerebral small vessel disease (SVD) in multicentre studies. *Clin Sci* 2017; 131: 1361–1373.
- 304 West J, Wright J, Tuffnell D, Jankowicz D, West R. Do clinical trials improve quality of care? A comparison of clinical processes and outcomes in patients in a clinical trial and similar patients outside a trial where both groups are managed according to a strict protocol. *Qual Saf Heal Care* 2005; 14: 175–178.
- 305 Ramirez J, Scott CJM, Black SE. A short-term scan-rescan reliability test measuring brain tissue and subcortical hyperintensity volumetrics obtained using the lesion explorer structural MRI processing pipeline. *Brain Topogr* 2013; 26: 35–38.
- 306 ter Telgte A, Wiegertjes K, Gesierich B, Marques JP, Huebner M, de Klerk JJ *et al.* Contribution of acute infarcts to cerebral small vessel disease progression. *Ann Neurol* 2019; 86: 582–592.
- 307 Brown RB, Tozer DJ, Loubière L, Hong YT, Fryer TD, Williams GB *et al.* MINocyclinE to Reduce inflammation and blood brain barrier leakage in small Vessel disease (MINERVA) trial study protocol. *Eur Stroke J* 2022; 7: 323–330.
- 308 Fernández-López D, Faustino J, Daneman R, Zhou L, Lee SY, Derugin N *et al.* Blood–Brain Barrier Permeability Is Increased After Acute Adult Stroke But Not Neonatal Stroke in the Rat. *J Neurosci* 2012; 32: 9588.
- 309 Gerhard A, Schwarz J, Myers R, Wise R, Banati RB. Evolution of microglial activation in patients after ischemic stroke: a [11C](R)-PK11195 PET study. *Neuroimage* 2005; 24: 591–595.
- 310 Patlak CS, Blasberg RG. Graphical evaluation of blood-to-brain transfer constants from multiple-time uptake data. Generalizations. *J Cereb Blood Flow Metab* 1985; 5: 584–590.
- 311 Taheri S, Gasparovic C, Shah NJ, Rosenberg GA. Quantitative measurement of blood-brain barrier permeability in human using dynamic contrast-enhanced MRI with fast T1 mapping. *Magn Reson Med* 2011; 65: 1036–1042.
- 312 Hudson HM, Larkin RS. Accelerated image reconstruction using ordered subsets of projection data. *IEEE Trans Med Imaging* 1994; 13: 601–609.
- 313 Burgos N, Cardoso MJ, Thielemans K, Modat M, Pedemonte S, Dickson J *et al.* Attenuation correction synthesis for hybrid PET-MR scanners: Application to brain studies. *IEEE Trans Med Imaging* 2014; 33: 2332–2341.
- 314 Tomasi G, Edison P, Bertoldo A, Roncaroli F, Singh P, Gerhard A *et al.* Novel reference region model reveals increased microglial and reduced vascular binding of 11C-(R)-PK11195 in patients with Alzheimer's disease. *Soc Nucl Med* 2008; 49: 1249–1256.

- 315 Yaqub M, van Berckel BN, Schuitemaker A, Hinz R, Turkheimer FE, Tomasi G *et al.* Optimization of Supervised Cluster Analysis for Extracting Reference Tissue Input Curves in (R)-[^{11}C]PK11195 Brain PET Studies. *J Cereb Blood Flow Metab* 2012; 32: 1600–1608.
- 316 Bright P, Hale E, Gooch VJ, Myhill T, van der Linde I. The National Adult Reading Test: restandardisation against the Wechsler Adult Intelligence Scale-Fourth edition. *Neuropsychol Rehabil* 2018; 28: 1019–1027.
- 317 Nikodemova M, Duncan ID, Watters JJ. Minocycline exerts inhibitory effects on multiple mitogen-activated protein kinases and I κ B α degradation in a stimulus-specific manner in microglia. *J Neurochem* 2006; 96: 314–323.
- 318 Yang F, Zhou L, Wang D, Wang Z, Huang QY. Minocycline ameliorates hypoxia-induced blood–brain barrier damage by inhibition of HIF-1 α through SIRT-3/PHD-2 degradation pathway. *Neuroscience* 2015; 304: 250–259.
- 319 Chen SP, Chou KH, Fuh JL, Huang YH, Huang CC, Lirng JF *et al.* Dynamic changes in white matter hyperintensities in reversible cerebral vasoconstriction syndrome. *JAMA Neurol* 2018; 75: 1106–1113.
- 320 Manso Y, Holland PR, Kitamura A, Szymkowiak S, Duncombe J, Hennessy E *et al.* Minocycline reduces microgliosis and improves subcortical white matter function in a model of cerebral vascular disease. *Glia* 2018; 66: 34–46.
- 321 Linn J, Halpin A, Demaerel P, Ruhland J, Giese AD, Dichgans M *et al.* Prevalence of superficial siderosis in patients with cerebral amyloid angiopathy. *Neurology* 2010; 74: 1346–50.
- 322 Dodd KC, Emsley HCA, Desborough MJR, Chhetri SK. Periprocedural antithrombotic management for lumbar puncture: Association of British Neurologists clinical guideline. *Pract Neurol* 2018; 18: 436–446.
- 323 Harris PA, Taylor R, Thielke R, Payne J, Gonzalez N, Conde JG. Research electronic data capture (REDCap)--a metadata-driven methodology and workflow process for providing translational research informatics support. *J Biomed Inform* 2009; 42: 377–381.
- 324 Bader S, Wolf L, Milenkovic VM, Gruber M, Nothdurfter C, Rupprecht R *et al.* Differential effects of TSPO ligands on mitochondrial function in mouse microglia cells. *Psychoneuroendocrinology* 2019; 106: 65–76.
- 325 NINDS NET-PD Investigators TNN-P, Fagan SC, Hart RG, Hovinga CA, Murphy DD, Dawson TM *et al.* A randomized, double-blind, futility clinical trial of creatine and minocycline in early Parkinson disease. *Neurology* 2006; 66: 664–71.
- 326 Howard R, Zubko O, Bradley R, Harper E, Pank L, O'Brien J *et al.* Minocycline at 2 Different Dosages vs Placebo for Patients With Mild Alzheimer Disease: A Randomized Clinical Trial. *JAMA Neurol* 2020; 77: 164–174.
- 327 Scott G, Zetterberg H, Jolly A, Cole JH, De Simoni S, Jenkins PO *et al.* Minocycline reduces chronic microglial activation after brain trauma but increases neurodegeneration. *Brain* 2018; 141: 459–471.
- 328 Deakin B, Suckling J, Barnes TRE, Byrne K, Chaudhry IB, Dazzan P *et al.* The benefit of minocycline on negative symptoms of schizophrenia in patients with recent-onset psychosis (BeneMin): a randomised, double-blind, placebo-controlled trial. *The Lancet Psychiatry* 2018; 5: 885–894.
- 329 Walsh J. *Blood-Brain Barrier Permeability and Inflammation in Cerebral Small Vessel Disease*. 2020. doi:10.17863/CAM.50869.

- 330 Carcel C, Woodward M, Balicki G, Koroneos GL, Aguiar De Sousa D, Cordonnier C *et al.* Trends in recruitment of women and reporting of sex differences in large-scale published randomized controlled trials in stroke. *Int J Stroke* 2019; 14. doi:10.1177/1747493019851292.
- 331 Haast RA, Gustafson DR, Kiliaan AJ. Sex differences in stroke. *J Cereb Blood Flow Metab* 2012; 32: 2100–2107.
- 332 Shi L, Zhao L, Yeung FK, Wong SY, Chan RKT, Tse MF *et al.* Mapping the contribution and strategic distribution patterns of neuroimaging features of small vessel disease in poststroke cognitive impairment. *J Neurol Neurosurg Psychiatry* 2018; 89: 918–926.
- 333 Soysal P, Arik F, Smith L, Jackson SE, Isik AT. Inflammation, Frailty and Cardiovascular Disease. *Adv Exp Med Biol* 2020; 1216: 55–64.
- 334 Gilhus NE, Deuschl G. Neuroinflammation — a common thread in neurological disorders. *Nat Rev Neurol* 2019 158 2019; 15: 429–430.
- 335 Glezer I, Simard AR, Rivest S. Neuroprotective role of the innate immune system by microglia. *Neuroscience* 2007; 147: 867–883.
- 336 Haruwaka K, Ikegami A, Tachibana Y, Ohno N, Konishi H, Hashimoto A *et al.* Dual microglia effects on blood brain barrier permeability induced by systemic inflammation. *Nat Commun* 2019 101 2019; 10: 1–17.
- 337 Potter GM, Chappell FM, Morris Z, Wardlaw JM. Cerebral perivascular spaces visible on magnetic resonance imaging: Development of a qualitative rating scale and its observer reliability. *Cerebrovasc Dis* 2015; 39: 224–231.
- 338 Tang Y, Le W. Differential Roles of M1 and M2 Microglia in Neurodegenerative Diseases. *Mol Neurobiol* 2015 532 2015; 53: 1181–1194.
- 339 McNamara NB, Munro DAD, Bestard-Cuche N, Uyeda A, Bogie JFJ, Hoffmann A *et al.* Microglia regulate central nervous system myelin growth and integrity. *Nat* 2022 6137942 2022; 613: 120–129.
- 340 Janssen B, Vugts DJ, Windhorst AD, Mach RH. PET imaging of microglial activation - Beyond targeting TSPO. *Molecules* 2018; 23: 1–14.
- 341 Staszewski J, Piusińska-Macoch R, Brodacki B, Skrobowska E, Stepień A. IL-6, PF-4, sCD40 L, and homocysteine are associated with the radiological progression of cerebral small-vessel disease: A 2-year follow-up study. *Clin Interv Aging* 2018; 13: 1135–1141.
- 342 Hijdra D, Vorselaars ADM, Grutters JC, Claessen AME, Rijkers GT. Phenotypic Characterization of Human Intermediate Monocytes. *Front Immunol* 2013; 4: 339.
- 343 Yamamoto H, Yoshida N, Shinke T, Otake H, Kuroda M, Sakaguchi K *et al.* Impact of CD14++CD16+ monocytes on coronary plaque vulnerability assessed by optical coherence tomography in coronary artery disease patients. *Atherosclerosis* 2018; 269: 245–251.
- 344 Engelhardt B, Coisne C. Fluids and barriers of the CNS establish immune privilege by confining immune surveillance to a two-walled castle moat surrounding the CNS castle. *Fluids Barriers CNS* 2011; 8. doi:10.1186/2045-8118-8-4.
- 345 Rustenhoven J, Kipnis J. Brain borders at the central stage of neuroimmunology. *Nat* 2022 6127940 2022; 612: 417–429.
- 346 Candelario-Jalil E, Dijkhuizen RM, Magnus T. Neuroinflammation, Stroke, Blood-Brain Barrier Dysfunction, and Imaging Modalities. *Stroke* 2022; 53: 1473–1486.

- 347 Pedragosa J, Salas-Perdomo A, Gallizioli M, Cugota R, Miró-Mur F, Briansó F *et al.* CNS-border associated macrophages respond to acute ischemic stroke attracting granulocytes and promoting vascular leakage. *Acta Neuropathol Commun* 2018; 6: 76.
- 348 Prinz M, Masuda T, Wheeler MA, Quintana FJ. Microglia and Central Nervous System-Associated Macrophages - from Origin to Disease Modulation. *Annu Rev Immunol* 2021; 39: 251–277.
- 349 Gerganova G, Riddell A, Miller AA. CNS border-associated macrophages in the homeostatic and ischaemic brain. *Pharmacol Ther* 2022; 240: 108220.
- 350 Nevola K, Sandin M, Guess J, Forsberg S, Cambronerio C, Pucholt P *et al.* OlinkAnalyse. Facilitate Analysis of Proteomic Data from Olink. 2017.
- 351 Albert JM, Li Y, Sun J, Woyczynski WA, Nelson S. Continuous-time causal mediation analysis. *Stat Med* 2019; 38: 4334–4347.
- 352 Tuladhar AM, Lawrence A, Norris DG, Barrick TR, Markus HS, de Leeuw FE. Disruption of rich club organisation in cerebral small vessel disease. *Hum Brain Mapp* 2017; 38: 1751–1766.
- 353 Maillard P, Fletcher E, Singh B, Martinez O, Johnson DK, Olichney JM *et al.* Cerebral white matter free water: A sensitive biomarker of cognition and function. *Neurology* 2019; 92: E2221–E2231.
- 354 Pettersson-Pablo P, Nilsson TK, Breimer LH, Hurtig-Wennlöf A. IGFBP-1 and IGFBP-2 are associated with a decreased pulse-wave velocity in young, healthy adults. *BMC Cardiovasc Disord* 2021; 21: 1–8.
- 355 Murthy S, Karkossa I, Schmidt C, Hoffmann A, Hagemann T, Rothe K *et al.* Danger signal extracellular calcium initiates differentiation of monocytes into SPP1/osteopontin-producing macrophages. *Cell Death Dis* 2022 131 2022; 13: 1–15.
- 356 Tozer DJ, Brown RB, Walsh J, Hong YT, Williams GB, O'Brien JT *et al.* Do Regions of Increased Inflammation Progress to New White Matter Hyperintensities?: A Longitudinal Positron Emission Tomography-Magnetic Resonance Imaging Study. *Stroke* 2023; 54: 549–557.
- 357 van der Poel M, Ulas T, Mizze MR, Hsiao CC, Miedema SSM, Adelia *et al.* Transcriptional profiling of human microglia reveals grey–white matter heterogeneity and multiple sclerosis-associated changes. *Nat Commun* 2019 101 2019; 10: 1–13.
- 358 Leng F, Edison P. Neuroinflammation and microglial activation in Alzheimer disease: where do we go from here? *Nat Rev Neurol* 2020 173 2020; 17: 157–172.
- 359 Paolicelli RC, Sierra A, Stevens B, Tremblay ME, Aguzzi A, Ajami B *et al.* Microglia states and nomenclature: A field at its crossroads. *Neuron* 2022; 110: 3458–3483.
- 360 Bridges LR, Andoh J, Lawrence AJ, Khoong CHL, Poon W, Esiri MM *et al.* Blood-brain barrier dysfunction and cerebral small vessel disease (arteriolosclerosis) in brains of older people. *J Neuropathol Exp Neurol* 2014; 73: 1026–1033.
- 361 Roberts JM, Maniskas ME, Bix GJ. Bilateral carotid artery stenosis causes unexpected early changes in brain extracellular matrix and blood-brain barrier integrity in mice. *PLoS One* 2018; 13: e0195765.
- 362 Powell E, Ohene Y, Battiston M, Dickie BR, Parkes LM, Parker GJM. Blood-brain barrier water exchange measurements using FEXI: Impact of modeling paradigm and relaxation time effects. *Magn Reson Med* 2023; : 1–17.
- 363 Iturria-Medina Y, Sotero RC, Toussaint PJ, Mateos-Pérez JM, Evans AC, Weiner MW *et al.*

- Early role of vascular dysregulation on late-onset Alzheimer's disease based on multifactorial data-driven analysis. *Nat Commun* 2016 71 2016; 7: 1–14.
- 364 Sweeney MD, Zhao Z, Montagne A, Nelson AR, Zlokovic B V. Blood-brain barrier: From physiology to disease and back. *Physiol Rev* 2019; 99: 21–78.
- 365 Iadecola C. The Neurovascular Unit Coming of Age: A Journey through Neurovascular Coupling in Health and Disease. *Neuron* 2017; 96: 17–42.
- 366 Holland PR, Searcy JL, Salvadores N, Scullion G, Chen G, Lawson G *et al.* Gliovascular disruption and cognitive deficits in a mouse model with features of small vessel disease. *J Cereb Blood Flow Metab* 2015; 35: 1005–1014.
- 367 Masamoto K, Tomita Y, Toriumi H, Aoki I, Unekawa M, Takuwa H *et al.* Repeated longitudinal in vivo imaging of neuro-glio-vascular unit at the peripheral boundary of ischemia in mouse cerebral cortex. *Neuroscience* 2012; 212: 190–200.
- 368 Hase Y, Chen A, Bates LL, Craggs LJL, Yamamoto Y, Gemmell E *et al.* Severe white matter astrocytopathy in CADASIL. *Brain Pathol* 2018; 28: 832–843.
- 369 Che Mohd Nassir CMN, Damodaran T, Yusof SR, Norazit A, Chilla G, Huen I *et al.* Aberrant Neurogliovascular Unit Dynamics in Cerebral Small Vessel Disease: A Rheological Clue to Vascular Parkinsonism. *Pharm 2021, Vol 13, Page 1207* 2021; 13: 1207.
- 370 Wendeln AC, Degenhardt K, Kaurani L, Gertig M, Ulas T, Jain G *et al.* Innate immune memory in the brain shapes neurological disease hallmarks. *Nature* 2018; 556: 332–338.
- 371 Abdelhak A, Foschi M, Abu-Rumeileh S, Yue JK, D'Anna L, Huss A *et al.* Blood GFAP as an emerging biomarker in brain and spinal cord disorders. *Nat Rev Neurol* 2022 183 2022; 18: 158–172.
- 372 Chouliaras L, Thomas A, Malpetti M, Donaghy P, Kane J, Mak E *et al.* Differential levels of plasma biomarkers of neurodegeneration in Lewy body dementia, Alzheimer's disease, frontotemporal dementia and progressive supranuclear palsy. *J Neurol Neurosurg Psychiatry* 2022; 93: 651–658.
- 373 Gaetani L, Blennow K, Calabresi P, Di Filippo M, Parnetti L, Zetterberg H. Neurofilament light chain as a biomarker in neurological disorders. *J Neurol Neurosurg Psychiatry* 2019; 90: 870–881.
- 374 Duering M, Konieczny MJ, Tiedt S, Baykara E, Tuladhar AM, van Leijssen E *et al.* Serum neurofilament light chain levels are related to small vessel disease burden. *J Stroke* 2018; 20: 228–238.
- 375 Egle M, Loubiere L, MacEski A, Kuhle J, Peters N, Markus HS. Neurofilament light chain predicts future dementia risk in cerebral small vessel disease. *J Neurol Neurosurg Psychiatry* 2021; 92: 582–589.
- 376 Nylén K, Öst M, Csajbok LZ, Nilsson I, Blennow K, Nellgård B *et al.* Increased serum-GFAP in patients with severe traumatic brain injury is related to outcome. *J Neurol Sci* 2006; 240: 85–91.
- 377 Khalil M, Pirpamer L, Hofer E, Voortman MM, Barro C, Leppert D *et al.* Serum neurofilament light levels in normal aging and their association with morphologic brain changes. *Nat Commun* 2020 111 2020; 11: 1–9.
- 378 Wallin A, Sjögren M. Cerebrospinal fluid cytoskeleton proteins in patients with subcortical white-matter dementia. *Mech Ageing Dev* 2001; 122: 1937–1949.

- 379 Pavlov AN, Khorovodov AP, Mamedova AT, Koronovskii AA, Pavlova ON, Semyachkina-Glushkovskaya O V. *et al.* Changes in blood–brain barrier permeability characterized from electroencephalograms with a combined wavelet and fluctuation analysis. *Eur Phys J Plus* 2021; 136: 1–9.
- 380 Livingston NR, Calsolaro V, Hinz R, Nowell J, Raza S, Gentleman S *et al.* Relationship between astrocyte reactivity, using novel 11C-BU99008 PET, and glucose metabolism, grey matter volume and amyloid load in cognitively impaired individuals. *Mol Psychiatry* 2022; 27: 2019–2029.
- 381 Garcia-Hernandez R, Cerdá AC, Carpena AT, Drakesmith M, Koller K, Jones DK *et al.* Mapping microglia and astrocyte activation in vivo using diffusion MRI. *Sci Adv* 2022; 8: 2923.
- 382 Poggesi A, Pasi M, Pescini F, Pantoni L, Inzitari D. Circulating biologic markers of endothelial dysfunction in cerebral small vessel disease: A review. *J Cereb Blood Flow Metab* 2016; 36: 72–94.
- 383 Van Dijk EJ, Prins ND, Vermeer SE, Vrooman HA, Hofman A, Koudstaal PJ *et al.* C-Reactive Protein and Cerebral Small-Vessel Disease. *Circulation* 2005; 112: 900–905.
- 384 Gu Y, Gutierrez J, Meier IB, Guzman VA, Manly JJ, Schupf N *et al.* Circulating inflammatory biomarkers are related to cerebrovascular disease in older adults. *Neurol - Neuroimmunol NeuroInflammation* 2019; 6: 1–14.
- 385 Heye AK. *Measurement of subtle blood-brain barrier disruption in cerebral small vessel disease using dynamic contrast enhanced magnetic resonance imaging.* 2016.
- 386 Rajani RM, Quick S, Ruigrok SR, Graham D, Harris SE, Verhaaren BFJ *et al.* Reversal of endothelial dysfunction reduces white matter vulnerability in cerebral small vessel disease in rats. *Sci Transl Med* 2018; 10: 9507.
- 387 Harrell Jr FE. *Regression Modeling Strategies.* 1st ed. Springer Verlag, 2013.
- 388 Austin PC, Steyerberg EW. The number of subjects per variable required in linear regression analyses. *J Clin Epidemiol* 2015; 68: 627–636.
- 389 Peduzzi P, Concato J, Kemper E, Holford TR, Feinstein AR. A simulation study of the number of events per variable in logistic regression analysis. *J Clin Epidemiol* 1996; 49: 1373–1379.
- 390 Ling Y, Chabriat H. Incident cerebral lacunes: A review. doi:10.1177/0271678X20908361.
- 391 Hayashida Y, Kakeda S, Hiai Y, Ide S, Ogasawara A, Ooki H *et al.* Diagnosis of intracranial hemorrhagic lesions: Comparison between 3D-SWAN (3D T2*-weighted imaging with multi-echo acquisition) and 2D-T2*-weighted imaging. *Acta radiol* 2014; 55: 201–207.
- 392 Yusuying S, Yusuyin S, Cheng X. Translocator Protein Regulate Polarization Phenotype Transformation of Microglia after Cerebral Ischemia–reperfusion Injury. *Neuroscience* 2022; 480: 203–216.
- 393 Ransohoff RM. A polarizing question: Do M1 and M2 microglia exist. *Nat Neurosci* 2016; 19: 987–991.
- 394 Olah M, Patrick E, Villani AC, Xu J, White CC, Ryan KJ *et al.* A transcriptomic atlas of aged human microglia. *Nat Commun* 2018; 9. doi:10.1038/s41467-018-02926-5.
- 395 Nutma E, Fancy N, Weinert M, Marzin MC, Tsartsalis S, Muirhead RCJ *et al.* Translocator protein is a marker of activated microglia in rodent models but not human neurodegenerative diseases. *bioRxiv* 2022; : 2022.05.11.491453.

- 396 Jordão JF, Thévenot E, Markham-Coultes K, Scarcelli T, Weng YQ, Xhima K *et al.* Amyloid- β plaque reduction, endogenous antibody delivery and glial activation by brain-targeted, transcranial focused ultrasound. *Exp Neurol* 2013; 248: 16–29.
- 397 Choi HJ, Han M, Seo H, Park CY, Lee EH, Park J. The new insight into the inflammatory response following focused ultrasound-mediated blood–brain barrier disruption. *Fluids Barriers CNS* 2022; 19: 1–21.
- 398 Silburt J, Lipsman N, Aubert I. Disrupting the blood–brain barrier with focused ultrasound: Perspectives on inflammation and regeneration. *Proc Natl Acad Sci U S A* 2017; 114: E6735–E6736.
- 399 Goldberg TE, Harvey PD, Wesnes KA, Snyder PJ, Schneider LS. Practice effects due to serial cognitive assessment: Implications for preclinical Alzheimer’s disease randomized controlled trials. *Alzheimer’s Dement Diagnosis, Assess Dis Monit* 2015; 1: 103–111.
- 400 Duff K, Lyketsos CG, Beglinger LJ, Chelune G, Moser DJ, Arndt S *et al.* Practice Effects Predict Cognitive Outcome in Amnesic Mild Cognitive Impairment. *Am J Geriatr Psychiatry* 2011; 19: 932–939.
- 401 Kumar A. Editorial: Neuroinflammation and Cognition. *Front Aging Neurosci* 2018; 10: 413.
- 402 Wakana S, Caprihan A, Fallon J, Panzenboeck MM, Fallon JH, Perry M *et al.* Reproducibility of Quantitative Tractography Methods Applied to Cerebral White Matter. *Neuroimage* 2007; 36: 630–644.
- 403 Ying C, Kang P, Binkley MM, Ford AL, Chen Y, Hassenstab J *et al.* Neuroinflammation and amyloid deposition in the progression of mixed Alzheimer and vascular dementia. *NeuroImage Clin* 2023; 38: 103373.
- 404 Low A, Mak E, Malpetti M, Passamonti L, Nicastro N, Stefaniak JD *et al.* In vivo neuroinflammation and cerebral small vessel disease in mild cognitive impairment and Alzheimer’s disease. *J Neurol Neurosurg Psychiatry* 2020; 0: jnnp-2020-323894.
- 405 Hill AB. The Environment and Disease: Association or Causation? *J R Soc Med* 1965; 58: 295–300.
- 406 Bowen NK, Guo S. *Structural Equation Modeling*. Oxford University Press (OUP), 2011.
- 407 Swardfager W, Yu D, Ramirez J, Cogo-Moreira H, Szilagyi G, Holmes MF *et al.* Peripheral inflammatory markers indicate microstructural damage within periventricular white matter hyperintensities in Alzheimer’s disease: A preliminary report. *Alzheimer’s Dement Diagnosis, Assess Dis Monit* 2017; 7: 56–60.
- 408 Iordanishvili E, Schall M, Loução R, Zimmermann M, Kotetishvili K, Shah NJ *et al.* Quantitative MRI of cerebral white matter hyperintensities: A new approach towards understanding the underlying pathology. *Neuroimage* 2019; 202. doi:10.1016/j.neuroimage.2019.116077.
- 409 Cai J, Sun J, Chen H, Chen Y, Zhou Y, Lou M *et al.* Different mechanisms in periventricular and deep white matter hyperintensities in old subjects. *Front Aging Neurosci* 2022; 14: 940538.
- 410 Sakamoto T, Ohashi W, Tomita K, Hattori K, Matsuda N, Hattori Y. Anti-inflammatory properties of cilostazol: Its interruption of DNA binding activity of NF- κ B from the Toll-like receptor signaling pathways. *Int Immunopharmacol* 2018; 62: 120–131.
- 411 Tardif J-C, Kouz S, Waters DD, Bertrand OF, Diaz R, Maggioni AP *et al.* Efficacy and Safety of Low-Dose Colchicine after Myocardial Infarction. *N Engl J Med* 2019; 381: 2497–2505.

- 412 Nidorf SM, Fiolet ATL, Mosterd A, Eikelboom JW, Schut A, Opstal TSJ *et al.* Colchicine in Patients with Chronic Coronary Disease. *N Engl J Med* 2020; 383: 1838–1847.
- 413 Askew KE, Beverley J, Sigfridsson E, Szymkowiak S, Emelianova K, Dando O *et al.* Inhibiting CSF1R alleviates cerebrovascular white matter disease and cognitive impairment. *Glia* 2023; : 375–395.
- 414 Deshmane SL, Kremlev S, Amini S, Sawaya BE. Monocyte Chemoattractant Protein-1 (MCP-1): An Overview. *J Interf Cytokine Res* 2009; 29: 313.
- 415 Guo Y, Li Y, Liu X, Cui Y, Zhao Y, Sun S *et al.* Assessing the effectiveness of statin therapy for alleviating cerebral small vessel disease progression in people ≥ 75 years of age. *BMC Geriatr* 2020; 20. doi:10.1186/s12877-020-01682-w.
- 416 Brickman AM, Zahodne LB, Guzman VA, Narkhede A, Meier IB, Griffith EY *et al.* Reconsidering harbingers of dementia: progression of parietal lobe white matter hyperintensities predicts Alzheimer’s disease incidence. *Neurobiol Aging* 2015; 36: 27–32.
- 417 Kim SJ, Lee DK, Jang YK, Jang H, Kim SE, Cho SH *et al.* The Effects of Longitudinal White Matter Hyperintensity Change on Cognitive Decline and Cortical Thinning over Three Years. *J Clin Med* 2020; 9: 2663.
- 418 Ma Y, Yilmaz P, Bos D, Blacker D, Viswanathan A, Ikram MA *et al.* Blood Pressure Variation and Subclinical Brain Disease. *J Am Coll Cardiol* 2020; 75: 2387–2399.
- 419 Al-Janabi OM, Bauer CE, Goldstein LB, Murphy RR, Bahrani AA, Smith CD *et al.* White Matter Hyperintensity Regression: Comparison of Brain Atrophy and Cognitive Profiles with Progression and Stable Groups. *Brain Sci* 2019, Vol 9, Page 170 2019; 9: 170.
- 420 Khalaf A, Edelman K, Tudorascu D, Andreescu C, Reynolds CF, Aizenstein H. White matter hyperintensity accumulation during treatment of late-life depression. *Neuropsychopharmacology* 2015; 40: 3027–3035.
- 421 Findlay MD, Dawson J, Dickie DA, Forbes KP, McGlynn D, Quinn T *et al.* Investigating the relationship between cerebral blood flow and cognitive function in hemodialysis patients. *J Am Soc Nephrol* 2019; 30: 147–158.
- 422 Maillard P, Carmichael O, Harvey D, Fletcher E, Reed B, Mungas D *et al.* FLAIR and Diffusion MRI Signals Are Independent Predictors of White Matter Hyperintensities. *Am J Neuroradiol* 2012; 34: 54–61.
- 423 Moon SY, de Souto Barreto P, Rolland Y, Chupin M, Bouyahia A, Fillon L *et al.* Prospective associations between white matter hyperintensities and lower extremity function. *Neurology* 2018; 90: e1291–e1297.
- 424 Nebes RD, Reynolds CF, Boada F, Meltzer CC, Fukui MB, Saxton J *et al.* Longitudinal increase in the volume of white matter hyperintensities in late-onset depression. *Int J Geriatr Psychiatry* 2002; 17: 526–530.
- 425 van Leijssen EM, de Leeuw F-E, Tuladhar AM. Disease progression and regression in sporadic small vessel disease - insights from neuroimaging. *Clin Sci* 2017; : 1192–1206.
- 426 Prins N, Straaten E van, Dijk E van, Simoni M, Shijndel R van, Vrooman H *et al.* Measuring progression of cerebral white matter lesions on MRI. *Neurology* 2004; 62: 1533–1539.
- 427 Wohl MA, Boone KB, Miller BL, Lesser IM, Mehringer CM. White matter hyperintensities in healthy older adults: A longitudinal study. *Int J Geriatr Psychiatry* 1994; 9: 273–277.
- 428 Garde E, Lykke Mortensen E, Rostrup E, Paulson OB. Decline in intelligence is associated

- with progression in white matter hyperintensity volume. *J Neurol Neurosurg Psychiatry* 2005; 76: 1289–1291.
- 429 Cho A-H, Kim H-R, Kim W, Yang DW. White matter hyperintensity in ischemic stroke patients: it may regress over time. *J stroke* 2015; 17: 60–6.
- 430 Silbert LC, Nelson C, Howieson DB, Moore MM, Kaye JA. Impact of white matter hyperintensity volume progression on rate of cognitive and motor decline. *Neurology* 2008; 71: 108–113.
- 431 Liu T, Sachdev PS, Lipnicki DM, Jiang J, Geng G, Zhu W *et al.* Limited relationships between two-year changes in sulcal morphology and other common neuroimaging indices in the elderly. *Neuroimage* 2013; 83: 12–17.
- 432 Valdés Hernández M del C, González-Castro V, Chappell FM, Sakka E, Makin S, Armitage PA *et al.* Application of Texture Analysis to Study Small Vessel Disease and Blood–Brain Barrier Integrity. *Front Neurol* 2017; 8: 327.
- 433 Van Sloten TT, Sigurdsson S, Van Buchem MA, Phillips CL, Jonsson P V, Ding J *et al.* Cerebral Small Vessel Disease and Association With Higher Incidence of Depressive Symptoms in a General Elderly Population: The AGES-Reykjavik Study. *Am J Psychiatry* 2015; 172: 570–578.
- 434 Wang X, Valdés Hernández MC, Doubal F, Chappell FM, Wardlaw JM. How Much Do Focal Infarcts Distort White Matter Lesions and Global Cerebral Atrophy Measures? *Cerebrovasc Dis* 2012; 34: 336–342.
- 435 Lee W-J, Jung K-H, Ryu YJ, Lee S-T, Park K-I, Chu K *et al.* Echocardiographic index E/e' in association with cerebral white matter hyperintensity progression. *PLoS One* 2020; 15: e0236473.
- 436 Jiaerken Y, Luo X, Yu X, Huang P, Xu X, Zhang M. Microstructural and metabolic changes in the longitudinal progression of white matter hyperintensities. *J Cereb Blood Flow Metab* 2019; 39: 1613–1622.
- 437 Cook I, Leuchter A, Morgan M, Dunkin J, Witte E, David S *et al.* Longitudinal Progression of Subclinical Structural Brain Disease in Normal Aging. *Am J Geriatr Psychiatry* 2004; 12: 190–200.
- 438 Sam K, Crawley AP, Conklin J, Poublanc J, Sobczyk O, Mandell DM *et al.* Development of White Matter Hyperintensity Is Preceded by Reduced Cerebrovascular Reactivity. *Ann Neurol* 2016; 80: 277–285.
- 439 Hooshmand B, Mangialasche F, Kalpouzos G, Solomon A, Kareholt I, Smith AD *et al.* Association of Vitamin B12, folate, and sulfur amino acids with brain magnetic resonance imaging measures in older adults a longitudinal population-based study. *JAMA Psychiatry* 2016; 73: 606–613.
- 440 de Bresser J, Reijmer YD, van den Berg E, Breedijk MA, Kappelle LJ, Viergever MA *et al.* Microvascular Determinants of Cognitive Decline and Brain Volume Change in Elderly Patients with Type 2 Diabetes. *Dement Geriatr Cogn Disord* 2010; 30: 381–386.
- 441 Wolfson L, Wei X, Hall CB, Panzer V, Wakefield D, Benson RR *et al.* Accrual of MRI white matter abnormalities in elderly with normal and impaired mobility. *J Neurol Sci* 2005; 232: 23–27.

APPENDIX A. Studies included in WMH progression review (chapter two).

Table A.1 shows the list of studies identified and included in the systematic review and meta-analysis, including cohort details, subgroups if relevant, baseline WMH volume, image analysis pipeline and annualised WMH growth.

Reference	Cohort	Subgroups (if applicable)	Number of participants	Annualised WMH growth (cc/y)	Baseline WMH (cc)	Image analysis pipeline	Sequence used to segment WMHs	Field strength (T)	Slice thickness (mm)
Dufouil et al. 2005 ¹⁶⁶	Perindopril Protection Against Recurrent Stroke Study (PROGRESS)	Control Perindopril	103 89	0.0006 [‡] 0.00013 [‡]	0.0018 [‡]	Manual	T2	1.0/1.5	5
Godin et al. 2011 ²⁷⁶	3C-Dijon	Controls Hypertensive patients	402 917	0.06 0.4	5.6	Semi-automated - segmentation in <i>SPM99</i> and in house multispectral Bayesian classifier (<i>Université Paris, France</i>)	T2	1.5	3.5
Ammirati et al. 2019 ¹⁶⁴	Asymptomatic patients with carotid stenosis		51	0.08 [#]	0.97	Semi-automated – local thresholding segmentation program (<i>Jim6, www.xinapse.com</i>)	FLAIR	1.5	
Guo et al. 2020 ⁴¹⁵	Population-based cohort and trial of rosuvastatin vs placebo	Control Rosuvastatin	662 119	0.11 0.23	5.05 4.29	Automated – in house (<i>Shandong First Medical University, Shandong, China</i>)	FLAIR	3	2
Markus et al. 2005 ²⁶⁴	Austrian Stroke Prevention Study (ASPS)		267	0.18 (years 1-3) 0.29 (year 4-6)	1.32	Semi-automated – (<i>DisplImage, University College London, UK</i>)	T2	1.5	5
Brickman et al. 2015 ⁴¹⁶	Dementia patients vs controls	Controls Alzheimer's disease	261 26	0.2	7.91 9.18	Semi-automated – in house (<i>Columbia, USA</i>)	FLAIR	1.5	1.3
Kim et al. 2020 ⁴¹⁷	MCI patients		87	0.22	40.58	Automated – in house tissue classifier algorithm (<i>Hanyang University, Seoul, Republic of Korea</i>)	FLAIR	3	2

Van der Veen et al. 2013 ²⁹⁴	Second Manifestation of ARterial disease – MRI study (SMART-MR)		663	0.23 [#]	2.8	Semi-automated – in house k-nearest neighbours clustering algorithm (<i>Utrecht, Netherlands</i>)	FLAIR	1.5	4
Nasrallah et al. 2019 ²⁴⁰	Systolic blood Pressure INtervention Trial – Memory and cognition IN Decreased hypertension (SPRINT-MIND)	Control Intensive BP treatment	200 249	0.23 0.37	4.57 4.4	Automated – in house deep learning based segmentation algorithm (<i>Pennsylvania, USA</i>)	FLAIR	3	1
Burton et al. 2006 ¹⁸⁴	Dementia patients vs controls	Controls AD DLB PD	33 14 14 13	0.23 0.74 0.28 0.75	5 14 5 6	Semi-automated – in house contouring algorithm (<i>Newcastle, UK</i>)	FLAIR	1.5	5
Callisaya et al. 2013 ⁵⁰	Tasmanian Study of Cognition and Gait (TASCOG)		225	0.24	5.6	Automated – segmentation in <i>SPM5</i> then in house adaptive boosting statistical classifier (<i>Monash, Austria</i>)	FLAIR	1.5	3
Ma et al. 2020 ⁴¹⁸	Rotterdam Scan study		1109	0.28 [#]	5.68	Semi-automated – in house k-nearest neighbours clustering algorithm (<i>Erasmus, Netherlands</i>)	FLAIR	1.5	
Whitman et al. 2001 ²⁶⁷	Healthy population (age 74-88)		70	0.28	3.1	Manual	T2	1.5	5
Al-Janabi et al. 2019 ⁴¹⁹	Alzheimer's Disease Neuroimaging Initiative 2 (ADNI2)		351	0.31	6.27	Automated – in house Bayesian classifier (<i>University of California Davis, USA</i>)	FLAIR	1.5	1.2
ter Telgte et al. 2019 ³⁰⁶	RUN-DMC InTENse		54	0.32	5	Automated – in house neural network (<i>Nijmegen, Netherlands</i>)	FLAIR	3	0.85
Khalaf et al. 2015 ⁴²⁰	Patients with late life depression	Remitters Non-remitters	23 24	0.35 0.69	0.41 0.71	Automated – in house fuzzy connectedness algorithm (<i>Johns Hopkins, USA</i>)	FLAIR	3	3
Nylander et al. 2018 ⁹⁸	Prospective Investigation of the Vasculature in Uppsala Seniors (PIVUS)		252	0.36 [#]	10.1	Automated (<i>CASCADE, ki.se/en/nvs/cas- cade</i>)	T2	1.5	3

Findlay et al. 2019 ⁴²¹	Patients with end-stage renal failure	Dialysis Renal transplant	24 10	0.38 [#] 0.01 [#]	2.96 0.28	Semi-automated	FLAIR	3	
ten Dam et al. 2006 ¹⁶⁷	Prospective Study of Pravastatin in Elderly at Risk (PROSPER)	Pravastatin Control	265 270	0.4 [#] 0.4 [#]	1.8 1.6	Semi-automated – in house segmentation algorithm (<i>Leiden, Netherlands</i>)	FLAIR	1.5	
Ramirez et al. 2016 ¹⁸⁵	Dementia patients vs controls	Controls AD without SVD AD with severe baseline SVD	44 56 57	0.4 0.16 1.0	4.4	Semi-automated (<i>Lesion Explorer, https://www.rotman-baycrest.on.ca/files/publicationmodule/@random45f5724eba2f8/Ramirez_etal2011.pdf</i>)	T2	1.5	3
Maillard et al. 2012 ⁴²²	Alzheimer's disease, mild cognitive impairment and controls	Control MCI AD	72 34 13	0.41 0.47 1.22	6.6 9.4 9.0	Semi-automated - segmentation in SPM99 and in house multispectral Bayesian classifier (<i>Université Paris, France</i>)	FLAIR	1.5	
Moon et al. <i>Neurol</i> 2018 ⁴²³	Multidomain Alzheimer's Preventive Trial (MAPT)		358	0.44	12.6	Automated (<i>White matter Hyperintensity Automated Segmentation Algorithm contrast based algorithm, WHASA</i>)	FLAIR		
Nebes et al. 2002 ⁴²⁴	Case of depression vs 12 controls	Controls Depressed	12 1	0.47 8.42	5.32 12.05	Semi-automated – in house border identification algorithm (<i>Massachusetts General Hospital, USA</i>)	FLAIR	1.5	3
van Leijsen et al. 2017 ⁴²⁵	RUN-DMC		276	0.5	5.8	Semi-automated (SPM12, https://www.fil.ion.ucl.ac.uk/spm/software/spm12/)	FLAIR	1.5	5
Promjunyakul et al. 2015 ⁹¹	Healthy population (age >65)		24	0.51 (incident within first five voxel layers of existing lesions)		Semi-automated - in house clustering algorithm (<i>Oregon, USA</i>)	FLAIR	3	2
Prins et al. 2004 ⁴²⁶	Dementia patients		20	0.57 [#]	3.3	Semi-automated (<i>Show_Images 3.6.1</i>)	T2	1.5	5
Gottesman et al. 2010 ⁸⁷	Atherosclerosis Risk in Communities (ARIC)		983	0.58	7.8	Automated – in house signal intensity classifier (<i>Johns Hopkins, USA</i>)	FLAIR	1.5	5

Wohl et al. 1994 ⁴²⁷	Healthy population (age 47-83)		16	0.58	2.74	Manual	T2	1.5	3
Garde et al. 2005 ⁴²⁸	Healthy population (age 80)		26	0.63 [#]	4.7	Automated – in house local thresholding algorithm (<i>Copenhagen, Denmark</i>)	T2	1.5	2
Van Dalen et al. 2017 ²³⁹	Prevention of Dementia by Intensive Vascular Care (PreDIVA)	Controls Intensive CVD treatment	36 24	0.7 0.73	5.7 6.3	Automated – in house k-nearest neighbours clustering algorithm (<i>Amsterdam, Netherlands</i>)	FLAIR	3	1.2
Johnson et al. 2016 ²⁷⁸	NeuroCognitive Outcomes of Depression in the Elderly (NCODE)	Depressed Control	130 110	0.74 0.72	6.7 5.18	Semi-automated (<i>MRX, GE</i>)	T2	1.5	3
Raz et al. 2007 ²⁷¹	Hypertensive patients vs controls	Controls Hypertensive	23 23	0.75 [#] 1.15 [#]	6.36	Manual	T2	1.5	5
Cho et al. 2015 ⁴²⁹	Stroke patients		100	0.865	2.78	Semi-automated (<i>Analyze 10.0, www.analyzedirect.com</i>)	FLAIR		4.5
Silbert et al. 2008 ⁴³⁰	Oregon Brain Aging Study (OBAS)		104	0.9	9.73	Semi-automated (<i>REGION</i>)	T2	1.5	4
Liu et al. 2013 ⁴³¹	Sydney Memory and Ageing Study		185	0.9	12.3	Automated – in house k-nearest neighbours clustering algorithm (<i>University of South Wales, Australia</i>)	FLAIR	3	
Mok et al. 2009 ²³⁸	Regression of Cerebral Artery Stenosis trial (ROCAS trial)	Control Simvastatin	106 102	0.95 [#] 1.5 [#]	1.1 1.6	Semi-automated (<i>Easy Vision 4.3, Phillips</i>)	T2	1.5	
Valdes Hernandez et al. 2016 ⁴³²	Patients with mild stroke		46	0.97 [#]		Semi-automated – multispectral classifier (<i>MCMxxxVI, University of Edinburgh, UK</i>)	FLAIR	1.5	
Peng et al. 2014 ²⁸²	Hypertensive patients aged >80		294	1.01	13.78	Automated (<i>Freesurfer, surfer.nmr.mgh.harvard.edu</i>)	FLAIR	3	1
Van Sloten et al. 2015 ⁴³³	Age, Gene/ Environment Susceptibility (AGES-Reykjavik)		1949	1.2	11	Automated – in house neural network-based classifier (<i>Reykjavik, Iceland</i>)	FLAIR	1.5	3

Wang et al. 2012 ⁴³⁴	Mild stroke patients		46	1.21 [#]	12.17	Semi-automated – multispectral classifier (<i>MCMxxxVI, University of Edinburgh, UK</i>)	FLAIR	1.5	
Lee et al. 2017 Radiol ¹⁵³	Healthy population (age 50-87)		450	1.27	9.66	Semi-automated (<i>NeuroROI, University of Nottingham, UK</i>)	FLAIR	1.5/3	3
Chappell et al. 2017 ²⁶²	First stroke patients		264	1.27	22	Semi-automated – multispectral classifier (<i>MCMxxxVI, University of Edinburgh, UK</i>)	FLAIR	1.5	5
Lee et al. 2020 ⁴³⁵	Patients attending routine healthcheck		392	1.35 [#]	10.01	Semi-automated (<i>NeuroROI, University of Nottingham, UK</i>)	FLAIR	1.5	4
Bernbaum et al. 2015 ¹⁵⁵	CATCH (Minor stroke/TIA patients)		40	1.83	9.21	Manual	FLAIR	3	3.5
Jiaerken et al. 2019 ⁴³⁶	Alzheimer's Disease Neuroimaging Initiative (ADNI)	Controls MCI AD	19 16 5	1.98 1.26 8.45	11.11 14.37 36.17	Semi-automated (<i>SPM12, https://www.fil.ion.ucl.ac.uk/spm/software/spm12 and in house manual correction</i>)	FLAIR	3	5
Sachdev et al. 2007 ⁸⁴	Healthy population (age 58-85)		51	2.15	16.38	Automated (<i>SPM99, https://www.fil.ion.ucl.ac.uk/spm/software/spm99, Analyze, www.analyzedirect.com and in house, University of New South Wales, Australia</i>)	FLAIR	1.5	4
Gouw et al.. 2008 ⁷⁰	Leukoaraiosis And DISability in the elderly (LADIS)		20	2.3	24.6	Semi-automated (<i>Show_Images 3.6.1</i>)	FLAIR	0.5/1.5	5
Cook et al. 2004 ⁴³⁷	Healthy population (age 60-89)		29	2.89	8.4	Semi-automated (<i>MRX, GE</i>)	FLAIR	1.5	3
Sam et al.2016 ⁴³⁸	Patients with SVD (Fazekas score >2 on MRI)		45	3.3	26.7	Semi-automated (<i>SPM8, https://www.fil.ion.ucl.ac.uk/spm/software/spm8, Lesion Explorer, https://www.rotman-baycrest.on.ca/files/publicationmodule/@random45f5724eba2f8/Ramirez_etal2011.pdf and AFNI afni.nimh.nih.gov</i>)	FLAIR	3	3

Moscufo et al. 2012 ⁵¹	Healthy population (age >75)		77	3.3	13.9	Semi-automated (<i>Freesurfer, surfer.nmr.mgh.harvard.edu and 3D Slicer</i>)	FLAIR	3	1.3
Lambert et al. 2016 ³⁰⁰	St George's Cognition and Neuroimaging Study (SCANS)		99	5.62	31.9	Semi-automated (<i>SPM12, https://www.fil.ion.ucl.ac.uk/spm/software/spm12 using group averaged tissue probability maps, and ITK-SNAP, www.itksnap.org/</i>)	FLAIR	1.5	5
<i>Studies reporting values other than cubic centimetre/millilitre equivalent:</i>									
Hooshmand et al. 2016 ⁴³⁹	Swedish National Study on Aging and Care in Kungsholmen (SNAC-K)		299	0.00005% TBV		Semi-automated (<i>SPM12, https://www.fil.ion.ucl.ac.uk/spm/software/spm12/</i>)	T2		
Goldstein et al. 2005 ²⁷⁷	Healthy population (age 55-79)		121	0.0066% TBV	0.094% ICV	Manual	T2	1.5	3
Firbank et al. 2007 ⁸³	Study in COgnition and Prognosis in the Elderly (SCOPE)	Normotensive Hypertensive on Candesartan Hypertensive on placebo	41 45 47	0.021% TBV 0.0285% TBV 0.036% TBV		Automated (<i>SPM99, https://www.fil.ion.ucl.ac.uk/spm/software/spm99/</i>)	T2	1.5	5
de Bresser et al. 2010 ⁴⁴⁰	Type 2 diabetes patients vs controls	Controls Type 2 DM	34 68	0.03% TBV 0.035% TBV		Semi-automated – in house k-nearest neighbours clustering algorithm (<i>Utrecht, Netherlands</i>)	FLAIR	1.5	4
Dickie et al. 2016 ²⁷⁴	Lothian birth cohort		351	0.86% TBV	0.76% ICV	Semi-automated – multispectral classifier (<i>MCMxxxVI, University of Edinburgh, UK</i>)	FLAIR	1.5	4
Wolfson et al. 2005 ⁴⁴¹	Mobility-impaired patients vs controls 14	Controls Patients	7 7	0.02% TICV 0.1% TICV		Automated – 3D expectation-maximisation algorithm (<i>Harvard, USA</i>)	T2	1.5	3
Gu et al. 2019 ³⁸⁴	Washington Heights-Hamilton Height-Inwood and Columbia		310	0.92% TICV	-6.02 (log WMH /ICV ratio)	Automated – in house seed-growing algorithm (<i>Columbia, USA</i>)	FLAIR	1.5	3

	Aging Project (WHICAP)								
Liu et al. 2016 ²⁸⁰	Healthy population (age >80)		232	6.39% of baseline lesion volume	5.11	Semi-automated (<i>Freesurfer</i> , <i>surfer.nmr.mgh.harvard.edu</i> and <i>FMRIB Automated Segmentation Tool</i> , https://fsl.fmrib.ox.ac.uk/fsl/fslwiki/FAST)	FLAIR	3	1

APPENDIX B. MRI sequence details (chapters four to eight).

Table B.1 shows the MRI sequence parameters used for imaging in the PET-MRI cohort of patients with SVD and healthy control participants.

Sequence	Acquisition parameters
T ₁ -weighted	Axial 3D fast-spoiled gradient echo sequence (BRAVO), flip angle = 12°, inversion time = 450ms, field of view = 28 mm, slice thickness = 1mm, number of slices = 192, reconstructed matrix size = 512 × 512
T ₂ -weighted	Axial T ₂ fast-spoiled gradient echo sequence angled anterior commissure-posterior commissure (AC-PC), flip angle = 111°, TE = 85 ms, TR = 6000ms, field of view = 22mm, slice thickness = 5 mm, number of slices = 31, reconstructed matrix size = 1024 × 1024
FLAIR	Axial T ₂ FLAIR, angled AC-PC, flip angle = 160°, TR = 8800ms, TE = 120ms, TI = 2445ms, field of view = 22mm, slice thickness = 5 mm, number of slices = 28, reconstructed matrix size = 256 × 256
Susceptibility-weighted	Axial susceptibility weighted imaging, flip angle = 17°, repetition time = 40.6ms, echo time = 24.2ms, field of view = 22 mm, slice thickness = 2mm, number of slices = 70, reconstructed matrix size = 256 × 256
DTI	Axial DTI, angled anterior commissure-posterior commissure with the diffusion gradients applied in 63 directions with a b-value = 1000s/mm ² , TE = minimum, TR = 15763ms, field of view = 19.2mm, slice thickness = 2 mm, number of slices = 65-70 depending on slice angulation reconstructed matrix size = 256 × 256
DCE-MRI	3D radiofrequency spoiled gradient echo, TR = 6.3ms, TE = 1.784ms, number of slices = 16, reconstructed matrix size = 256 × 256, final resolution = 0.94 × 0.94 × 3mm, flip angles = 2°, 5°, 12°, 17°, 22°, 27°, temporal resolution = 15 seconds per flip angle with interphase interval 15 seconds (eight cycles)

APPENDIX C. Intra- and inter-assay reliability data for proteomics panel data.

Table C.1 shows the distribution of intra-assay coefficients of variance across the 92 biomarkers in the Olink CVD III panel.

Coefficient of variance range	<5%	5-10%	10-15%	>15%
Number of biomarkers	12	59	19	2

Table C.2 shows the distribution of inter-assay coefficients of variance across the 92 biomarkers.

Coefficient of variance range	<10%	10-20%	20-30%	>30%
Number of biomarkers	31	53	8	0

APPENDIX D. Univariate regression model results for individual Olink biomarkers as predictors of radiological features of SVD (chapter six).

Table D.1 shows the univariate regression model β coefficients and p values for WMH volume, lacune count, CMB count and brain volume for each individual biomarker in the Olink CVD III panel. Green cells represent protective associations (i.e. negative correlation with WMHs, CMBs and lacunes, and positive correlation with brain volume) and red cells represent deleterious associations. Uncorrected p values are highlighted yellow at <0.05 .

Marker	WMHs		Lacunes		CMBs		Brain volume	
	β	p value	β	p value	β	p value	β	p value
BLM.hydrolase	0.402	0.002	0.148	0.273	0.272	0.037	-0.230	0.070
MB	0.387	0.004	0.060	0.665	0.151	0.261	0.056	0.666
Gal.4	0.390	0.005	0.007	0.961	0.249	0.064	-0.083	0.538
TNFRSF10C	0.320	0.021	-0.145	0.310	0.003	0.982	-0.086	0.525
TR	0.280	0.046	-0.015	0.919	0.085	0.532	-0.096	0.469
PECAM.1	-0.262	0.077	-0.218	0.167	-0.030	0.837	-0.095	0.535
ITGB2	-0.244	0.080	-0.157	0.256	-0.276	0.037	-0.127	0.335
DLK.1	-0.243	0.081	-0.178	0.200	-0.210	0.116	-0.003	0.980
CHIT1	-0.226	0.104	-0.131	0.340	-0.155	0.246	-0.091	0.478
TIMP4	0.217	0.120	0.131	0.350	0.147	0.274	-0.009	0.945
NT.proBNP	0.209	0.134	0.091	0.517	-0.086	0.525	-0.170	0.206
CCL24	-0.207	0.136	0.010	0.940	-0.186	0.161	0.085	0.506
OPG	0.185	0.180	0.239	0.076	0.127	0.338	-0.207	0.120
SELE	-0.187	0.180	-0.079	0.571	-0.028	0.836	-0.183	0.197
LTBR	-0.186	0.186	0.174	0.260	-0.068	0.615	-0.054	0.715
TNFSF13B	0.183	0.190	-0.094	0.524	-0.039	0.770	0.072	0.599
SELP	-0.184	0.195	-0.128	0.361	-0.157	0.247	0.051	0.724
RETN	0.181	0.216	0.237	0.098	-0.158	0.258	-0.145	0.284
TR.AP	0.166	0.232	-0.037	0.790	0.010	0.939	-0.116	0.371
CTSD	-0.165	0.236	0.147	0.283	-0.060	0.654	0.064	0.622
PRTN3	-0.170	0.240	-0.159	0.263	0.073	0.600	0.002	0.990
ICAM.2	-0.160	0.254	-0.054	0.698	-0.059	0.660	-0.143	0.299
LDL.receptor	-0.159	0.256	-0.052	0.737	-0.101	0.454	0.084	0.562
Notch.3	0.158	0.271	0.175	0.222	0.002	0.988	0.197	0.141
Ep.CAM	-0.146	0.293	0.093	0.498	0.058	0.664	-0.014	0.915
MMP.9	-0.145	0.301	-0.167	0.225	-0.207	0.118	0.008	0.955
GP6	0.143	0.303	0.033	0.808	0.060	0.652	-0.028	0.829

CD163	0.140	0.313	-0.134	0.330	-0.295	0.023	-0.015	0.908
SHPS.1	-0.139	0.324	-0.091	0.525	-0.034	0.800	0.016	0.903
PLC	-0.138	0.329	0.111	0.431	0.156	0.245	-0.199	0.134
TLT.2	0.139	0.335	0.012	0.937	-0.016	0.909	0.162	0.236
CHI3L1	-0.138	0.341	-0.107	0.477	-0.086	0.535	-0.038	0.789
AZU1	-0.131	0.350	-0.267	0.052	-0.284	0.030	-0.091	0.485
CD93	0.124	0.375	0.120	0.381	0.145	0.275	-0.007	0.954
GDF.15	-0.132	0.378	-0.010	0.945	-0.032	0.821	-0.279	0.042
ST2	-0.130	0.389	-0.003	0.985	-0.094	0.514	0.099	0.510
vWF	0.124	0.396	-0.055	0.707	0.047	0.739	-0.052	0.707
TFF3	0.117	0.403	0.133	0.338	0.181	0.174	0.030	0.816
TFPI	-0.117	0.403	-0.064	0.652	0.150	0.260	0.267	0.047
OPN	-0.115	0.411	0.157	0.251	-0.066	0.625	0.074	0.567
IL2.RA	0.111	0.428	0.136	0.333	0.191	0.150	-0.122	0.365
TNFRSF14	-0.109	0.438	0.078	0.574	0.033	0.804	-0.012	0.926
Gal.3	0.112	0.440	0.045	0.775	0.174	0.208	-0.223	0.135
MPO	0.107	0.442	0.152	0.285	0.123	0.353	-0.161	0.226
CCL16	0.102	0.466	0.079	0.565	0.159	0.233	-0.023	0.857
PSP.D	0.099	0.486	0.004	0.978	-0.034	0.803	0.039	0.770
CSTB	-0.100	0.489	0.263	0.065	0.195	0.153	-0.032	0.817
ALCAM	-0.100	0.505	-0.155	0.327	-0.010	0.944	-0.123	0.429
MCP.1	-0.088	0.524	-0.123	0.375	-0.168	0.200	0.125	0.336
MMP.2	0.086	0.544	-0.081	0.570	-0.145	0.283	0.146	0.274
CCL15	-0.085	0.545	0.020	0.889	0.089	0.505	-0.045	0.734
IL.17RA	0.087	0.555	0.021	0.884	-0.035	0.805	0.021	0.877
PGLYRP1	-0.080	0.563	0.038	0.794	-0.028	0.830	0.094	0.490
CASP.3	-0.079	0.570	0.104	0.447	0.136	0.301	-0.011	0.933
t.PA	-0.076	0.583	0.032	0.816	0.060	0.648	0.076	0.550
uPA	0.073	0.600	0.145	0.308	0.083	0.532	0.193	0.141
GRN	-0.075	0.606	-0.043	0.771	-0.069	0.615	-0.018	0.895
JAM.A	0.068	0.629	-0.086	0.536	-0.043	0.747	0.116	0.368
IL.6RA	-0.065	0.643	0.021	0.881	0.010	0.940	-0.154	0.254
PI3	-0.060	0.667	-0.017	0.910	0.003	0.982	-0.173	0.232
IGFBP.2	-0.059	0.675	-0.128	0.355	-0.198	0.138	-0.071	0.581
CDH5	-0.056	0.689	0.018	0.900	-0.045	0.737	0.202	0.115
AP.N	0.055	0.696	0.128	0.350	0.167	0.209	-0.022	0.867
MEPE	0.058	0.697	0.116	0.425	0.176	0.210	0.000	0.999
TNF.R2	-0.055	0.699	-0.016	0.909	-0.030	0.822	0.102	0.433
IGFBP.7	0.054	0.699	0.090	0.520	0.077	0.562	0.119	0.358
IL.18BP	-0.055	0.700	-0.130	0.353	0.019	0.891	0.015	0.913
IL.1RT1	0.054	0.701	-0.080	0.578	-0.231	0.082	0.062	0.643
PCSK9	0.046	0.738	0.099	0.468	0.210	0.109	-0.117	0.359
CPB1	-0.042	0.761	0.210	0.120	0.010	0.941	0.057	0.656
RARRES2	-0.041	0.766	0.064	0.645	0.014	0.914	-0.128	0.326
EGFR	-0.041	0.768	-0.046	0.735	-0.061	0.648	0.241	0.057
PAI	-0.040	0.777	0.019	0.891	-0.089	0.506	0.122	0.349
U.PAR	0.037	0.796	0.180	0.193	0.173	0.198	-0.118	0.362
CTSZ	0.035	0.804	-0.186	0.175	-0.163	0.215	-0.010	0.937

IGFBP.1	-0.033	0.820	-0.150	0.289	-0.414	0.002	0.007	0.959
PDGF.subunit.A	0.030	0.829	-0.158	0.251	-0.086	0.515	-0.276	0.034
MMP.3	-0.029	0.833	-0.024	0.860	-0.098	0.463	-0.132	0.304
EPHB4	-0.031	0.834	-0.050	0.742	-0.103	0.457	-0.166	0.241
FABP4	0.030	0.835	0.026	0.861	0.011	0.935	0.242	0.071
CXCL16	0.024	0.866	0.129	0.356	-0.019	0.888	-0.236	0.066
TNF.R1	-0.023	0.869	-0.046	0.737	-0.118	0.374	-0.144	0.253
COL1A1	0.021	0.880	-0.112	0.422	-0.043	0.747	0.021	0.872
SCGB3A2	-0.020	0.887	-0.034	0.804	-0.025	0.848	0.281	0.026
CNTN1	0.020	0.890	0.070	0.628	-0.015	0.913	0.019	0.885
KLK6	0.017	0.904	-0.047	0.734	0.025	0.852	-0.095	0.466
IL.1RT2	0.015	0.917	-0.033	0.813	0.141	0.292	0.159	0.223
SPON1	-0.010	0.944	0.252	0.064	0.171	0.201	-0.100	0.446
PON3	0.007	0.960	-0.205	0.134	-0.157	0.237	0.045	0.729
CPA1	-0.007	0.963	-0.256	0.065	-0.146	0.268	0.173	0.190
FAS	-0.001	0.995	-0.084	0.546	-0.026	0.846	0.192	0.133
AXL	0.000	0.998	0.086	0.538	-0.176	0.185	0.056	0.677

APPENDIX E. Univariate regression model results for individual Olink biomarkers as predictors of BBB permeability (chapter seven).

Table E.1 shows the univariate regression model β coefficients and p values for BBB hotspot proportion and Q_{alb} for each individual biomarker in the Olink CVD III panel. Green cells represent protective associations (i.e. negative correlation with WMHs, CMBs and lacunes, and positive correlation with brain volume) and red cells represent deleterious associations. Uncorrected p values are highlighted yellow at <0.05 .

Marker	BBB hotspot proportion		Q_{alb}	
	β	p value	β	p value
PI3	0.443046	0.005792	-0.32745	0.398358
TFPI	-0.37208	0.018902	0.097236	0.817167
TLT.2	-0.31233	0.038136	0.119474	0.68094
SELE	-0.28572	0.044741	0.079589	0.751475
PAI	-0.25225	0.097695	0.160039	0.733123
CD93	-0.20191	0.157602	0.030701	0.911777
U.PAR	-0.2064	0.176832	-0.08477	0.743395
CCL16	-0.19658	0.179994	-0.1255	0.648303
PSP.D	0.205789	0.182729	-0.0058	0.983546
IL.18BP	-0.19551	0.183265	-0.03033	0.905885
MEPE	-0.20505	0.183986	-0.09796	0.711297
AXL	-0.18958	0.205565	0.158463	0.706815
SPON1	0.182436	0.222912	-0.20588	0.491555
PDGF.subunit.A	0.182775	0.23192	0.483523	0.035466
CDH5	-0.1758	0.24494	-0.0241	0.9304
FABP4	-0.18526	0.253844	-0.03518	0.889439
SCGB3A2	-0.16432	0.273323	0.09247	0.709318
TNFRSF14	-0.15983	0.281325	0.163958	0.544138
NT.proBNP	0.17421	0.29846	-0.47981	0.298124
IGFBP.7	-0.14992	0.314997	0.10251	0.796533
JAM.A	-0.15543	0.315052	-0.11189	0.687636
Ep.CAM	0.13256	0.359324	-0.17	0.565647
PECAM.1	0.163928	0.360754	0.766174	0.003159
MPO	0.137596	0.36331	0.142032	0.584792
TNFSF13B	0.166954	0.365254	-0.88419	0.163671
PCSK9	0.135592	0.365502	-0.25721	0.331734
TR.AP	-0.137	0.371099	0.460166	0.301347
EGFR	-0.12955	0.378157	0.144523	0.553393
SHPS.1	0.159083	0.382606	-0.64545	0.177083
AP.N	-0.12499	0.384778	0.061251	0.864985
OPN	-0.12549	0.392179	-0.09234	0.761706

ALCAM	-0.14479	0.393798	-0.37198	0.389315
BLM.hydrolase	0.142113	0.394276	-0.0675	0.870352
Gal.4	-0.12839	0.414018	-0.01285	0.974176
CHI3L1	-0.12826	0.422888	0.427033	0.171815
IL.17RA	-0.12101	0.426113	0.234062	0.391374
PGLYRP1	-0.11582	0.456375	-0.14369	0.631653
SELP	-0.10703	0.481657	0.096514	0.771688
uPA	-0.10867	0.487975	0.762964	0.06754
MCP.1	-0.11006	0.488308	-0.423	0.2191
t.PA	-0.10365	0.500319	0.386765	0.221159
Notch.3	-0.10073	0.502324	-0.11705	0.667913
ST2	-0.1253	0.507508	0.408046	0.269318
TIMP4	0.101778	0.516733	-0.46552	0.26194
DLK.1	-0.09396	0.527927	-0.07774	0.818151
RARRES2	-0.09592	0.528182	0.804445	0.001761
GDF.15	-0.0973	0.538326	-0.05916	0.80433
PRTN3	0.097066	0.587374	-0.36009	0.412862
CPA1	-0.08687	0.591864	-0.13423	0.635172
CTSZ	0.085019	0.59319	-0.01813	0.970717
GP6	0.075072	0.621256	0.230633	0.483439
CHIT1	-0.07199	0.62769	0.21884	0.494485
TFF3	-0.07162	0.630368	-0.17638	0.518677
MB	-0.08078	0.639955	-0.73998	0.149782
vWF	-0.07846	0.64847	0.622766	0.016426
KLK6	0.06565	0.656229	0.323802	0.202109
CCL24	-0.06582	0.659655	-0.31976	0.439291
CTSD	-0.06445	0.662446	-0.24286	0.509182
IL.1RT2	-0.0604	0.687301	-0.22384	0.561461
IL.1RT1	-0.06257	0.693828	-0.04345	0.890601
AZU1	0.058962	0.694015	0.187554	0.504863
EPHB4	0.062373	0.712812	0.198604	0.596574
IL2.RA	0.056975	0.71709	-1.04626	0.016179
CASP.3	-0.05697	0.719201	0.240859	0.423102
TNFRSF10C	-0.05537	0.72192	0.080989	0.80129
TNF.R2	0.050734	0.729607	0.304471	0.269951
CNTN1	0.058389	0.737424	-0.06376	0.859092
FAS	-0.05391	0.744985	-0.47723	0.287869
PON3	0.048419	0.774386	-0.01709	0.960323
CSTB	-0.04218	0.791474	-0.0176	0.958321
IL.6RA	0.03639	0.801084	-0.31648	0.428191
CCL15	0.041229	0.805942	-0.22346	0.495234
CPB1	-0.03205	0.826254	0.508677	0.106598
ITGB2	0.033441	0.826828	0.376718	0.397033
Gal.3	-0.03636	0.835212	0.229244	0.603627
LDL.receptor	-0.03586	0.844922	0.569347	0.149686
IGFBP.1	0.028665	0.847676	0.132755	0.676483
TNF.R1	0.026397	0.856212	0.341134	0.140561
OPG	0.028441	0.859018	-0.60437	0.053284

MMP.9	-0.02407	0.867987	0.396281	0.300263
GRN	0.024556	0.872436	-0.24785	0.563468
RETN	0.024097	0.878934	0.090317	0.809094
TR	-0.01932	0.899954	0.144937	0.674086
ICAM.2	-0.01509	0.919219	0.427004	0.096919
PLC	0.016012	0.922855	0.013763	0.958815
IGFBP.2	0.014026	0.925172	0.400323	0.098275
CD163	0.01279	0.933913	-0.17496	0.622555
LTBR	-0.01414	0.934143	-0.07012	0.790865
MMP.3	0.009474	0.948334	-0.01019	0.981507
COL1A1	-0.0104	0.949186	-0.06788	0.855419
MMP.2	0.003001	0.985063	0.015497	0.954421
CXCL16	0.001438	0.99217	-0.02149	0.946107